UNIVERSITY OF STELLENBOSCH
FACULTY OF ENGINEERING
DEPARTMENT OF MECHANICAL ENGINEERING

"DESIGN EVALUATION AND REDESIGN OF A REFRIGERATED SEMI-TRAILER STRUCTURE USING THE FINITE ELEMENT TECHNIQUE"

by

Johannes Francois du Toit

Thesis presented in partial fulfilment of the requirements for the degree of Master of Engineering (Mechanical Engineering) at the University of Stellenbosch.

Promoter: Mr. E Terblanche

STELLENBOSCH NOVEMBER 2000

Declaration

I, the undersigned, hereby declare that the work contained in this thesis is my own original work and that I have not previously in its entirety or in part submitted it at any university for a degree.

Abstract

The finite element technique was used to do an in-depth design evaluation and optimisation of a 15.45-metre refrigerated semi-trailer. Although the emphasis is placed on finite element modelling and its application on a heavy transport vehicle, the paper covers the whole design evaluation and redesign process. Special consideration is also given to the manufacturing process as to ensure that the data generated can be implemented in an effective manner.

Opsomming

Eindige element spannings analises was gedoen op `n 15.45-meter verkoelingsleunwa. Die doelwit was om die huidige ontwerp te evalueer en die ontwerp veral vanuit `n koste en sterkte oogpunt te optimeer. Die fokus van hierdie tesis is die eindige element analises en ontwerpskommentaar hierop gebaseer. Die verhandeling hanteer egter die hele ontwerp en vervaardigingsproses sodat die data hierin versamel en verwerk, prakties uitgevoer kan word.

Dedicated to GOD for my talents and my parents, Jannie and Ann du Toit.

Acknowledgements

The list is rather extensive, and help came from various and sometimes unexpected sources. All of who became good friends, if they weren't before. In the 4 years that I've been active with my research and analyses my knowledge of engineering and more importantly, being an engineer were greatly influenced by the following people. To these people I am immensely grateful.

Instrumental to this thesis and my engineering schooling on the whole is my promoter and mentor, Eugéne Terblanche. His calm, collective, and professional approach towards problem solving has given me insight not available in textbooks. His genuine friendship is also greatly treasured. Johan Barry has taught me many engineering qualities, but the one I appreciate the most, and I'll try to remember, is: "Wees net rustig". This is especially applicable to the transport industry! Also his extensive knowledge of transport engineering, which he is always willing to share, has made my research far easier. Robert Herring has taught me the imperative value of being honest and polite towards all people in a manufacturing environment. He is also an excellent example when it comes to thoroughness and attention to detail.

The professional advice and friendship of Peter Doyle of NCS Resins is greatly commended. Deon Prinsloo of Busaf Cape has also made my life far easier by understanding my situation and giving his support. All the factory workers at Busaf have also participated in helping me to understand semi-trailers and especially the manufacturing process. There are a few I would like to mention who impressed me with their knowledge and friendliness. At the GRP side: Kenneth, Julian and Collin. In the steel section: Joe de Wet, Jackson, Limba, Wiseman, Davie Syster, Johnnie Graaf and Willy. In the offices Brenda and Gina also deserve special mentioning.

My fellow postgraduate students have made it all a bit more bearable. Hano, you have kept me sane, or at least tried to. Thank you for all the help, advice and listening. Anthony, I'm glad that I took 4 years to finish; otherwise I would not have had the privilege to meet you. Thank you for the late night coffee breaks and other

extracurricular activities! I would furthermore like to thank our lab technician Ferdi Zietsman for all the favours, advice and true friendship.

To my friends in general, thank your for the support. I feel it would be proper to mention the following people, without going into particular detail. JP du Plessis, Mariette Grobbelaar, Christine Steinmann, Hennie Roodt, Oom Jan Nel, Tannie Brenda Nel, Suzanne Terblanche, Mariana van Rooyen, Susan Rossouw, Clarissa Meyer, Nicollette Tredoux, Hilda Tredoux, Heilet de Jager, Marnus van Wyk and André Shwack. They each mean a great deal to me, and made sure I'll remember my masters as a great time.

I would like to end my acknowledgements with those who mean the most to me: My family, especially my parents and my heavenly father. You know why I did my masters, and you know how I did it. Thank you for the continuous support, motivation and prayers, and thank you that I can trust on you for future support.

Table of Contents

List of Figures

List of Tables

List of Photos

Chapter 1: Project Background & General Description

Due to the increasing competitive nature of the South African transport industry, semi-trailer design has become much more technologically advanced in the past few years, even more so after historical import barriers were removed. The transport market is continually placing higher demands on the manufacturing industry to deliver lighter and stronger semi-trailers with even more cargo carrying capacity. Transport legislation is also adapting to modern international standards on a continuous basis. From a manufacturers viewpoint the only way to assure survival in an economically unstable market sector is to deliver the required product, faster and at a lower price than the competition. Alternatively you can deliver a superior product, even at a higher cost, which would give the operator an operational advantage over his competitors. For these reasons, advanced manufacturing and state of the art design techniques are a pre-requisite for real success in the South African semi-trailer market. If you don't deliver technological superior products, your company will not survive. The days are gone where the price and past negotiations were the only considerations when buying semi-trailers.

The specific trailer is chosen for various reasons, but the most motivating criteria are the economical benefits of optimising the particular vehicle structure. In the transport industry, semi-trailers of this nature are in high demand. A new, lighter and more reliable semi-trailer would most certainly result in higher sales figures. Increased financial reward is the main driving force behind this project. The main objective is simple: Building a superior product at a competitive price.

This is by no means an easy task. Firstly, what is the definition of superior and what would the Rand value of a competitive price be. Questions like this need to be answered before a design evaluation of this nature could begin. The redesign needs to be optimised with regard to various criteria, with the three most prominent being weight, cost and strength. These three objectives are however opposing design criteria, and in this is the real design problem. To reach the optimal design, various design-aids and experimental measurements were necessary - far more than the traditional intuitive feeling widely used in the manufacturing community at large.

Chapter 2: Introduction to and Description of Analysed Semi-trailer.

As mentioned earlier, the analysed trailer is a 14.45-metre tri-axle refrigerated semi-trailer. What make this semi-trailer unique is its added payload capabilities. Instead of the standard 28 pallets being allowed on tri-axle reefers, this semi-trailer can carry 30 pallets, thus increasing the allowed payload volume with just over 7%. It is important to note that the restrictions on the standard 28 pallet semi-trailer is not dimensional, but rather axle overloading. It is legal to extend a semi-trailer behind its rear axle to 60% of the wheelbase. If however you do this, the payload centre of gravity will shift even more to the bogie[1] support. The bogie will then be overloaded, rendering the layout illegal. For a more in-depth weight distribution discussion refer to Appendix A.

Figure 2.1: Finished GRP semi-trailer

[1] Bogie: Similar to undercarriage. A structural sub frame complete with suspension and axle-wheel assemblies

The semi-trailer design is quite conventional in the sense that it comprises of the same basic structural elements as was used for the past 20+ years. The only real thing that changed was the materials and the manufacturing processes, albeit to a small degree. Henred Fruehauf did break away from the standard design method by introducing a chassis-less refrigerated semi-trailer in the early eighties. This however did not render any long-term solutions, and they returned to the previous, and current, design methods with slight changes in the early nineties. The main reason the industry design stayed so conservative is the low manufacturing volumes. This necessarily leads to low capital investment in research and development projects. Manufacturing companies are not willing to spend large amounts of money on new designs, while they still sell enough of their current designs. The market also accepted this, since it was not economically feasible to import semi-trailers. However, one of the big setbacks of the American and European trailers is that they are not adapted to our local conditions. It's more a question of inadequate payload capabilities, and vulnerability to operator misuse than our apparent worsening road conditions.

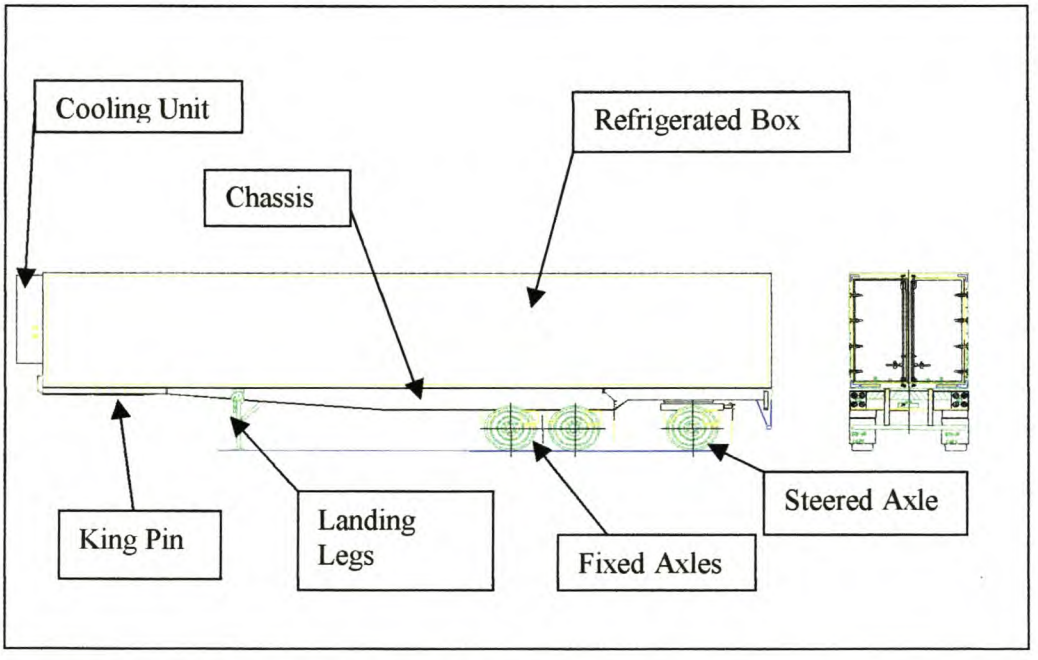

Figure 2.2: Side and rear view of refrigerated semi-trailer

With the above drawings and photograph the basic traditional refrigerated semi-trailer design could be introduced briefly. The main load carrying structure is two I-beams. Attached two these two beams are the suspension, and front linkage point, called the

kingpin. On top of the load-carrying structure is a refrigerated compartment, with the cooling unit supported at the front. This type of semi-trailer is used to carry perishable goods at temperature levels from +5 to a minimum of -20 degrees Celsius. The cargo is usually in the form of standardised 1m x 1.2m pallets, weighing a maximum of approximately 1000kg each, although this may vary considerably.

To substantiate this rather basic description of the semi-trailer one can take a closer look at some of the applied loads. Form a static viewpoint there is a large bending moment present caused by the distributed payload. This load is the fundamental shape-forming factor if the two main I-beams are assessed. An I-beam is exceptionally well adapted to carry these high bending loads for minimal material weight, in torsion it is however not very stiff. To accommodate the torsion forces the main I-beams are stiffened by means of cross-members as well as vertical web stiffeners.

The refrigerated box structure is also stressed in a bending fashion by the payload, as the chassis and box assemblies are connected quite rigidly. The box is constructed by an inner and outer layer of chop strand mat (CSM) together with polyurethane and wood core sections. The structure is quite capable of resisting the imposed bending load. The refrigerated box also increases the chassis structure's torsion stiffness considerably. These torsion stresses are primarily induced during dynamic loading cases.

The dynamic loads are divided into two classifications. First there is long duration dynamic loading, e.g. braking moments, severe manoeuvring, unsymmetrical payload configuration, transverse wind loads, and steady state transverse acceleration. Under the classification of short duration dynamic loading are events like pot-hole impact and forklift floor impact. The long duration dynamic loading is reasonably easy to visualise, but the short duration loading and especially its influence on the overall structure is not easily understood or calculated. At this point in time the effect of both of these dynamic load scenarios will not be explained, but rather left for analysis at a later stage. It could however be mentioned that historically they did not play a dominant role in the overall shape forming of the semi-trailer structure.

Chapter 3: Design and Manufacturing Processes

The trailer manufacturing process is different form most other manufacturing processes in the sense that manufacturing is done on a job-shop basis. There is seldom a situation that a trailer is built without a predetermined customer. The customer places an order and only then can manufacturing commence. The main reason is the high manufacturing costs combined with a perpetually unstable market.

This situation makes process optimisation a bit different. It is difficult to predict you income for a long period in advance, and that in turn makes it hard to rationalise large capital investments. Change must be incorporated on continuous, and low cost fashion. On the design side, optimisation is possible in theory, but difficult to pull through to production. It is much easier to sell a complete physical product to a customer, especially if he does have of these current designs in his fleet, than to convince him to buy a new concept. The danger always exists that a substantial capital investment might have design or manufacturing flaws, and this might lead to unacceptable down times, which could throw the return on investment balance to the negative side.

A way to overcome the "new product" fear is to build a prototype, but unfortunately this is a high capital investment for the manufacturing company. Usually the manufacturer obtains a development partner, where both parties can share the risk of new development. In this arrangement the client does pay for the vehicle, and agrees to a fair amount of modification downtime after the vehicle has been sold. Unfortunately this does not always work properly since there is seldom-effective feedback between the end user and the original designer. If feedback does reach the designer, it is usually third or higher party information. All the relevant detail is lost, and it is mostly based on negative comments. At this stage the problem is highly exaggerated, and to convince the management on both sides that it is not that serious is a rather difficult procedure, much more than it would have been just to rectify the original mechanical failure or design deficiency.

This is where finite element modelling and accurate analyses are highly advantageous. For a fraction of prototyping cost, an idealised model can be created and structural functionality and integrity tested. Even more so if complete mechanical design packages are utilised where vehicle parametrics and handling characteristics are analysed. With this approach the end client can be assured than the first unit will be capable of handling the imposed loading and operating conditions. Also, different designs can be compared without either of them ever seeing the light.

Today this design approach is a given for the high technology and high production volume companies, with various software packages available. For the transport industry, especially for the parametrics and handling characteristics, ADAMS®[2] is the preferred software solution. From the mechanical simulations it is then easy to obtain the stress solutions for given worst-case scenarios with packages like Nastran®[3]. Unfortunately the smaller manufacturing companies believe they do not have access to these high-end software solutions due to the perceived high cost. The ironic side of it all is that this software is not as inaccessible as what was originally the case. The capital investment for these high solutions are in-fact in-reach of most manufacturers, it is only a mindset that has to be changed. In the past it was not an everyday option and the older companies are not used to analysing concepts with complete simulations before they start manufacturing. They would build a new prototype based on experience rather than on technology. With this approach however you are not effectively using available technology, and success won't come easy at all.

If one considers the large capital investment into trailers, and the associated high cost a design oversight might have, the use of this software is not expensive. It would not necessary be cost effective for each manufacturer to obtain his own license at first, but to make use of outside contractors, until enough work is done to substantiate the investment. The only problem in South Africa is the current availability of competent outside contractors in this field, but the situation will change if the demand increases.

---

[2] ADAMS®: © Mechanical Dynamics Inc
[3] Nastran®: © MacNeal-Schwendler Corporation

For this thesis a full mechanical simulation was not done. Only detailed finite element analyses were undertaken. The use of a package like ADAMS® would however greatly improve the design quality and time to market of vehicle systems. In chapter 13 a detailed investigation into ADAMS® with possible applications specifically directed towards the trailer manufacturing industry, was undertaken.

The manufacturing process differs from order to order. The client might order a standard trailer with no special features. Often however the trailer is custom build for the specific needs of the client. The variables are not always considerable, but even a slight variant might require a new set of drawings according to the ISO9001 specifications.

The order will start with the sales department enquiring about the pricing influences of certain design changes. Also the engineering department will contact the client to obtain engineering specific details and design the vehicle layout for the specific payload and operating conditions. In this optimisation process, different vehicle layouts are considered where the winning layout is the one that will best fit in with the customer's current fleet, operating conditions and just as important, his peculiar likes and dislikes. After the design is fixed, the price is calculated and a formal quote is prepared. In the next step the client might place and order, or not. If an official order is placed, further engineering details are obtained and then the design drawings are created. Only for special designs, or products varying considerable from the standard design, strength calculations are done.

If one considers this process, there is not really opportunity for design personnel to optimise or improve current designs. Every job is handled in isolation, and design changes are not easily adopted into the system. If for instance the engineering department wants to change the side panel construction, the sales department has to agree on this before they sell the product to a potential customer. The sales department are rather conservative regarding design changes, and they will much rather sell proven technology, instead of taken a leap of faith. As described above, this is where accurate finite element modelling can assist.

After the design phase, the material requirements are loaded into a material requirements program (MRP) system[4]. The drawings are issued and manufacturing can begin. The GRP and steelwork usually runs parallel, with the GRP work the more labour intensive activity.

The production processes will now be discussed together with some detail factory issues as to clearly define the original and baseline manufacturing process. Deviations from this process will be given in the design and process modification chapters where it is believed changes could lead to improvement in quality or decreased production cost. In the following chapter a manufacturing cost breakdown is given, from this it is more obvious where production and manufacturing costs can be saved. Also a weight breakdown would indicate where to effectively save weight.

Photo 3.1: Guillotine

The cutting and bending process are the first stage. Standard brake presses and guillotines are used. The guillotine can cut up to 12 mm plate, 3 m in width. The presses can handle up to 8 mm plate, also 3 m in width. The material loading is manual, with no readily available mechanical assistance.

---

[4] At Busaf Cape the Impact Encore® © Software suit is used

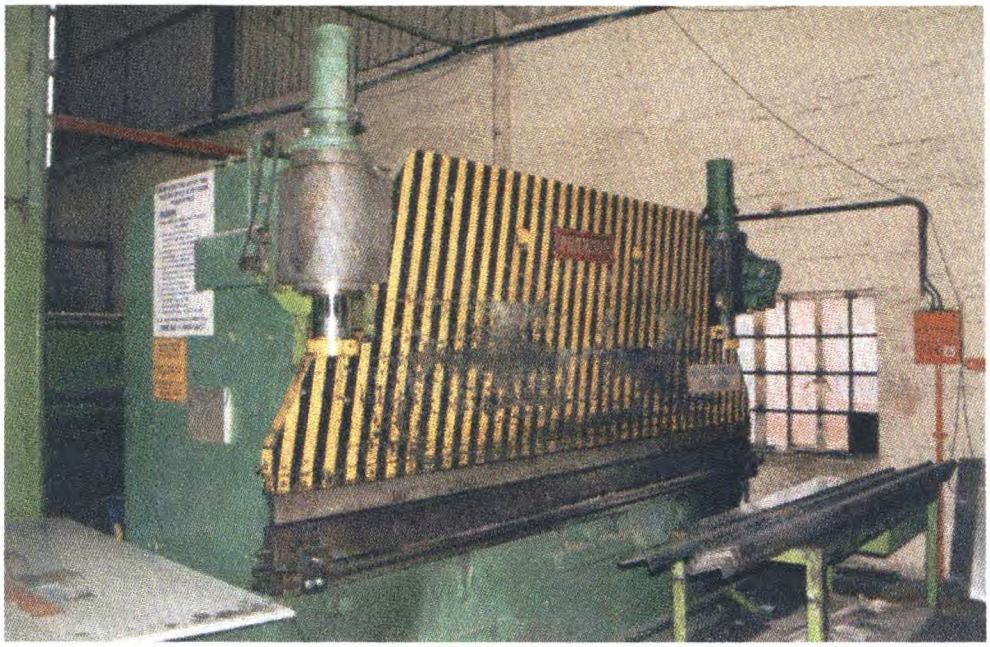

Photo 3.2: Brake press

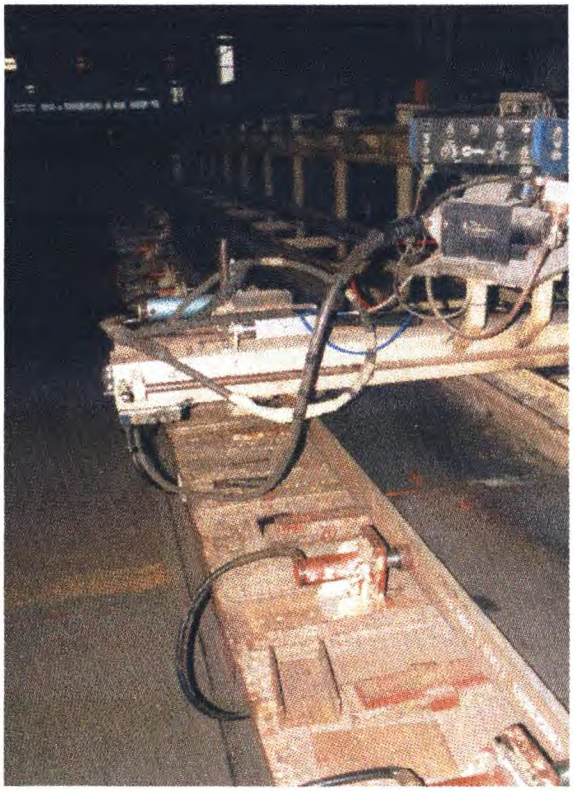

Photo 3.3: Beam welding machine

The I-beams are welded with an automated cam assisted welding machine. A cam follows the upper or lower flange and the welding head will follow the welding groove. The beams are held in place with hydraulic clamps. Before the longitudinal weld is started the beam is tacked together to prevent distortion. Only linear speed control is used. Also only one side of the I-beam can be welded. The flanges of the I-beams are folded with a mobile hydraulic press. Up to 25×150 mm flats can be bent to suit the web profile.

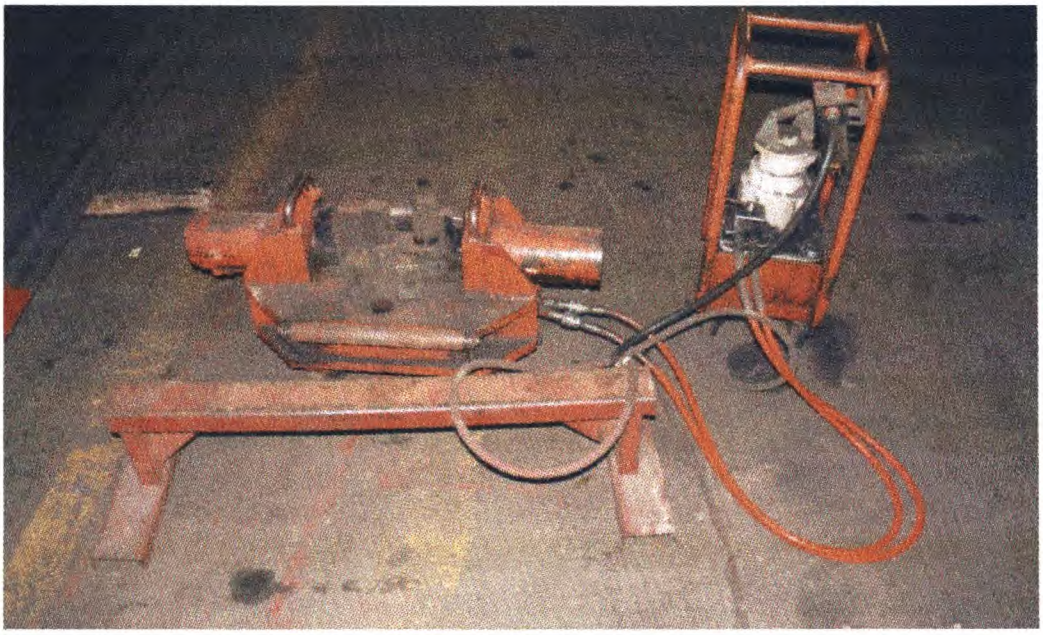

Photo 3.4: Flange bender

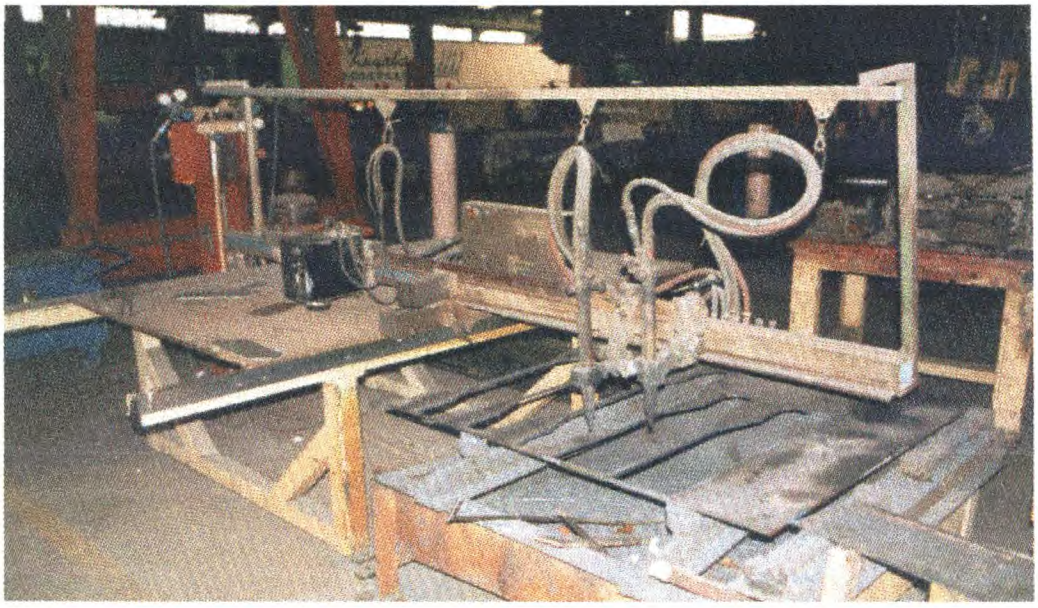

Photo 3.5: Plasma cutter

Profile cutting is achieved with a plasma profile cutter. The machine uses an optical eye to follow a printed profile drawing. Maximum cutting size is 2.5×1.5 m. Material thickness is between 4 and 50 mm. The average cutting speed varies between 3 to 7 mm/s, depending on material thickness.

After the beams are welded, they are placed in a jig at the correct chassis centre distance. In this jig the axle hanger brackets and axles themselves are welded on the chassis assembly. All the cross-members and apron plate support structures, as well as the landing legs are also welded into place. For the steering axle trailer the front steering system is installed, as well as the rear steering bogie. For the whole of stage two the trailer is upside down.

During the stage three process the chassis construction is finished. The rear under-run protection, lightbox and toolboxes are welded onto the chassis. The chassis is sprayed, where after the tyres are fitted. The chassis are now ready for the GRP box section.

Photo 3.6: Finished glass fibre skin panels

The refrigerated cooling box process starts with the manufacturing of the glass fibre skins. The floor, roof and side beams are also manufactured in advance. The skins have to stand for at least three days to allow for the styrene to escape from the lay-up.

After the skins are cured sufficiently they are placed on the lay-up table. During this process the different parts included into the panel construction, which are sandwiched

Photo 3.7: Floor beam moulds

together between the two glass layers with bonding resin. The panel is held under a vacuum, until the resin has cured. After the floor, sides, roof and bulkhead panels are finished, the box assembly starts. The assembly starts with the floor. The front bulkhead is placed unto the floor and fixed with epoxy glue and rigid angle

assemblies. Thereafter the sides are fixed to the floor with epoxy and also bolts where the rigid floor beams are in place. The sides are held vertical with overhead cranes

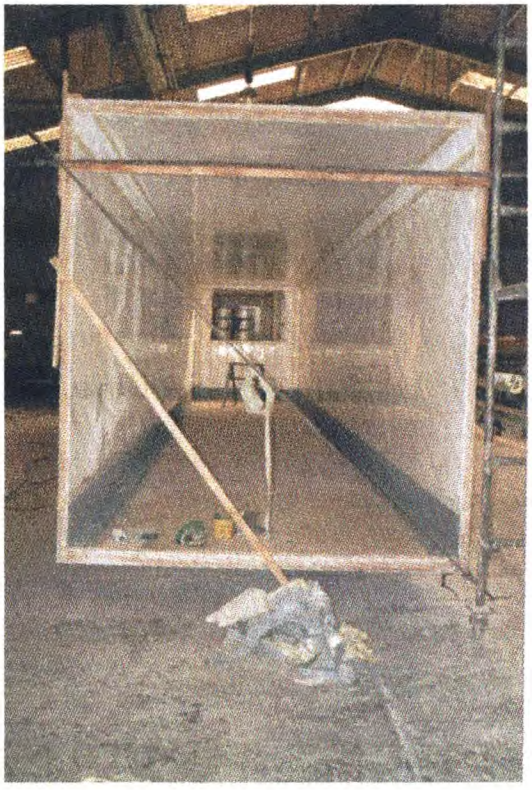

Photo 3.8: Rear view of box assembly

until the glue is cured and all the bolted connections are in place. The complete assembly is held square with large clamps. The roof is next to be adhered to the assembly. After these parts are in place, the interior, exterior and inside floor surface are hand laminated for extra strength and to act as vapour barriers. After this the bottom and top corner cappings are fastened to the assembly with pop-rivets. Next the doorframe is installed, after being manufactured separately. The doorframe is adhered with self-drilling screws and epoxy. The rear doors are the last to be hung. The GRP box is finished off, and then bolted onto the waiting steel chassis.

The trailer is now ready for the finishing stage. During this stage the brake and electrical installation are completed. Finishing detail such as mud-flaps and required logos are also attached. After this the trailer is sent away to install the refrigeration

unit, and after a final quality check the trailer are sent for its roadworthy clearance and it is deliverable to the end client.

During the manufacturing process various welding machines are used. The three most prominent being the MIG, TIG and stick welding machines. The MIG machines are the standard type used. The TIG machines are used when aluminium flooring is installed, or when delicate aluminium work need to be done such as for the bulkhead protector and corner capping finishing. For the beam welding machines, fluxed core welding wire is used to increase weld consistency and speed. The stick welding is sometimes used for the small parts manufacturing processes, e.g. spare wheel carriers, toolboxes.

The current GRP manufacturing environment and process were evaluated with a grid given in an article by Bob Lacovara, "The Optimum Composites Shop" © CFA, 1994 [3]. The grid was slightly altered to suit trailer manufacturing, and is given in appendix B. The situation that currently describes Busaf's situation is the bolt-faced choice. In this grid "worst", "better" and "best" workshop practises are listed. Clearly from this grid the current processes tend to be the "worst" or "better" selection.

As mentioned in this rather out-dated article, to succeed in the future, a company must strive and achieve the "best" rating for the various activities. The change to meet these requirements will either come by choice and economic survival, or by regulatory force. Lacovara also states that: "Today's optimised composites shop, which employs the latest facility design and production capabilities will be the norm in the not too distant future". The article is written from an European viewpoint so it might be a bit harsh to directly apply it to a South African context. However, the global village concept has made the world a small place and to survive you have to be the best, or at least equivalent to. The processes as used in Busaf falls far short of an advanced or optimum composite shop, and if Busaf would like to participate as a world class manufacturing company, certain changes would need to be implemented.

To incorporate these changes will necessarily lead to capital investment, and if the company's investors will feel the need to comply with international trends, is

doubtful. Or rather it will be difficult to convince them, given the unstable South African transport market. If however Busaf want to compete in world markets such investments would surely be worthwhile.

Chapter 4: Material Cost Breakdown

The trailer is manufactured from various types of materials and sub assemblies. The processes are normally labour intensive, as could be expected. The cost of these

Item	Contribution	Outsourced
Chassis	**50.00%**	
Axles	10.14%	Yes
Suspension	10.10%	Yes
Tyres	7.48%	Yes
Steering Kit	6.30%	Yes
Brake Kit	4.08%	Yes
Rims	2.12%	Yes
Paint	0.66%	Yes
Wheel Alignment	0.35%	Yes
L/Leg Kit	0.13%	Yes
Chassis Assembly	2.58%	
Beams	1.79%	
Rear Dolly	1.67%	
Extras	0.74%	
Lightbox and Bumper	0.55%	
Finishing	0.45%	
Electrical	0.44%	
Spare Wheel Carrier	0.26%	
Toolbox	0.16%	
GRP Refrigerated Box	**27.28%**	
Floor Assembly	8.23%	
Side Panels	8.22%	
Roof Panel	4.13%	
Box Assembly	2.82%	
Door Frame	1.57%	
Door Panel	1.11%	
Bulkhead	0.88%	
Bulkhead Protector	0.33%	
Labour	**22.72%**	
GRP Labour	10.86%	
Steel Assembly	4.74%	
Cutting & Bending	3.95%	
Paint / Finishing Labour	1.78%	
GRP Doors / Fittings Labour	1.38%	
Total Cost	**100.00%**	

Table 4.1: Overall trailer cost breakdown

manufacturing processes and materials is arranged here to identify the most expensive components, to help with the cost optimisation.

With this type of breakdown it is easy to see on what structural components the finite element analyses should focus to optimise the cost. The pricing structure is for a standard trailer without the optional extras such as aluminium flooring, hubodometers, etc. It also excludes the refrigeration unit, which can cost anything from R85 000 and upward. No absolute values are given; only percentage of complete cost is shown.

From the breakdown is clear that for the grouping as per table 4.1 the chassis with its' running gear is the most expensive part of the trailer. If however the outsourced parts, e.g. those that are bought as a unit and are only assembled into the overall structure, are ignored the breakdown changes considerably.

Process	% of Complete Trailer
Outsourced	40.69%
GRP	27.28%
Labour	22.72%
Chassis	9.31%

Table 4.2: Pricing breakdown summary

With this grouping, the steelwork has the least influence on the overall costing, in fact, it is almost three times less than the GRP work. By far the most expensive component is the outsourced parts, which constitutes almost 41% of the total cost. The outsourced parts are normally referred to as high value parts in the manufacturing process. These parts are bought at given prices, which is difficult to change since they are fixed through the current market circumstances and economy of scales. From a design point of view it will also be difficult to omit these parts, since they are key components of the trailer structure, e.g. suspension, tyres, etc.

If only the high value components are examined as in table 4.3 it is apparent where the most effort must go into, to obtain better purchase prices. The axles are slightly more expensive than the suspension, but in reality these will come as a unit from one supplier. They therefore account for 20.24% of the total price. The end user usually

specifies these items. It is therefore difficult to negotiate lower prices with the supplier beforehand, since order quantities are not known long in advance. It is also risky to use inferior or less known suspension axle components if they are not specified due to the high warranty risks involved. A viable option is to obtain a large number of consignment stock from your supplier, which could lead to a noticeable price decrease. In a way the client is indirectly forced to use a certain make of axle and suspension.

High Value Cost Item	Contribution
Axles	**10.14%**
Suspension	**10.10%**
Tyres	**7.48%**
Steering Kit	**6.30%**
Brake Kit	**4.08%**
Rims	**2.12%**
Wheel Alignment	**0.35%**
L/Leg Kit	**0.13%**

Table 4.3: High value items pricing breakdown

Tyres quantity cannot be altered, except if the client opts for "super singles". The standard vehicle layout uses a dual tyre configuration per hub, e.g. twelve tyres for the three axles plus one spare wheel. It is possible to use only one tyre per hub, e.g. seven tyres in total, including the one spare wheel tyre, if the larger and more expensive tyres are used. The cost implications are detailed in table 4.4.

Cost Item	Dual	Super Single
Rims	100%	-27.96%
Tyres	100%	12.35%
Total	100%	0.98%

Table 4.4: Tyre configuration cost comparison

From this comparison there is not much cost difference as what might be expected. Further more when you have a tyre failure with super singles it is not possible to continue driving, whereas for a dual configuration it is possible to continue driving to the next repair centre. A major advantage of singe tyres is that of weight saving. With the super single configuration you save about 200 kg on the total trailer mass. In addition, if aluminium rims are used you can save up to 500 kg, which is about a

5.3% tare weight saving. The single tyres also have a much lower rolling resistance, which would reduce vehicle running costs considerably. For a dual tyre combination the danger also exists that uneven tyre pressure, or one misaligned tyre could cause excessive tyre wear. From the above it is clear that initial capital investment is about the same for the two options, but the super single option is more advantageous from a running cost viewpoint, even more so if the cost of super single tyres can be reduced further.

One part of the high value grouping for which the design can change to potentially decrease the cost, is the steering mechanism. This mechanism is a mechanical sub-system with a large number of parts. There is scope for design optimisation, not only from a cost viewpoint, but also from a reliability point. In the chapter dealing with reliability this will be considered further.

The brake installation is a given, and it must be of a high standard as specified in the SABS regulations. There are different options, but the breakdown as given above is for the standard kit. This price includes the parts and outsourced installation labour. If the labour were supplied in-house there will be a cost saving, but from a feasibility, capability and quality viewpoint this option is not advisable.

High quality wheel alignment is also of major importance. A severely misaligned set of axles can lead to tyre failure in a very short distance, since irregular tyre wear is usually non-correctable after it started. On a trip of a 1 000 km it is possible to loose the full set of tyres, which make the money spend on correct axle alignment a worthwhile investment. A steering axle trailer needs special attention when it comes to axle alignment. A special tool were designed and produced as to help with this specific alignment process. Detail of this is included in appendix G.

If the focus shifts to the remaining parts of the chassis group, the assembly process is the most expensive. Most of the steel labour is also allocated to this process. From a design viewpoint there is scope for improvement, not as much for material used, but rather processes used. This will be discussed in chapter 10. The beams are second, but the current manufacturing process constraints dictate their shape. To change their shape and manufacturing speed, will require large capital investments.

Chassis	50%
Chassis Assembly	2.58%
Beams	1.79%
Rear Dolly	1.67%
Extras	0.74%
Lightbox and Bumper	0.55%
Finishing	0.45%
Electrical	0.44%
Spare Wheel Carrier	0.26%
Toolbox	0.16%

Table 4.5: Chassis cost breakdown

From a strength viewpoint there are some shortcomings. This will be dealt with in the design evaluation chapters. The extras grouping include some miscellaneous commodities, and mostly also after-sales cost. These are unlikely to change much, since first maintenance services and other services are obligatory.

At first glance the lightbox and bumper does not seem that expensive, but if one considers that they are only 3.26 times less expensive than the I-beams, their cost suddenly features. The under run protection, strength is prescribed by the SABS specifications. The lightbox can be made lighter, and less expensive. As mentioned above, details about such structural changes will be discussed in chapter 10.

Under finishing is material costs such as decals, emergency equipment, reflectors and the like. Legislation and general appearance specify these, and change is not likely. In studying the production of the refrigerated box, or GRP work as it is frequently referred to, it is clear that this structural part and process account for a large fraction of the total cost. From a labour viewpoint the GRP labour amounts to 47.83% of the total labour allocated. This process would be the ideal area to cut on labour costs. Various GRP labour saving concepts is discussed in the design and production chapter.

The floor is the single most expensive assembly. This assembly is also the structural component that showed the most failure in the past. The high production cost and failure rate made this component a main focus point for structural optimisation.

GRP Refrigerated Box	27.28%
Floor Assembly	8.23%
Side Panels	8.22%
Roof Panel	4.13%
Box Assembly	2.82%
Door Frame	1.57%
Door Panel	1.11%
Bulkhead	0.88%
Bulkhead Protector	0.33%

Table 4.6: GRP cost breakdown

Detailed finite element models were created to analyse the floor behaviour. In table 4.6 the side panels appear to cost the same as the floor section. The values stated above are however for material only, and it must be mentioned that the floor is much more labour intensive than the side panels. Another aspect that must be remembered is that the side panels are one of the single most important components when it comes the overall appearance. The large reflective surface will instantly show any surface irregularities, or even substrate deficiencies. There is scope for structural change, not only to improve appearance, but also to lower production cost, increase strength and reduce weight.

The roof cost is almost equivalent to one side panel, and as for the side panel there is room for improvement.

The assembly process is cumbersome, it is also not as material intensive as what it is labour intensive. Given high enough production volumes and inventive design changes this process can be improved to a great extent.

For the remaining parts structural optimisation is possible, but their influence on the total price might not be so significant. However design changes for all of these parts were proposed and some analysed.

The labour is grouped as per the different work areas inside the factory. The labour issues were discussed as it applied to the different manufactured sub assemblies above. However it can be repeated that the glass fibre work is the most labour

intensive and methods to decrease the allocated hours must be found. Further the cutting and bending process are also rather expensive considering what the actual process entails. Methods to decrease this cost effectively were also investigated.

An important aspect of the labour cost that has to be remembered is that the labour costs are direct and immediate costs. The workers have to be paid weekly, whereas manufacturing costs can only be recovered after production and the payment has been received. In this period interest is being paid on this money, which can easily change the percentage values above with a percent or two. Also labour cost can escalate due to unforeseen circumstances. Public holidays, political strife, and the like can make your workforce highly unproductive. These costs cannot be predicted, or worse recovered. The only way to minimise this risk is to minimise actual labour hours, or use outside contract workers, or companies, who doesn't work at a hourly rate, but rather on a Rand per assignment basis. However with this approach quality control can become an obstacle, where the feedback loop is removed from the system. For the same reason design mistakes can slip through the system.

From the above discussions it is clear that the biggest cost influence is the high value components. Management and purchase department can have the biggest cost influence if these supplied prices can be lowered by buying at a premium. The refrigerated box as a whole is the next biggest contributor. Especially this manufacturing process needs to be refined, or altered.

Chapter 5: Material Weight Breakdown

Similar to the material cost breakdown, the weight contribution of different sub-structures were estimated as to help with the optimisation process. The three main categories were running gear, chassis and GRP box section. These were further divided into the various substructures as indicated in the table below. The detailed semi-trailer weight breakdown is as calculated in the FEA model. The truck and trailer tare weights are as per weighbridge measurements. In some instances the detailed breakdown may not be precisely correct, but for there comparative analyses it is considered adequate.

Sub-assembly	Weight [kg]	Weight Contribution [%]
Gross combination mass	**50 798**	**100.00%**
Payload	30 000	59.06%
Truck tractor	8 320	20.86%
Semi-trailer tare weight	11 120	20.09%
Running gear	**3 483**	**34.13%**
Axles + suspension	1 695	16.61%
Rims	520	5.10%
Tyres	1 040	10.19%
Brakes + other	228	2.23%
Chassis	**1 507**	**14.77%**
I-beams	983	9.63%
Apron plate	314	3.08%
Steering bogie	90	0.88%
Light box + bumper	120	1.18%
GRP box	**4 319**	**42.33%**
Floor	1 929	18.90%
Sides	1 489	14.59%
Roof	538	5.27%
Bulkhead	160	1.57%
Door frame	110	1.08%
Door panels	93	0.91%
Refrigeration unit	**780**	**8.77%**

Table 5.1: Estimate weight breakdown

In appendix A the overall vehicle mass distribution is discussed further. From the above data the GRP box section is clearly the biggest contributor. Next is the running gear and the chassis construction is only third. The refrigeration unit are the smallest contributor with 8.77%.

The GRP section is the most likely area to achieve weight saving, but the loading and stress distribution of this construction is rather complex and intuitive design techniques will not easily deliver optimal designs. The floor is the main contributor. Between the sides and roof the side panels seem the more likely candidate to achieve weight savings. The bulkhead, doorframe and door panels are not that big a contributor that extensive redesign is thought necessary, not from weight considerations anyway.

From a design viewpoint not much can be done to the running gear and refrigeration unit, since these assemblies are outsourced as complete units. The importance of using low weight running gear is however stressed considering its 43.13% contribution. A 10% weight saving in the running gear is more than two times as effective as a 10% weight saving in the chassis construction. The axle and suspension manufactures do realise this weight importance and almost all of their new development focuses on lightweight construction. The tyres are also heavy, and lighter alternatives than the standard 13 off 12R22.5's should be investigated. The refrigeration units are also continuously getting lighter and smaller. Especially the obtainable front swing-clearance has decreased considerably in past few years, allowing extended front overhang.

Traditionally the first place most semi-trailer designers would try to cut on weight is the chassis assembly. This sub-assembly accounts for 14.77% of the overall semi-trailer tare weight, and weight saving here will not be so dramatic and effective. However there is some weight to be saved in these structures. Probably the best way to save weight in the chassis construction is to eliminate the chassis completely, e.g. mount suspension and kin pin assemblies directly to a reinforced refrigerated box section. This concept is referred to as a chassis-less design and is not uncommon in the USA and Europe. The main setback of such designs is the decreased thermal

isolation, and complex reparations procedures. Another interesting weight breakdown is to differentiate with regard to material type rather than to sub-structures. The out-sourced parts such as the suspension and refrigeration unit was left out of this particular breakdown. The volume and a comparison of stiffness multiplied by the volume of the different materials were also calculated as to evaluate effective usage. The stiffness effectiveness comparison does not take distance from neutral axis in account, so from a theoretical viewpoint this is not strictly correct.

Material	Weight [kg]	Weight Contribution [%]	Density [$kg.m^{-3}$]	Volume [m^3]	Young's Modulus [$GN.m^{-2}$]	Stiffness Effective-ness
Steel	2744	40.83%	7850	0.35	200	70.00
Wood	1374	20.45%	480	2.86	13	37.18
CSM[5]	1239	18.44%	1400	0.89	8	7.12
PU[6]	544	8.10%	55.38[7]	9.82	0.018	0.18
Bonding resin	535	7.96%	1280	0.42	3.5	1.47
Aluminium	284	4.23%	2670	0.11	70	7.70
Total	**6720**	**100.00%**		**14.44**		

Table 5.2: GRP Box and chassis material property weight breakdown

From table 5.2 it can be seen that steel is by far the heaviest structural material and its usage has to be investigated in detail. It is also the main stiffness contributor, and removal of steel will inevitably lead to major structural changes.

Wood is the second largest weight contributor, as well with regard to stiffness. Combined with its rapid degradation when exposed to moisture the use of wood needs to be investigated.

The aluminium does not actually add that much to the stiffness as what might seem from the calculation above, structurally it doesn't really feature in the design. Its use is limited to the bulkhead protector and corner capping finishing, in both cases more for aesthetic reasons than strength.

---

5 CSM = Chopped strand mat
6 PU = Polyurethane

7 This is a usage weighted average between the 40 and 80 kg.m-3 density foam.

Chopped strand mat and woven roving is the basis material for the GRP box section. Its use is automatically associated with refrigerated transport, and change in this material usage will not be easy, or even attainable. The strength to weight ratio is excellent, and given the prescribed manufacturing procedures are adhered to, excellent surface appearance is possible.

PU foam is used extensively for its thermal insulation properties. The density is low and from a weight saving viewpoint there is not much scope for reduction by altering the design or material specifications. Also the thermal insulation cannot be reduced, since this will directly increase operations cost. It might however be a viable option to use a material with better strength and stiffness characteristics. The material will now have a dual purpose, structural and thermal. The insulation material has to be distributed in an uniform manner, also highly advantageous from a stress viewpoint.

The weight data for the semi-trailer as currently built by Busaf was further compared with a European design. Data for a Spanish design from the mid 90's was available from a paper by E. Larrodé, from the University of Zaragoza.[8]

Sub-Assembly	Spanish Design [kg]	Busaf Design [kg]	Modified Spanish [kg]
Floor	1900	1929	2034
Side	1200	1489	1284
Roof	515	583	551
Bulkhead	105	160	112
Total	**3720**	**4161**	**3982**

Table 5.3: GRP weight comparison

Considering that the Spanish design conformed to European standards the length is only 13.5 m, almost 1 m shorter that the Busaf design. The height and width is similar. In column three of the table the Spanish design is extrapolated linearly to the equivalent Busaf length. The Busaf design is 7% heavier than its European rival.

[8] Design and analysis of a lightweight frigorific semi-trailer by means of a numerical simulation procedure. Department of Transport Engineering, University of Zaragoza.

This is not a large difference, and considering maximum payload capabilities, the Busaf semi-trailer will have a better payload to tare weight ratio. In the paper it is mentioned that using Carbon and Kevlar composite material instead of steel for a chassis-less construction, a 30% theoretical weight saving was achieved. It is further mentioned that production cost stayed the same. This is however a doubtful statement, and it requires further investigation before it can be believed as such.

From the above breakdowns and comparisons it is clear that the GRP box is probably the best place to save weight and detailed analyses will be beneficiary. Chassis changes or total removal is also an option. Furthermore our South African designs are not lagging European manufactures, considering tare weight and cargo carrying capability.

Chapter 6: Welding

Welding is used extensively as a method of joining pre-cut sheet metal in semi-trailer manufacturing. Fillet and butt-welding are the most prominent, with fillet weld types more prone to fatigue failure where excessive bending or transverse shear stress situations exists. It is important to note that welding was not built into the overall semi-trailer finite element model. Doing this would have lead to an immense increase in the solving-matrix size to ensure acceptable element aspect ratios. The finite element analyses results were rather used to do analytical checks using standard welding formulas and listed acceptable stress values. The American Welding Society (AWS) code was used to evaluate the welding [22,24]. Terms and definitions used in these paragraphs are as defined in the AWS code.

The manual shielded metal arc process (MIG) is used as the basis for strength calculations, since it is used extensively throughout the manufacturing process. The default filler wire used in the factory is of the E70 strength classification. The maximum ultimate tensile stress for this filler material is listed [23] as 496 MPa and the yield strength is in the order of 413 MPa.

From the AWS code the maximum shear stress allowed in a groove or fillet weld shall not exceed 0.3 times the ultimate electrode stress. For the E70 electrode this is equivalent to 149 MPa.

The minimum fillet or groove weld sizes for different plate thickness are listed in table 6.1. The table was converted from inches and rounded to the nearest logical decimal standard. The standard plate thicknesses used in semi-trailer manufacturing are 4, 4.5, 5, 6, 8, 12 and 16 mm. The average thickness is about 5 mm. (For welding calculations the thinner plate of the welded assembly is used for strength calculations.)

Plate thickness from [mm]	to [mm]	Minimum throat size [mm]
0	6	3
6	13	5
13	19	6.5
19	→	8

Table 6.1: Plate thickness

From the table it is fair to assume that a minimum fillet size of 5 mm must be specified as a company standard. Also from the AWS code the maximum allowed shear flow is listed for various weld throat leg sizes. The original kips[9] / linear in. was directly converted to the SI values and not rounded.

Leg size [mm]	Unit Force [N.mm^{-1}]
25.40	1828.43
22.23	1599.41
19.05	1371.63
15.88	1142.61
12.70	913.60
11.11	800.32
9.53	685.81
7.94	571.31
6.35	456.80
4.76	342.29
3.18	229.02
1.59	114.51

Table 6.2: Maximum unit force

These two tables serve as a rough guide for allowed weld stresses but doesn't allow for fatigue and particular weld design. The actual allowed stress is also dependent on actual weld orientation and the method the member is loaded. Similar to the British Standard (BS) welding specification the AWS classify welds into seven design types. These seven weld classifications each has its own limit design stress for different load repetitions as indicated in table 6.3 below.

[9] kips = kilo pounds

	Load cycles			
Weld Category	**20 000 – 100 000**	**100 000 – 500 000**	**500 000 - $2x10^6$**	**$2x10^6$ +**
A	434	255	165	165
B	338	200	124	110
B'	269	159	103	83
C	241	145	90	69
D	193	110	69	48
E	152	90	55	34
E'	110	62	41	21
F	103	83	62	55

Table 6.3: Allowable fatigue weld stress [MPa]

Note that the 'A' classification in table 6.3 above is referring to the original base metal and not a specific weld type. The most commonly used welds in semi-trailer manufacturing are classified in table 6.4 [21].

Description	**Class**	**Comment**	**Stress [MPa]**
I-beam flange to web fillet	B	Only longitudinal loads	124
Intermittent I-beam flange welds	E		55
I-beam vertical stiffener	C	Applicable to base metal	90
I-beam flange to flange connection	F	If radiography (B)	62
I-beam doubling strap	E	Longitudinal or transverse	55
Cross member flange to I-beam flange	E	Applicable to I-beam	55
Cross member web	E	Applicable to I-beam	55
Plug weld, base metal	E	For shear in plug (F)	55
Axle hanger brackets	D	Flange wider than bracket	69
Bolted connections	B		124
Miscellaneous small fittings	C	If larger (D) or (E)	90

Table 6.4: Typical semi-trailer welds and their fatigue allowable stresses

As a conservative estimate it can be assumed that a semi-trailer will experience two events per kilometre travelled that would lead to a significant stress amplitude variation. At a realistic design limit of 18 500 km travelled per month this ads up to 2.22×10^6 fatigue load cycles for a five year period. If a three-year period is considered this value reduces to 1.33×10^6. The five-year period is just above the 2×10^6 group and 3-years fall in the 500 000 to 2×10^6 range as listed in table 6.3. It was consequently decided that the 500 000 to 2×10^6 range is sufficient for semi-trailer design and this will be an acceptable structural design lifetime. The maximum

allowed stress value associated with this cycle range is listed in the last column of table 6.4 above [20].

The listed allowable stress values can be reduced further by a factor of 1/(1-K) where 'K' is the relation of the minimum stress over the maximum stress. For a predominant bending load as present in the semi-trailer it is unlikely that the load will change in sign. The stress stays positive or negative, only the amplitude varies. For this scenario the value of 'K' above is set to zero and the stress reduction factor is equal to unity, e.g. no reduction. If however there is a complete sign change in the stress, which might arise for torsional loading, K is equivalent to –1 and the allowed fatigue stress is half of the values listed in table 6.3 and 6.4.

Considering weld quality and general connection design, a rule of thumb maximum stress value is estimated at 55 MPa for all weld types. When the stress is higher than this limit in the FEA's the welded interfaces is investigated in more detail.

If table 6.4 is studied in more detail some interesting observations are made. If the I-beam flanges are hand welded and start-stop situations arise, the allowed maximum stress falls from 124 to 55 MPa. This is a high price to pay, and for this reason automated beam-welding machines is a necessity. Also the allowed stress for a single I-beam with a higher section height is considerably more than that for a beam with doubling plates. With doubling plates fitted the maximum allowed stress is again reduced from 124 to 55 MPa. If the addition of a doubling plate does not reduce the stress by a factor of 2.25 the estimated fatigue life actually decrease even though the bending stress decreases.

In the book "Design of welded structures" [22], published by the Lincoln welding foundation, guidelines are given as to adapt your design to be more resistant to fatigue failure. These guidelines will be listed below and adopted to be applicable to the semi-trailer design [20].

Fatigue design rules

1 Reduce the maximum stress range. Prevent large and rapid fluctuations in stress values, e.g. remove stress raisers and stress concentration factors. The load cannot be altered to remove peak stresses in the case of semi-trailer design. The method of load distribution can however be adapted.

2 Use butt weld instead of fillet welds. Also grind critical welds smooth. Stress relieving welds have no appreciable effect on fatigue strength.

3 Where critical loading exists, orientate plate so that force is in line with rolling direction. For the I-beam neck area this would mean that the rolling directing should be vertical since the web transfer a large shear load.

4 Form member into shape it would tend to assume under loading, this would reduce flexure under loaded conditions. This might be difficult to achieve for the semi-trailer structure since the chassis is designed with a positive camber so that when it's loaded the effective displacement is zero.

5 Avoid operating near the critical resonant frequency of individual members or whole structure to avoid excessive amplitude. This is especially applicable when the trailer is operated with no payload. Much higher frequencies are generated and certain members vibrate loose instead of being broken by external forces.

6 Consider prestressing beams to reduce amplitude variation. This is the same as prestressing bolted connections. This can be achieved by welding practise, e.g. weld a beam that there is a tensile force in the top flange due to heat shrinkage. Again, this is opposing the negative camber required to cancel out loading deflection.

7 Avoid eccentric application of loads since this will cause more flexure when the load is applied.

8 Stiffeners decrease flexibility of panels and result in better fatigue strength, unless they cause an abrupt change of section. This is readily applicable to the apron plate and high rear I-beam web sections.

9 A rigid frame design of a statically indeterminate type will be better suited than a simple structure since the load is shared by other members; hence its less likely to collapse immediately if a fatigue failure starts in one member. The failure can then be repaired if a crack is spotted during maintenance

inspection. Examples of this would be to connect cross members not only by welding them to the I-beam, but also to insert gusset plates. Load will now be transferred.

10 Avoid biaxial and triaxial stresses. Stresses of this nature is created when the I-beam is loaded transversely, e.g. a cross member pressing against the web section. When a member presses against the web section the web must be supported on the opposite side to reduce the stress amplitude.

Stresses in I-beam fillet welds

The main I-beams are subjected to reasonably high levels of bending, torsion and transverse stresses. Since these beams are of a plate girder design, the top and bottom flanges are welded to the web plate with fillet welds, as shown in figure 6.1.

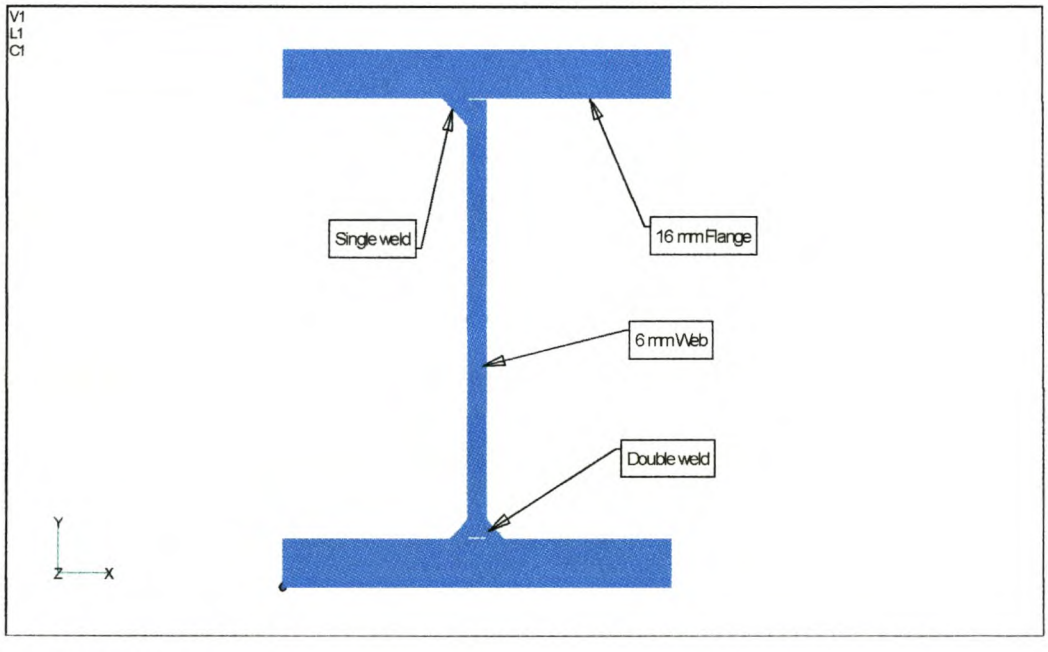

Figure 6.1: Girder type I-beam

In practice it are these welds that are the most probable location of severe failure, either due to fatigue or overloading.

The beams are welded with a semi-automated beam-welding machine. The machine only controls linear, e.g. along length of beam, velocity. When there is a taper in the

beam design the effective speed of the welding head increases to keep the linear speed constant. This effectively reduces the amount of filler wire that is deposited in the fillet weld. Failures due to this defect have been noted, especially at the drastic depth variations at the rear axle frame clearance.

The most effective and economical solution to this problem without obtaining new equipment is to reduce the taper angle. Another shortcoming of the machine is that only one side of the beam can be welded at a time. To reduce production time the other side is never welded in the machine, but only hand welded in the critical beam areas. As mentioned above the maximum allowed stress values decrease considerable if the weld is hand deposited instead of a continuous machine welded type.

Detailed finite element models of such welded assemblies were made, especially to investigate the practice of one-sided beam welding. The single sided weld was larger than the double fillets to the extent that the same amount of filler material was deposited at the top and bottom flanges. The beam was loaded in a pure bending (vertical), torsion and horizontal bending fashion. A section in the middle of the beam away from the applied loads was used for comparative analyses.

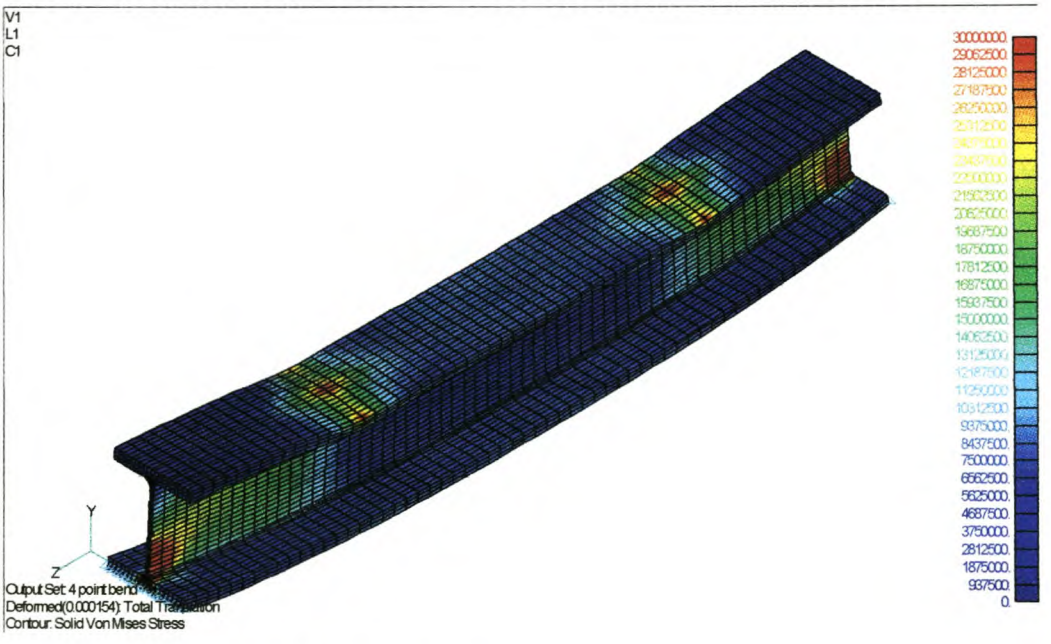

Figure 6.2: 4 Point pure bending weld test

For the pure bending case the shear stress in the single weld is noticeably higher, albeit very localized. In figure 6.3 the deformation plot clearly indicates that the beam top flange will twist, whereas for the double-sided configuration the flange stays flat. This flange buckling will lead to further high stress points where cross members connect to the main beams. Also if the close-up of the fillet weld, figure 6.4, is inspected, the high stresses at the weld inside root is visible, clearly an undesirable situation.

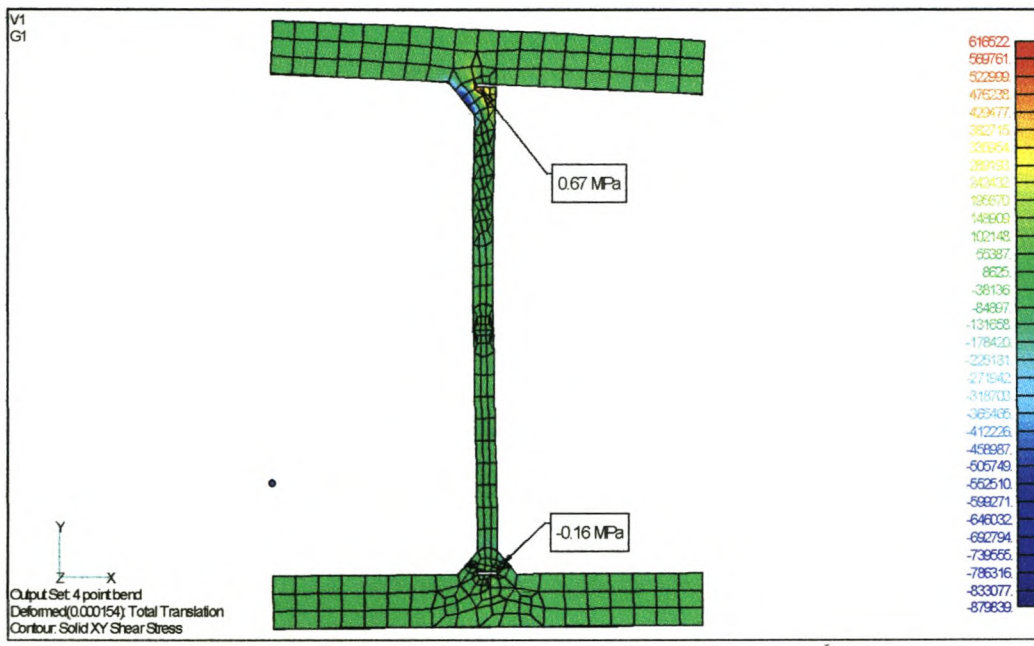

Figure 6.3: Pure bending weld comparison

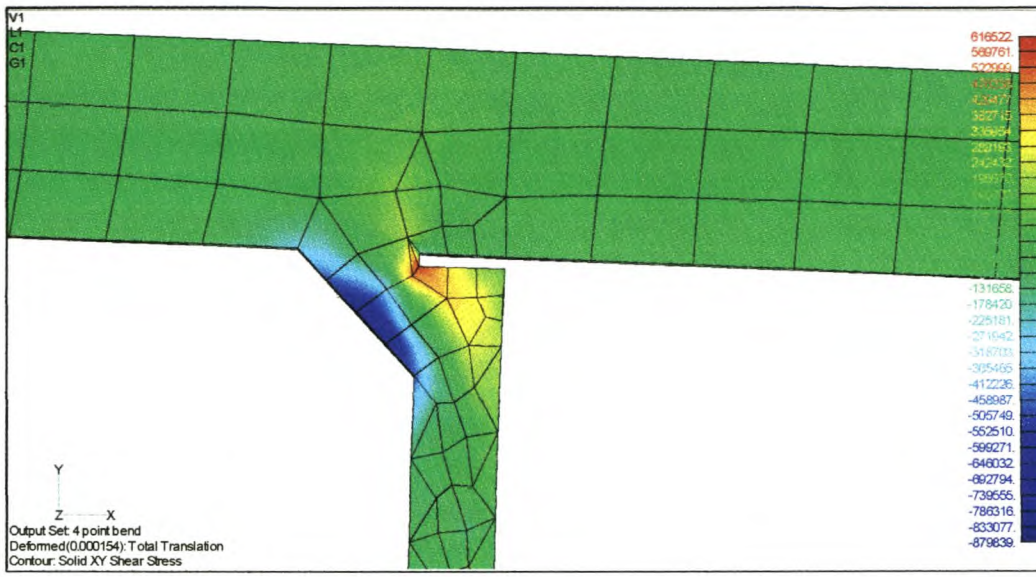

Figure 6.4: Close-up of fillet weld

For the torsion load case the one end of the beam was fixed and to the load were applied on the other end, as per figure 6.5. Again the double-sided weld is the more favourable option, but not to the same extend as for the bending test comparison.

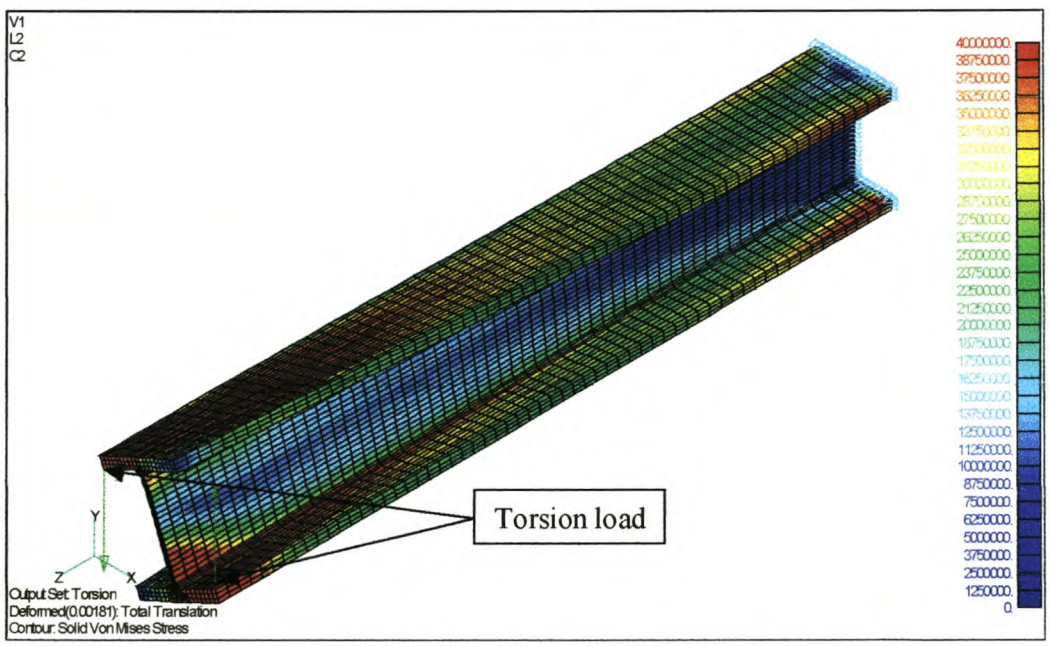

Figure 6.5: Torsion weld test beam layout

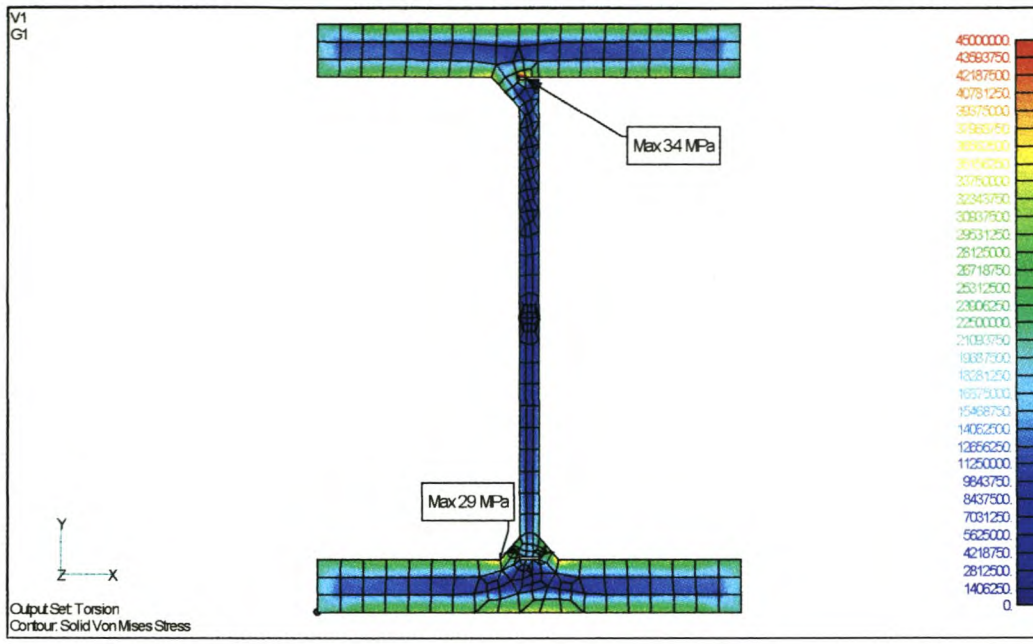

Figure 6.6: Detailed torsion stresses

For the transverse bending test the two sides of the beam were held fixed, and the transverse load applied at two equidistant locations. Again from the detailed stress contours the single weld is worse off.

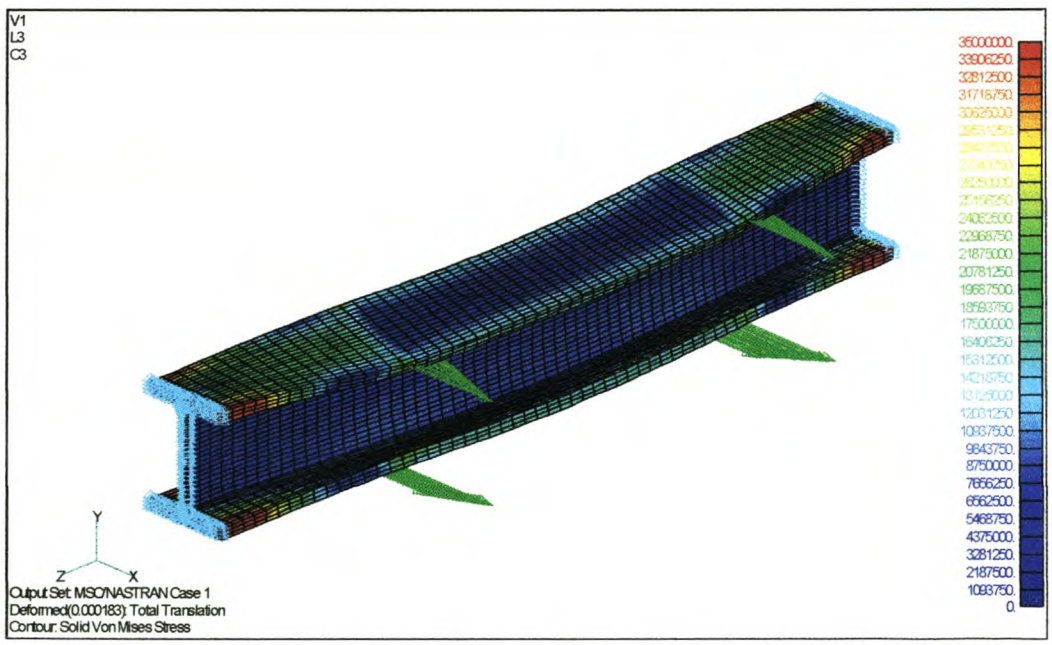

Figure 6.7: Transverse bending weld test comparison

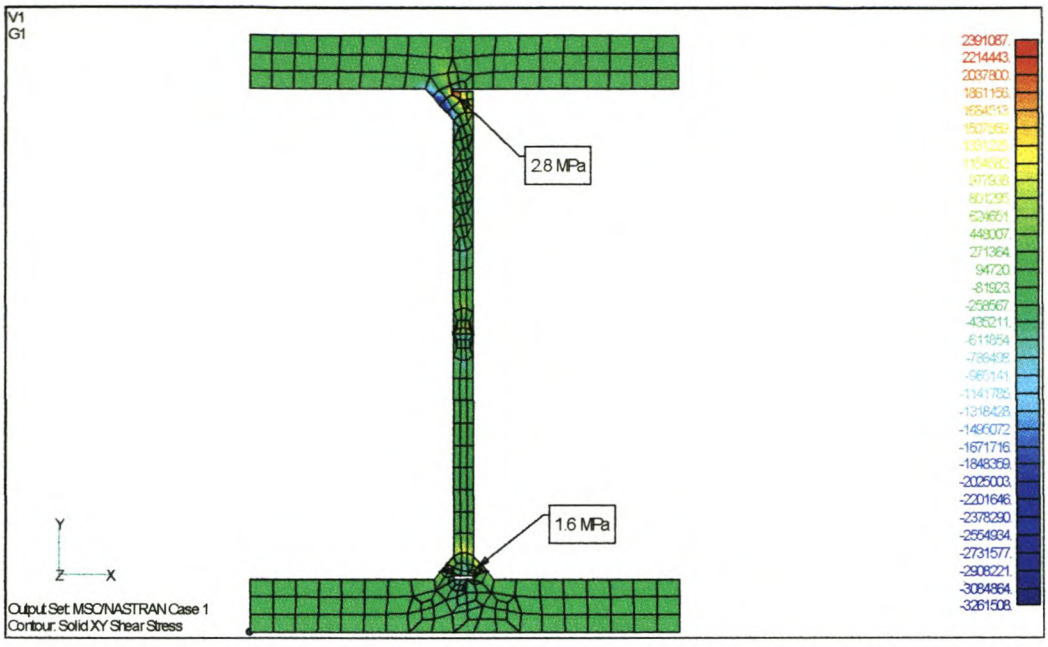

Figure 6.8: Detailed stresses for transverse bending test

Load type	Single large fillet	Double smaller fillets	%
Bending	0.67	0.16	319%
Torsion	34	29	17%
Transverse	2.8	1.6	75%

Table 6.5: Stress comparison for single and double fillet welds

Clearly the advantages from welding both sides of the I-beam are greater than the extra cost implications. This is even more the case if material weight is to be saved by reducing the I-beam flange thickness in the lower stressed areas. The mean stress can now increase since the welds are capable of transferring the shear loads.

Chapter 7: Description of Finite Element Models

A comprehensive and detailed FEA model was created as to investigate the effect of various load and constraint scenarios on the semi-trailer structure. Due to the nature of semi-trailer design, the model comprised of a large variety of different materials and structural properties. From a model creation viewpoint the complex property variation combined with the slender aspect ratio of most of these structural shapes made auto meshing rather impossible. Only in a few cases could the auto mesh function be used with success, for most of the rest manual element creation was the only viable solution. The assembled model comprised of 52 253 nodes and 69 196 elements.

For brevity it will not be attempted to discuss the creation of the model in full detail. Plots of the different sub-assemblies and some important comments will however be given as to give insight into the trailer structure and how the FEA model was created to simulate its behaviour. For most of the figures below, unless clearly visible or stated differently, the semi-trailer is seen from the curbside, e.g. driving from the viewer's right to left. This orientation is an industry standard. Colour differences are indicative of different structural properties, or occasionally different material properties.

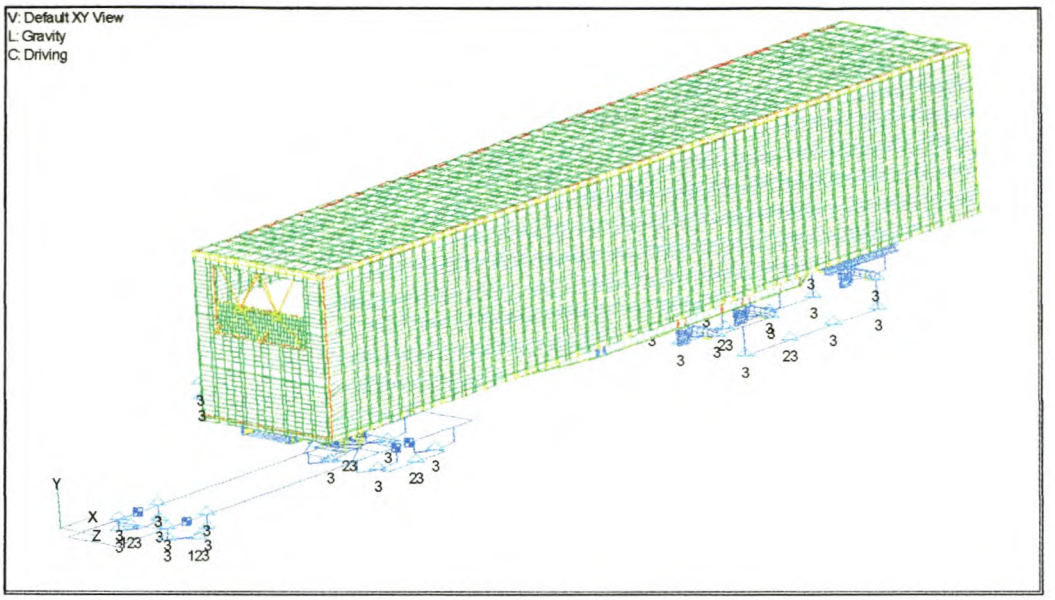

Figure 7.1: Overall FEA model of GRP semi-trailer

In figure 7.1 the complete model is shown. The truck was also included in the model as to accurately simulate the complete vehicle response to the applied loading. The truck was however only modelled with beam and spring elements, as an accurate stress distribution for the structure was not required. To correctly simulate the truck response, mass elements were included with the beam and spring elements. These were altered so that the mass properties were similar to the actual front and rear axle

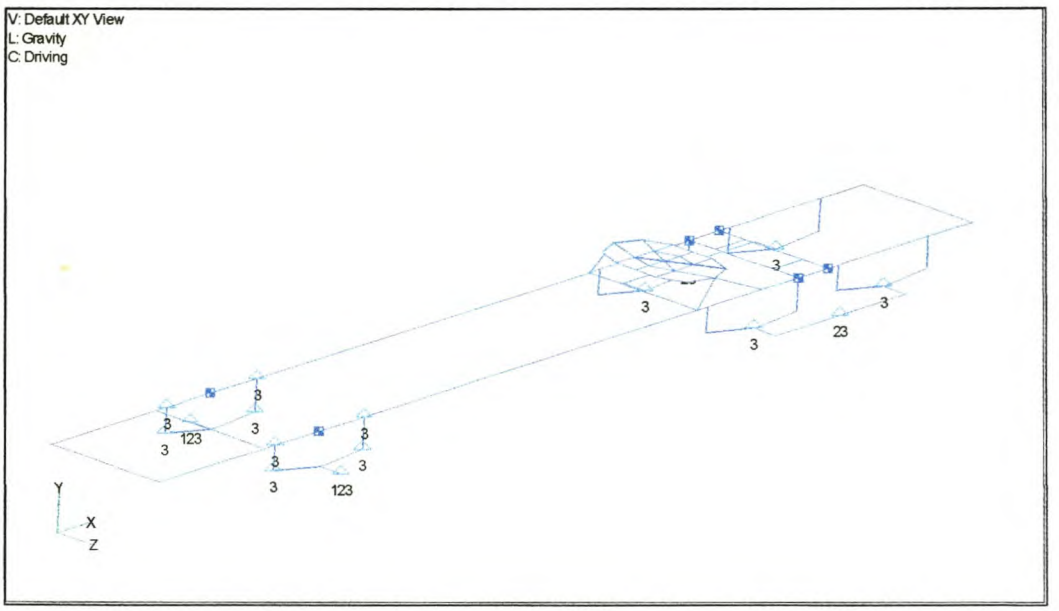

Figure 7.2: Approximate FEA model of truck

tare weights. Refer to figure 7.2. The suspension of the semi-trailer was modelled in more detail, since these members directly influence stresses within the analysed structures. Spring, beam, plate and mass elements were used to create the rear bogie. The airbag spring unit was modelled with some constant property spring elements. The full effect of air damping and shock absorbing, both having non-linear behaviour, was therefore not accurately modelled. This is not seen as a shortcoming since only quasi-static situations were modelled, and stresses within the suspension itself are not investigated. The data for the suspension stiffness were obtained form BPW, the OEM[10] supplier in Germany.

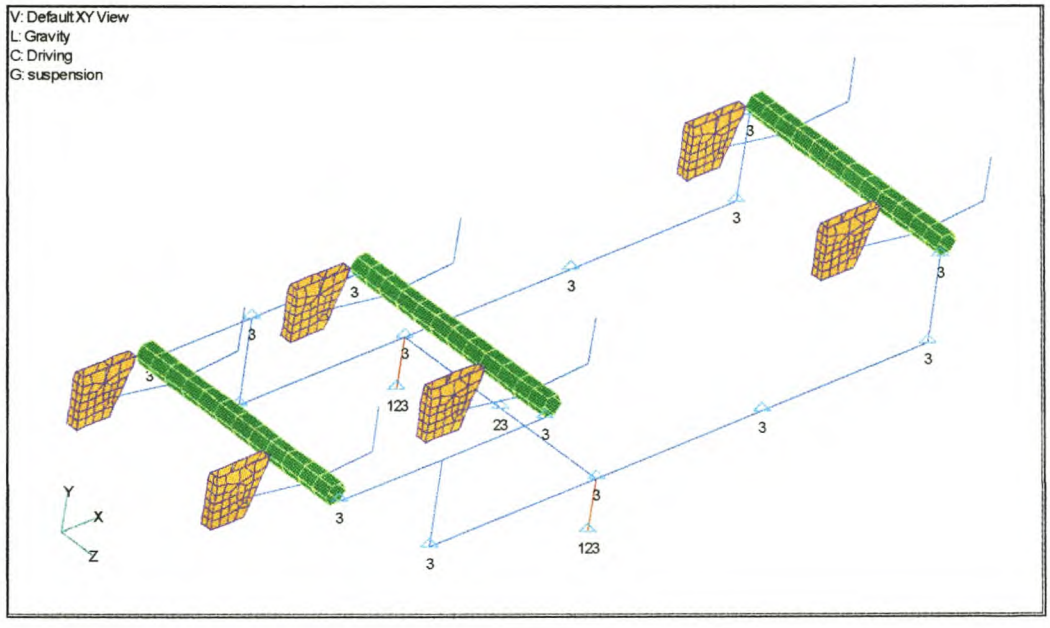

Figure 7.3: FEA model of suspension sub-assembly

As can be seen in figure 7.3 for the "driving" constraint set, the rear bogie set was allowed to move rearwards, e.g. no constraint in the axial direction but it was not allowed to move in a sideways direction. For most of the analyses the axles were located in this fashion. The airbag suspension system will always attempt to maintain the same pressure in all the bags, e.g. the load is distributed evenly among all the wheels. The complete rear bogie was supported by one point, and from this point the

[10] Original Equipment Manufacturer

support was transferred to the different axles via beam linkages. The suspension can however only transfer the load to a certain degree. To accommodate this behaviour gap elements were placed at the outer support positions. If the axle lowers more than 30 mm[11] the mechanism will lock. To analyse this, a non-linear analysis is necessary, one such an analysis was done. From this it was evident that this locking is not present.

The steel chassis were also modelled in detail, since failures in this structure are of a critical nature. This structure is also a candidate for weight reduction due to the high density of the steel used. As can be seen in figure 7.4 the chassis is constructed from a large variety of different steels and plate thickness.

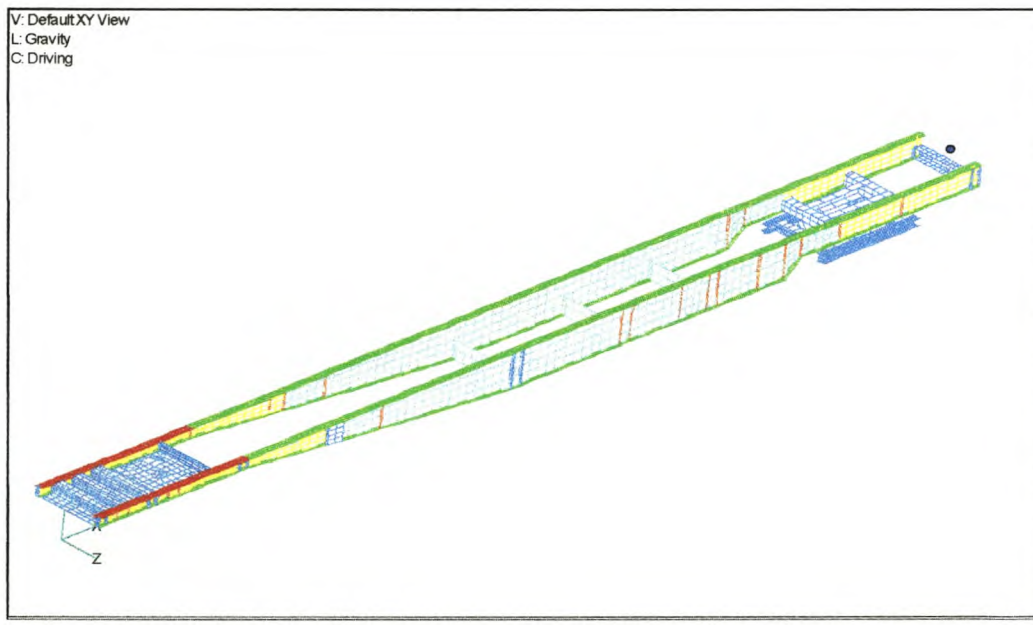

Figure 7.4: GRP chassis assembly FEA model

Welding was not built into the overall FEA model due to the large differences in the element size ratios, which would either lead to foolishly large or highly inaccurate modelling. Where deemed necessary detailed models of certain welding interfaces were created in separate models. For the chassis assembly the steering mechanism

[11] Value obtained from D. van de Wall, BPW S.A. applications engineer

was not included in the structural model. The rear axle and steering arrangement were such that straight line driving was modelled.

The GRP box section was the most complex part of the model to create. The panels each comprised of different layers, each layer with completely different material properties. Also inside the panel lay-ups various wood and steel inserts are included for structural strength. These had to be included in the model, as they will definitely influence overall stresses. Observed failures were mostly near these structural inserts, so care had to be taken as to ensure that the FEA modelled, was representative of the actual construction.

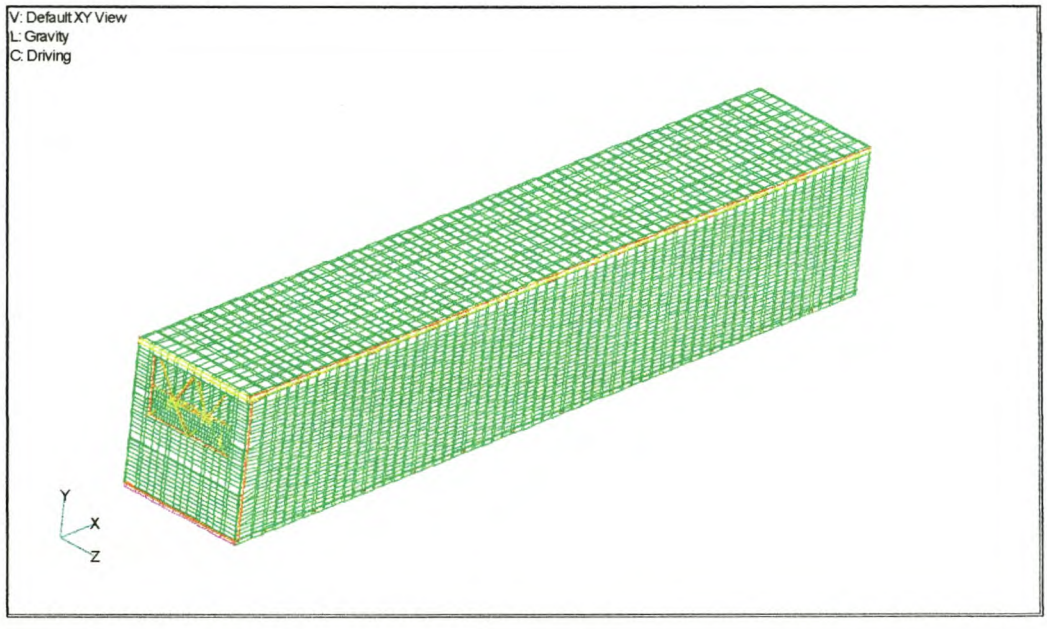

Figure 7.5: Box section of GRP semi-trailer FEA model

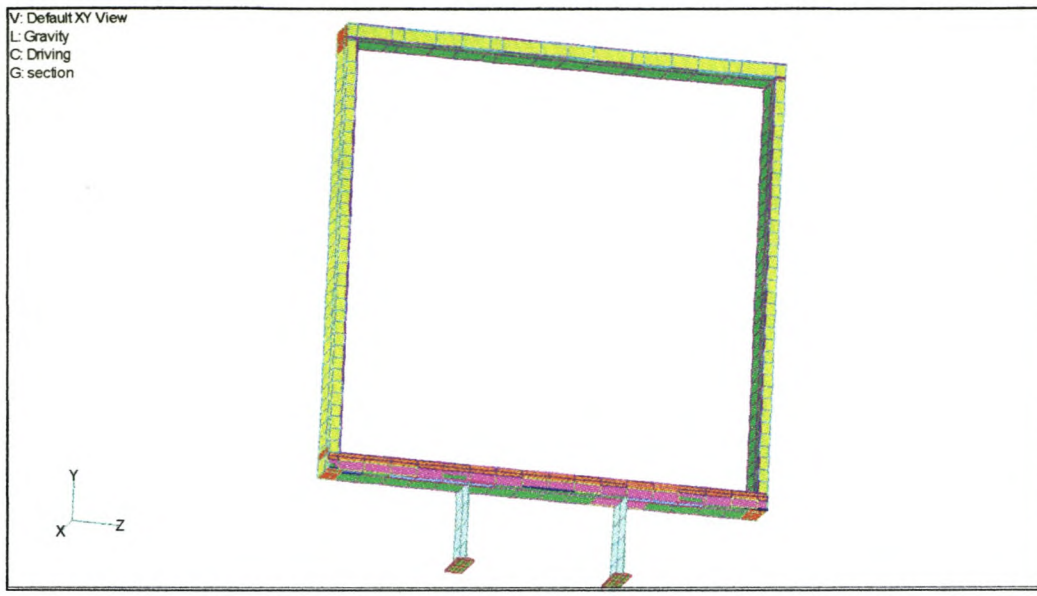

Figure 7.6: Section through GRP semi-trailer

Figure 7.5 is a complete GRP assembly and figure 7.6 is a section through the semi-trailer near its mid section. For this model most of the elements are not clearly visible since they are below the outer plate elements or they are too thin with regard to the thicker solid elements. As described in the manufacturing chapter the GRP box is assembled form six different sub-assemblies, e.g. the floor, bulkhead, sides, roof, doorframe and also the rear doors. They are assembled in the order as given above. A representative figure for each of these sub-assemblies is given. For clarity purposes some of the layers were omitted in some of the figures.

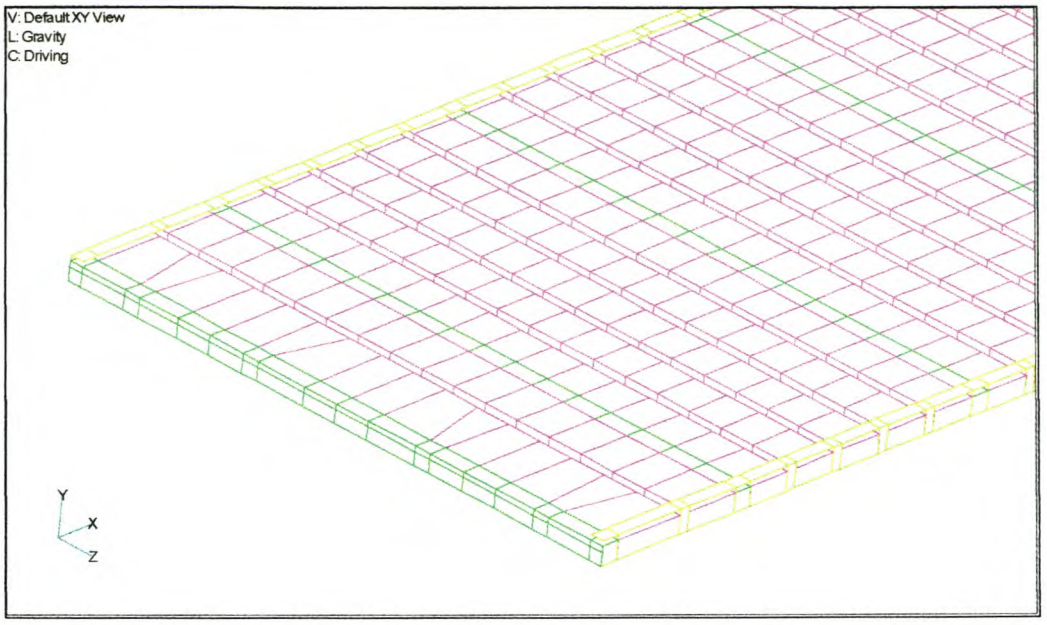

Figure 7.7: Floor FEA model

For figure 7.7 the upper CSM layer, wood layer and interior wood beams were not plotted. The purple indicates the 80 $kg.m^{-3}$ polyurethane foam inserts. The dark green elements are representative of a rigid floor beam. The pale green side beams are the folded steel inserts. The floor was also analysed in a separate model to investigate forklift loading in more detail.

The bulkhead section includes the bulkhead protector constructed of CSM and wood, which protect the actual bulkhead from damage inflicted during loading/offloading of the payload. With the outside skin removed the interior wood beams are clearly visible. The refrigeration unit were modelled as beam and mass elements, not shown in figure 7.8, but visible in figure 7.1.

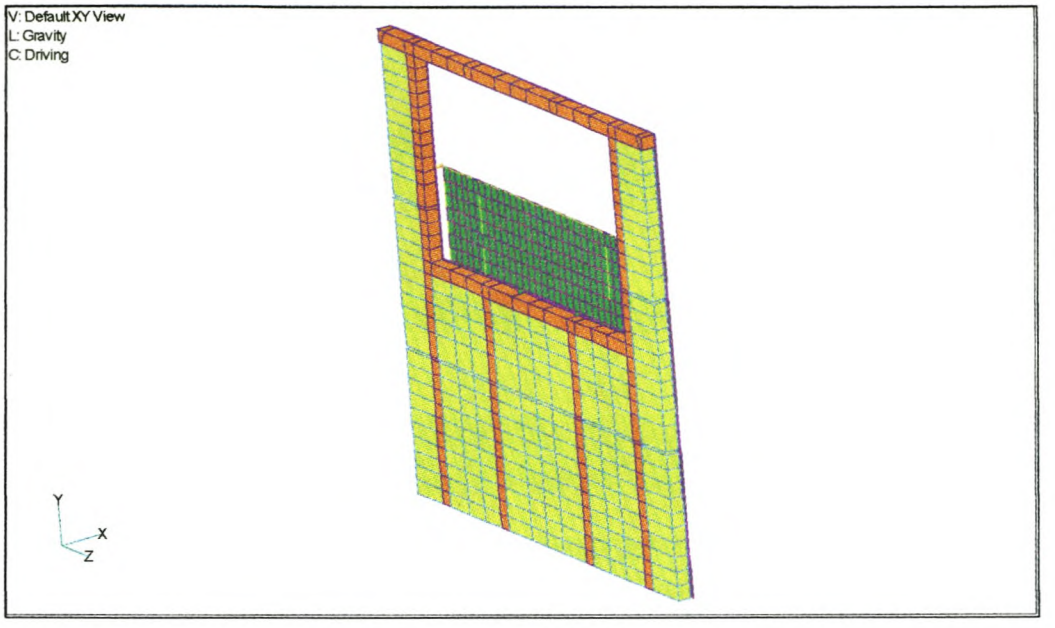

Figure 7.8: Bulkhead section of GRP semi-trailer

The side panel comprises of a 2×450 CSM, 40 kg.m^{-3} PU foam, 6 mm laminated pine and a 2×300 CSM layer as seen from the out- to the inside. The wood and foam elements were modelled as solid elements whereas the CSM layers were idealized with plate elements. This construction is typical for the GRP panels. The interior wood layer is inserted to give the panel more penetration strength.

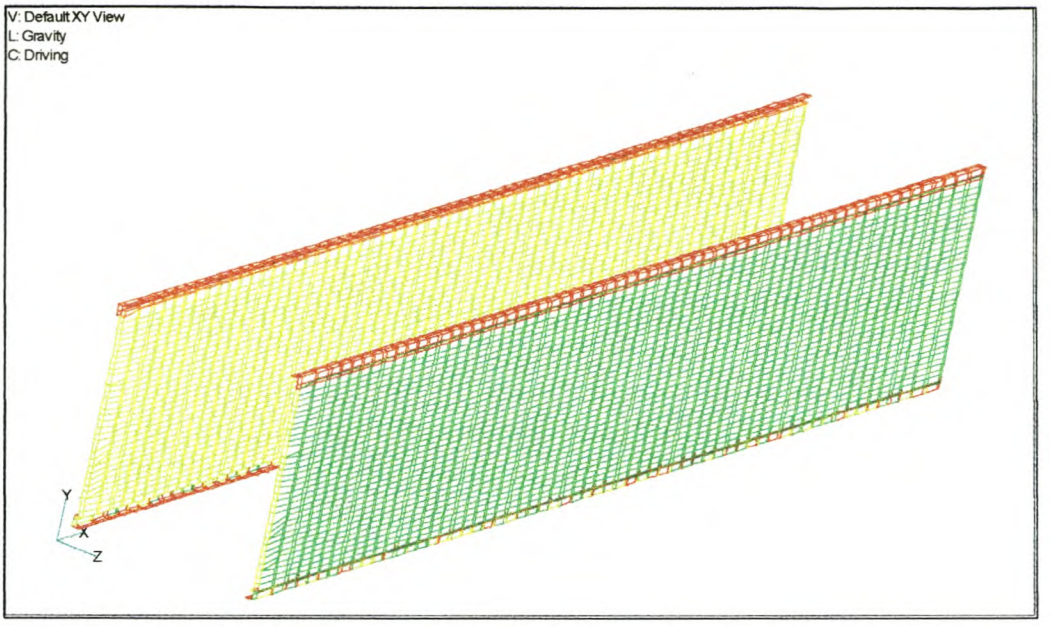

Figure 7.9: GRP semi-trailer side panels

In figure 7.9 the aluminium corner capping (red) is also visible. The bottom half doesn't seem continuous, this is however only a plotting algorithm phenomenon. Not visible in figure 7.9 is the internal Z-sections. These Z-sections are made of CSM laminated in-between the PU foam slabs. The effectiveness of these sections were also analysed in a separate model.

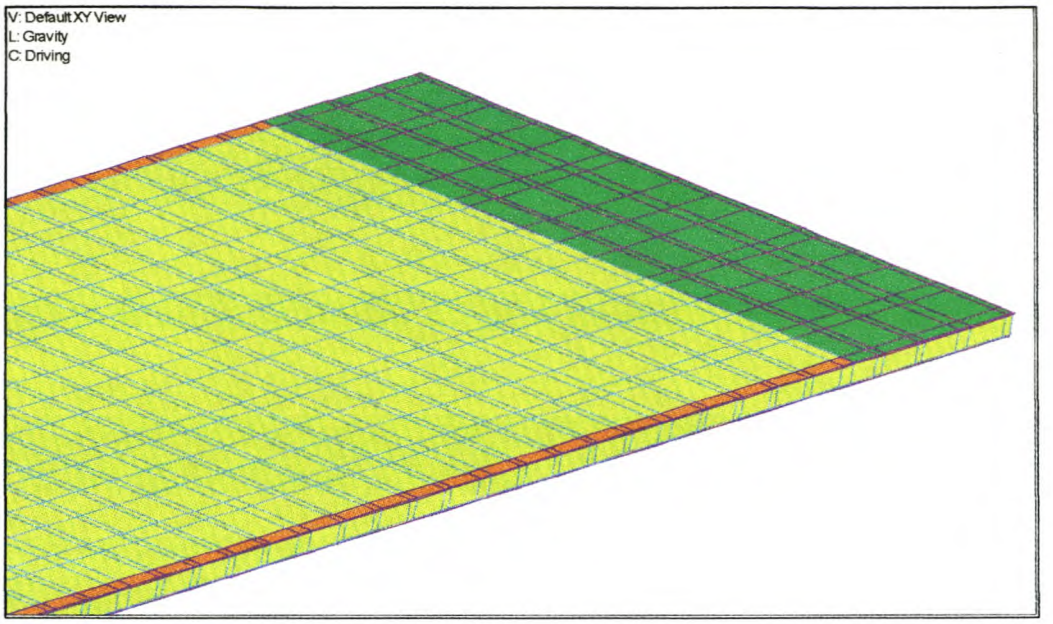

Figure 7.10: GRP Roof panel FEA model

In figure 7.10 the rear section of the roof panel is shown. The upper CSM layer is only shown for the last metre. The construction of the roof panel is similar to the side panels, with the Z-sections and wood layer omitted.

The rear doorframe is constructed of 3CR12 corrosion resistant steel. The bottom sill plate was also included in the FEA model. The door panels themselves were omitted in the structural analyses, as rather flexible sealing rubbers, which will isolate them structurally from the rest of the structure, surround them. Also the hinges do allow for some play and the forces won't be transferred easily into the door panels. For the thermal analysis the doors were included as a single panel with the same composition as the two separate door panels. The weight influence of the two door panels were assumed negligible.

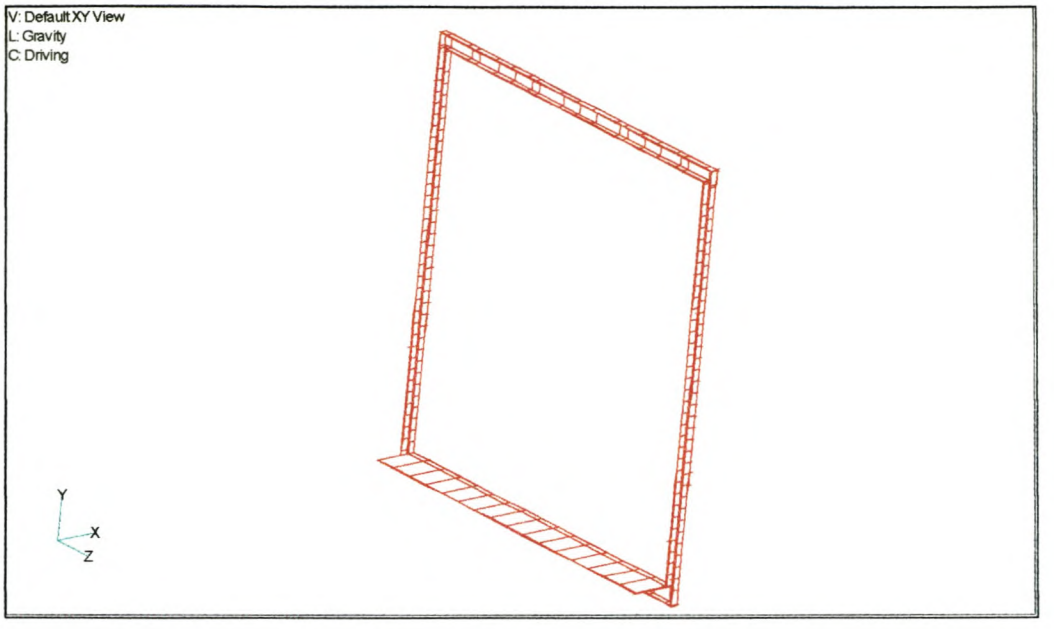

Figure 7.11: Rear doorframe for GRP semi-trailer

The payload was also included in the FEA model. Not for strength properties, but as to accurately simulate mass properties. For the analyses a 30 000 kg payload was inserted into the semi-trailer. The stiffness of the payload was 5 $GN.m^{-2}$, and its thermal properties were taken to be similar to that of apples. From figure 7.12 it can be seen that rather than been spaced uniformly through the length, it was placed as close as possible to 1×1 m pallet sizes while still connecting to floor nodes. It was also assumed that the payload is only standing on the floor, and has not toppled over.

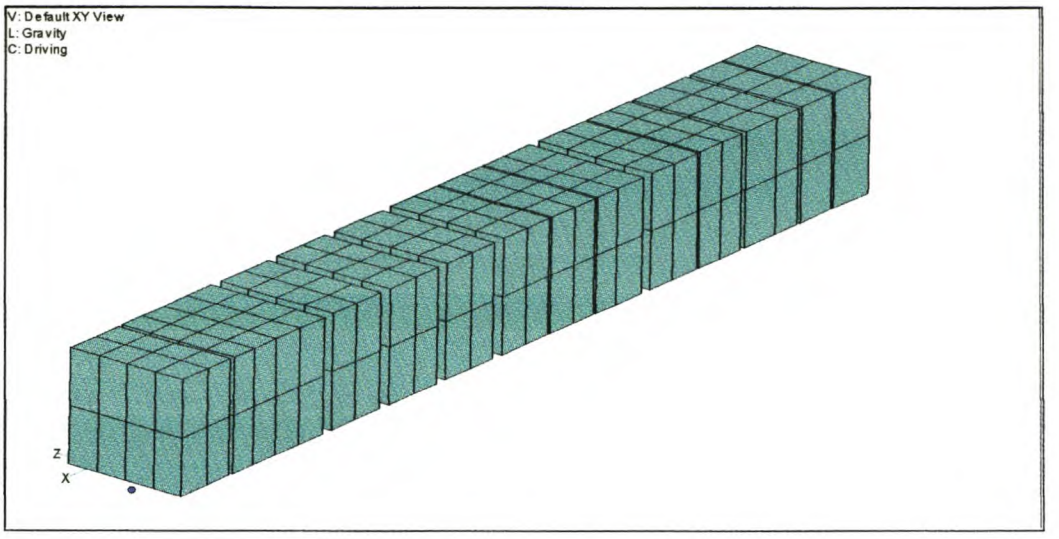

Figure 7.12: FEA model of cargo inside GRP semi-trailer

Material properties

A large number of different materials are used in semi-trailer manufacturing. Especially for the refrigerated box section the material properties vary considerably. To accurately analyse the structure, care had to be taken to ensure that the material properties resembled the materials as used and manufactured in-house by Busaf. Various literature sources were used to obtain the engineering material properties as listed in tables 7.1 and 7.2. The particular source of the data is included as footnotes below the table.

If the material properties were not readily available, or if it was suspected that actual properties may vary from the stated values, experimental verification was conducted. In appendixes C, D and E the experimental procedure and results for respectively polyurethane foam, wood and glass are given.

To use more convenient analysis methods all the materials were assumed to be isotropic and linear. For materials such as wood the weakest, or experimentally estimated aggregate values were used.

Description	Tensile Ultimate[12] [MPa]	Tensile Yield [MPa]	Young's Mod. [MN.mm^{-2}]	Poisson's Ratio	Density [kg.m^{-3}]	Thermal Expansion deg. C. 10^{-6}	Thermal[13] Conductance W/mK	Cost Index[14]	Comment
30 Oak	618	463	210	0.3	7850	11	45	1.11	*Common flange material*
Supraform TM 380	450	380	200	0.3	7850	11	45	1.26	*Use for suspension members, X-members*
Supraform TM 420	490	420	200	0.3	7850	11	45	~	*Not used commonly*
300 WA	450	300	200	0.3	7850	11	45	1.00	*Commonly used*
300 WC	450	300	200	0.3	7850	11	45	1.10	*Improved brittle fracture resistance*
Com Quality[15]	~	(230)	200	0.3	7850	11	45	0.8	*Used for non-structural members*
BS4360-50 A	490	345	210	0.3	7850	11	45	1.2	
BS4360-50 B	490	335	210	0.3	7850	11	45	1.2	*Used for apron plates, suspension members*
BS4360-50 C	490	355	210	0.3	7850	11	45	1.2	
ROQ-Tuff	852	791	224	0.3	7850	11	45	2.5	*Occasionally used for beams flanges*
ROQ-Last	1095	739	211	0.3	7850	11	45	~	*High wear resistance*
Alum 5454[16]	220	125[17]	70	0.33	2670	24	45	~	*Used for high strength aluminium applications*
BS4360-43A/B/C	430	275	200	0.3	7850	11	45	1.01	*Used frequently for small parts*
Domex – 690 XP[18]	750	690	210	0.3	7850	11	45	~	*Good forming, high strength*
Corten	480	345	210	0.3	7850	11	45	1.18	*Fair corrosion resistance*
3CR12[19]	530	380	200	0.3	7700	9	23	2.25	*Good corrosion resistance*
Stainless 304[8]	600	310	195	0.3	7900	17	15.7	4.1	*Excellent corrosion resistance*

Table 7.13: Engineering material properties for metallic materials

12 Unless otherwise stated material properties obtained from **ISCOR** material data sheets.
13 Standard value obtained from **Heat Transfer**, J.P. Holman, 7th ed, 1992.
14 300WA used as base index.
15 Properties not guaranteed.
16 Data obtained from, **Strength of Aluminium**, Alcan Canada Products Limited, 5th ed, 1983.
17 For Al. 545 Shear yield = 75 MPa, Bearing ultimate 440 MPa.
18 Data obtained from, **Sheet Steel Handbook**, SSAB Tunnplåt AB, 2nd ed, 1996.
19 Data obtained from, **Pocket guide to stainless steel & 3CR12**, Middelburg Steel and Alloys.

Description	Thickness [mm]	Tensile Ultimate [MPa]	Tensile Modulus [GN.mm^{-2}]	Compress. Strength [MPa]	Compression Modulus [GN.mm^{-2}]	Shear Ultimate [MPa]	Shear Modulus [GN.mm^{-2}]	Poisson's Ratio	Density [kg.m^{-3}]	Water Absorption Max%	Thermal Expansion K. 10^{-6}	Thermal Conductance W/m.K
2x300 CSM + 0.6 Gelcoat[20]	2.1	63-140	2.5				2.8-3.0		1200		22-36	0.24-0.28
2x450 CSM + 0.6 Gelcoat	3.0	63-140	2.2				2.8-3.0		1125		22-36	0.24-0.28
2x450 WR+ 0.6 Gelcoat	3.0	84	2.5				3.0-3.5		1500		11-16	0.7-0.31
CSM Only	Various	100	8	150				0.26	1400		30	0.2
WROnly	Various	250	15	150				0.26	1600		15	0.24
Gelcoat	0.6					7			1100			
Resin Bond[21]	Various	70	3.5						1280	0.2	100	0.2
Pekay Polystyrene Adhesive[22]	Various					8						
Sikadur 31 Epoxy Adhesive	Various											
Pultrusion - Roving[23]	Various	689	41.4	414				0.26	2020	0.25	5.2	
Pultrusion – Mat[24]	Various	207(45)	15.9(5.5)	1389(69)	15.9(5.5)	31(31)			1650	0.7	5.2	
Corematt XX4 – Core only	1/2/3/4/5	2.3	0.350	7	0.200	2.5	0.050		550-750			
Corematt + 2x450 CSMx2	9.2	45.4	3.79						9.0			
Polyurethane 40[25]	Various	0.134		0.259	0.005	0.172	0.0015		40	0.3	80	0.0301
Polyurethane 80	Various			0.741	0.051				80			
Polystyrene[26]	Various	0.140		0.3					35	1.0	70	0.25 (5 years)
Ply	Various	31	9.3	36		6.2(1.9)	0.7				6.1	
Wood Douglas Fir	Various	130(2.3)	13.7	50(6.0)		8.2			480		3.7(15.8)	0.12
Wood Phenol	Various	60	11(2.2)						470			
Balsa	Various		2.86	8		1.1			140			

Table 7.14: Engineering material properties for non-metallic materials

---

20 Values obtained from experimental measurements and **Crystic Polyester Handbook**, Scott Bader, 1994.
21 Typical values obtained from, **Crystic Polyester Handbook**, Scott Bader, 1994.
22 From Pekay Chemicals (PTY) Ltd. Shawn Doyle
23 Values obtained from Composite Profiles cc. **CP Design Guide**
24 Values in brackets ( ) indicate material properties in transverse direction, where applicable.
25 Data obtained from **Linpac Insulation Products** report, 26 April 1995. Ref. DSA-015. Also www.Matweb.com, Baydur polyurethane. Experimental analyses were also used.
26 Specifically, **ISOBOARD RF**, values from product catalogue.

Load and Constraints Cases

As mentioned before, different load cases were analysed to investigate structural behaviour under various driving and load conditions. In table 7.3 the loads as applied to the complete model are listed. Suggestion of load sets 1 to 7 and 9 were obtained from "Analysis of commercial vehicle structures", H.J. Beermann, 1998[12]. The actual loading data was obtained from various other sources as described below.

No.	Analysis description	Constrain set
1	Static load, full payload	Driving
2	Braking	Inertia relieve
3	Axial deceleration	Driving
4	Transverse acceleration	Driving
5	Torsion	Driving Special
6	King pin shock	Inertia relieve
7	Bogie shock	Inertia relieve
8	King pin load	Parked
9	Asymmetrical longitudinal braking	Inertia relieve
10	Asymmetrical payload	Driving
11	Forklift	Parked 1
12	Wind loading	Driving

Table 7.15: Load sets for complete vehicle analysis

Static load

The static load scenario is the situation the semi-trailer would probably experience to a slightly lesser or greater extent for ninety plus percent of its life. The total payload was assumed to be equal to 30 000 kg, distributed over the length of the refrigerated cargo area. This will render the vehicle combination slightly overloaded, but it will definitely arise in normal operational conditions.

Braking

SABS regulations SV 1051: Braking, Part 1 states that for a category O_4 vehicle, e.g. trailers having a maximum mass of more that 10 t, the minimum attainable braking force shall not be less than 45% of the weight borne by the wheels of the semi-trailer. For this analysis this weight was taken to be equal to the maximum legal rear bogie weight plus the five percent overload tolerance allowed, e.g. 25 200 kg. This load was

applied at the axle hub positions, and will effectively be transferred to the chassis via the axle hanger brackets. Also this load will cause a bending moment on the suspension assembly. This moment of 9.92 kNm per wheel set was calculated by multiplying the wheel radius (0.535 m) with the brake force at road surface (18.54 kN). The moment was applied at the hub position. For this analysis the inertia relieve constraint method was used to simulate the force resisting vehicle momentum. Also from SV 1051 the maximum thrust on the trailer coupling mechanism shall not be greater than 0.06 G_A, where G_A is the maximum allowed weight of the trailer, e.g. 39 000 kg. This is a force of 2 340 kg, which was applied as a compressive force at the king pin location in the same analysis as the above tensile axle loads. This force is generated when the truck applies it brakes before the trailer, and the trailer actually pushes the truck forward. This is a highly unsafe situation since the vehicle can easily jack-knife[27].

Axial and transverse acceleration

For the axial deceleration load case, the driving constraint set was used. This analysis simulates structural integrity in an accident situation. Based on SABS 1398:1994, "Road tank vehicles for petroleum-based flammable liquids", this deceleration value was taken as 1g. The SABS specifications actually advise 2g deceleration, but this value seems a bit severe for GRP semi-trailers. In the cornering load case a similar approach was followed with a 0.5 g transverse acceleration body load.

27 Situation when the tractor is at an angle of more than 90 degrees relative to the semi-trailer direction of travel. At moderate to high speed this will cause definite damage or even a severe accident.

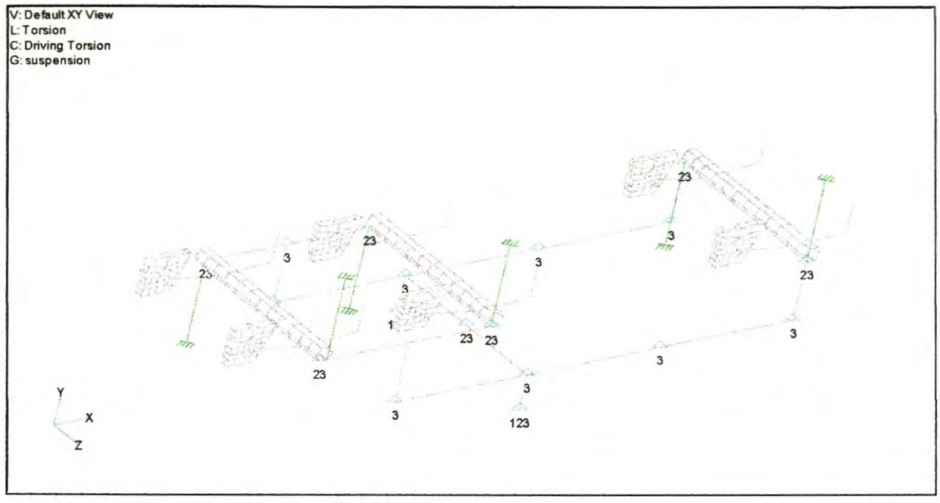

Figure 7.13: Torsion loading of rear bogie

Torsion

To investigate the semi-trailer's behaviour for severe torsional loading, displacement loads were applied at the axle hub positions. The truck bogie was twisted such that the left side was forced 50 mm downward while the right side was twisted upward with the same amount. The semi-trailer bogie was twisted to the same extent in the opposite direction. This load case is rather severe, and it is not believed that the chassis will be twisted to this extent in a continuous static situation. This analysis does however give insight into the general torsional behaviour of the semi-trailer structure.

King pin and bogie shock

While using the inertia relieve constraint set, an additional 1 g shock load was applied quasi-static at the front king pin position and rear bogie in two separate analyses. The maximum allowed bogie (25 200 kg) and king pin loads (16 000 kg) were used as the 1 g basis. This will simulate severe overloading in events like pothole impact and the like. The results of this analysis were added linearly to the gravity load case.

King pin tension load

Analysis 8 simulates the event when the semi-trailer's park brake is applied, and the truck pulls the semi-trailer forward. Assuming the truck can exert enough pull the maximum load will be equivalent to the brake resistance force. The maximum

coefficient of friction for tyres is estimated at 0.6. This will produce a force of 148 kN applied at the king pin location while the wheels are held in place.

Asymmetrical longitudinal braking

If only one side of the brakes is activated the semi-trailer will experience a transverse bending moment. The braking load was taken at 45% of half of the effective vertical weight, as per load case two.

Asymmetrical payload

The effect of unsymmetrical payload placement was investigated in analysis 10. The payload was placed with a 160 mm offset. This will induce a bending moment of 47 kNm along the semi-trailer's longitudinal axis.

Forklift manoeuvring

The effect of forklift manoeuvring inside the GRP box was also investigated. The forklift data was obtained from Kymmene Schauman Wood, a German vehicle component manufacturer. The data is according to the experimental testing as set out in the CEB 283 procedure [11]. The data is summarised in table 7.4.

Forklift axle load	5 460 kg
Axle track width	760 mm
Wheel foot print	180×80 mm
Effective pressure	1.86 MPa

Table 7.2: Forklift data used for floor FEA investigation

Side wind pressure

Following SABS 0160-1989 procedures, a strong transverse wind loading was applied as an 1100 $N.m^{-2}$ pressure load on one side of the GRP box. No negative / wake pressure was applied on the other side since this drag effect is believed negligible.

For the smaller sub assembly analyses the loads were applied as to represent apparent loading as what would be induced by the above analyses. The sub assembly analyses were used to economically compare different designs or concepts as to obtain a general view of stresses. The load cases for these analyses will not be summarised at this point, but will be explained when referred to and when deemed necessary.

Chapter 8: Analyses Result Discussion

After the FEA model was loaded and constrained in the correct fashion the strain and stress solution was obtained. Each load case took approximately two hours to analyse on an Intel PIII-500 machine with 394 MB of memory and SCSI hard drives swapping 25.883 GB of data, solving the 272 675 simultaneous equations.

After an analysis is completed, the first step is to validate the results. The most effective way to evaluate the data is to study the general displacement shape and values. It is not easy to visualize and quantify apparent stress distributions and values within a structure even if the applied loading is known. Displacement is however something you can develop an intuitive feeling for, and if the displaced shape and values do not seem acceptable, the resulting correctness is queried and the analysis parameters reconsidered.

The overall structure is divided into its logical sub-assemblies, e.g. the chassis and refrigerated box section for ease of interpretation. Where necessary the chassis and GRP section is in turn divided into their respective sub-components

To effectively visualise structural response on account of the applied loading, stress contour plots for various structures are included. Discussions will be included with the relevant contour plots. Unless stated otherwise the stress values are in Pa, with dark blue indicating the lowest stress value, and bright red the highest average elemental stress. The highest legend value is not always representative of the highest stress present; in some instances the legend scale is changed to suit visual interpretation. Unless stated otherwise the von Mises equivalent stress criteria is plotted as the default stress contour. The particular stress component is indicated in the lower left corner of the plot, whereas applied load and constraint cases are indicated in the upper left corner.

Analysis 1– Gravity

As mentioned in chapter 7 this is the stress distribution the semi-trailer will experience for most of its lifetime. This simulates the standard driving condition and the only loading is a one g vertical accelerating of -9.81 $m.s^{-2}$.

From the analysis results the vehicle weight distribution is as shown in the table 8.1 below. The weight distribution is not ideal from a legal viewpoint, but for this stress analysis it is realistic enough.

Weight Point	Load [kg]
Truck Front	7 716
Truck Bogie	17 401
Trailer Axle 1	9 153
Trailer Axle 2	9 153
Trailer Axle 3	8 573
Trailer Bogie	26 879
GCM	51 996

Table 8.1: Weight distribution

The mid-span of the semi-trailer deflects with approximately 17.4 mm. This displacement is the suspension deflection combined with structural deflection. The rear suspension lowered with 14.6 mm and the king pin with 10.7 mm. Hence the semi-trailer deflects with about 3 mm. In figure 1 the chassis deformation is plotted. From this deflection data it can be concluded that the structure is rather stiff in bending, considering that it deflects only 3 mm for the 30 tonnes it carries.

The maximum chassis stress clearly occurs in the neck area. In figure 8.2 the stress distribution for this area is shown. To make the model conservative the slewing ring assembly was omitted, only the 12 mm apron plate was modelled with the rear reinforcing plate in place.

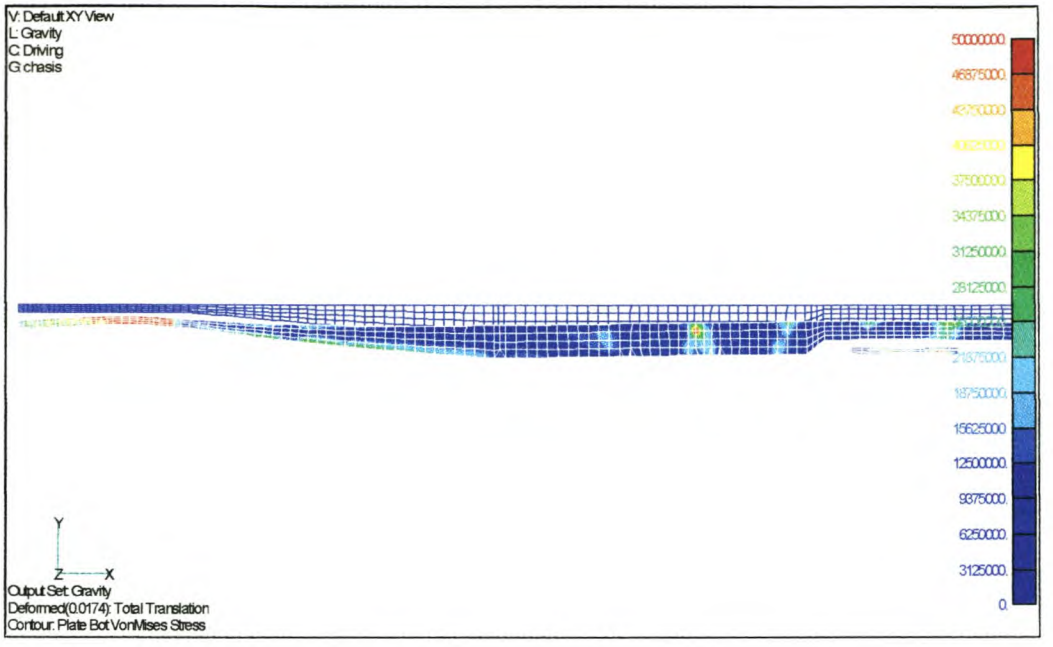

Figure 8.1: Chassis stresses and deflection for gravity load case

As is indicated in figure 8.2 the maximum upper flange stress is in the order of 105 MPa and in the lower flange it is 128 MPa. Considering that the 30 Oak material does have a yield strength of 461 MPa, these stress values are not excessively high. In the web the stress rise to about 150 MPa. This might lead to long term welding

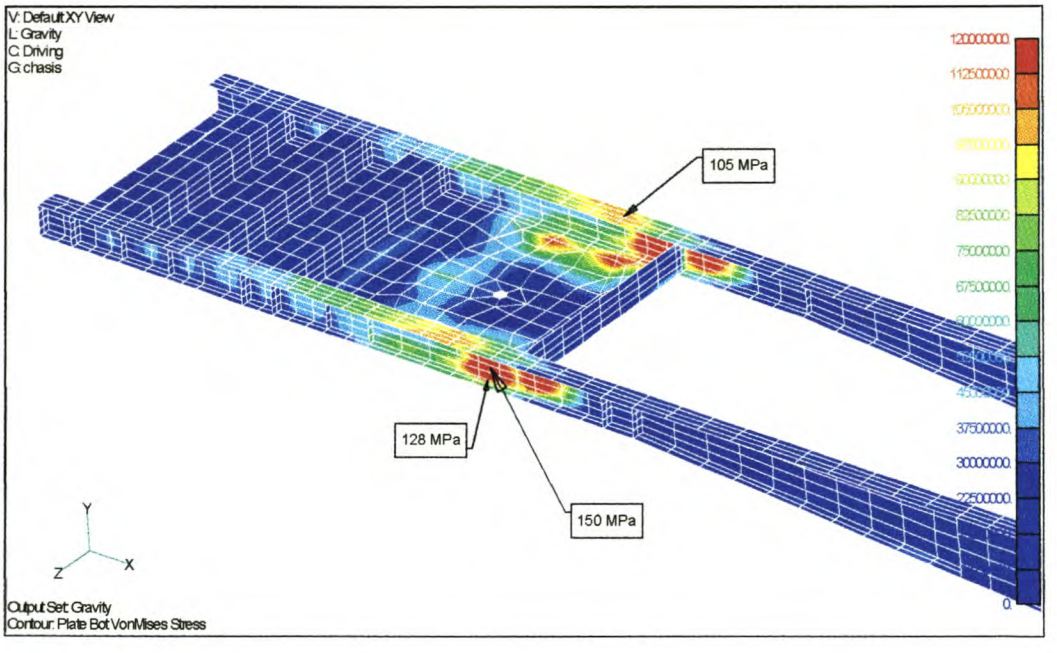

Figure 8.2: Neck stresses for gravity load case

failures, especially if other load cases also induce stresses in this area. The web is welded to the flanges with fillet welds, and these are not capable of transferring these high stresses. Fortunately the stress does reduce a little from the web centre to the outer welded connection. The effective stress is about 110 MPa at the weld interface, as can be seen in figure 8.3.

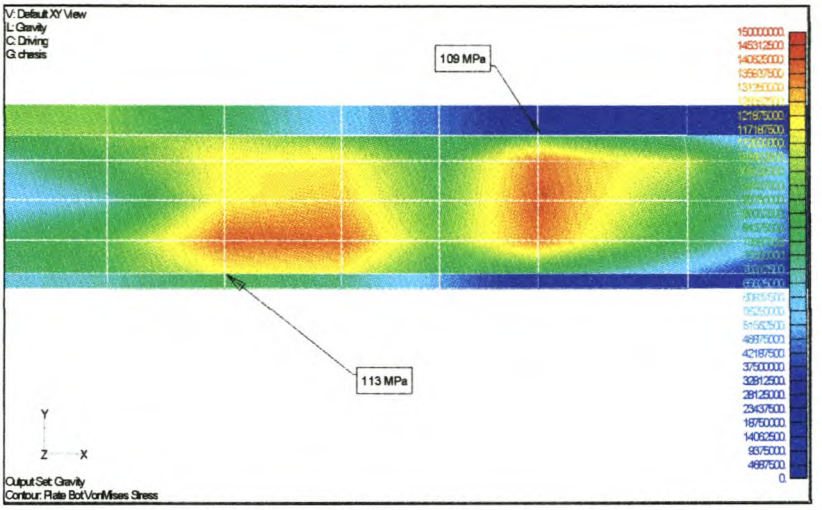

Figure 8.3: Side view of neck area, von Mises stress contour plot

As expected the stresses are due to the high shear stress in this vicinity, as indicated in figure 8.4. The best way to decrease the stress would therefore be to increase the web thickness; extra flange material would not be so effective since the web section are the predominant shear carrying member.

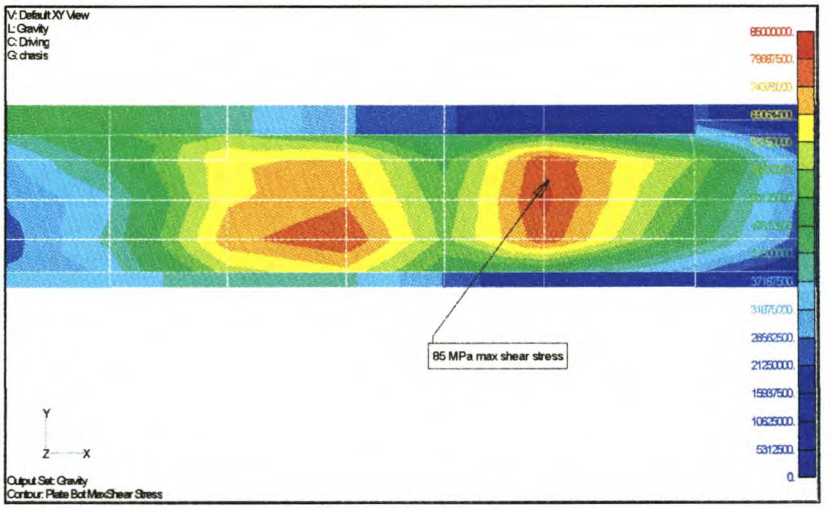

Figure 8.4: Maximum shear stress in neck area

Adequate stiffeners in this area would also help reduce the stress effectively. The remainder of the stresses within the chassis construction are acceptable, and even tend to be on the too low side. If only this bending load is considered the rear chassis is over designed and the beams can be made of a lighter construction. It is however premature to make assumptions based only on this one load case.

The stresses within the GRP box are distributed as would be logically expected. The highest stress is just behind the king pin support and then transferred to the rear bogie support. This tendency can be seen in figure 8.5. The upper roof and corner capping

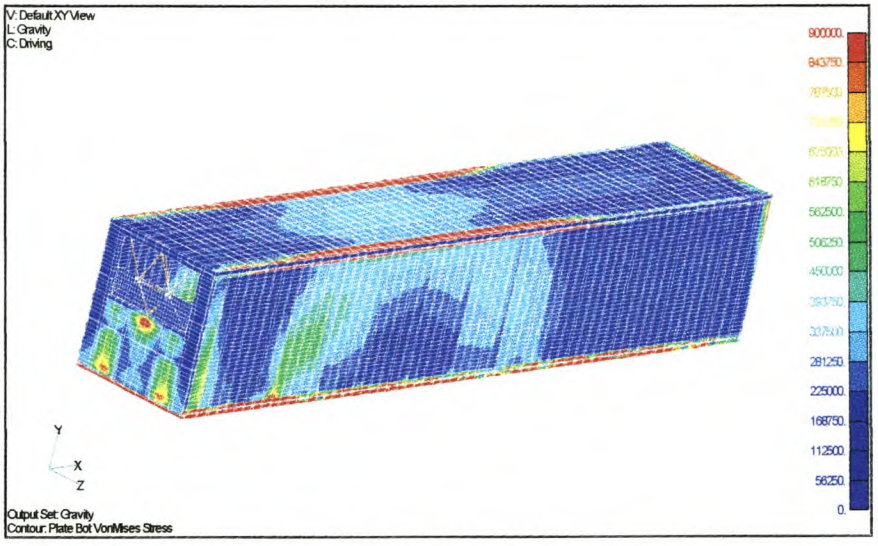

Figure 8.5: Stress distribution through GRP box section

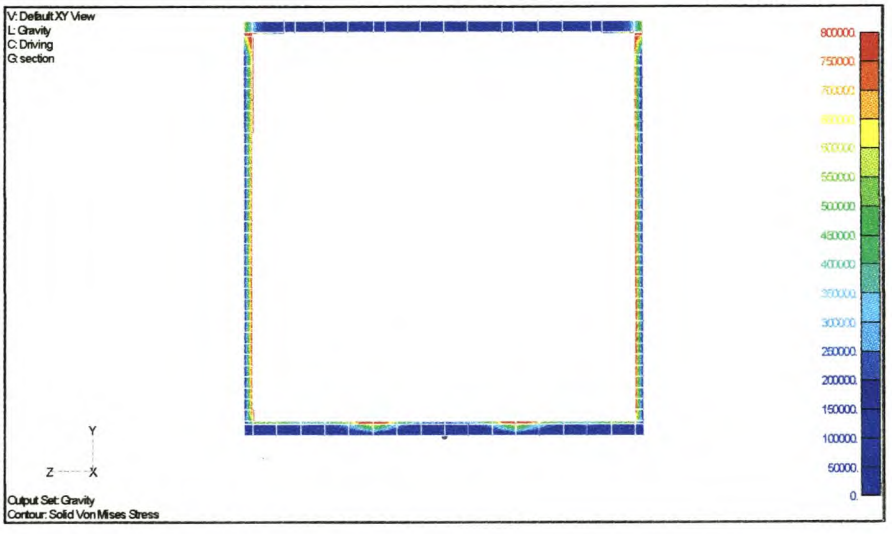

Figure 8.6: Section through GRP box section

also participate to transfer the load. In figure 8.6 a cross section cut is made. From this it is clearly visible that the inside of the GRP box section is stressed the highest when subjected to bending.

For the GRP box section the structural member that is stressed the highest is the floor panel. The stresses in the wood boards are the most representative of the actual stress distribution. The material is assumed isotropic, with the weakest direction used in the analyses models. Since this assumption is made the von Mises stress criteria can be used as an indication of failure, which doesn't take material direction into account. This is believed the more conservative approach since wood orientation is not always assured during the manufacturing process. The stresses as indicated in figure 8.7 are still within material specification, albeit to a small degree. The effective factor of safety is only 1.5, for this static load scenario. Most design manuals state for impact loading on heavy equipment and transport vehicles a load scale factor of 2 must be applied. Since this analysis is linear the stress will double if the load is doubled, indicating possible structural failure.

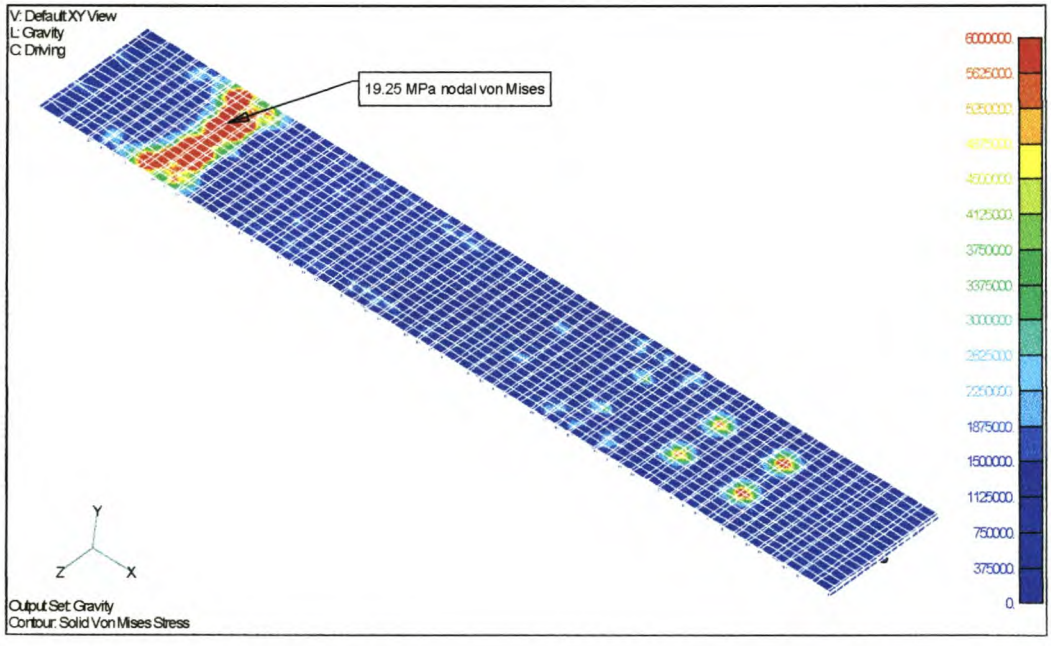

Figure 8.7: Stress in wood floorboards

Not indicated in the figure above are the polyurethane (PU) foam floorboards just below the wooden boards. The stresses in this material are above the design limits.

This will lead to severe material destruction inside the floor itself. If the PU-foam disintegrates, cavities will be created inside the floor. Moisture can accumulate in this area, which in turn could lead to wood degradation, leading to complete floor failure.

The floor outer (bottom) skin is the highest stressed skin panel, refer to figure 8.8. Stresses inside this panel are however still acceptable. The positions of the floor beams are clearly visible. From this analysis results it is not necessary to increase the strength of the whole floor area. However from the stress distribution it is necessary to strengthen the skin in the vicinity of the king pin, and above the two main I- beams. Strips of woven roving can be cut and applied in a lengthwise manner in the bottom skin. This will prevent outer skin cracking above the I-beam top flanges and king ping area.

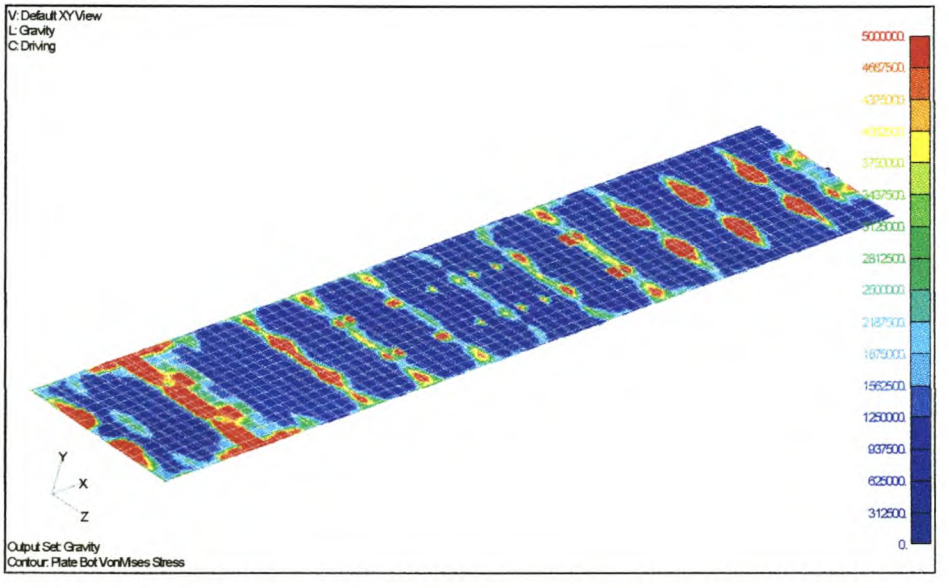

Figure 8.8: Stresses in outer floor skin

If the stresses on the inside floor skin are examined, the distribution is different from the outer skin. The stresses are still within material specifications, but again the big stress contour variations at the outer king pin position indicate possible locations for extra layers of mat reinforcement to lessen the abrupt change in stress. Also, a layer of woven roving in this area will reduce the stresses in the wood and PU foam layers.

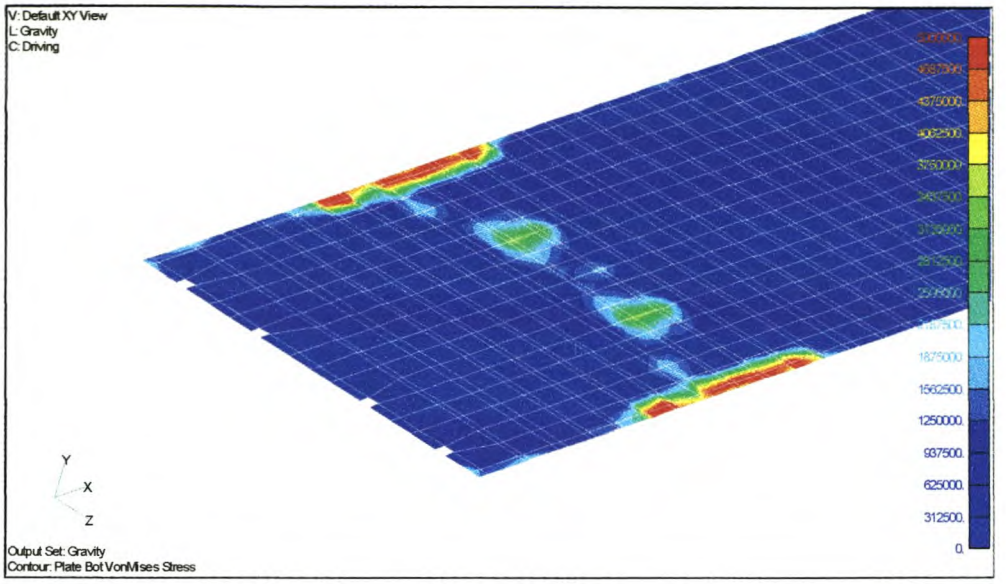

Figure 8.9: Interior floor skin

As indicated below, the side inside skin generally carries more load than the outside skin. The wood layer just below this skin is also stressed noticeably as per figure 8.10. Again the stresses are not high, but might indicate further investigation for other load cases.

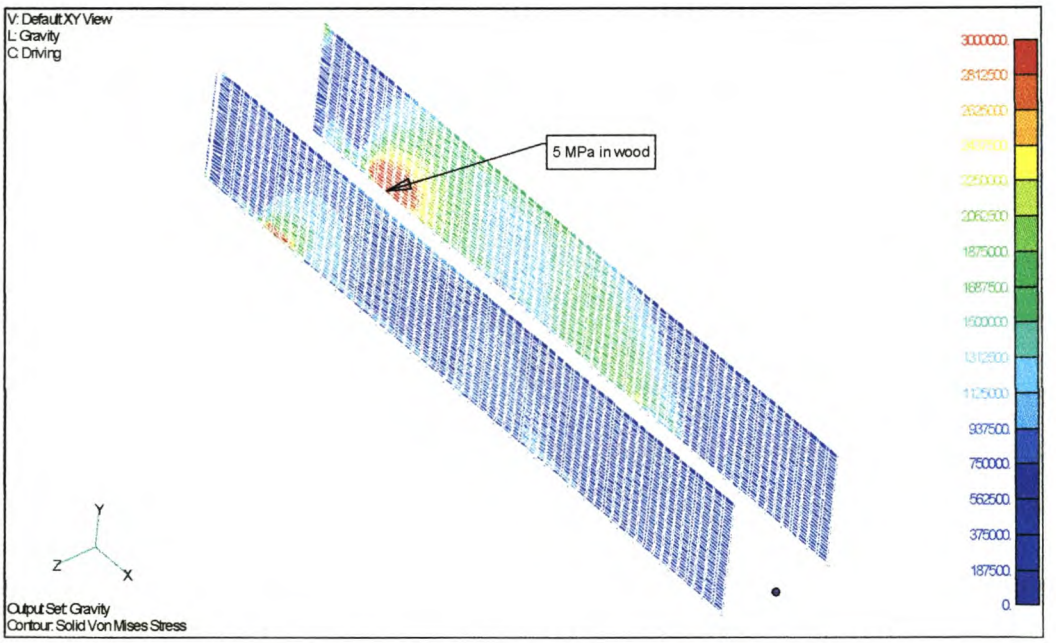

Figure 8.10: Stresses in side wood layer

The stresses within the bulkhead structure are also within design limits. The high stresses are also away from the beam-to-beam connection areas. In figure 8.11 the outside skin is plotted together with the Meranti beams. Clearly the stresses are acceptable and given that the beams and skin are assembled correctly during the vacuum bonding process, failure of this structure due to gravity loading alone is unlikely. It is however important that corner laminations be applied around the internal open area. This will prevent skin de lamination and moisture from entering the panel assembly.

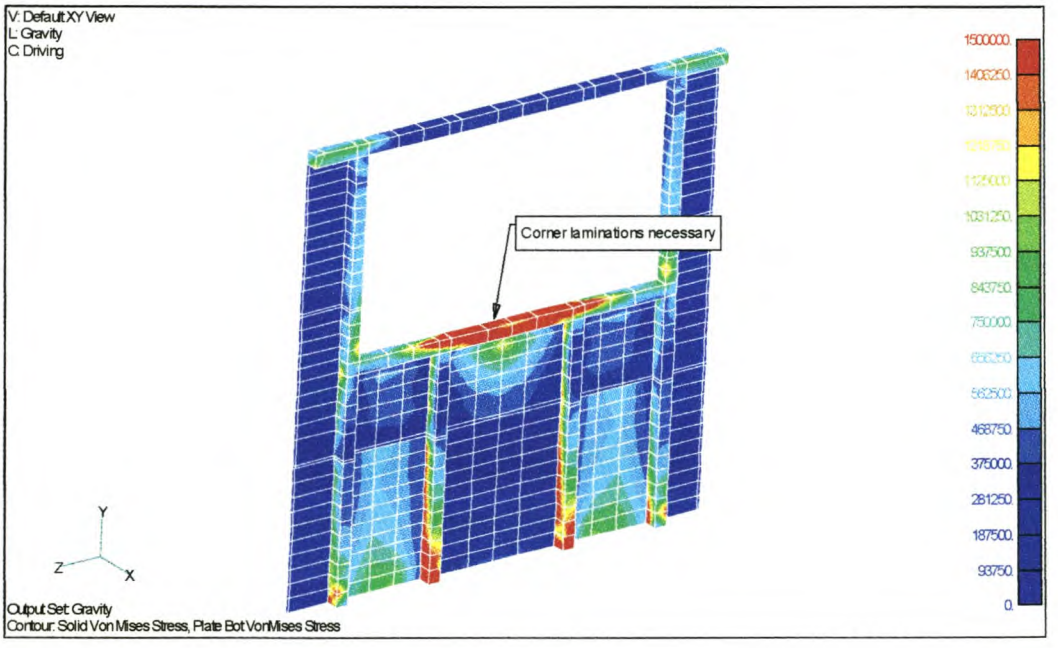

Figure 8.11: Stresses within bulkhead beams and outer skin

For the rest of the GRP box section the stresses are very low. For the door frame the maximum stress is only 8 MPa, and for the aluminium corner capping the highest stress is only 20 MPa. The gravity load case is however a very simple structural load and no torsion is applied. It is not really possible to comment on overall design efficiency at this stage.

Analysis 2 – Braking

When the semi-trailer applies its brakes the rear bogie will exert a tensile force on the chassis construction. Combined with this tension load a braking moment is generated as set out in chapter 7. This moment will increase the bearing load at the king pin area while increasing the applied bending moment over the length of the trailer. For this analysis only the braking effect was investigated and gravity ignored. The stresses due to braking must be added linearly to the gravity load case to obtain the full stress condition. In figure 8.12 the stress distribution due to the braking component is shown together with vectors indicating the applied loading. It is not possible to comment on chassis deflection since the inertia constraint method was used and whole body movement dominates the results. The increased neck stresses are considerable, as detailed in figure 8.13.

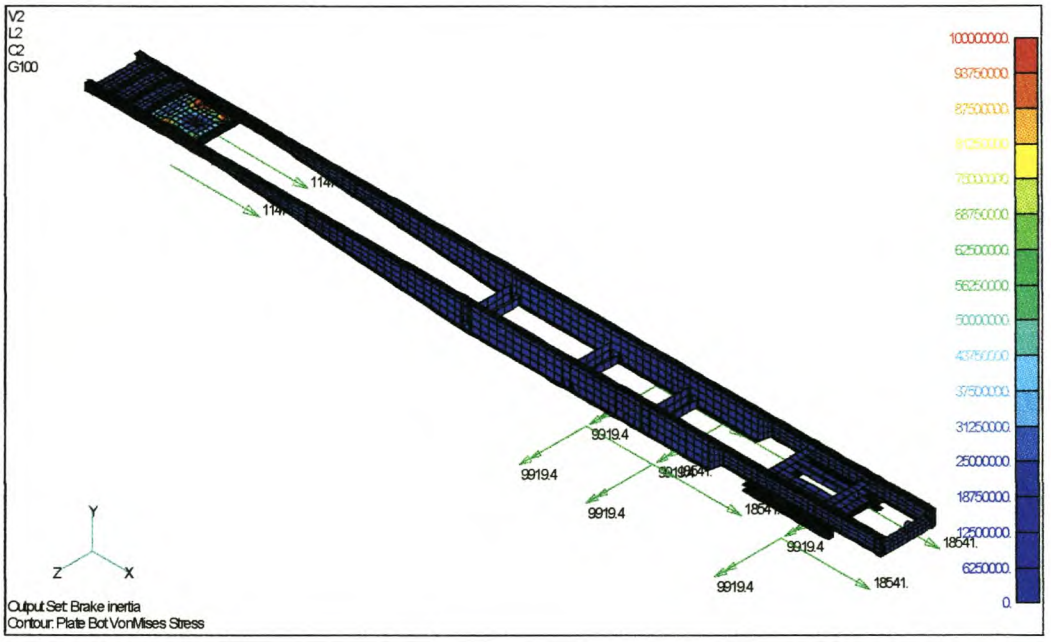

Figure 8.12: Forces and stresses due to braking

If figure 8.13 is compared with figure 8.2, some differences are observed. The location of the high braking stresses is situated more to the front than that for the bending. Also from figure 8.13 it is evident that the load is carried predominantly in the bottom flange.

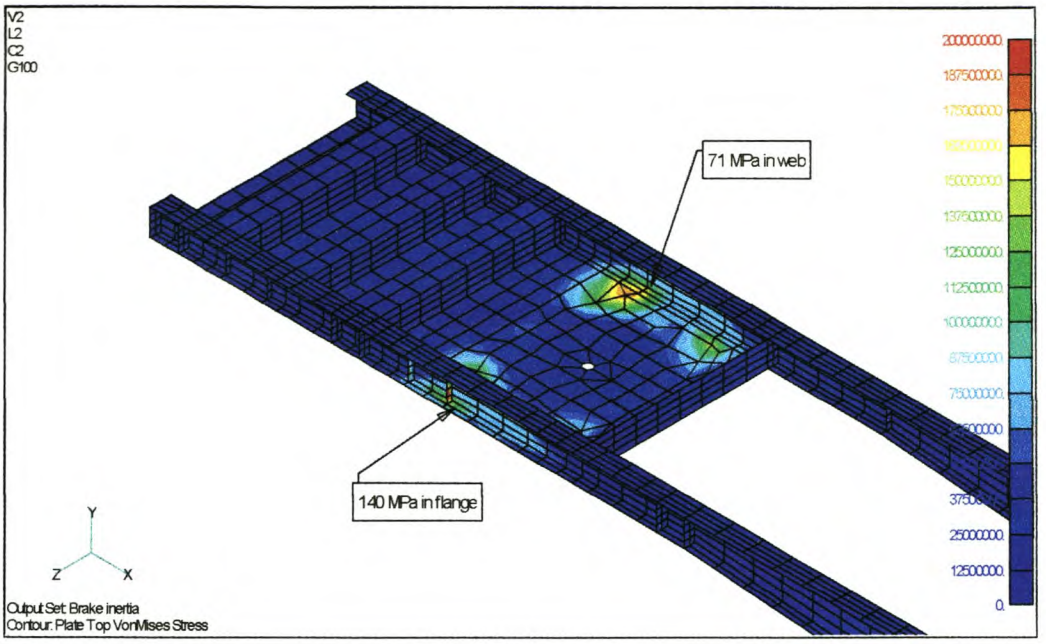

Figure 8.13: Detailed neck stresses

This is the logical stress distribution since the axial load is summed with the bending load in the bottom flange whereas for the top flange they oppose each other. In figure 8.14 the braking stress distribution is combined with the gravity stress distribution.

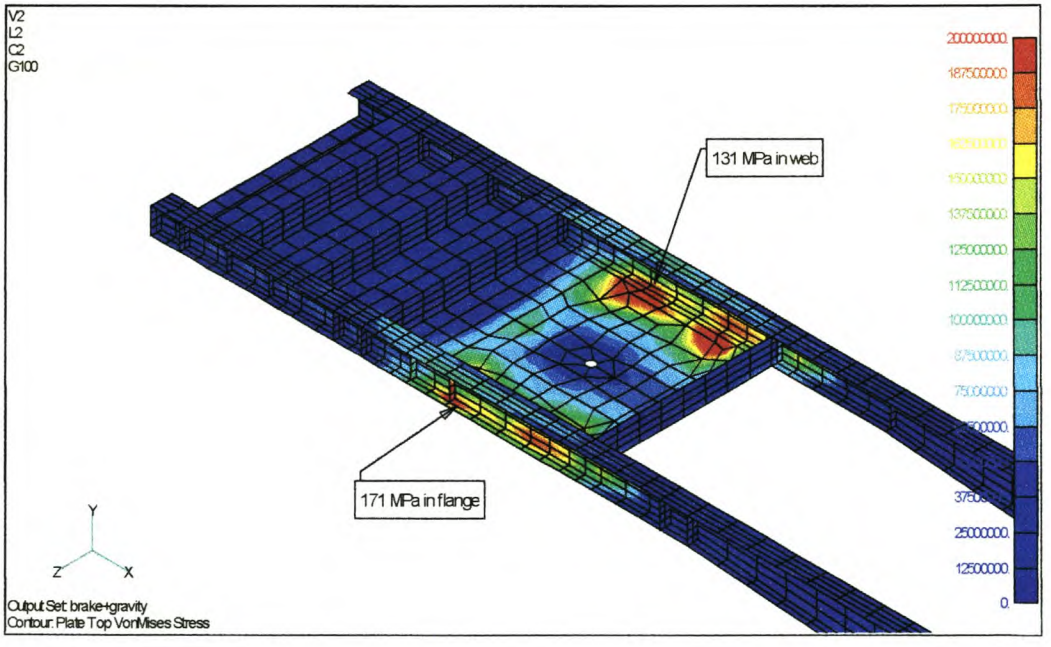

Figure 8.14: Combined gravity and brake stresses

The structural stresses are fairly high, especially for the web section. For the neck web area the use of 8 mm web plates are advised. Also from the stress contours it may be concluded that the front skid plate support beams are over designed. This might be a risky assumption since the actual load these members will experience during the hitching process will be considerably higher that the static scenario depicted above. However it is still believed that the current construction is over designed and thinner sections, say, 4 or 5 mm plate, can be used, especially for the first two beams. The last one directly in front of the apron plate assembly can be kept at the current 6 mm plate.

For the rest of the semi-trailer structure the braking induced stresses are very low and only in front of the hanger brackets there is a noticeable stress increase.

Analysis 3 – Axial deceleration – driving constraint

This load set induced very high stresses at the king pin location. The structure can clearly not withstand an axial deceleration of 1 g applied at the king pin location. The apron plate assembly will definitely deform plastically as figure 8.15 indicates since the stresses are far above the linear limits. This is however not considered a design shortcoming; it would be unrealistic to expect the structure to accommodate this severe loading. As mentioned in chapter 7, this analysis is included to investigate structural behaviour in the event of a vehicle accident situation. If only the king pin assembly are damaged and the rest of the chassis are intact the damage is relatively easy to repair.

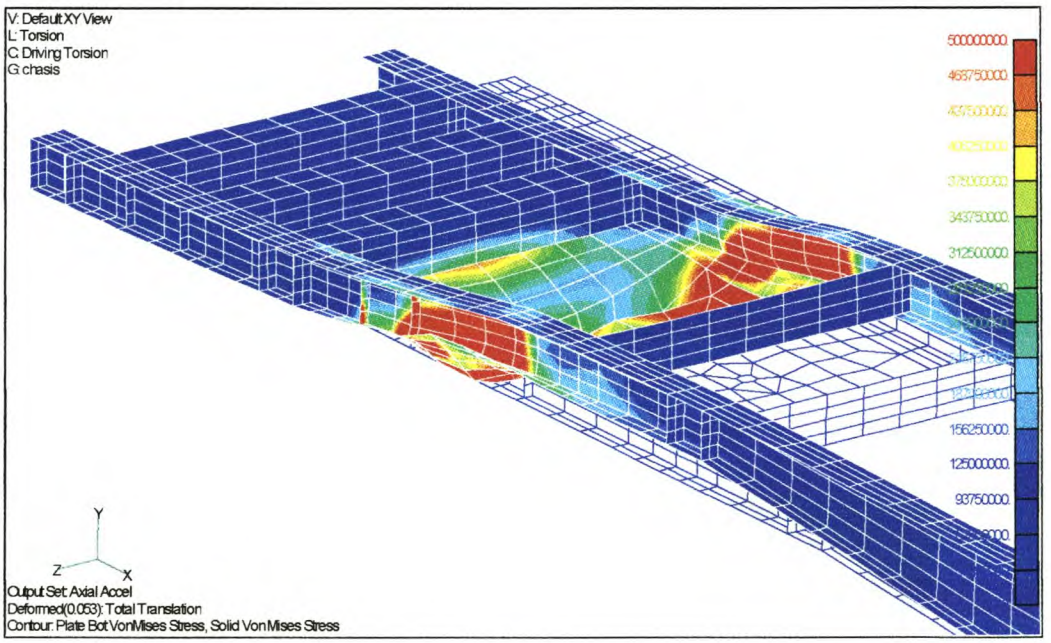

Figure 8.15: Neck stresses for 1 g axial deceleration

Analysis 4 – Transverse acceleration – driving constraint

The king pin area and rear suspension cross members are stressed to the same extent, as per figure 8.16, for this load case. This load is generated during severe sideways manoeuvring. Although the stresses are reasonably high it is not believed to be of a big concern. This load is by no means a fatigue load, and the structure will not experience this type of loading often in its service life. It must be remembered that the stresses in figure 8.16 have to be summed with the gravity load case to obtain the complete stress picture. For the neck area the stresses add up to about 300 MPa, for the rear the gravity load did not produce high stresses so its only the sideways acceleration that plays a role here with the maximum staying about 145 MPa.

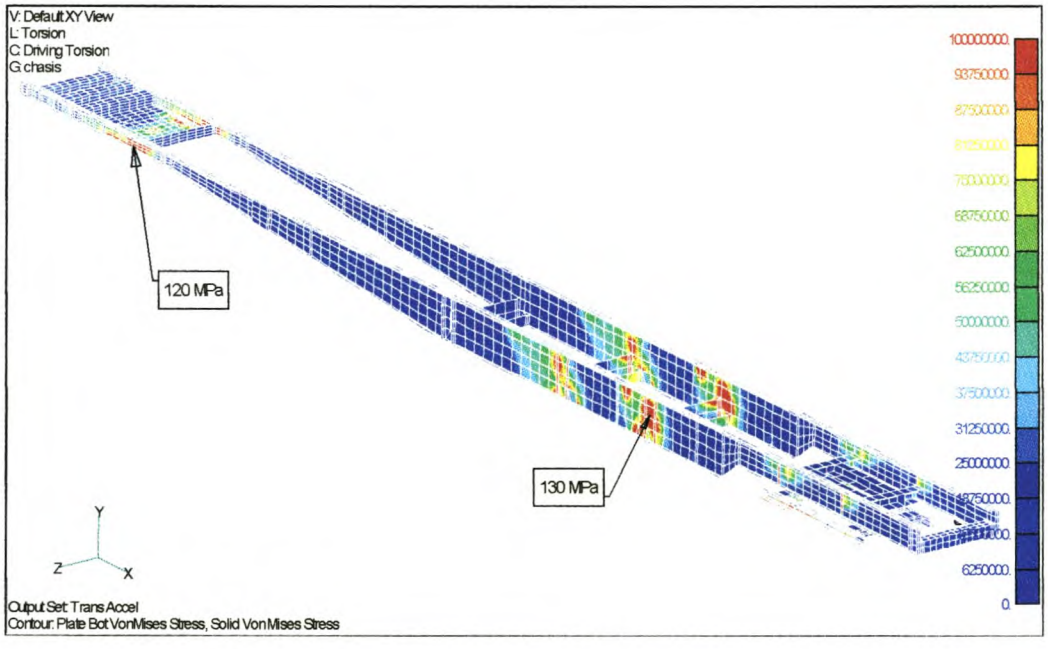

Figure 8.16: Chassis stresses for transverse acceleration

Analysis 5 – Torsion

The 50 mm asymmetrical suspension displacements induced a severe torsion load on the structure. As with the braking load case, gravity is not included with this analysis, again to make it easier to investigate torsional loading in isolation. In figure 8.17 the extent to which the suspension is deformed is indicated. The displacement loads are illustrated as the green lines with the 0.050 m load value.

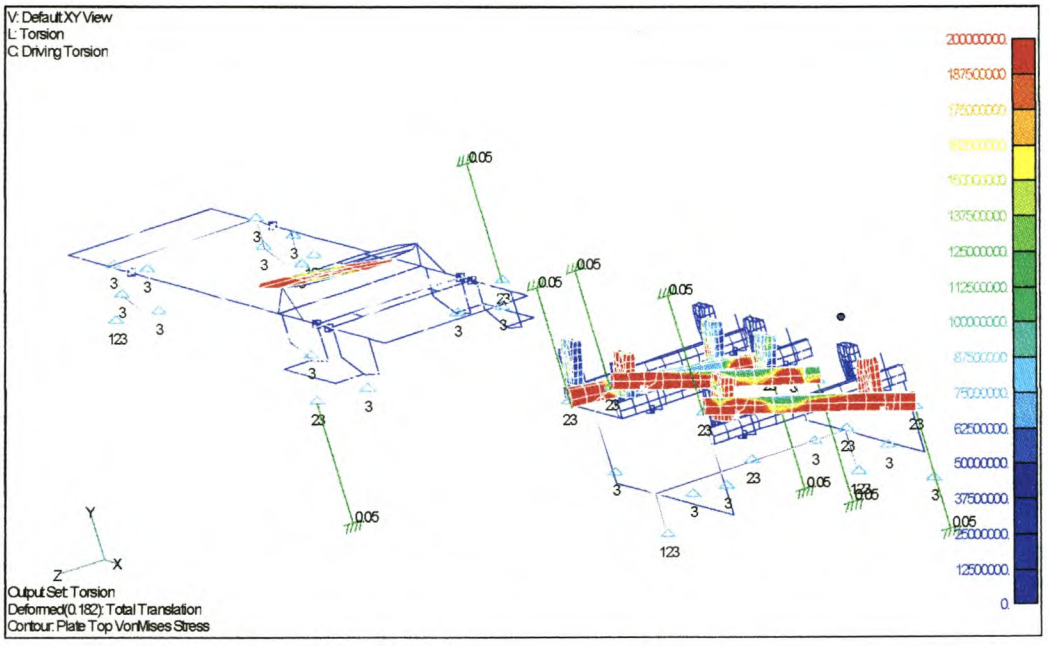

Figure 8.17: Displacement torsion load at truck and semi-trailer bogie

The stress produced by this deformation is considerable. In figure 8.18 the deformed chassis and GRP box is viewed directly from the front. Viewed from this angle it is evident that the steel structure is the main contributor to vehicle torsional stiffness, e.g. it is over stressed before the GRP section. If the chassis is examined alone, the front apron plate and the rear suspension cross members are clearly affected in an adverse manner. In figure 8.19 the highest critical stresses are indicated.

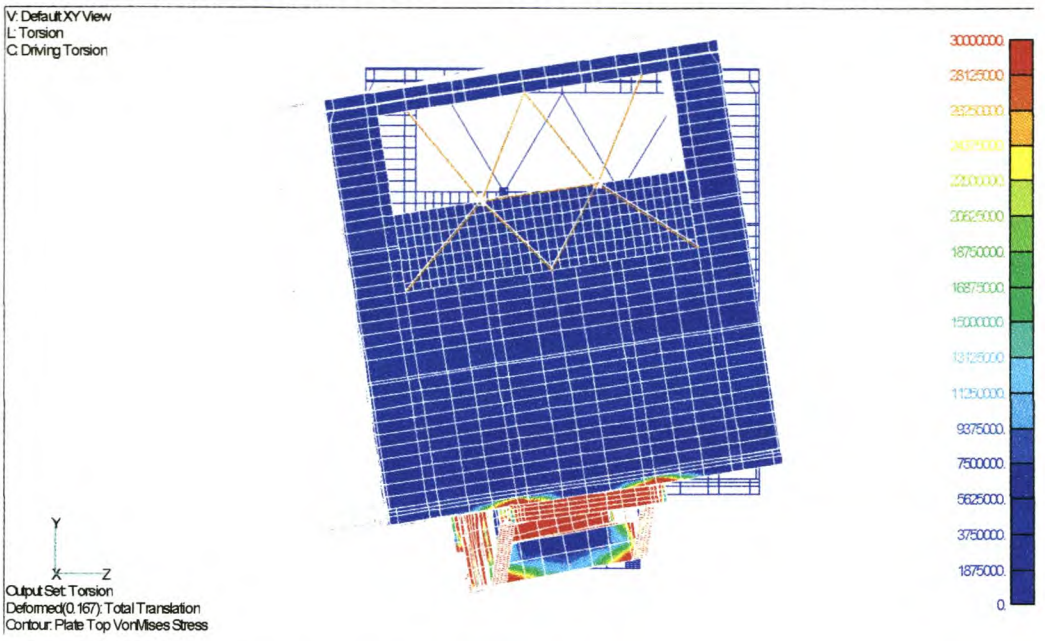

Figure 8.18: Torsion deformation of chassis and GRP box

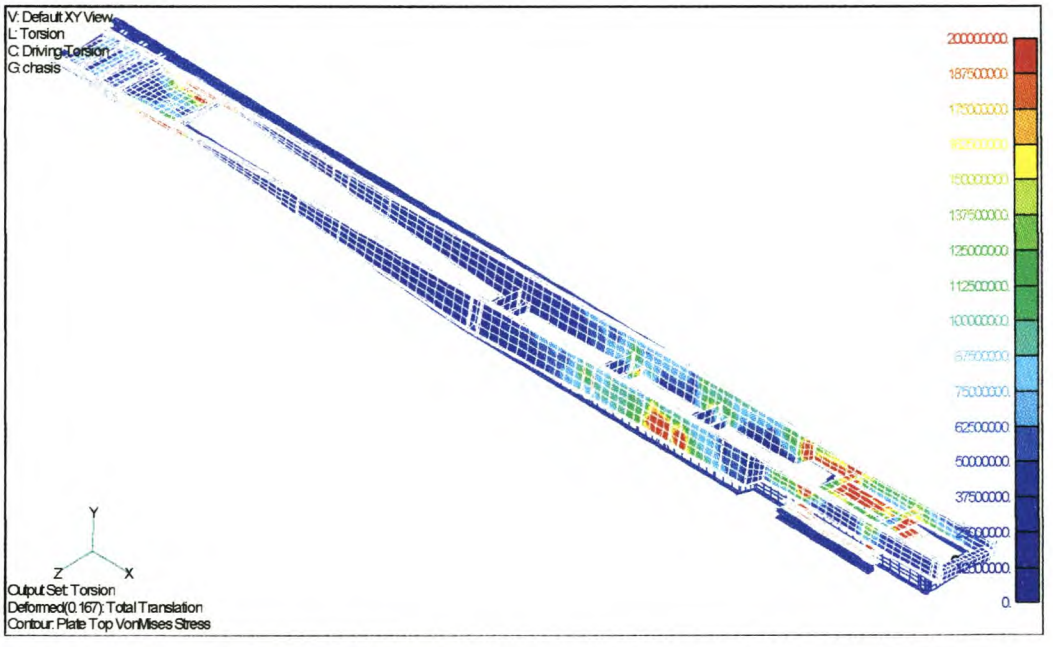

Figure 8.19: Chassis stresses due to torsion loading

In the welding chapter it is shown that a safe fatigue stress limit for welds is 55 MPa. If for the layout in figure 8.19 the maximum legend value is set at 55 MPa, an indication can be obtained where chassis welds must be of a superior quality, and where the I-beams must be welded on both sides. The first quarter and rear half of the chassis falls in this category. If all the welds are of the automated machine welded

type, the limit is set to 124 MPa. It appears that it would be the best to use automated machine welding at the rear section and the neck area on both sides of the web plate.

From a design viewpoint the I-beam webs need to be stiffened in the vicinity of the suspension cross members. Also the neck web area needs more strength, as was the case for the bending loads above.

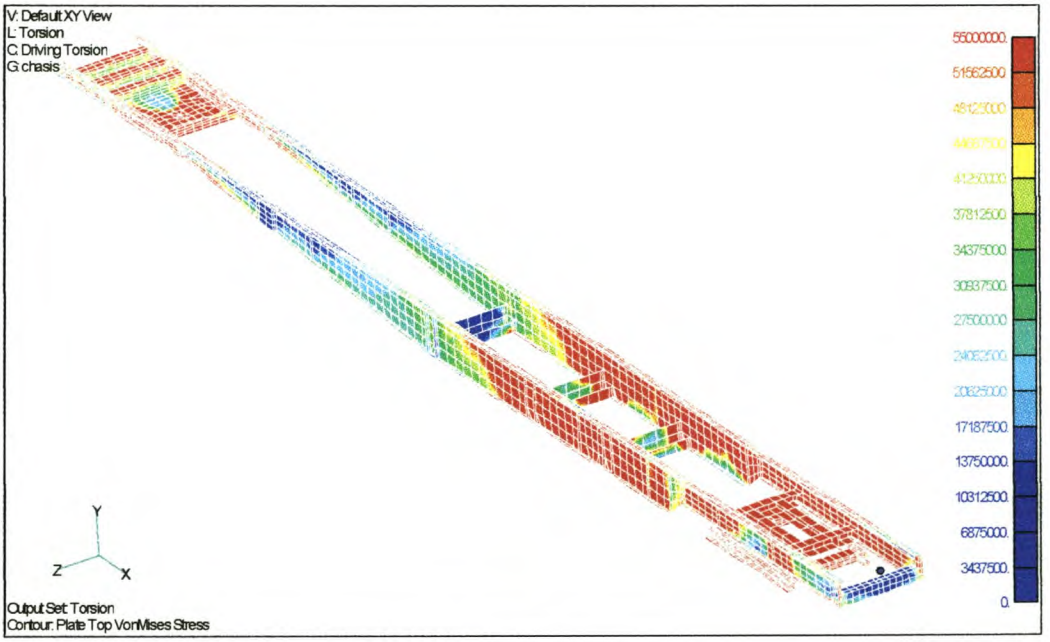

Figure 8.20: Areas where welding are critical

If the GRP box section is examined the effect of the torsional loading is also visible. In the wood floorboards high stresses are generated at the king pin area and above the rear suspension locations, as per figure 8.22. These stresses are still within the material design limits and from this it is fair to assume that the semi-trailer chassis will start cracking under such severe torsional loading before the floor is damaged. If figure 8.21 is compared to figure 8.6, the difference in load distribution is marked. Not only are values considerably lower, but also the torsion load is predominantly absorbed by the floor and not the complete structure.

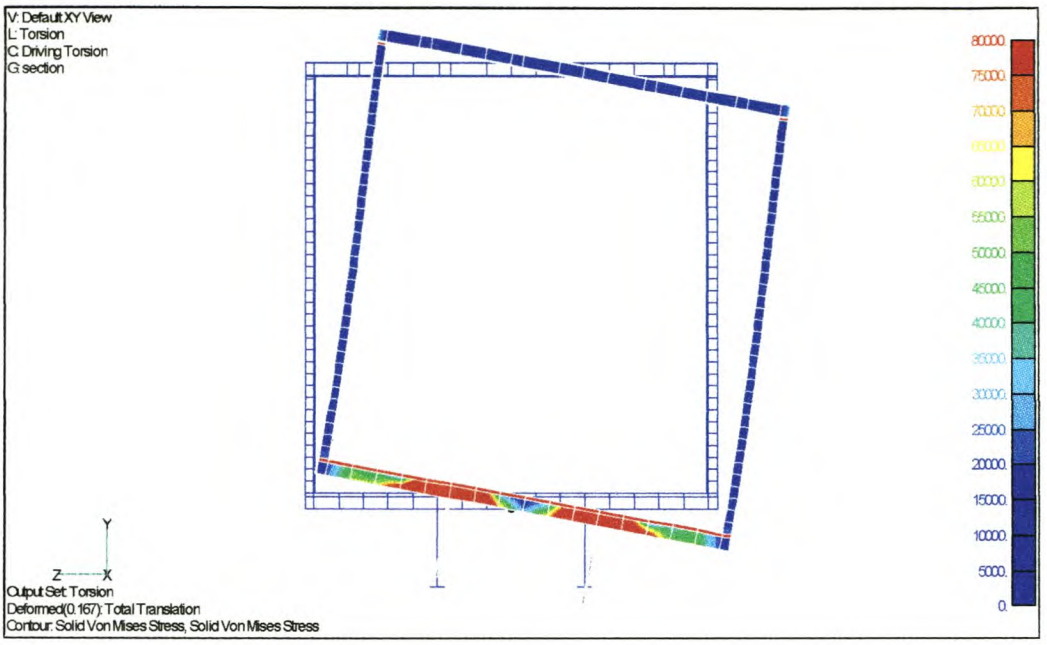

Figure 8.21: Section through GRP box for torsion load

In the side panels the torsion load does induce stresses, but only two a limited degree. Again the wood layer is stressed the highest with 5.5 MPa as indicated in figure 8.23. This value is still within material capabilities, and side panel failure on account of torsion loading is also unlikely.

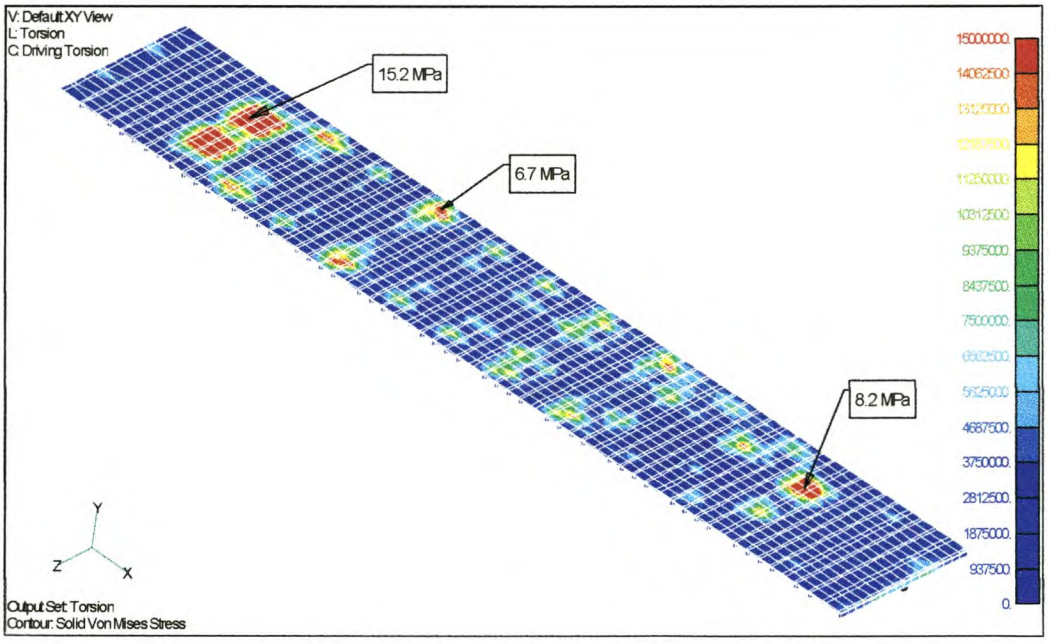

Figure 8.22: Torsion induced stresses in wood floorboards

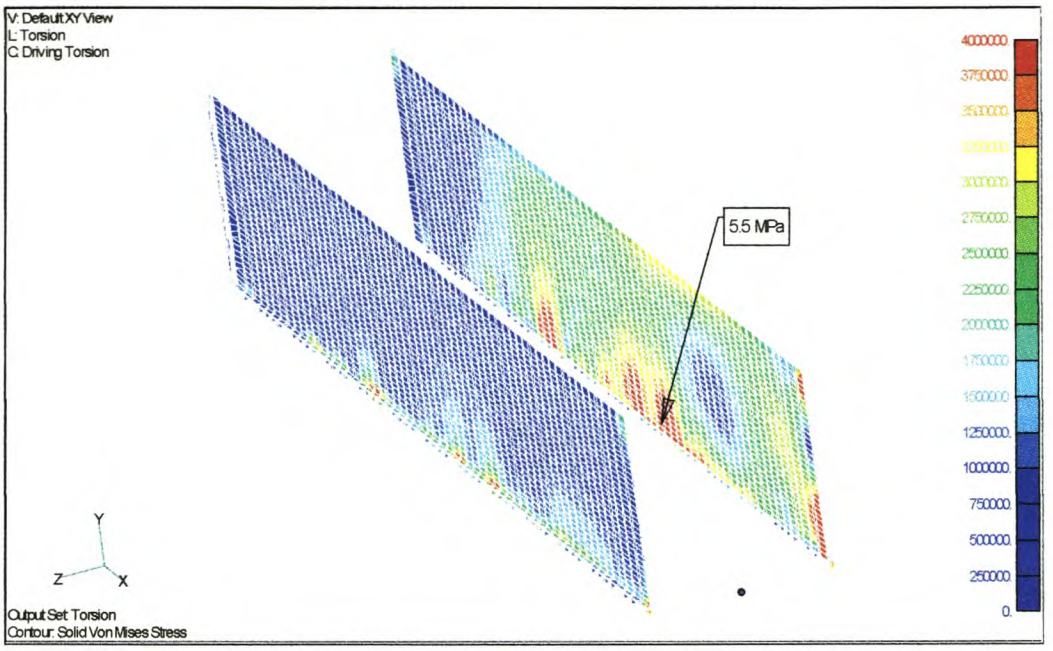

Figure 8.23: Torsion induced stresses in side wood layer

For the bulkhead structure the stresses are reasonably low and should not present any problems. There may be one point where attention to bonding should be given, and that is where the two main upright beams are bonded to the floor panel. As can be seen in figure 8.24, the stress at this location is 9 MPa. It is not so much the high

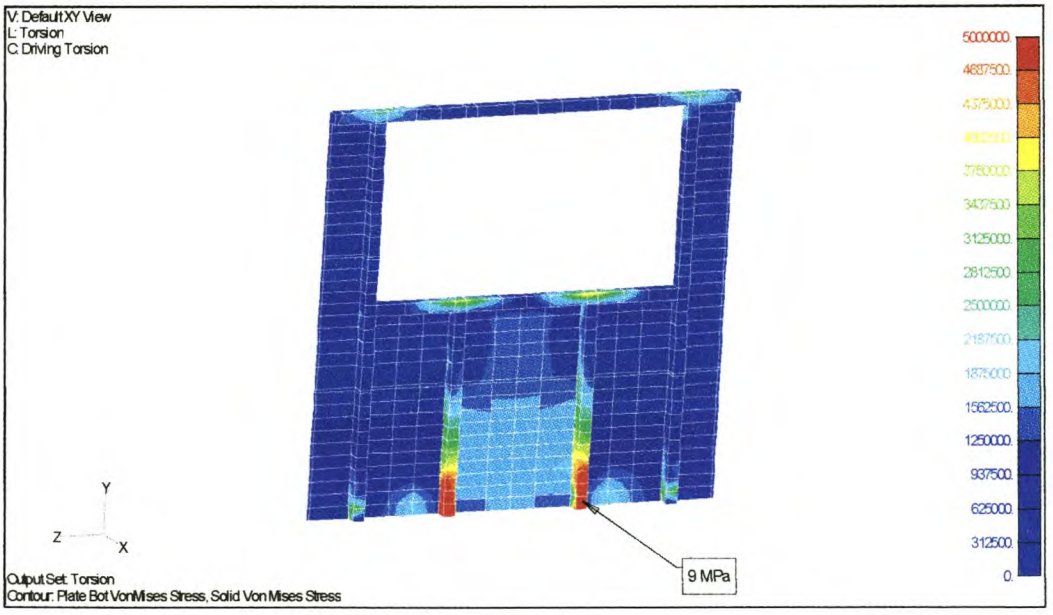

Figure 8.24: Bulkhead stresses for torsion load case

stress, but rather the rapid stress increase at this point that might cause fatigue failures. Failure in this vicinity is however not common.

The doorframe is the highest stressed member in the GRP box section. The maximum stress is about 164 MPa, and this is at a welded joint. The doubling plate at this location was not included into the model, and it is clear that the doubling plate is in fact necessary. As can be seen in figure 8.25, all 4 the corner positions should be strengthened and the welded joints grinded smooth to increase the fatigue life. Care should also be taken to ensure that the panels are adequately strengthened where they fit into the doorframe. Currently composite manufactured beams are fitted within the side panels at the rear end. These side beams are made from wood, steel and glass mat. It is advised that pultruded beams replace these assembled beams. The use of pultruded sections will be discussed further in chapter 11. As mentioned above it is evident that the GRP section does not contribute greatly to the torsional load carrying capability of the semi-trailer. The stresses are comparatively low and before torsional displacement will damage the GRP box, the chassis would have failed.

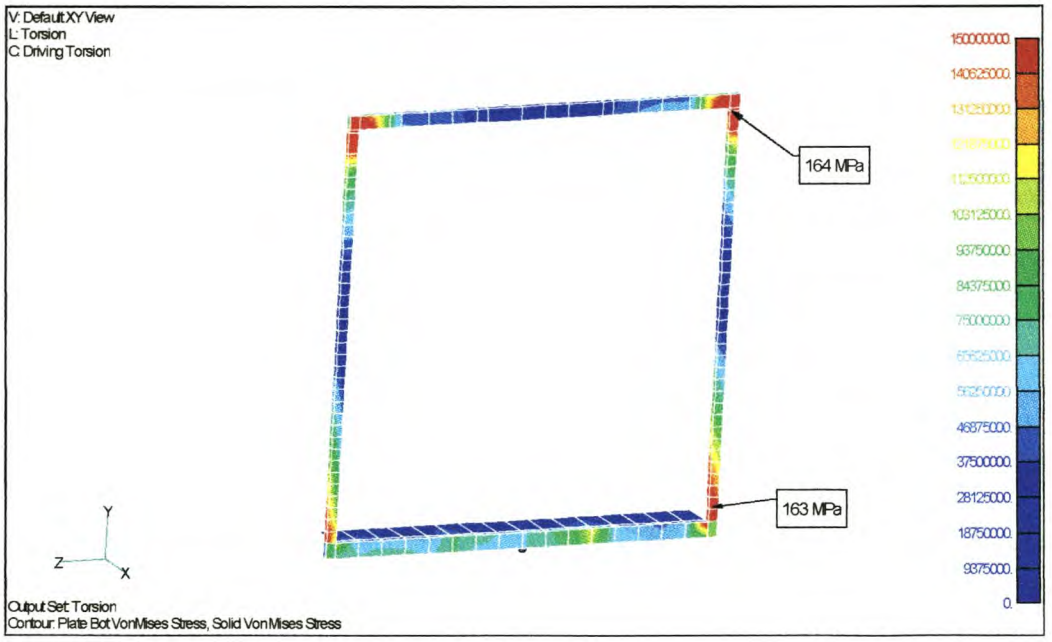

Figure 8.25: Doorframe stresses for torsion load case

It is however important to remember that the model as simulated here assumes a perfect bond between the different materials and panel layers. From actual

manufacturing samples there are often voids between the bonded surfaces. This would definitely lead to increased stresses and potential crack initiation areas. The allowed stresses might be highly exaggerated if all these flaws have to be taken into account. It is not possible to build these voids and inferior bonds into the FEA model; therefore care must be taken during the manufacturing process to eliminate such voids as far as possible. Another way around the problem is to allow for a greater factor of ignorance, e.g. decrease allowed stress by factor of 4 to accommodate realistic and sometimes inferior manufacturing practises. This is however not an effective way to optimise the structure; it will be better to build it according to design specification than to alter the design to cater for inferior manufacturing.

Analysis 6 – King pin shock

The extra 1 g load was applied at the front fifth wheel mounting points with inertia as the constraint mechanism. This stress vectors of this analysis is then added linearly to the standard 1g gravity stress vectors. The end result is an analysis, which will simulate an additional 1 g shock load while driving. This is believed to be the most realistic way to simulate these types of events with a linear analysis.

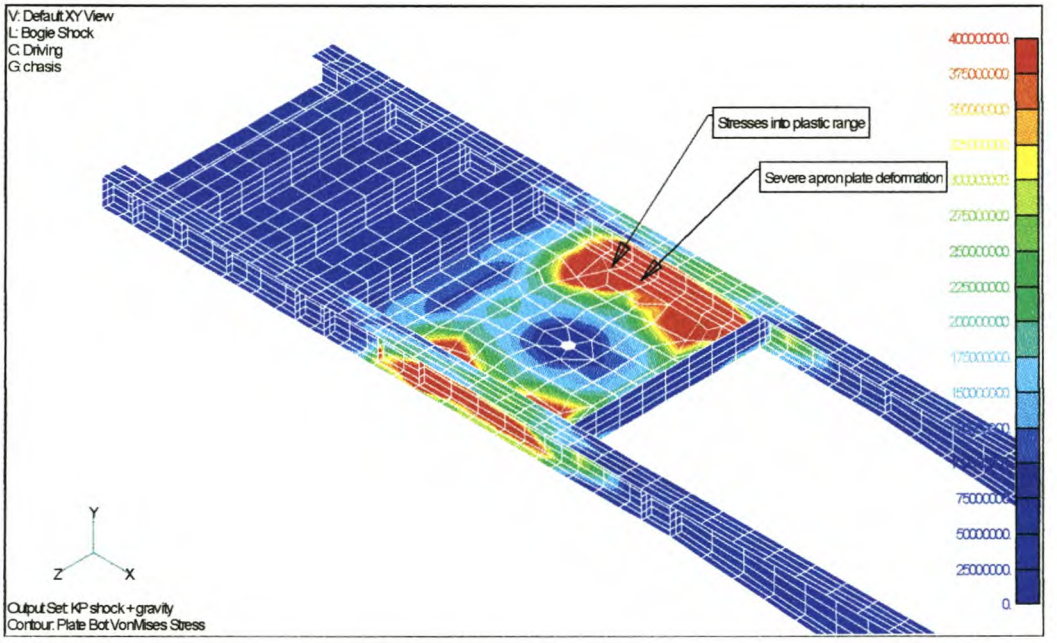

Figure 8.26: Stresses in neck area for combined gravity and king pin shock

The stresses for this analysis is high. At the outer edges of the apron plate the stresses are far into the plastic range. It is therefore not possible to give precise stress values. As mentioned the slewing ring is not included into the model. The slewing ring structure is reasonably stiff and would tend to stiffen the neck area, and in doing so decrease the stresses to a certain extent. The analysis does however clearly indicate that the forces transmitted between the slewing ring and outer apron plate is considerable. Also the apron plate will deform to a great extent under such loading, leading to uneven distribution of loads between the slewing ring mounting bolts. This will increase the stresses in these mounting bolts far above safe design values. Failures in these bolts are frequently noted, and the only why to eliminate this is to

prevent apron plate flexibility. In the original design the whole king pin support load was transmitted through the M16 bolts. This design was changed to allow for direct contact between the bottom of the slewing ring and the chassis structure, greatly decreasing bolt stresses. The stresses in the I-beams are acceptable, albeit high. For the rest of the structure no damage is predicted; the floor above the king pin being the worst affected, and localised stresses touching the 6 MPa range.

Analysis 7 – Bogie shock

As per analysis 6 the gravity load was added linearly to an additional 1 g bogie shock load. At the rear suspension area the shock did produce higher than gravity-induced stresses, but still within an acceptable range, refer to figure 8.27.

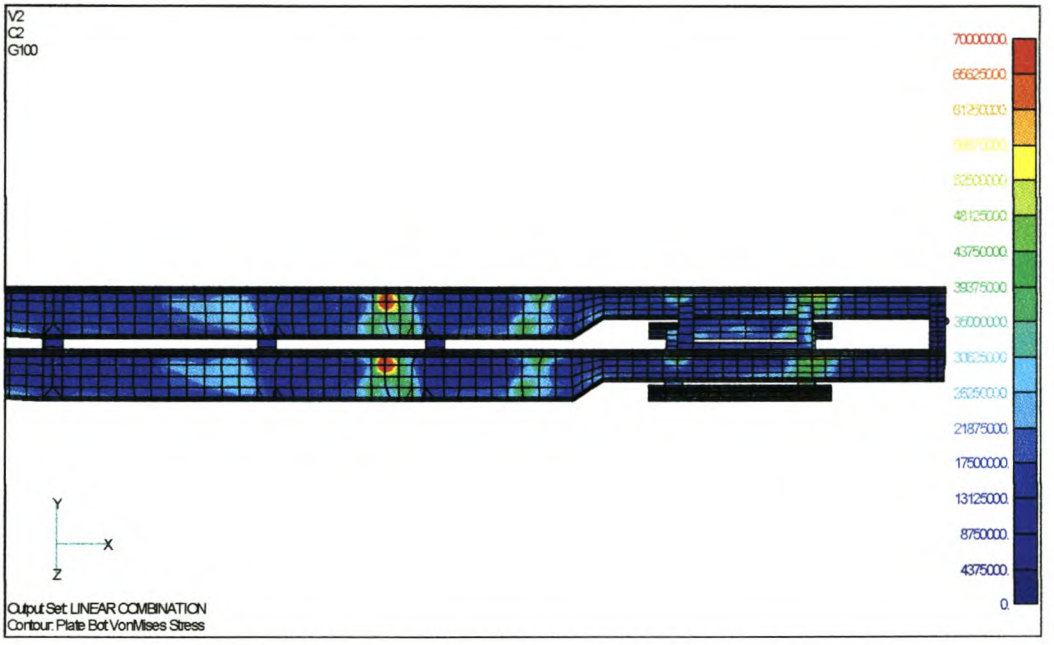

Figure 8.27: Rear chassis stresses for bogie shock

The highest stress is still in the neck area as per figure 8.28. If these stresses will be generated to this extent is debateable. In the model they are caused by the truck's inertia. It is doubtful if the king pin mechanism will transfer a downward force to this extent. In theory it would have been better to omit the truck mass elements for this analysis, but since the stresses are already below the king pin shock induced stresses, there is not much additional insight to gain from such an analysis.

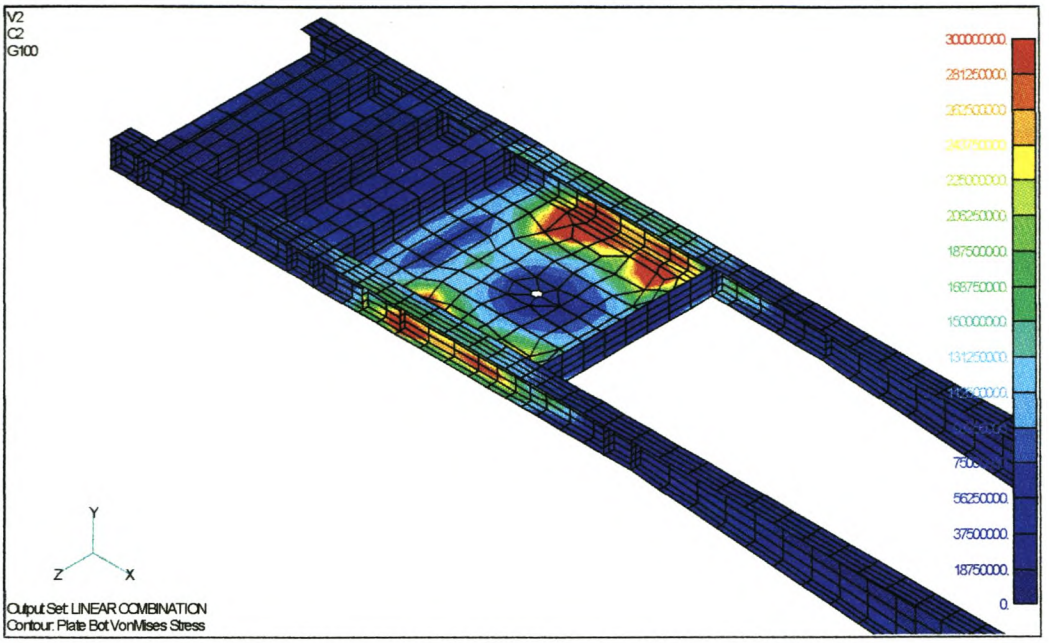

Figure 8.28: Neck stresses due to rear bogie shock

Analyses 8 – Park and pull

The stress distribution is as would be expected, and the analysis predicts that the semi-trailer lengthens with 11.38 mm. As with the other analyses the king pin area is again the highest stressed region, combined with gravity the stress levels is high enough to cause permanent plastic deformation. It is however unlikely that these stresses will be generated within the structure since the tyres would rather start slipping. Except for the neck no other problem areas were noted.

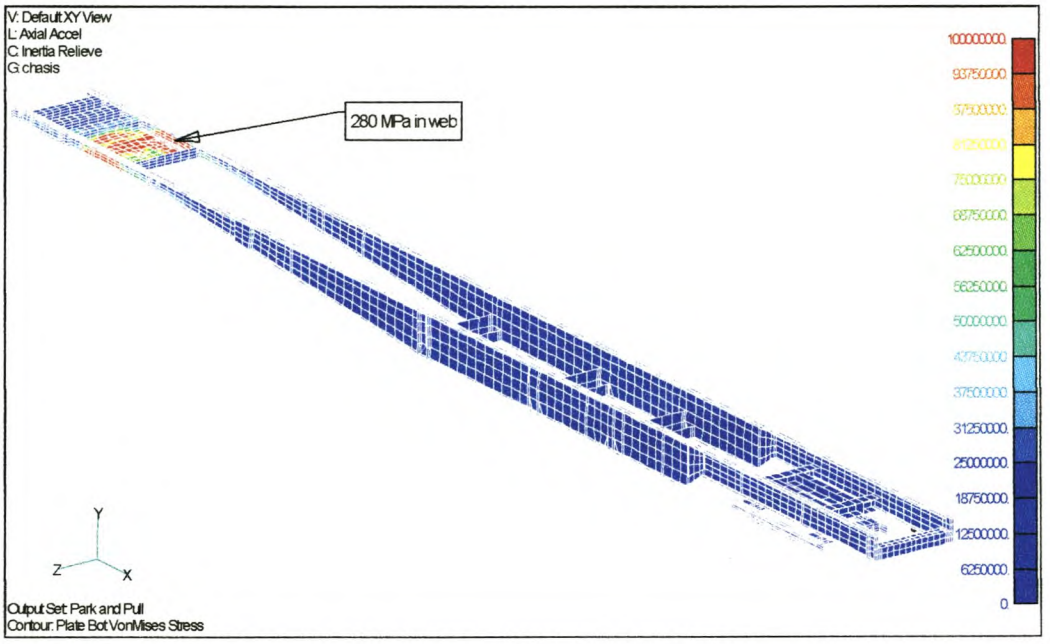

Figure 8.29: Axial pull in parked situation

Analysis 9 – Asymmetrical braking

If only one side of the semi-trailer's tyres have sufficient bearing pressure an asymmetrical tensile load is applied to the structure when the brakes are applied. From the analysis results no unacceptable high stress areas are noted, and as could be expected the deformation and neck stresses are about half of that of the full braking analysis.

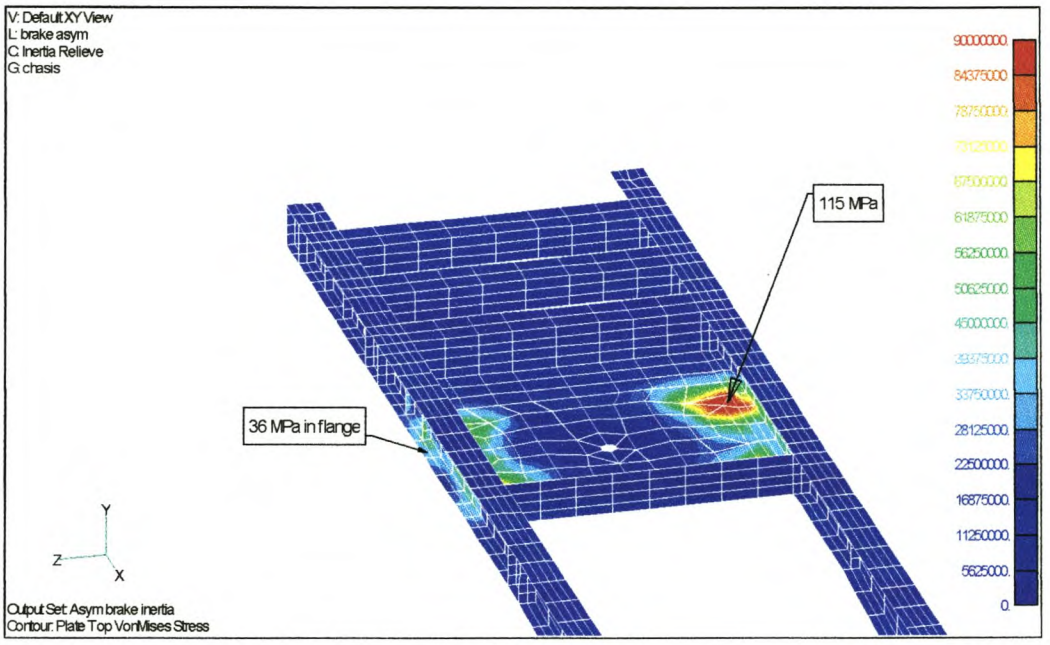

Figure 8.30: Stresses due to asymmetrical braking

Analysis 10 – Asymmetrical payload

This load case led to higher stresses than was anticipated. As usual the neck area is the only problem area. The stresses show similar distributions than the torsional analysis. If the design is adopted to bear the bending and torsion loads, this asymmetrical payload will not lead to failures.

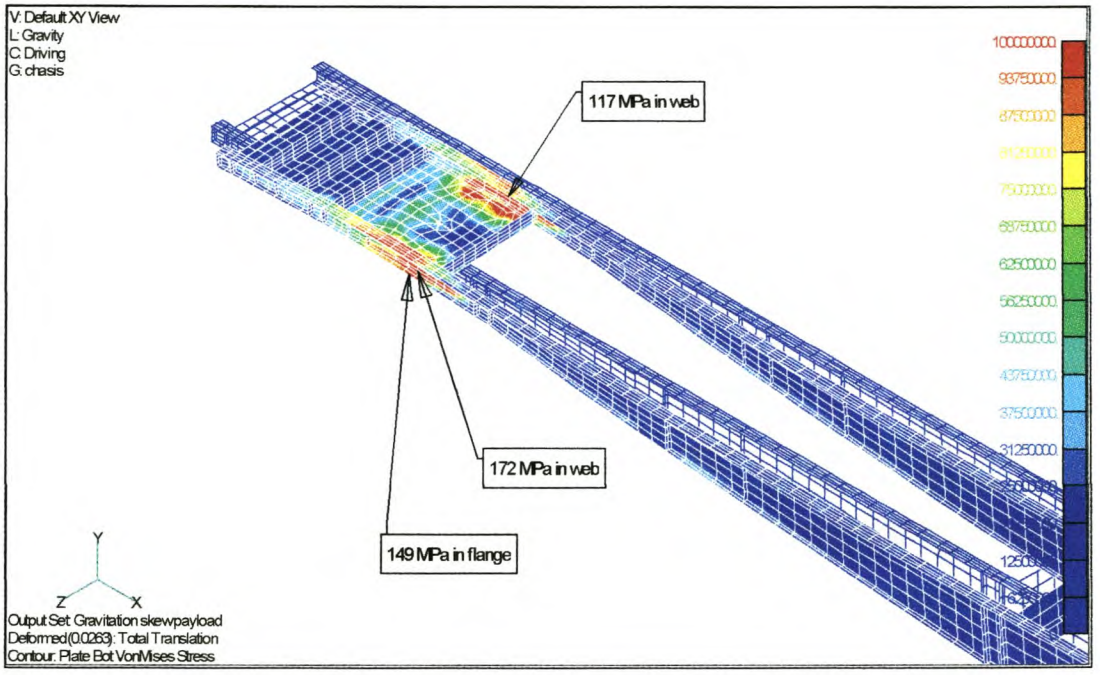

Figure 8.31: Neck stresses for asymmetrical payload

No other chassis or GRP box areas showed excessive stress values.

Analysis 11 – Forklift

The pressure force was applied almost midway between the suspension and king pin position to induce maximum bending moment together with the bearing pressure. Also the positioning was such that it did not align with the main floor beams, but rather above the standard 50×80 mm lamitico floor beams.

In figure 8.32 the floor is seen from above. Clearly the applied loading doesn't lead to severe or even noticeable stresses within the top CSM layer. The maximum stress is 1.3 MPa.

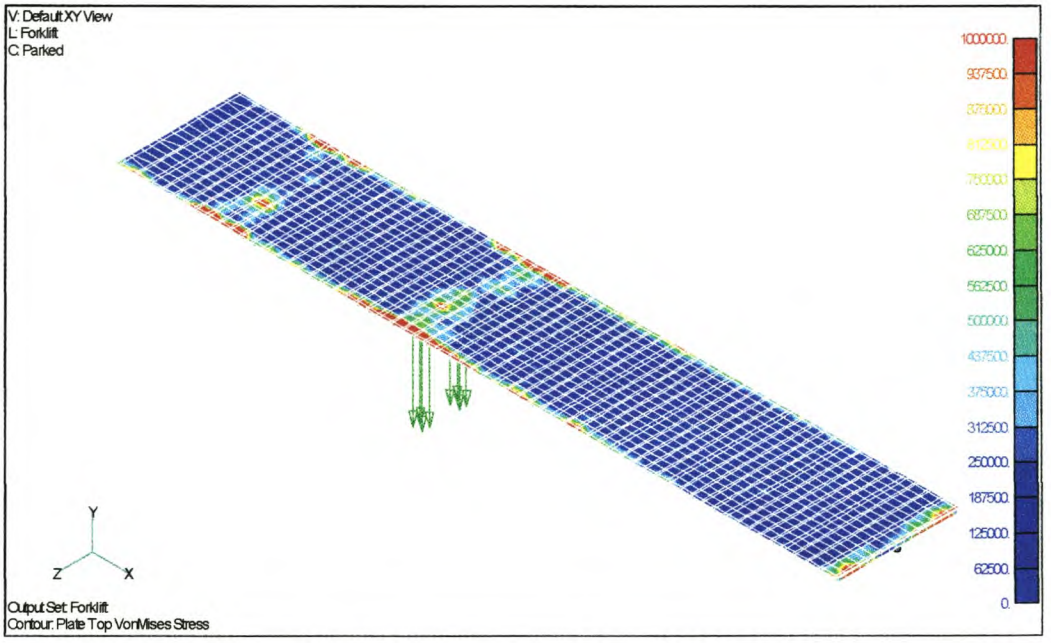

Figure 8.32: Stresses in top CSM floor layer due to forklift mass

If the wood panels are examined, the stresses directly under the forklift wheel is 3.6 MPa. This value is still acceptable, and wood failure is not likely, even after repeated load cycles. In the polyurethane foam the stresses are also acceptable at a 100 kPa maximum. In figure 8.33 the foam inside the nearby floor beam is also visible. The rest of the GRP structure and chassis assembly are hardly influenced by the forklift loading.

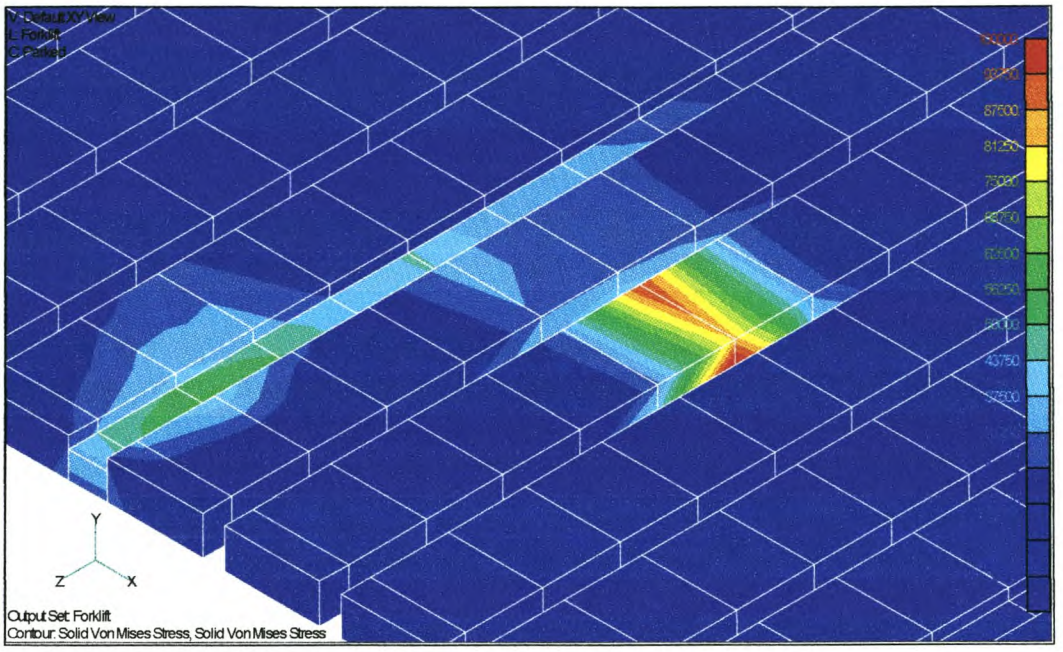

Figure 8.33: Stresses in PU-foam floor panels

A perfect bond between the floorboards and cross beams was assumed. This is not always the case, and if there is slip between the glass layer, wood floorboards and support beams considerable local stresses can be generated. The importance of a proper vacuum bonding process is again highlighted.

Analysis 12 – Side wind load

The stresses in the chassis is low, the highest stress is 50 MPa at the outside stiffeners of the centre suspension cross member to I-beam connection. In the GRP box the side to floor panel connection are the highest stressed area with peak stresses in the vicinity of 7 to 10 MPa. The stresses are not excessively high considering that the aluminium, wood and glass are capable to withstand these stresses. However, if these materials are not bonded properly, the assembly can quickly disintegrate as described in the torsion paragraph above. In figure 8.34 the effect the internal Z-sections have

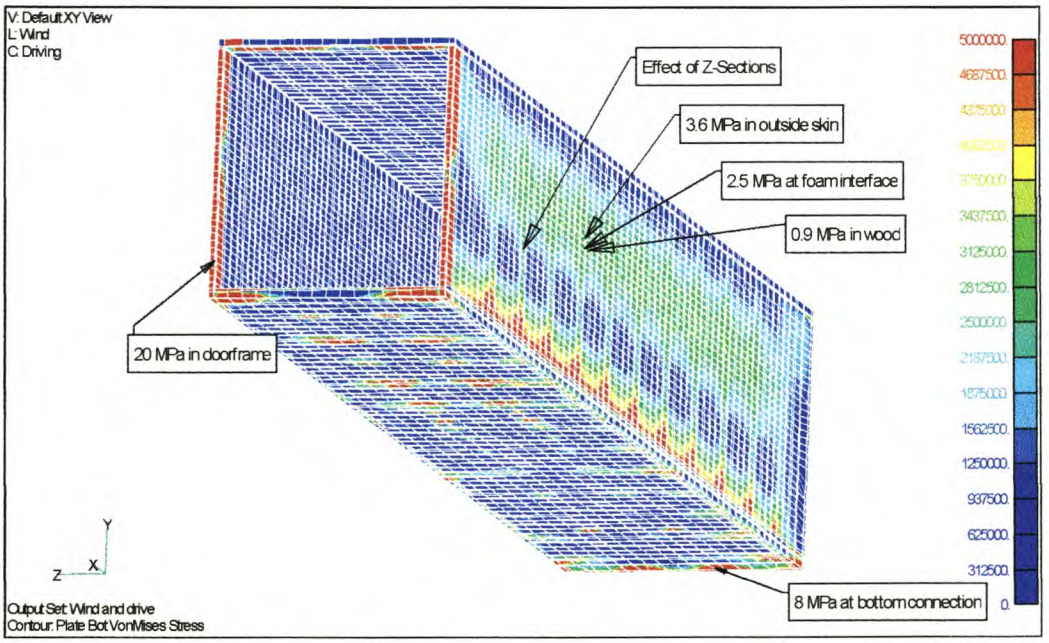

Figure 8.34: GRP box stresses due to wind loading

Is also clearly visible. Another area where the wind loading does lead to a stress increase is in the upper roof corner capping, albeit not visible in figure 8.34. The stress touches the 10 MPa range and again the bond quality needs to be of a high quality.

Analyses summary

Considering all of the above analyses, the following design comments will briefly summarise the current semi-trailer design. These paragraphs will not try to go into detailed design changes; the current design deficiencies will only be highlighted and explained in some detail.

Clearly the only severe chassis design shortcoming is the neck area. As repeatedly mentioned above, the neck would need reinforcing if an acceptable fatigue life is to be achieved. The main stress contributor is the high shear stress in this vicinity. Effective neck reinforcement will reduce the shear stress.

The relatively flexible mounting surface for the front slewing ring will further cause fatigue failures. The steering arrangement will need extra stiffening if service life is to be extended to 5 years.

It is assumed that if the semi-trailer is not of the steering axle type, the standard 8 mm apron plate, when being adequately stiffened by cross members referenced above, will be sufficient. In addition, from these analyses the use of 6 mm apron plates is not advised, except if it is supported sufficiently.

The girder type I-beam flanges themselves are not overstressed, however the stress at the flange to web interface is critical, and currently it is above the safe fatigue limit in numerous positions. If hand welded joints are used, the safe weld stress is 55 MPa. The largest part of the main I-beams are to some extent close to this design limit. If however the beams are machine welded on both sides for the whole length, the limit stress is raised to 124 MPa, giving the designer much more freedom and scope for beam weight reduction. For the load cases considered the beam mid section is never stressed to high levels, and a few kilograms could be saved if thinner flange material is used. If the flange section is changed at certain positions, careful attention needs to be given to weld quality. Radiography testing of this location might be necessary to ensure adequate weld strength.

The cross members are also never stressed above material capabilities. The highest stresses are usually at the cross member to I-beam joints. Gusset plates at cross member joints should always be in place for added fatigue failure resistance. The cross members can be made of less expensive material, the Supraform is not necessary.

The GRP box section is also generally not overstressed. The load distribution between the GRP box and chassis is different from what was expected. The chassis is the main load-carrying member for bending as well as torsion. It was thought that the box section would add more to the torsional stiffness.

Again it must be emphasised that the numerical simulation did not take bonded joints into consideration. Structural failure will almost always begin at these joint surfaces, except for severe accidental damage. Especially at the floor and side interface considerable stress variations might lead to fatigue failure. The same is applicable to the bulkhead to floor and side to roof interface.

In general the floor design is suited to withstand the applied loading. The only area where failure might arise is the section just above the king pin area. Stresses in the wood are close to the material design limits. Given that the different layers are bonded according to design specifications, the floor can withstand the bending, torsional and forklift loading. If the interior glass mat is severely worn, failure in the wood might arise. Even more so if moisture induced degradation is present in the wood panels.

The stresses in the polyurethane core is also high in some instances, noticeably in the floor section above the king pin area. As mentioned, a stronger and stiffer core material might be beneficial, even if only situated in this area.

Relative high stresses in the side Z-sections indicate that they are effective in transferring the load form the outer to inner skin sections. They will naturally lead to an increased heat loss since the glass mat's heat transfer coefficient is ten times higher than that of the polyurethane core material. Considering the small area they take up this effect is probably negligible.

Chapter 9: Sub-Component Finite Element Analyses

Detailed analyses are done to investigate particular design alternatives. These comparisons are done in separate models instead of the complete model to save modelling and analysis time. Even though the load cases are fictive they represent realistic stress distributions and will highlight potential design shortcomings.

The specific models are chosen to investigate observed failures in practise, or where high stressed areas are apparent from the complete finite element model. They also investigate semi-trailer design principles in general.

Chassis cross members

The first detailed model was made to compare different cross member to I-beam connection alternatives. This construction is typical for the suspension cross members. Two 400×100 mm I-beams of 2 m length and at 1 m separation with uneven legged U-channels in-between is modelled. First a torsional load is applied in a symmetrical manner, as indicated in figure 9.1. No constrain except for inertia relieve is applied, which conveniently removed all constraint stress concentrations.

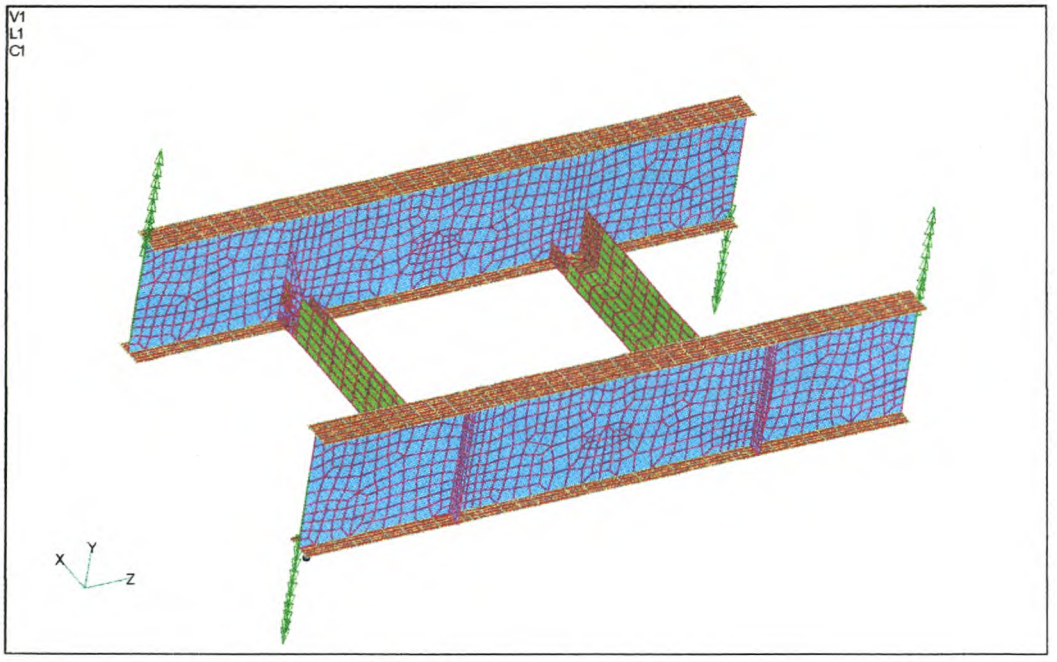

Figure 9.1: Cross member investigation model

As a second load scenario a shear load is applied, by means of two opposing forces, but one on either side, as per figure 9.2. Again the inertia relieve constraint method is applied.

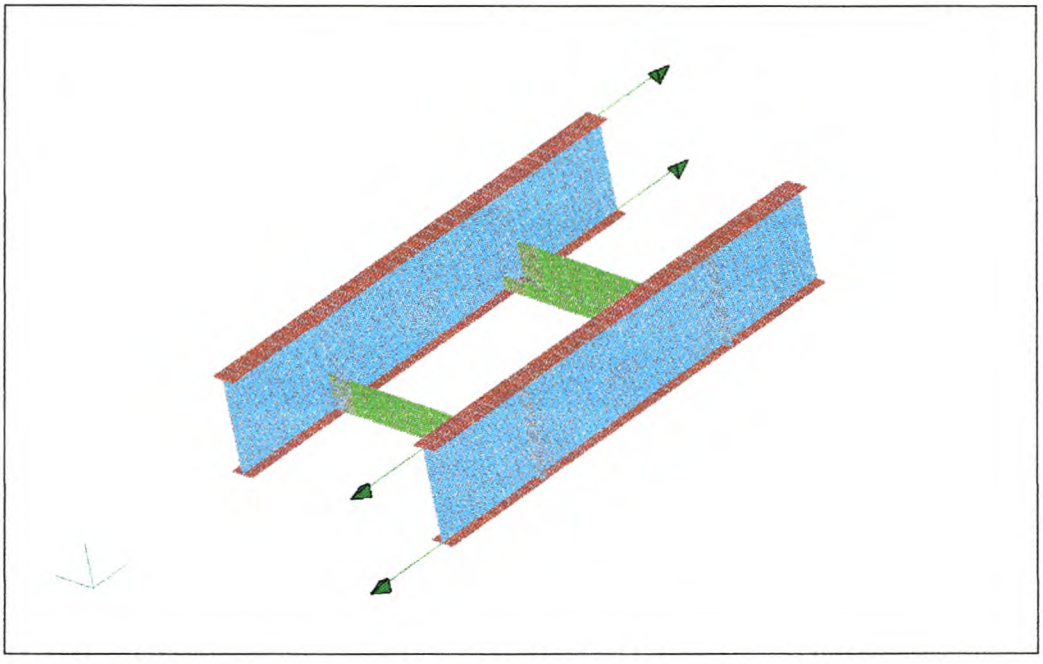

Figure 9.2: Shear load case for cross member investigation

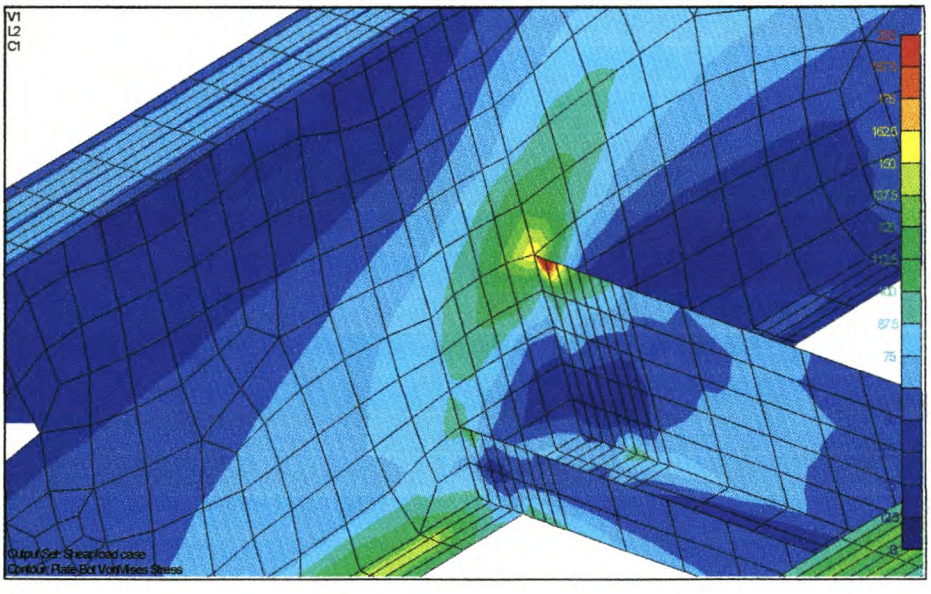

Figure 9.3: Plain connection, torsion

Four different connection methods are considered. The first one where the cross member is plainly welded to the I-beam web and flange. Complete full round welds

are assumed. As per figure 9.3 and 9.4 the stress increase around the upper point is considerable. Legend values for analyses are in MPa.

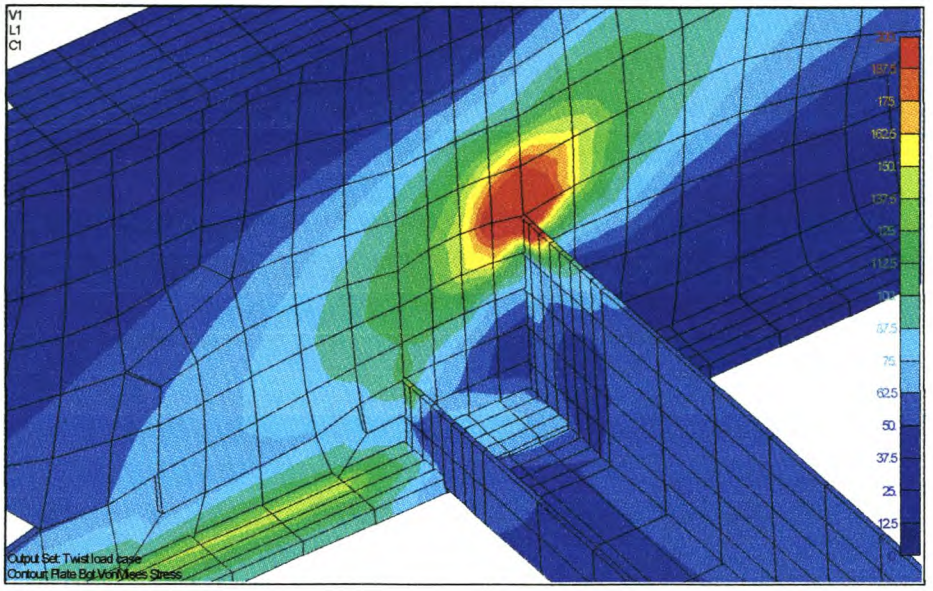

Figure 9.4: Plain connection, shear

If the stress directions are considered it is clear that the predominant cause of the high stresses is due to a load applied perpendicular to the web surface. The web easily gives way under such loading. For the torsion case the maximum von Mises stress in the I-beam web plate is 257 MPa, and for shear it is 160 MPa. For shear the maximum stress is actually in the cross member itself, being 229 MPa.

As a second connection type a vertical stiffener is placed on the outside of the I-beam, directly in-line with the vertical web of the cross member. It is assumed that the stiffener is welded all round.

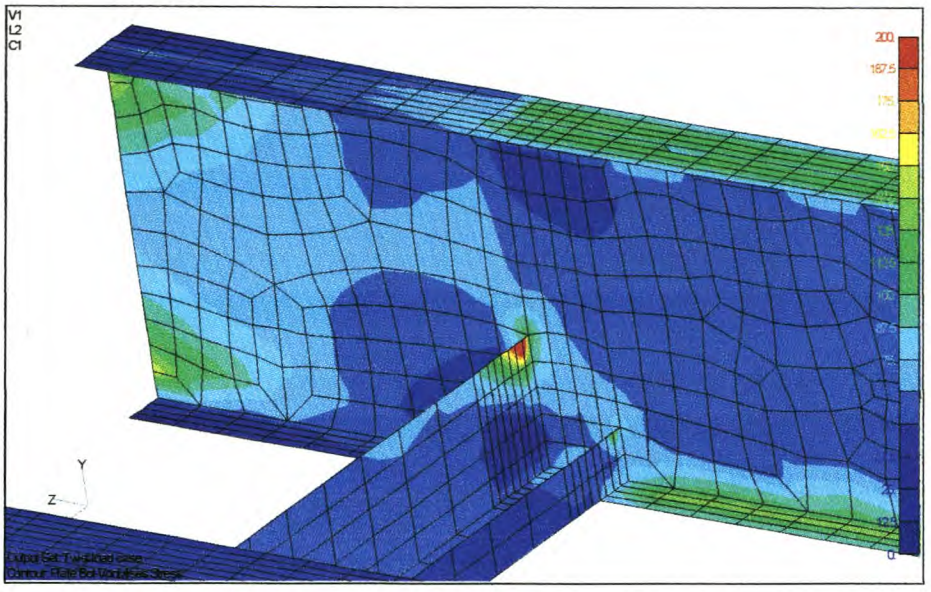

Figure 9.5: Outside stiffener, shear

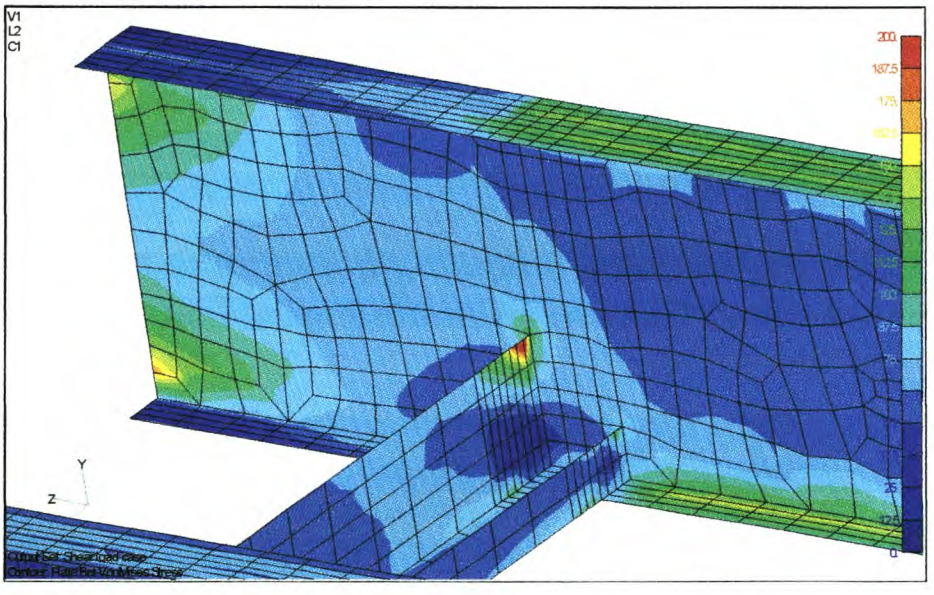

Figure 9.6: Outside stiffener, torsion

Again a stress concentration emerges at the upper, inner corner. For this scenario the maximum stress is lower and not in the I-beam anymore, but transferred to the cross member upper lip. The web stresses for the torsion and shear load case are respectively 111 and 106 MPa. This is a considerable improvement from the first design, especially if the I-beam is already carrying a high shear load.

The third case considered is the fitment of an internal gusset plate. The plate is completely joined to the I-beam, and only edgewise to the cross member. The mismatched element appearance is a plotting algorithm shortcoming.

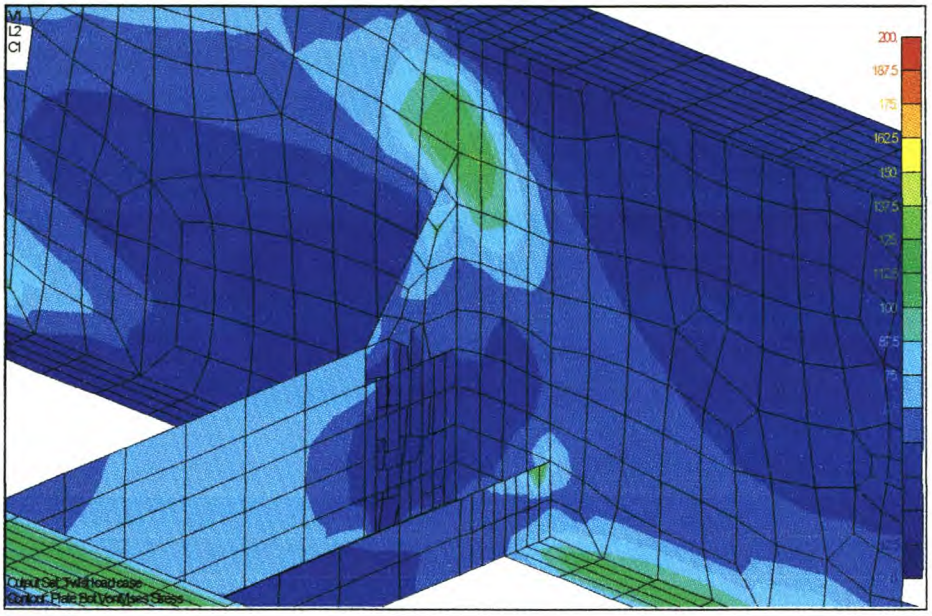

Figure 9.7: Gusset plate, torsion

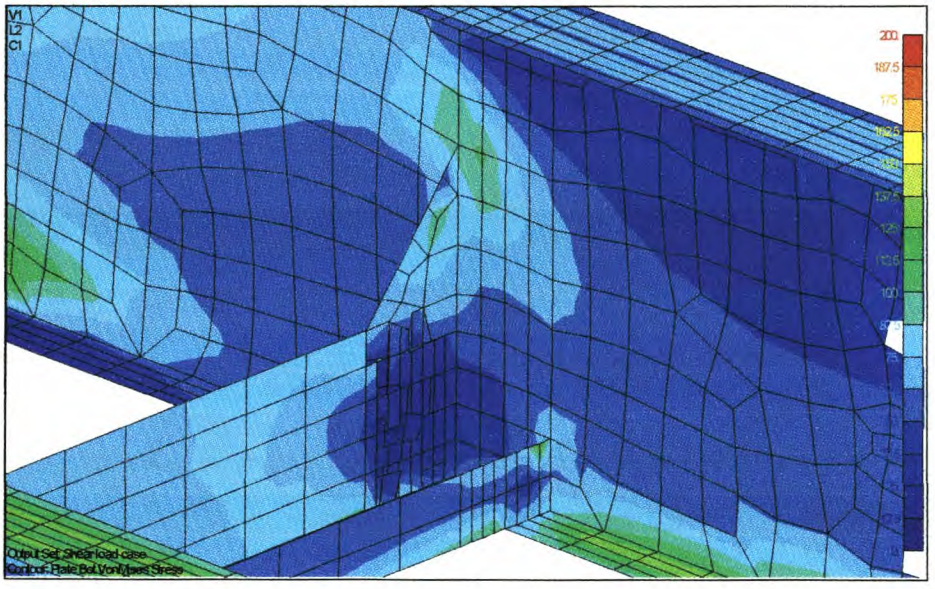

Figure 9.8: Gusset plate, shear

For both load cases the maximum stress is in the web plate, torsion induces 124 MPa and shear 94 MPa.

In the last considered design both the outside stiffener and gusset plate is included. The web stresses drop to 78 and 94 MPa for the torsion and shear load cases respectively. This maximum is not at the upper corner, but rather slightly downwards. Welding at this point will be of a better quality than that around the upper corner. As can be seen in figure 9.9 and 9.10 the maximum stress is in the gusset plate, at 154 and 145 MPa.

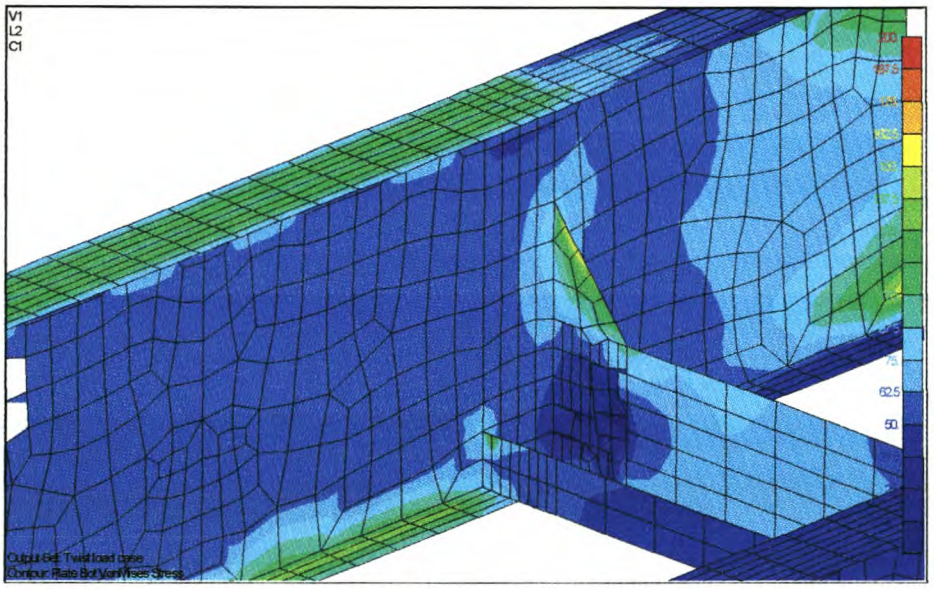

Figure 9.9:Gusset and stiffener, torsion

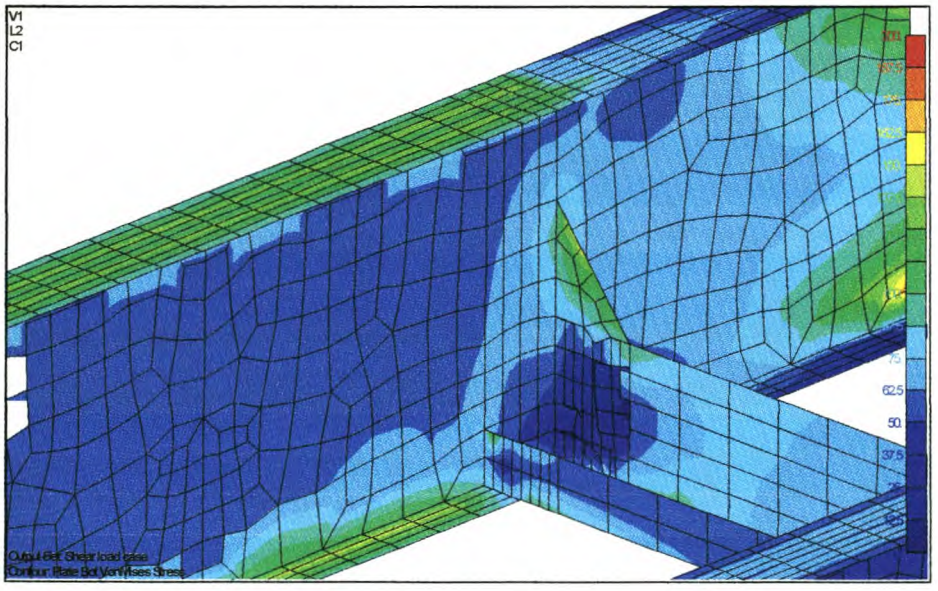

Figure 9.10: Gusset and stiffener, shear

In table 9.1 the four designs are compared. The values in brackets indicate the maximum stress inside the cross member, if it is higher than the I-beam web plate stresses. The mean stress is the sum of the torsion and shear stress compared to the sum of the plain connection design. Clearly the combined gusset and cross member design is the best alternative from a stress viewpoint. This design will necessarily cost more in terms of material and labour hours.

Connection type	Torsion [MPa]	Shear [MPa]	Mean% difference
Plain connection	257	160 (229)	100
Outside stiffener	111 (270)	106 (242)	52
Gusset plate	124	94	52
Gusset and outside stiffener	78 (154)	94 (145)	41

Table 9.1: Cross member maximum stress comparison

Considering the ease with which the outside stiffener can be fitted this seems to be the second best alternative. The mean stress is about 27% higher than that of the gusset plate combined with the outside stiffener design. From a fatigue viewpoint the gusset plate is still the best design since the design is redundant[28].

It is advised that a gusset plate combined with an outside stiffener be fitted at all high load carrying cross members. The gusset plate thickness should be comparable to the I-beam web plate thickness. The outside stiffener should be about 1.5 times the web plate thickness. For cross members where forces are lower, the placement of an outside vertical stiffener is recommended as standard. Actually, the stiffener should be in place whenever there is transverse I-beam loading, be-it from a cross member or any other beam attachment.

---

28 Refer to the fatigue resistance guidelines in the welding chapter

Detailed cross member welding

To investigate cross member connection in more detail a model utilising solid elements was created. The design is of type 4, as indicated in the previous section, with the same dimensions. The applied loading is also the same. With this solid model more detail can be obtained for the stresses at the welding interfaces.

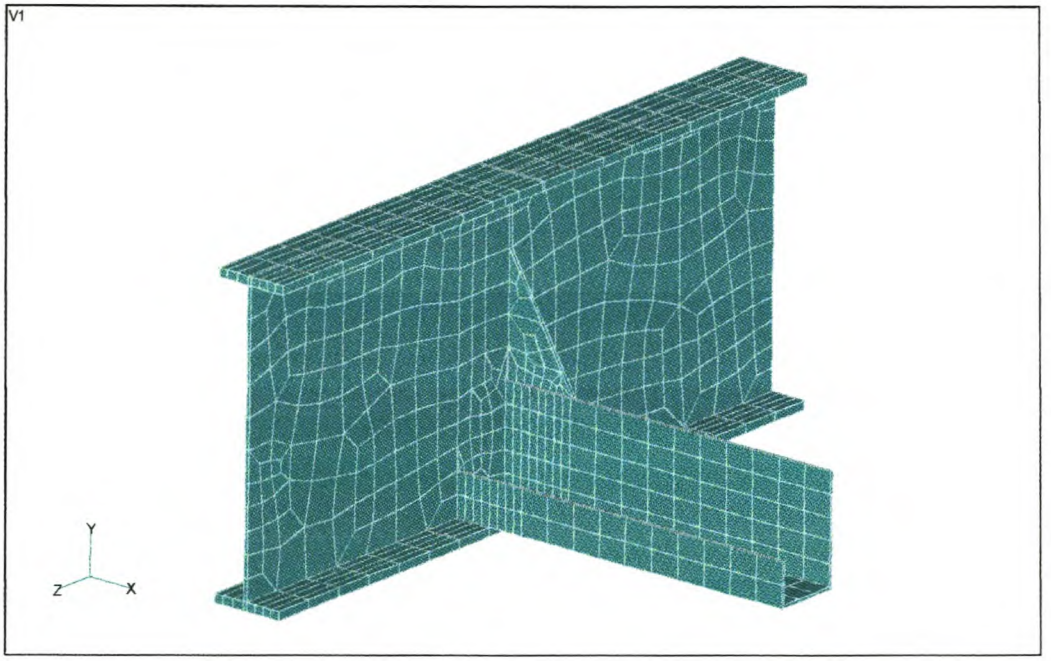

Figure 9.11: Solid model of cross member connection

The maximum stress values show excellent correlation with the analysis above. The stresses are listed in table 9.2 below.

Location	Torsion [MPa]	Shear [MPa]
I-beam web	79	81
Gusset plate	162	147

Table 9.2: Solid model cross member stresses

In figure 9.12 the torsion stress distribution is shown. It's resemblance to figure 9.9 is apparent.

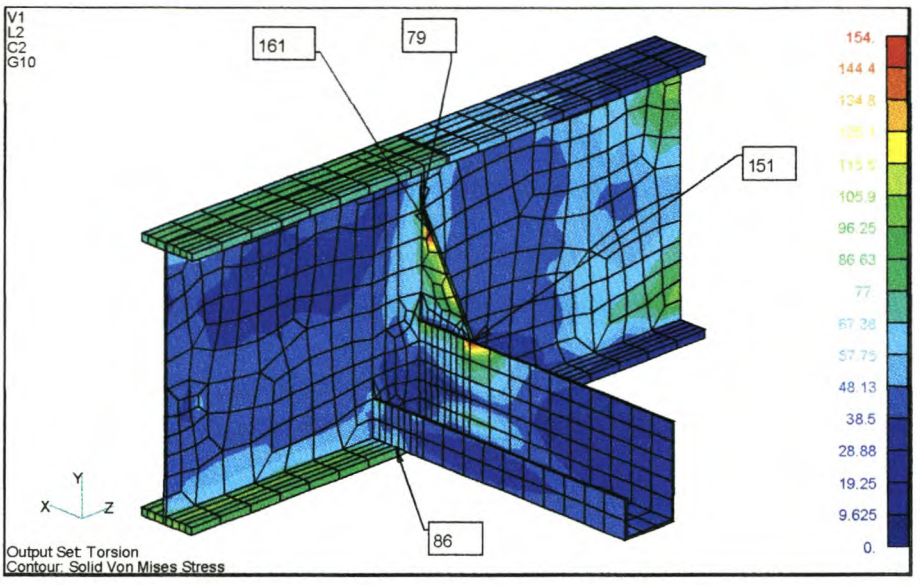

Figure 9.12: Torsion stresses for cross member solid model

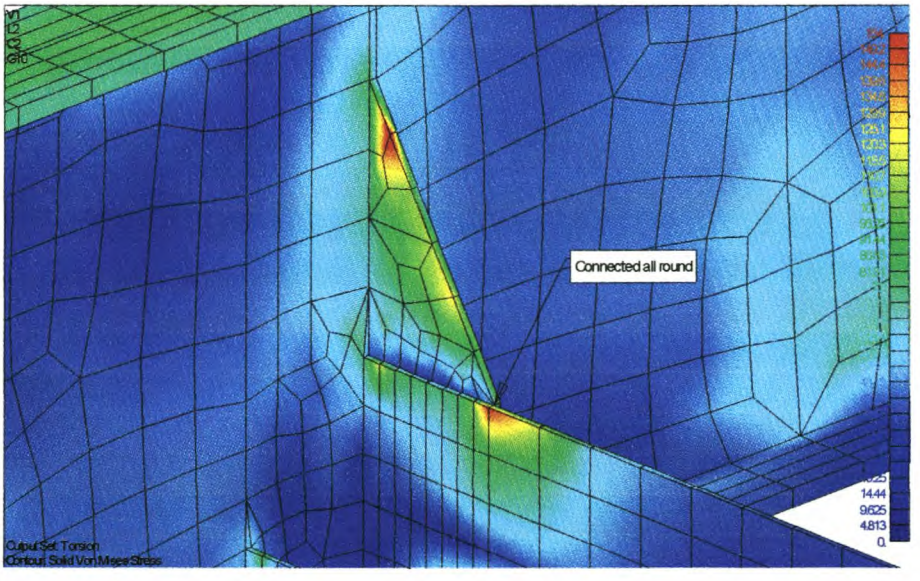

Figure 9.13: Detailed view of figure 9.12

In figure 9.13 it is clear that at the bottom connection between the gusset plate and the cross member itself there is a high stress area. A second modified model is made where the plate is not connected (welded) to the edge.

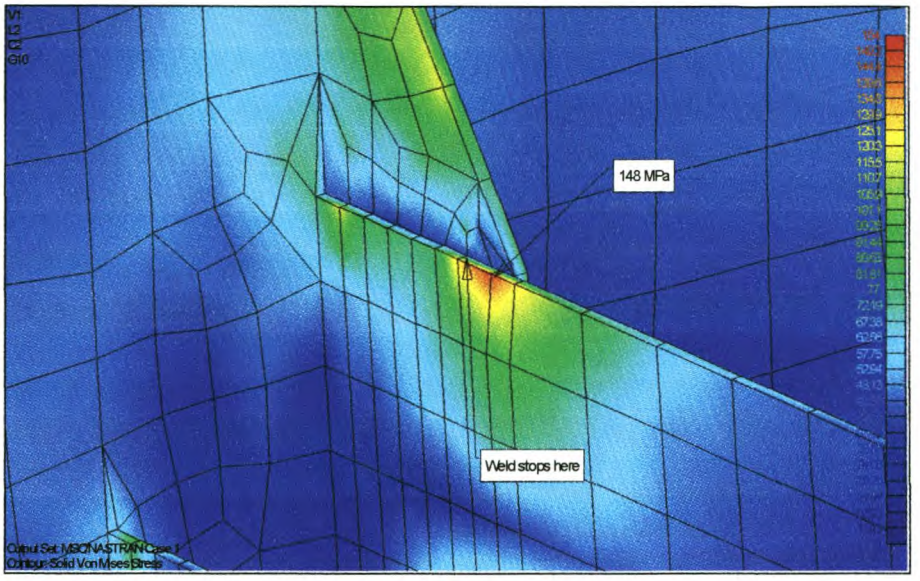

Figure 9.14: Modified gusset plate weld

If the weld is not pulled around the corner, but stopped a distance away, the stresses drop only slightly as indicated in figure 9.14. The big advantage is that the high stress area is now not near a weld.

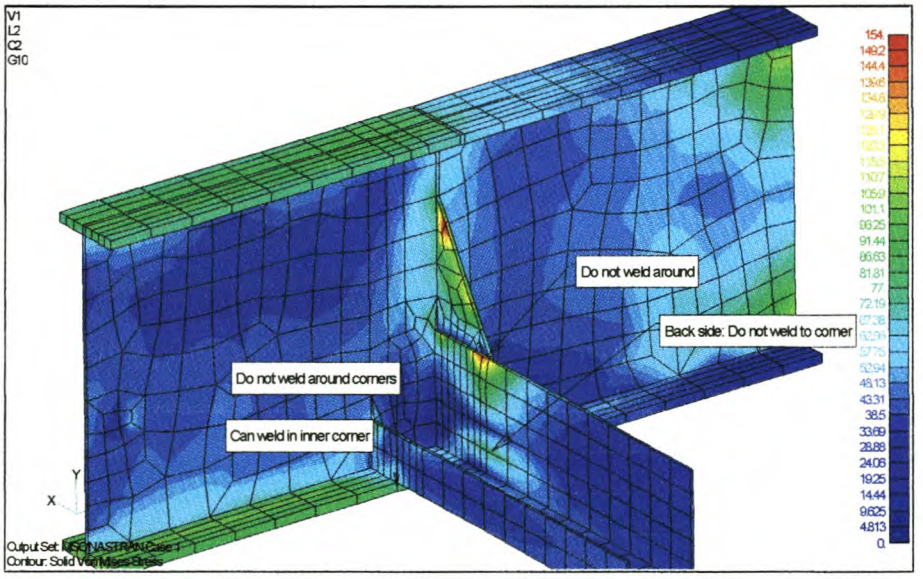

Figure 9.15: Welding directions for cross member joint

In figure 9.15 some design considerations is given as to extend structural fatigue life and increase ultimate construction strength.

Stiffener welding

Another debateable point is whether I-beam web stiffeners should be inserted where the beam is already loaded with a high bending moment. A 4-point bending, e.g. constant bending moment for mid-section, model was created. The stress around the stiffener position is compared with the stress elsewhere. Also the effect of the insertion of a cross member as per the previous section is investigated. At a first glance the stress influence does not appear noticeable.

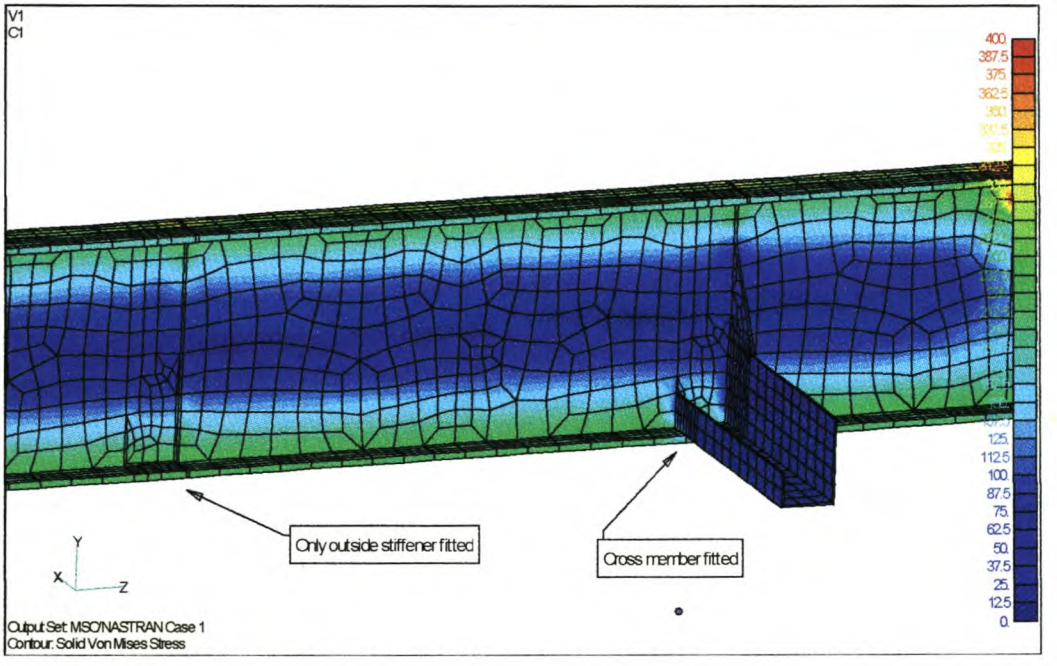

Figure 9.16: Effect of I-beam stiffening

An easy noticeable and undesirable effect however is the unsymmetrical twisting of the beam under a symmetrical load. Viewed at a slight angle from the front this twisting is clearly visible, figure 9.17. To prevent this in plane twisting of the I-beams, stiffeners must be placed on both sides of the web.

At closer inspection the stiffeners do however also induce negative stresses influence. If the stiffener is welded to the bottom flange there is an effective stress increase as

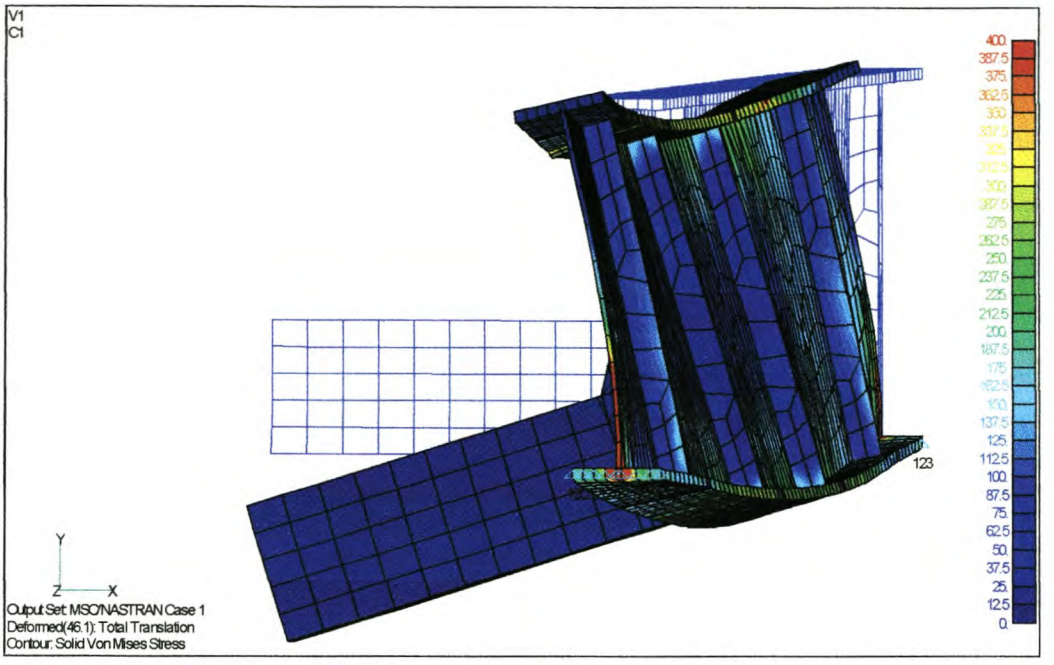

Figure 9.17: Twisting of I-beam due to unsymmetrical stiffener placement

visible in figure 9.18. The von Mises stress in the bottom flange increases with 10.9%. The welding around the stiffener bottom flange further also decreases the allowed stress, changing the allowed stress values form condition A to C according to the AWS code. This is a drop of 75 MPa. The effective change is therefore 40.23%.

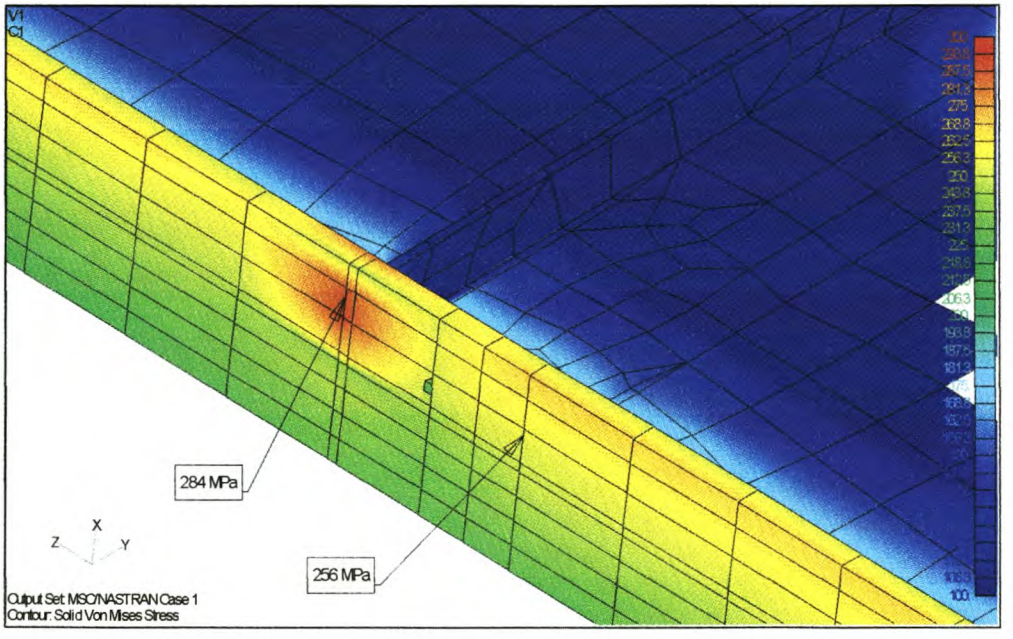

Figure 9.18: Adverse effect of stiffener on I-beam bottom flange

This is a high price to pay for web stiffening. In the top flange the effect is not as problematic since the flange is under compression, and fatigue failure not that likely.

The AWS advises that the stiffener be cut short from touching the bottom tension flange for fatigue applications. This will still absorb the web loading without the negative flange stress influence. An analysis was done to investigate this and as could be seen in figure 9.19, there is no flange or web stress increase.

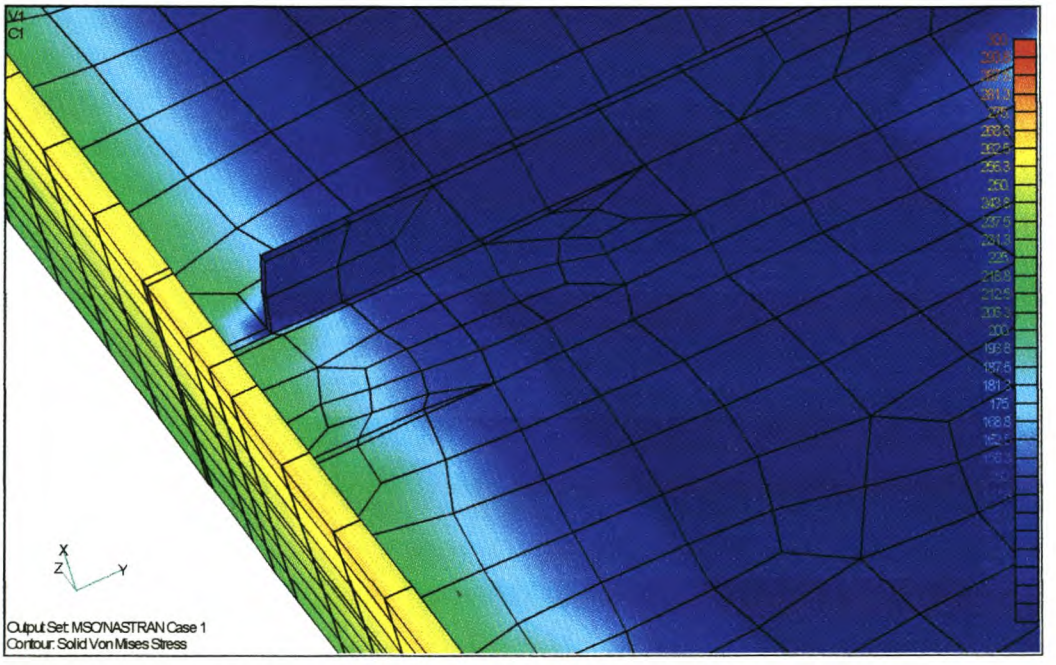

Figure 9.19: Stiffener cut short from bottom flange

This method of stiffener welding is however not common in semi-trailer chassis manufacturing, and there might be some negative implications. On the other hand it might be that it just was not implemented up to now.

I-beam top flange

To investigate possible weight saving the top and bottom I-beam flanges were changed from 12 mm to 8 mm material. For comparative reasons the analysis is done on the chassis-only model. Only the bending mode is investigated since this induces the highest stresses in the structure near the point of interest. Figure 9.20 and 9.21 are close-up views of this area.

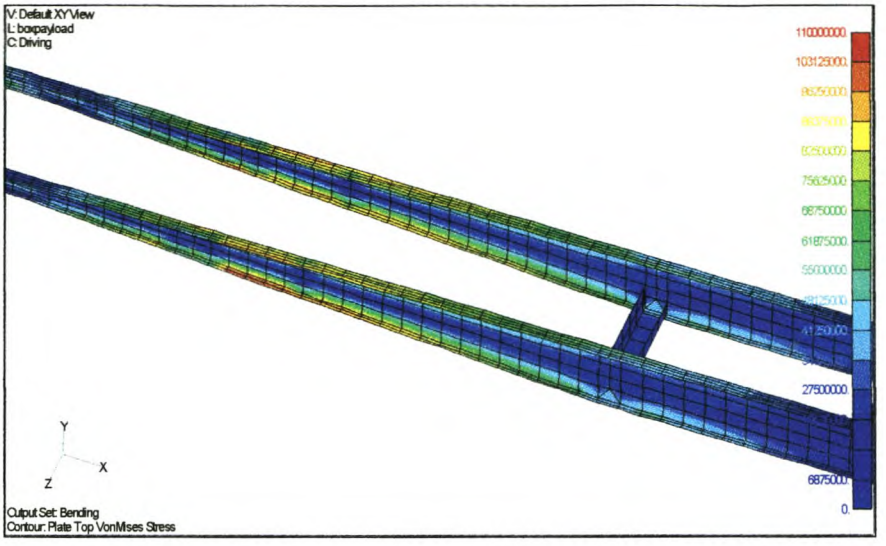

Figure 9.20: Original chassis, bending load

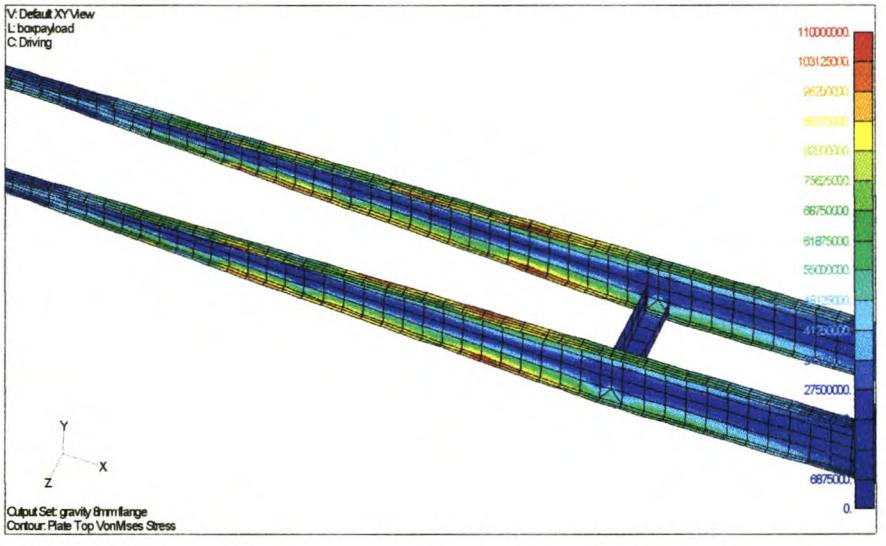

Figure 9.21: 8 mm flange material, bending load

Even though the position of the peak stresses does move backward the actual peak values increases with less than 10%. The change to 8 mm flange material is definitely an alternative to consider. Care must just be given to flange joints and that joint surfaces are not in line.

Side to floor panel joint

The current design is as shown on the right-hand side of drawing 9.22. For this configuration only exterior aluminium cappings are placed over the interior wood, steel and fibreglass assembly. Not only can this assembly method easily lead to misalignment, and insufficient bonding strength, it is also time consuming. If an extruded section, which will closely fit on both sides of the floor and side panels, are used the combined strength are considerable higher. Also from a manufacturing process there is a lot to gain. Not only is assembly time less, but quality will increase as well. Finite element models were created to compare the two designs from a strength viewpoint.

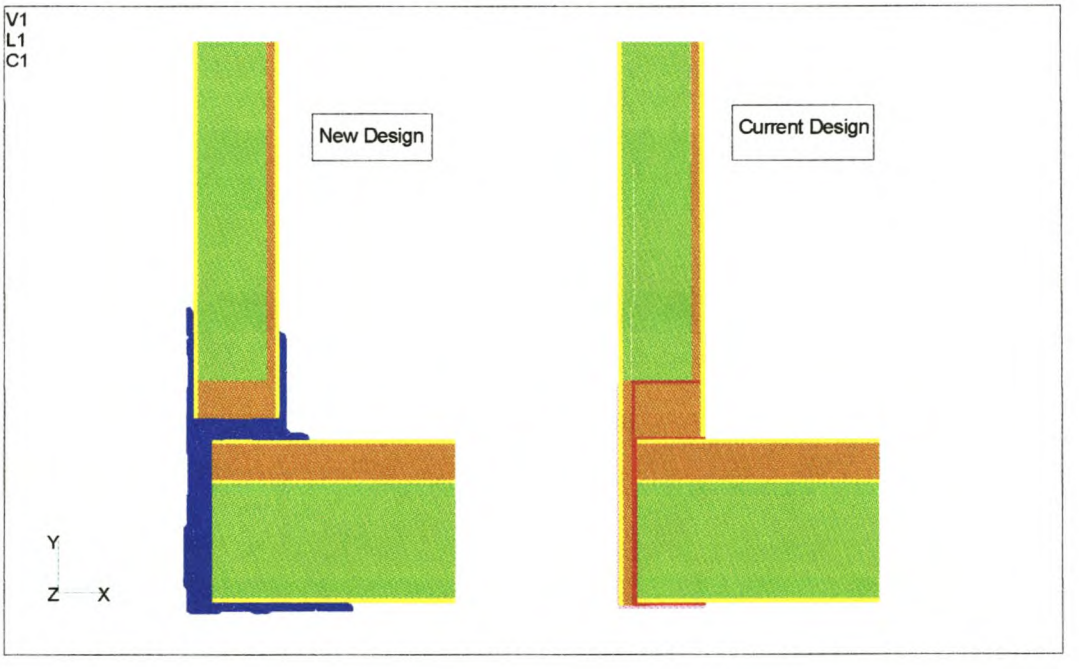

Figure 9.22: Corner assembly FEM comparison

Legend for above figure:

Blue:	Pultrusion
Green:	Polyurethane Foam
Brown:	Wood
Yellow:	CSM Skin

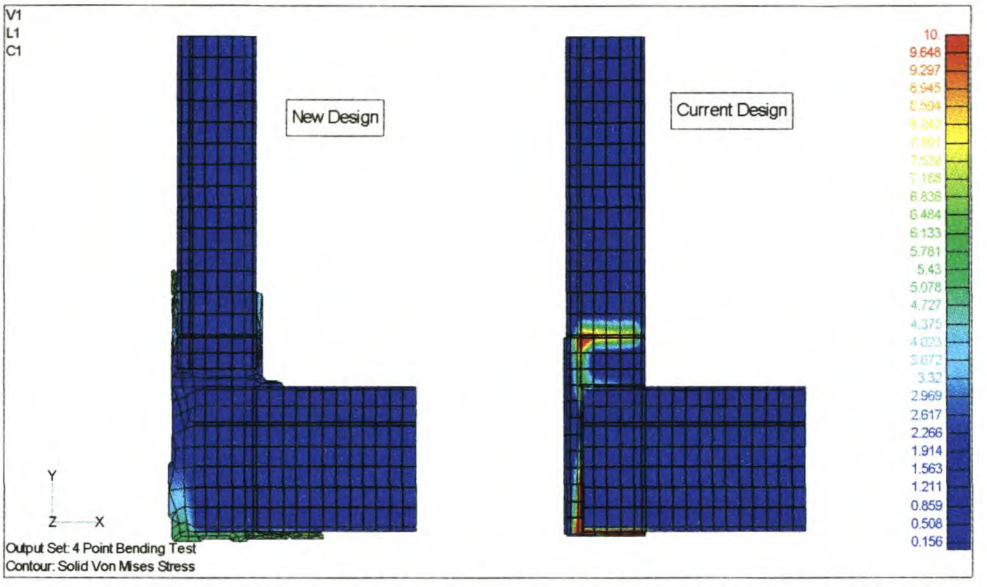

Figure9.23: Stresses in side to floor connection

The stresses in the new design are far superior to the current design. Not only are the stresses of a lower magnitude, the distribution are also better. Where the previous high stressed areas were at bonded surfaces, the new design move this stresses to the outer fibres. The high stresses are also away from pop-rivet joints. The internal high stress area of the current design is also effectively removed.

If fibreglass pultrusions are used it is guessed the cost for a die of this nature would be in the vicinity of R25 000 to R30 000. As with the floor beams this cost will be recovered rapidly given the labour savings, and decrease in warranty costs. The same section used for the floor to side panel connection can also be used for the side to roof connection.

Chassis outriggers

A design modification that is already implemented is the placement of outriggers beneath some of the box main floor beams. It is believed that these outriggers will improve the transfer of torsional loading and reduce the high floor stresses at the king pin location. The complete finite element model is used to analyse this concept. In total seven floor beams are supported on both sides with 4 mm folded beams. Two pairs are placed at the front and rear beam locations and the other five pairs spaced as

evenly as possible between them. The outriggers are tapered for weight saving and aesthetic reasons.

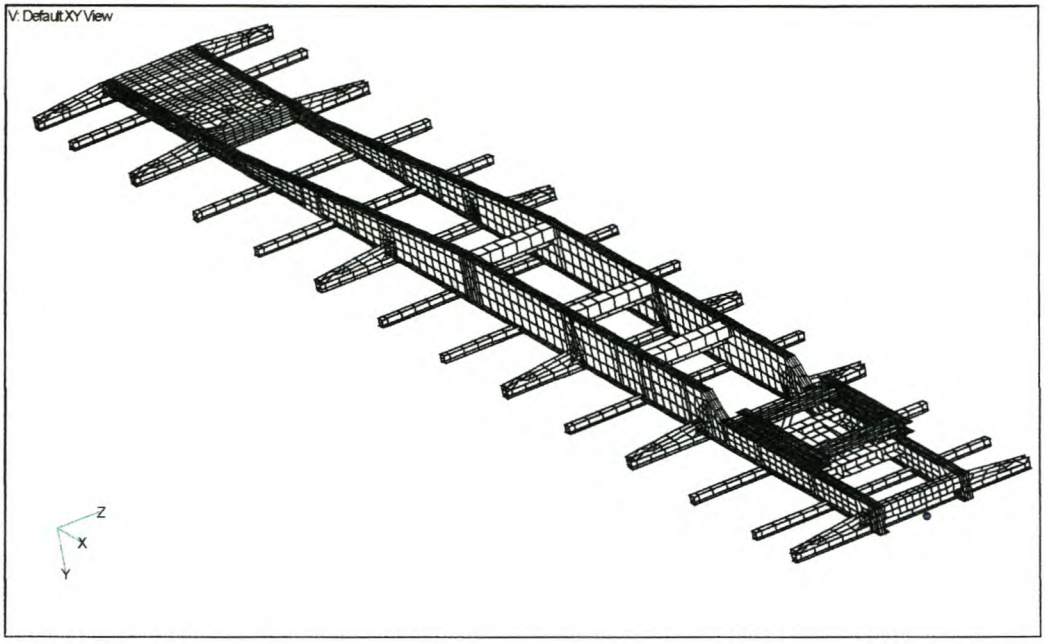

Figure 9.24: Chassis showed with floor beams and outriggers

In figure 9.24 the placement is shown. The same beam shape is used for all the outriggers. Two other structural changes are also incorporated into this model. A neck diffuser plate is fitted, together with thicker web plates.

Only gravity and torsion load cases are considered for this investigation. For the gravity load case the outrigger most heavily loaded is the second, or king pin outrigger. In the model this outrigger was not welded to the bottom flange, and the complete load is transferred through the web fillet welds. Stresses in this outrigger is high, but still acceptable since they are not located near a welded joint. The effect the outriggers have on floor stresses is significant. If figure 9.25 and 9.26 are compared there is a reduction of 24.7% in the wood floorboard stresses for the gravity load case.

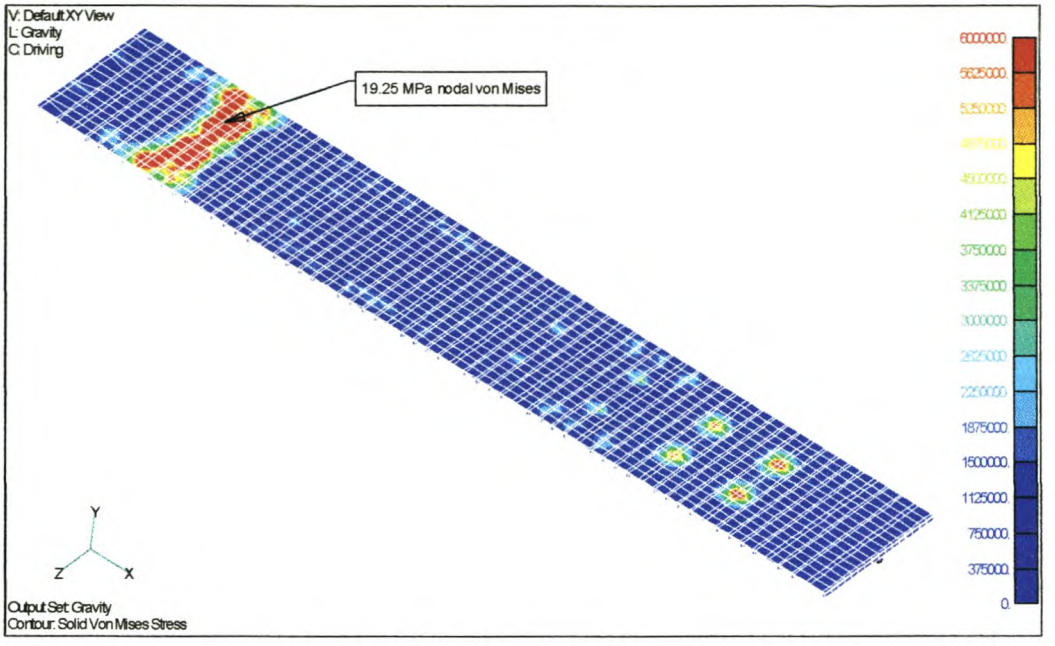

Figure 9.25: Stresses in wood floorboards, without outriggers

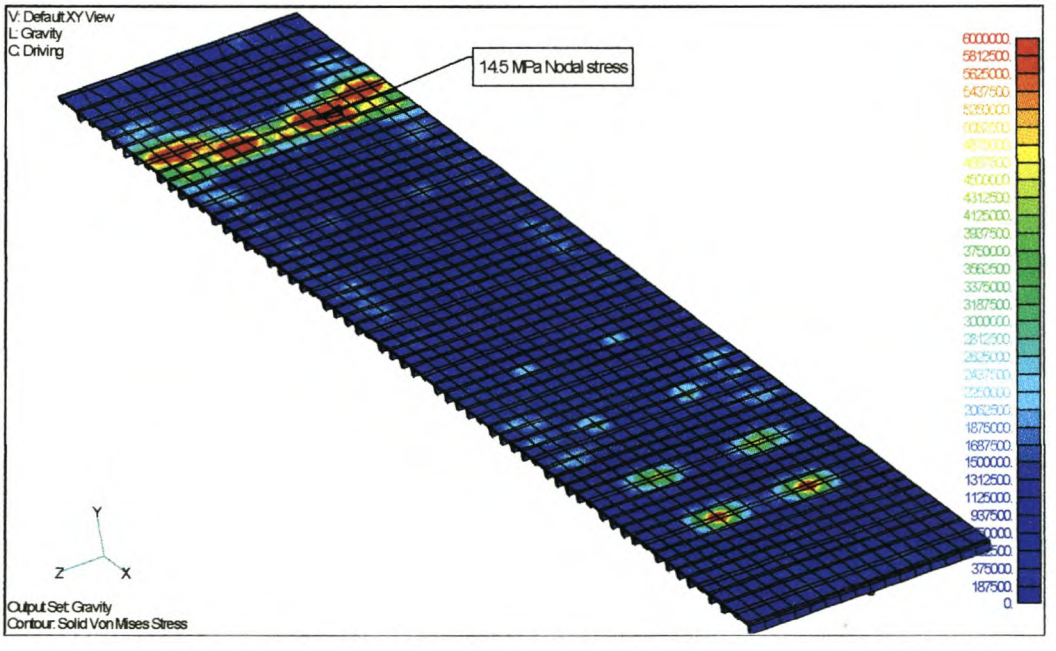

Figure 9.26: Stresses in floorboards with outriggers fitted

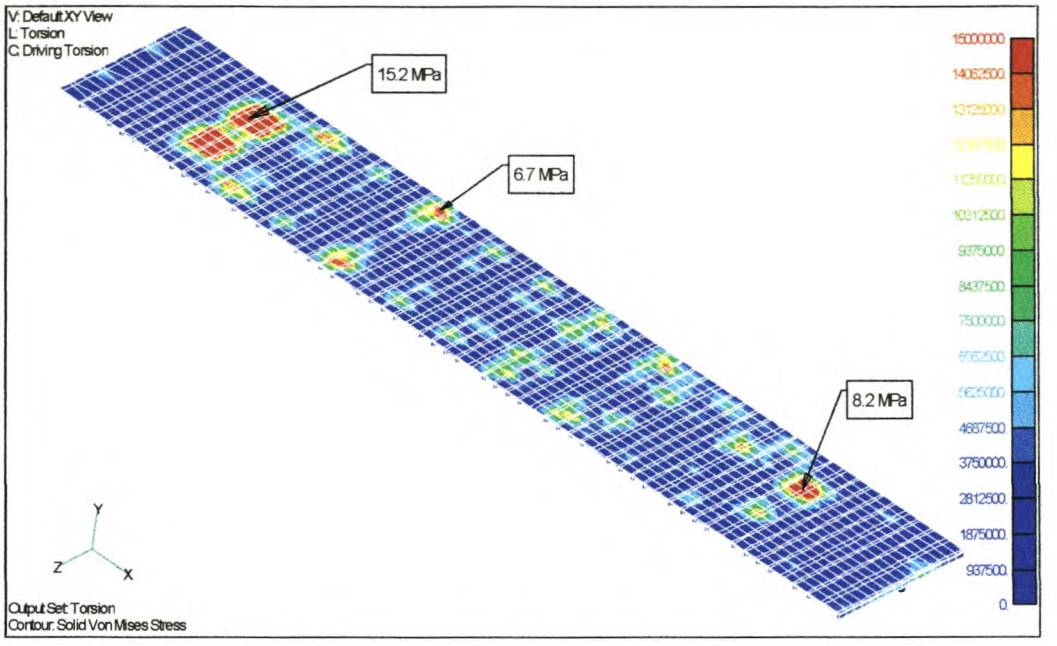

Figure 9.27: Floorboard stresses for original design, torsion load

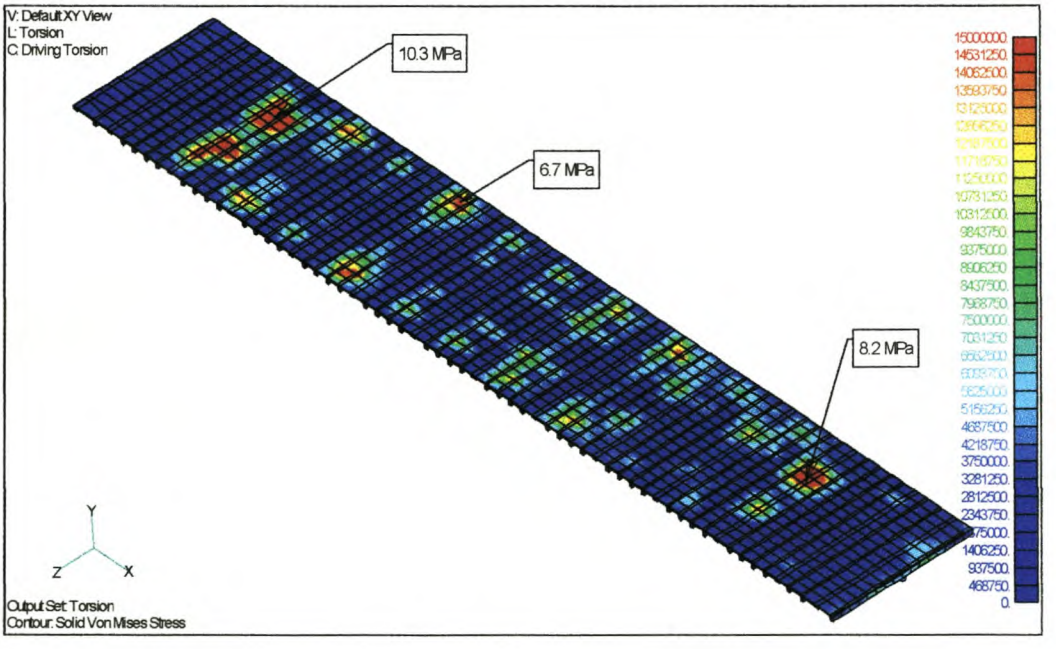

Figure 9.28: Floorboard stresses with outrigger, torsion load

For the torsional loading the stress also reduces, with 32%. In the side, roof and rear door panel the effect of the outriggers is noticeable, but only to a small degree. In the front bulkhead however the effect is significant for both the gravity and torsion load as is visible in figure 9.29 and 9.30.

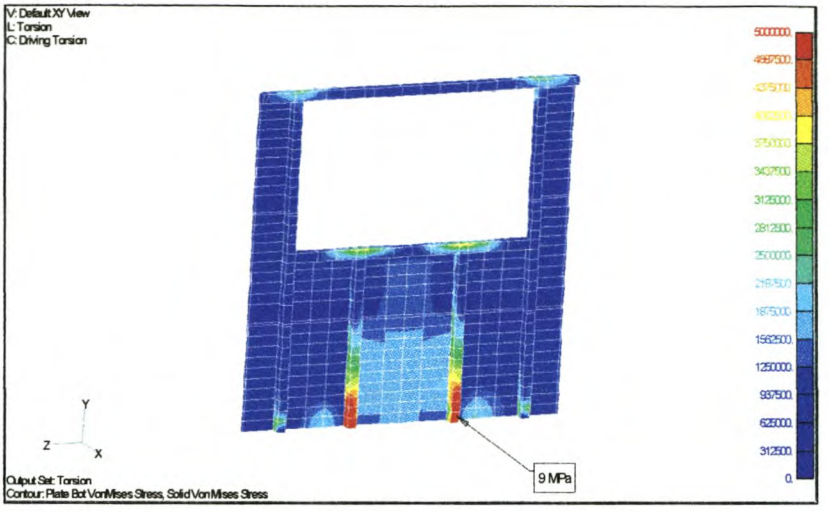

Figure 9.29: Bulkhead stresses for original design, torsion load

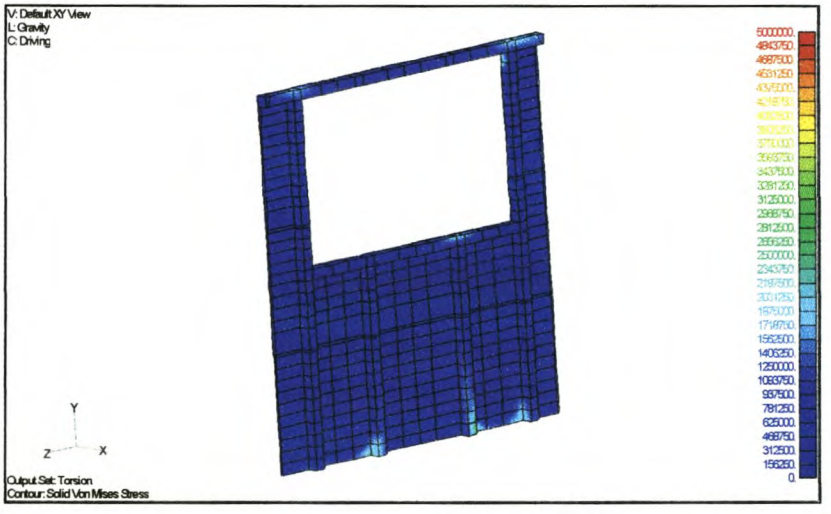

Figure 9.30: Bulkhead stresses with outriggers fitted, torsion load

Considering the above stress reductions the use of outriggers is advised. For the 7 pairs as indicated above the total added weight, excluding welding, is about 80 kg. It might be better to alter the manner in which they are distributed. Those that are at the front and rear positions can stay in place. One more pair need to be inserted near the king pin area to further distribute floor stresses. Those further down the chassis can be omitted to save weight.

Even though the stresses within a outrigger are low it is not advised to use plate material thinner than 4 mm. The use of aluminium bolted to the I-beam is possibility

to further save weight. Even though the aluminium is far more flexible than the steel it is still considerably stiffer than the wood and GRP material used for the box construction.

Chassis only analysis

For estimate strength calculations it is often assumed that the GRP box section doesn't contribute to the overall vehicle strength. The chassis is assumed to be the only load-carrying member. To evaluate this approach the results of the complete finite element model is compared to a chassis only model. The load is applied as a distributed load on all the upper I-beam flange nodes. Together with the payload of

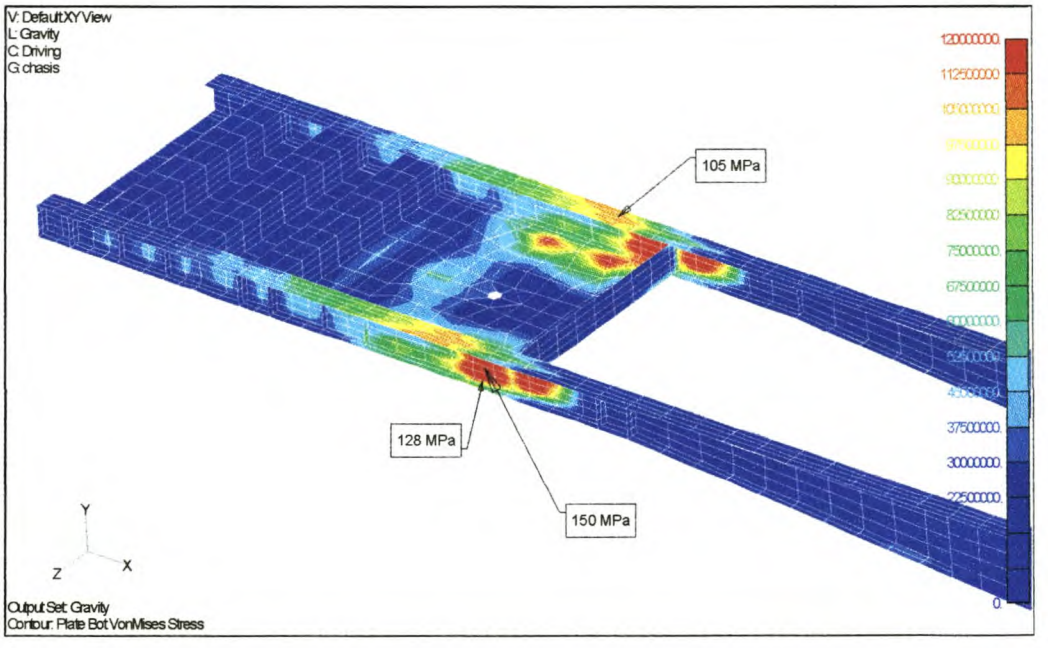

Figure 9.31: Complete model neck analysis, gravity load case

30 000 kg, the weight of the GRP box section of 4 561 kg is added. Only the gravity and torsional load cases are compared. From figures 9.31 and 9.32 it can be seen that the absolute stress values are not much different between the estimate and full analyses. For the three stress measurements the average difference is 8%. The positions of the maximum stresses do however differ. The estimate analysis is conservative, and for general design verification the stresses seem realistic.

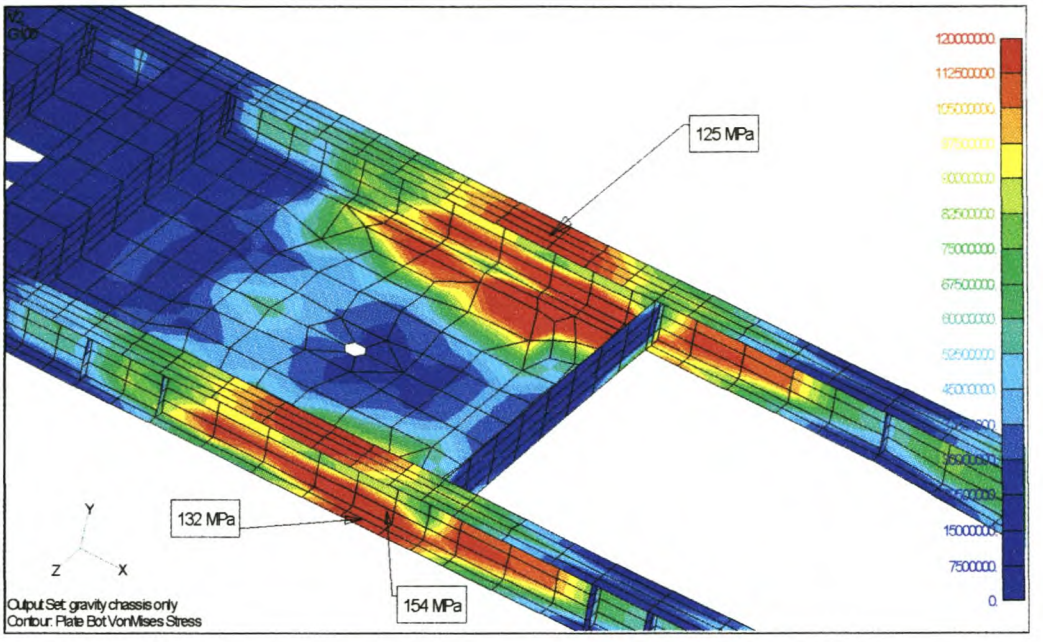

Figure 9.32: Estimate model neck analysis, gravity load case

Considering further that the chassis only model takes 3 minutes to analyse versus the 2 hours for the full model, the results are indeed helpful if minor chassis modifications need to be investigated.

If total chassis deflection is considered, the result starts to differ considerably. For the full model the mid-chassis deflection was just over 3 mm. For the estimate model it is 32 mm. Also the mid-span stresses for the I-beams are higher, as seen in figure 9.33. Apparently the GRP box section greatly stiffens the semi-trailer in bending. Considering this, the estimate model cannot be used for accurate chassis deflection calculations.

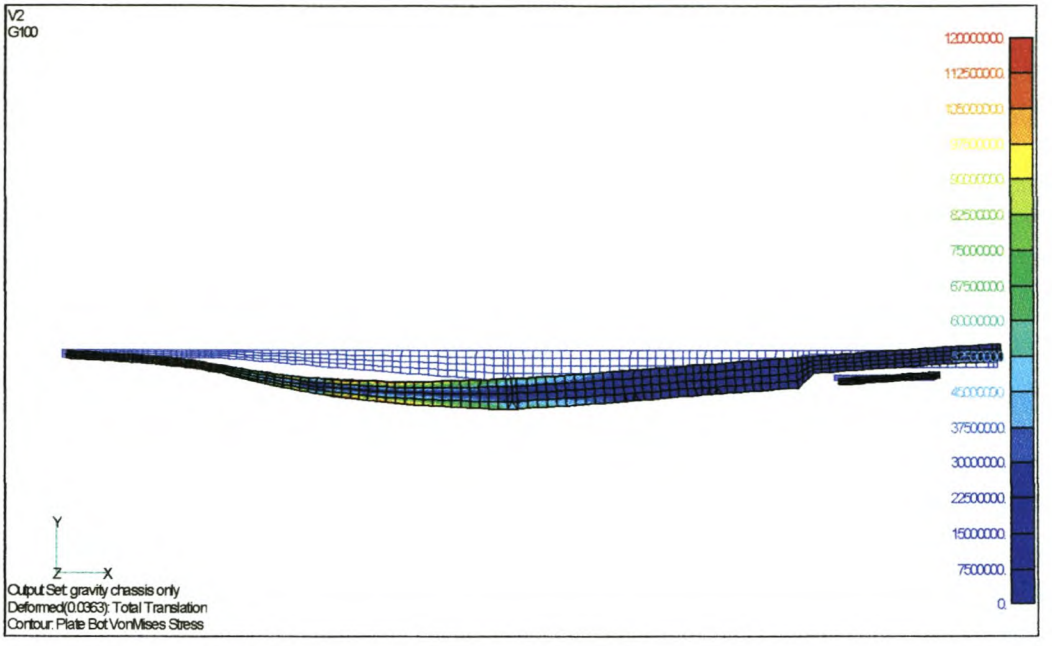

Figure 9.33: Estimate analysis chassis deformation

For the torsional load case the overall stress pattern is also similar, but the values differ more than that of the gravity load case. Considering the same three measuring points as for the gravity scenario the maximum stress is 21% lower for the estimate

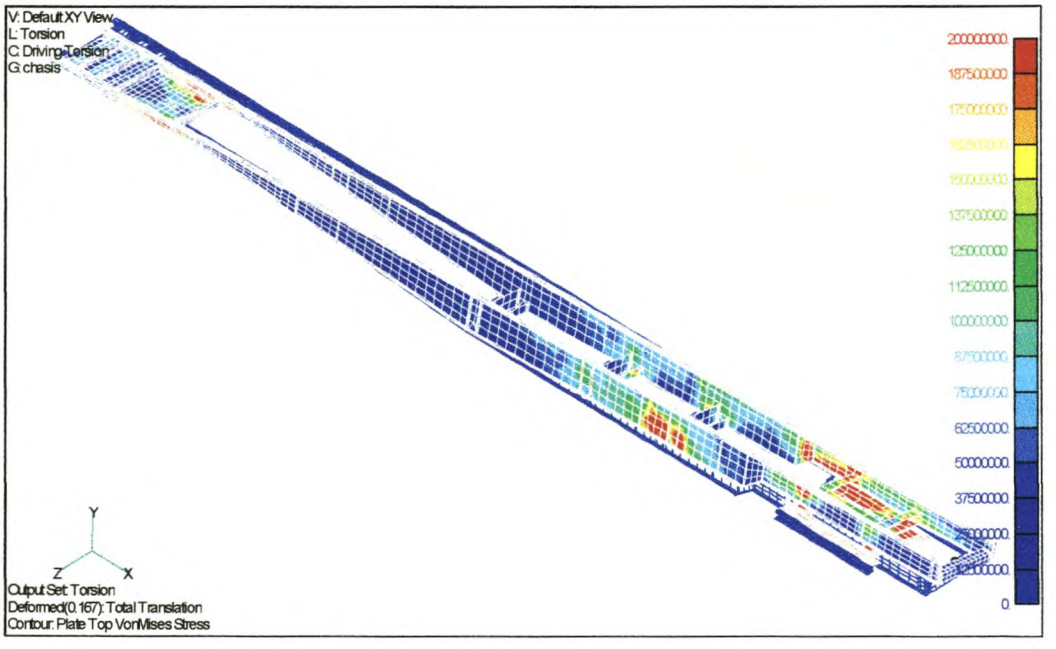

Figure 9.34: Full model, chassis torsional stresses

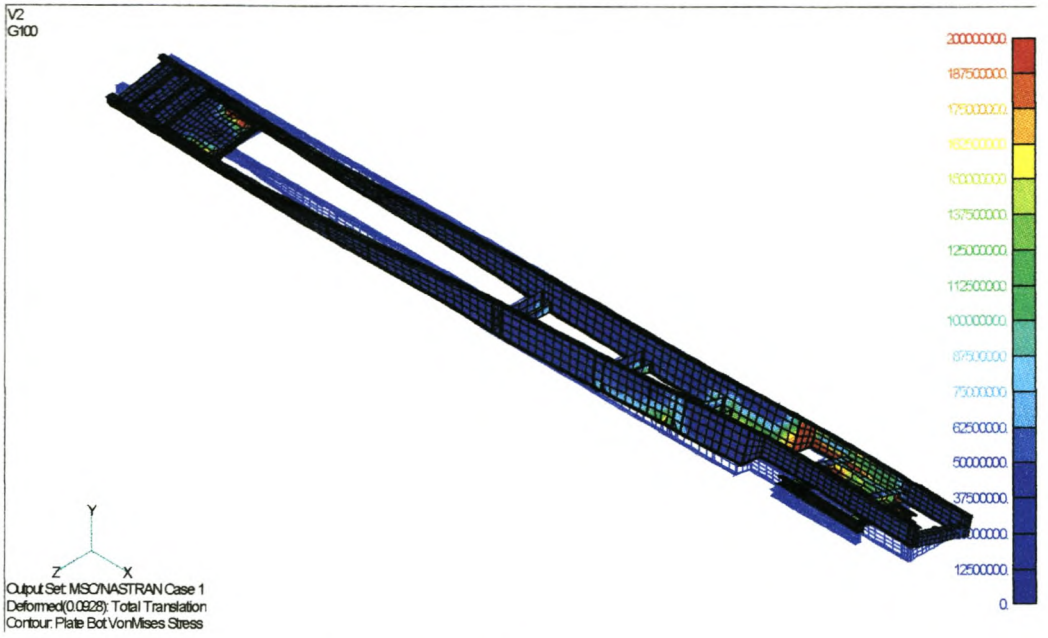

Figure 9.35: Estimate model, chassis torsional stresses

analysis. For comparison, the values are listed in table 9.3 below.

Location	Full [MPa]	Estimate [MPa]	Difference [%]
Neck flange	258	192	-25.58%
Neck web	360	257	-28.61%
Apron plate	348	311	-10.63%

Table 9.3: Stress comparison

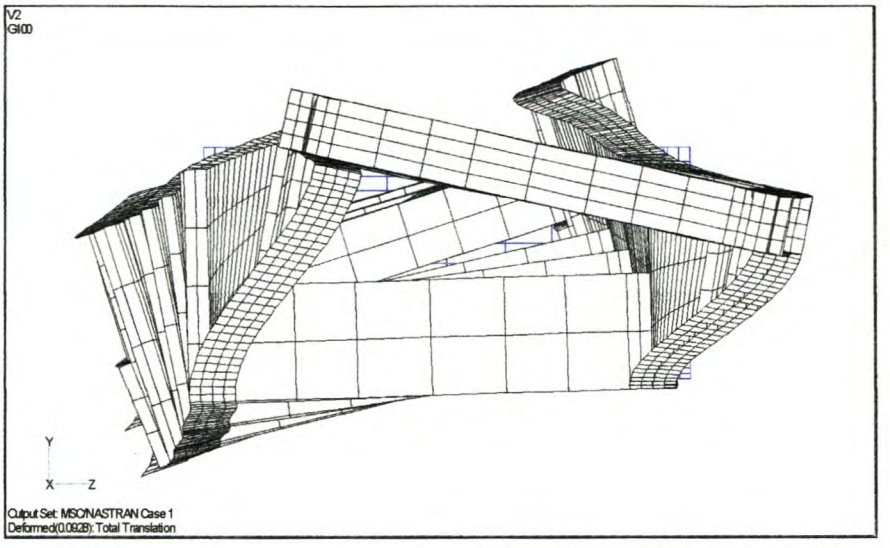

Figure 9.36: Chassis deformation for estimate model, torsion load

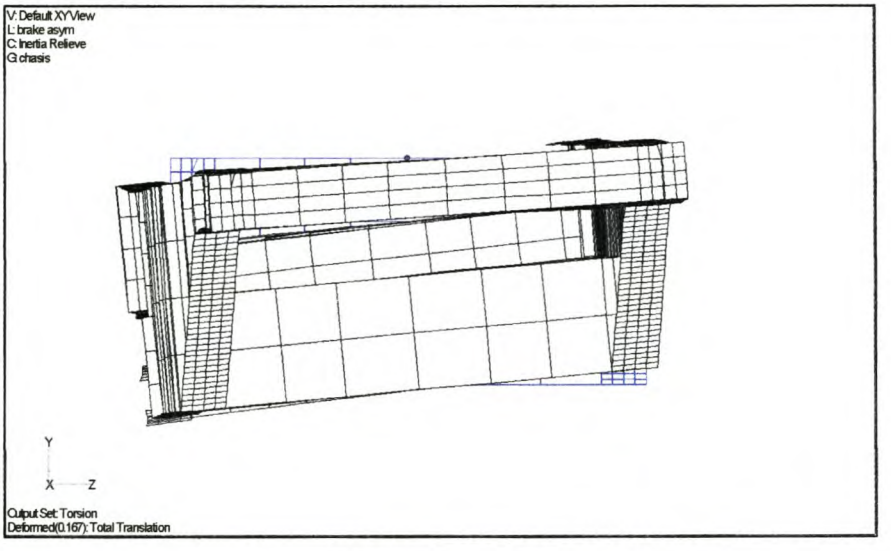

Figure 9.37: Chassis deformation for full analysis, torsion load

For the torsion load case chassis deflections are completely different. The refrigerated box does not only change the deflection values, but also the direction as indicated in table 9.4 below.

Position	Full [mm]	Estimate [mm]	Difference [%]
Front curb-side	16.82	- 28.20	-267.66
Front off-side	-17.60	+ 34.38	295.34
Rear curb-side	16.82	+ 52.38	211.41
Rear off-side	-26.03	- 27.81	-6.84

Table 9.4: Displacement comparison

As for the gravity load case it can be concluded that the estimate model cannot predicts chassis torsional deformation. Also from these analyses it is clear that the GRP box section have a great influence on torsional stiffness, but due the major material stiffness difference the chassis is the main load carrying member.

Neck reinforcing

To reduce the stresses within the neck area, various structural changes are investigated.

The first modification is the fitment of a stress diffusing plate between the two I-beam top flanges above the king pin area. In figure 9.38 a proposed design is shown, viewed from the upper rear. This 5 mm plate is welded with butt welds between the two I-beam flanges.

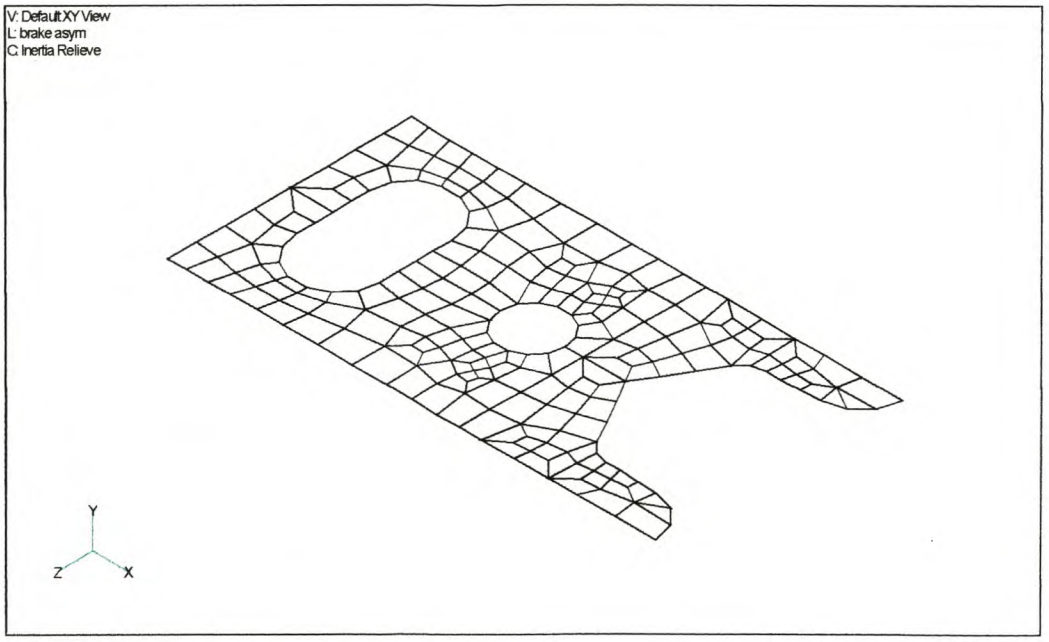

Figure 9.38: Neck stress diffusing plate

It was hoped that the insertion of this top plate will reduce stresses in the GRP floor boards which showed excessively high values. The plate did however not reduce the floor stresses to a great extent. In the wood the von Mises stress only dropped with about 1 MPa, or 6%.

In the chassis the reduction in stress is however marked. If figures 9.39 and 9.40 are compared, the effect of this modification is clearly visible. The stress within the diffuser plate is low, except for the one location at the cut-out.

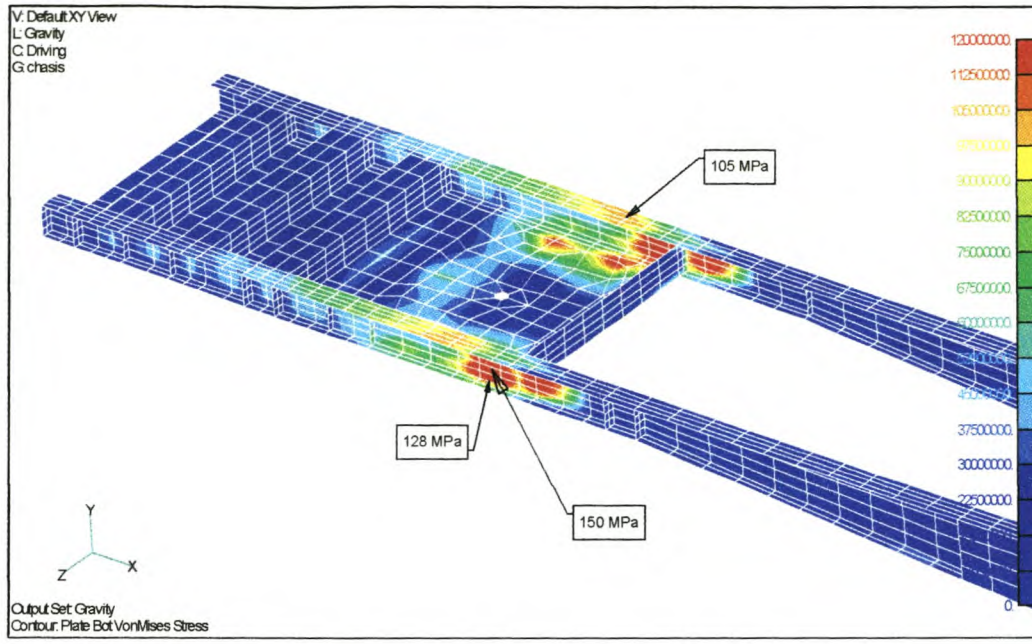

Figure 9.39: Gravity neck stresses for original design

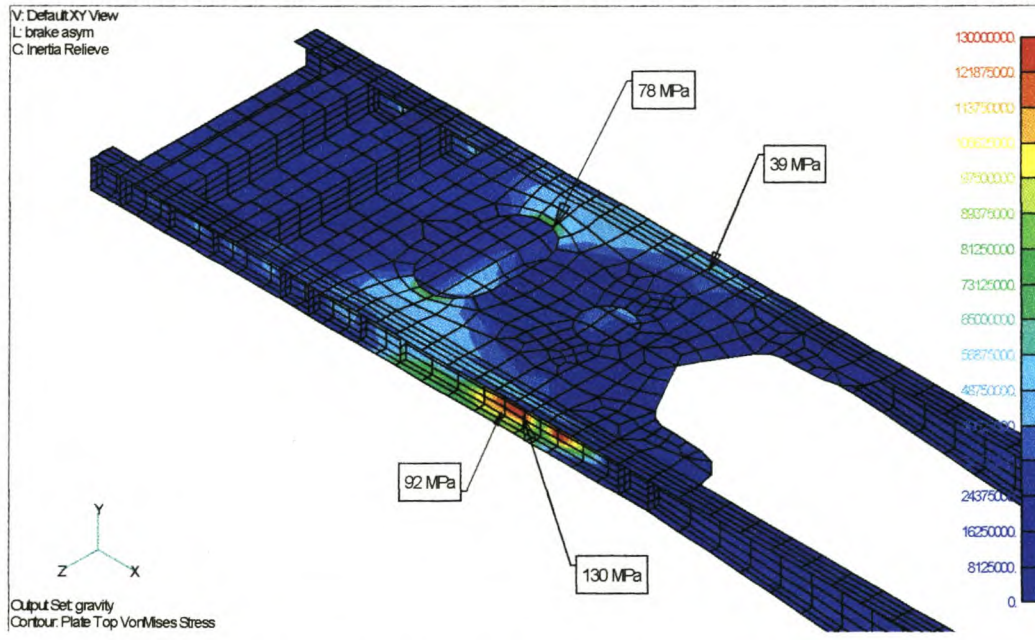

Figure 9.40: Gravity neck stresses with upper diffuser plate

The reduction of stress in the upper flange is remarkable. The weight of this diffuser plate is 40 kg, excluding welding. The standard method of neck reinforcing is to add a doubling strap. Considering weight, 40 kg is equivalent to a 3.5 m length of 120×12 mm flat bar. This length of flat bar cannot reduce the stress so effectively, keeping fatigue and weld quality in mind. The cost of the diffuser plate is low. It can be manufactured from 300 WA and furthermore it doesn't have to be cut out of one plate. The stress is sufficiently low to allow for welded joints in the plate itself.

Considering the small effect the chassis modification has on floor internal stresses, further neck analyses are done on the chassis-only model to save analysis time.

Since the diffuser plate successfully decreased upper flange stresses, a modified neck assembly is constructed where there is a gradual change of the apron plate assembly as well. The profile of the upper diffuser plate was also changed. Evidently the change led to considerable stress increase, as per figure 9.41.

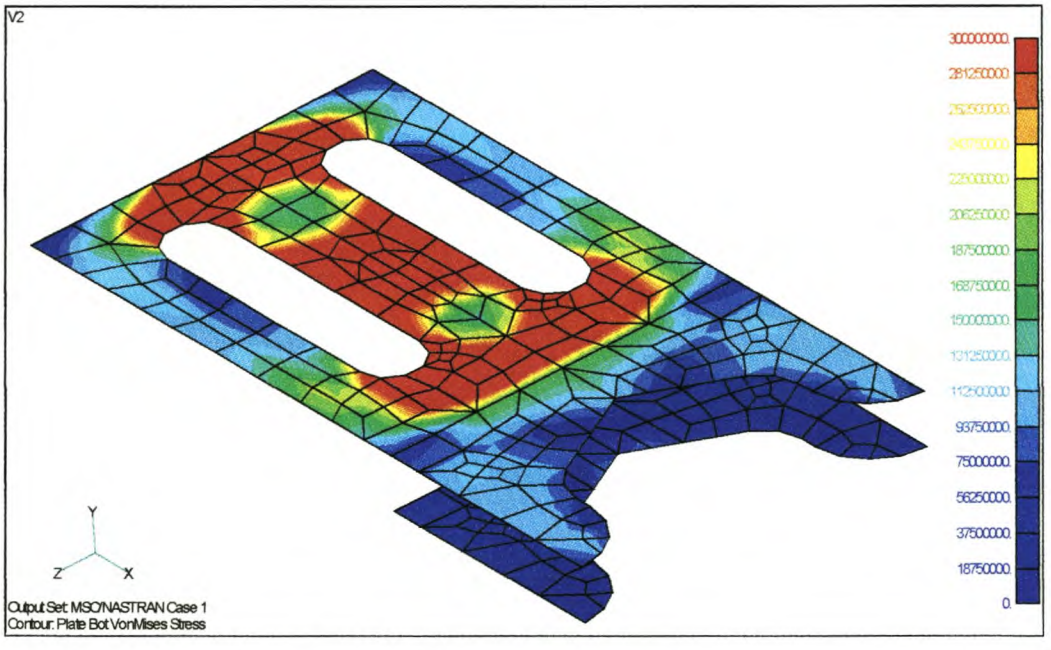

Figure 9.41: Modified neck, inappropriate diffuser plate design

The profile was changed again and this time the results were more favourable. As indicated in figure 9.42 the plate thickness for the rear section was changed to 8 mm.

The total added weight is 64 kg. Compared to the stress values of the original design, as per figure 9.42, the changes are definitely advisable.

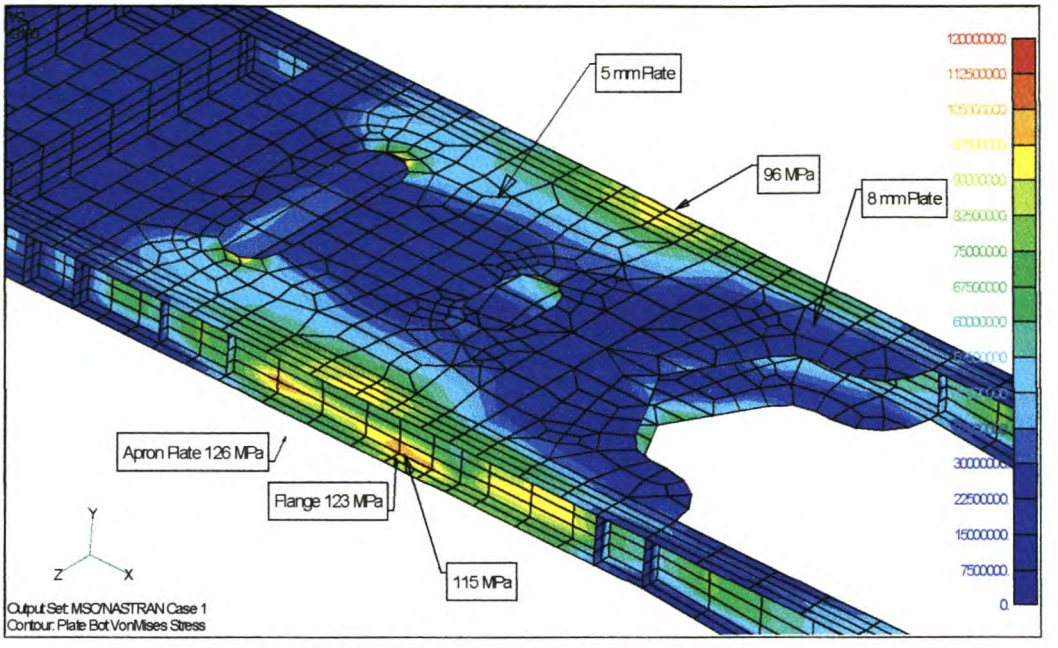

Figure 9.42: Modified neck area, gravity load

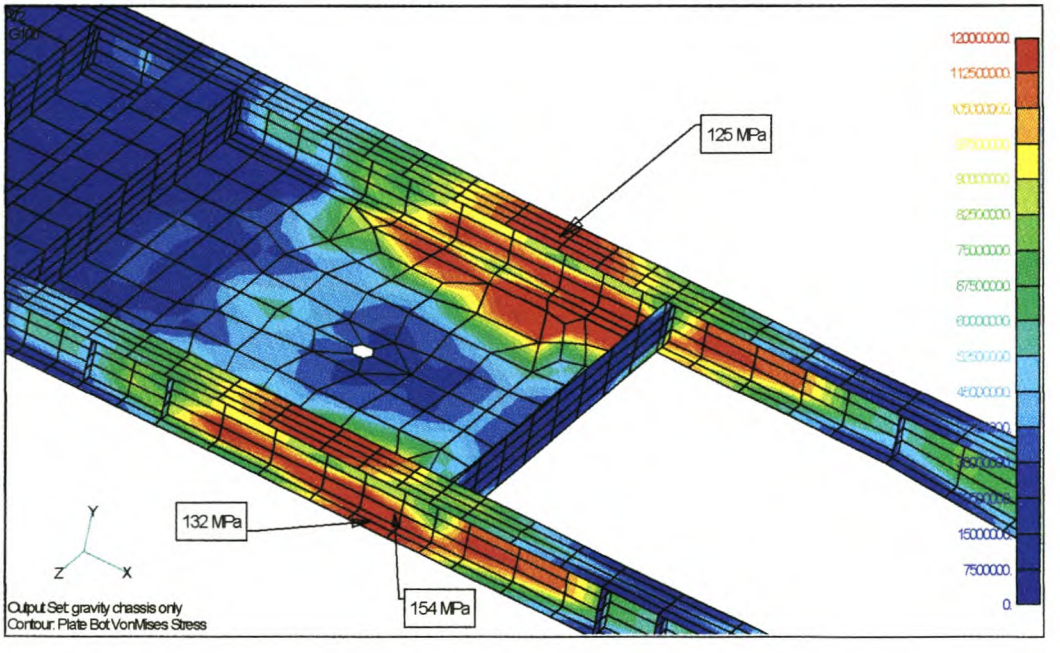

Figure 9.43: Original neck area, gravity load

In a third analysis the shape of the top diffuser plate is changed again to save weight, furthermore the I-beam web is made of thicker material. Stiffeners are also inserted

in high stress areas to absorb web shear stresses. The legend levels for figure 9.43 is the same as for 9.41 and 9.42. The reduction in stress values is obvious. An area that is still overstressed is the apron plate itself. As mentioned earlier the slewing ring support is not included in this model. It is believed that the stiffening effect of the slewing ring will reduce the stresses in the apron plate to acceptable levels.

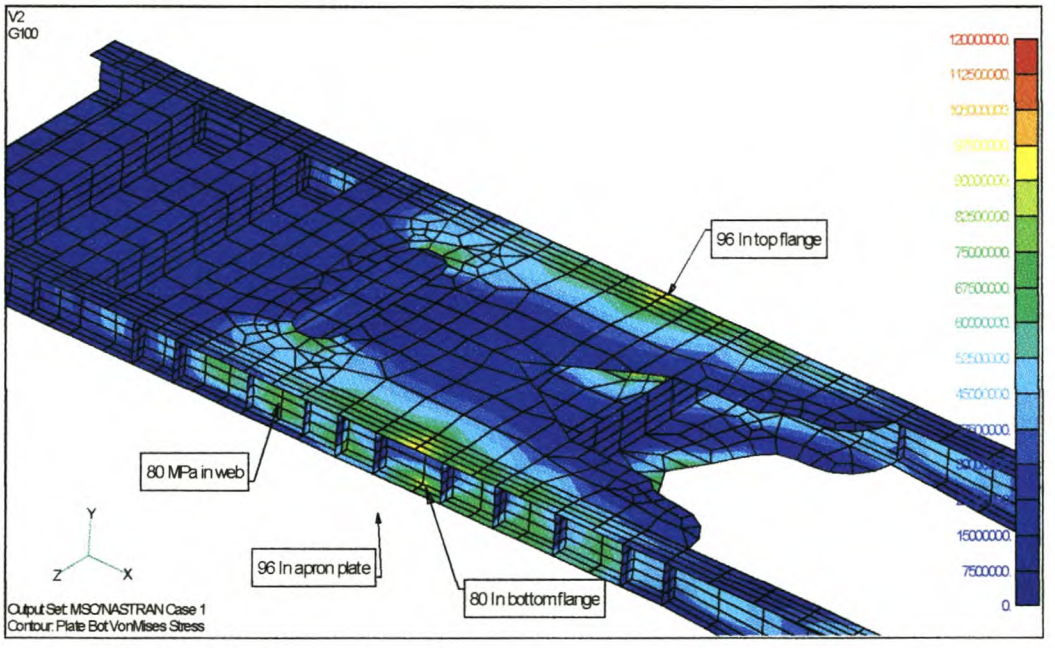

Figure 9.44: Modified neck rev.2 gravity stresses

The total weight addition is 80 kg. The stress is however reduced considerably, and the modification will greatly extend fatigue life, given that welding is designed to resist fatigue failure.

The above design changes must also be investigated when it is subjected to a torsional loading. The stresses in the front king pin section decreases. This is expected since the whole assembly is changed into a boxed section. Where this box section ends, however, a rapid increase in flange stresses arise. This will lead to fatigue failure. The torsional stiffness of the main I-beams is obviously far lower than that of the king pin assembly. The first investigation is the insertion of diagonal braces. Two 5 mm flat bars where placed between the top flanges to investigate their effectiveness in transferring the torsional load. In figure 9.45 the dramatic effect is visible.

The stresses at the diffuser plate drop radically. In the flanges the stress also falls to acceptable levels. Obviously the braces do not extend enough to the rear, and a second model was made with the extended braces at the top and bottom flange in place. This design with its stress contours is shown in figure 9.46.

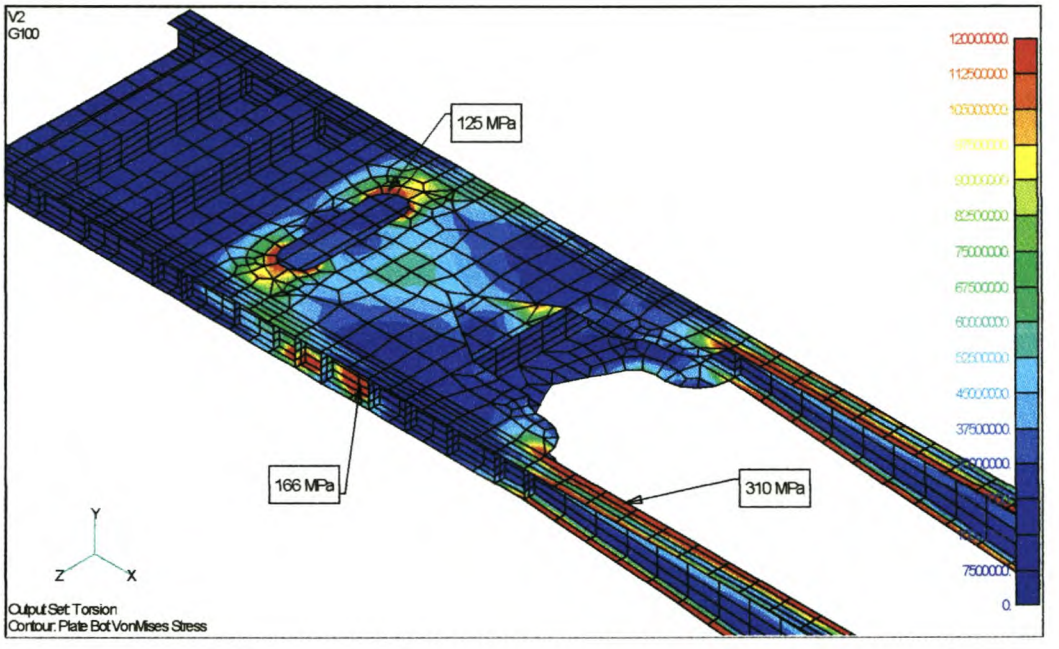

Figure 9.45: Modified neck area torsion stresses

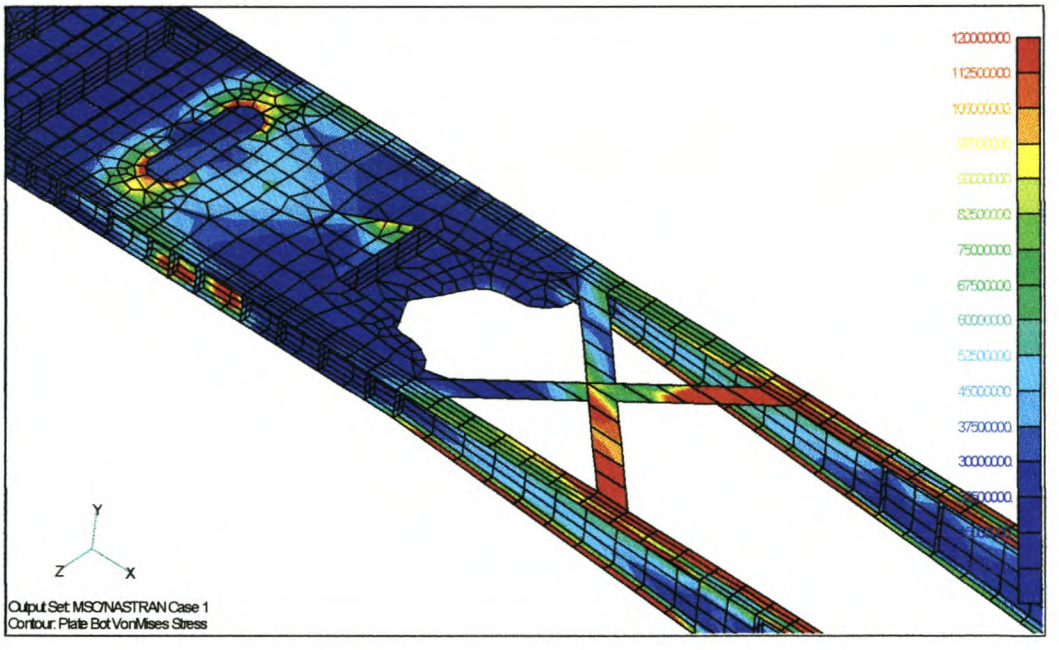

Figure 9.46: Braces to reduce torsional stress

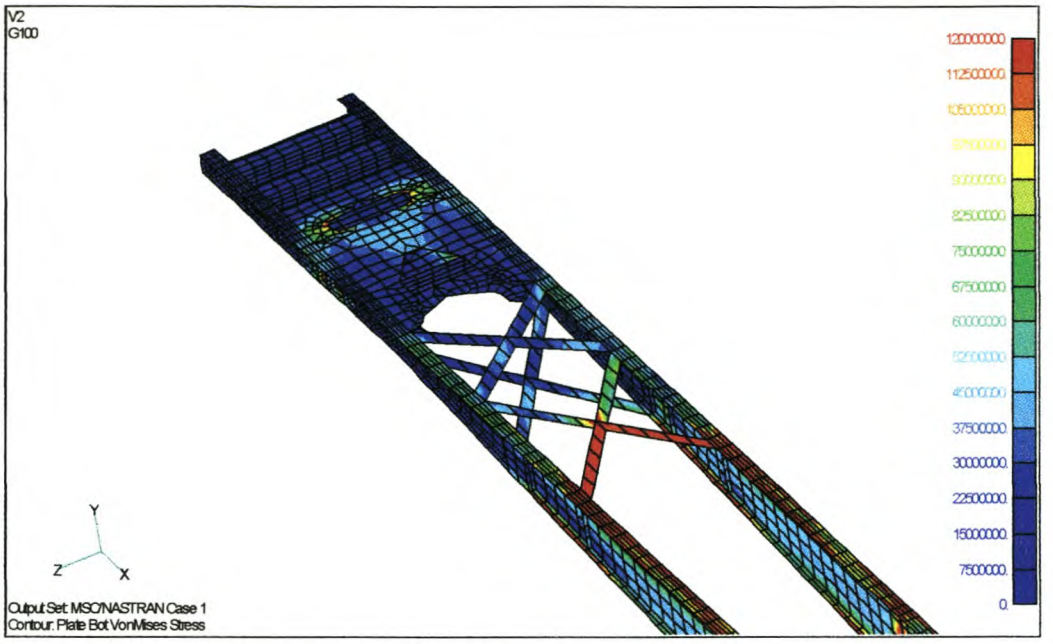

Figure 9.47: Modified braces for torsional loading

The braces are quite capable of removing the stresses from the neck area. Unfortunately the stresses are not removed completely, but rather moved backwards. Where the braces end a new high stress area is generated. This area will keep moving backwards as more braces are welded in place. A next model was made where another set of braces was included. The high stress area moved to the first axle cross member, causing a considerable stress increase within this member and its connection to the I-beams. Cross-braces further to the rear than shown in figure 9.47 is therefore not advised. The main advantage of the stress distribution as shown in figure 9.47 is that the area of high torsional stress is moved to an area where the beam bending load is low. Furthermore the braces doesn't weigh or cost much, but their welding to the I-beam flanges might cause fatigue failure if it is not of a high quality. An analysis that was done to investigate this problem was to insert gusset plates where the braces connect to the I-beams. Again the stresses rose at the termination of this plate, but the welding of this location will be better adapted towards fatigue failure, and their use is advised. In figure 9.48 this gusset plate effect is shown. The overlapping elements are due to the display algorithm.

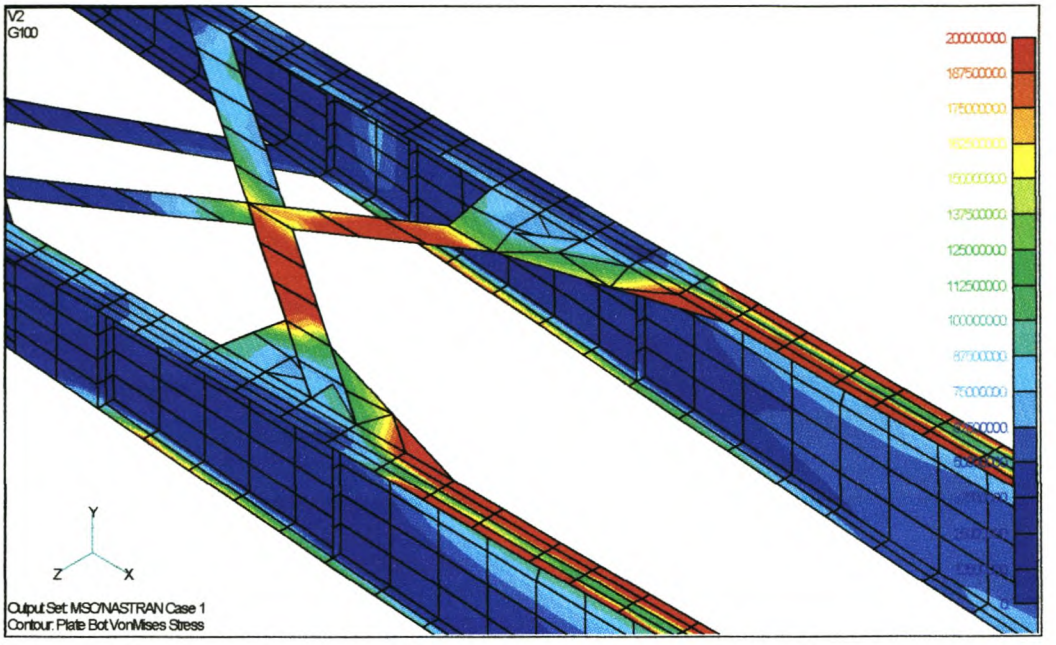

Figure 9.48: Gusset reinforced brace connection

Considering all of the above the boxing of the king pin area is advised, furthermore the use of braces just after the neck area is also advisable. Even though there are still high stress areas, the stress values are lower and at a more fatigue friendly location.

Chapter 10: Design Modifications

The advised design modifications are divided into four basic groupings. First are those that will increase vehicle strength and life expectancy. The second modifications will, if implemented, reduce weight and the third group is intended to reduce vehicle-manufacturing cost from a materials viewpoint. The manufacturing process changes are the fourth grouping, in which mostly quality issues and labour costs are addressed.

These modifications are based on the finite element analyses results, cost and weight breakdowns, manufacturing experience and general engineering design and manufacturing principles. The idea is not that these paragraphs will define a complete new design, rather proposals and concepts that can be implemented as given. Where deemed necessary the proposals are refined and linked to physical Rand and stress values.

Strength considerations

Some of the proposed changes given here were investigated in the sub-component finite element analyses. They are repeated here in a summarised manner.

The first obvious shortcoming of the current design is a weak neck area. The FEA's showed that this deficiency can be rectified with diffuser plates, thicker web plate material in the worst affected areas together with effective web reinforcement. Also the importance of a gradual change in section torsional stiffness was pointed out. The cross braces seemed to be the lowest mass solution. Later research, and specifically the SSAB Sheet Metal Handbook[29] further advises that these cross braces are inserted in a vertical manner when the structure is subjected to fatigue loading.

The floor area above the king pin is slightly over-stressed. Given the sometimes-inferior vacuum lay-up procedure the allowed stresses are low. Reinforcement of this

---

29 Sheet Metal Handbook: SSAB TUNNPLÅT © 1996

area is advised. Extra layers of 1×450 woven roving in this area will help to diffuse the localised high stress area. These layers can extend 1 m to the front and rear of the king pin. It is further advised that it will extend through the complete width of the floor, to successfully transfer the load to the stiffer side panels. Since the wood layer is the obvious main load-carrying member, a layer of woven roving just above and below the wood panels might be the best location for this additional material. Considering cloth and resin weight this modification will lead to a 13.5 kg increase for a 2:1 mixing ratio, where the 2:1 ratio allows for bonding as well.

The same principle might be applied at the rear doorframe and possibly in strips above the suspension mountings. At the door frame a 1 m wide U-shape insertion will work the best, with the sides of the U aligning with the semi-trailer sides and the bottom beneath the rear sill plate. Again the weight increase is about 12 kg.

The current corner capping design is insufficient to transfer the load from the floor to the side panels. A more rigid and less labour intensive design is called for. Since the labour savings would be the biggest benefit, this design change is discussed in the process paragraphs below. In the sub-assembly analyses this design was also investigated.

The use of chassis outriggers is also advised, as their effectiveness in reducing floor stresses is clear from the finite element analyses. These outriggers can be aligned with cross members to further stiffen the I-beams where transverse web loading exists. When the outrigger is in place where there is no back support, web stiffeners must be inserted. As mentioned earlier, the web stiffeners must not be welded to the bottom flange since this might initiate fatigue failure. This is where the stiffeners are inserted to resist web loading. When they are inserted to reinforce the I-beam in a torsional load fashion, they must be welded full around at the top and bottom.

Weight considerations

As indicated in appendix A, there is a need to reduce the semi-trailer tare weight with about 950 kg to make the layout legal with a 1610 mm king pin offset. Even with an 1800 mm offset there is a great deal to gain with a decreased tare weight.

As showed, the main weight contributor is the running gear, and its contribution was discussed in the weight breakdown chapter. The GRP box is the next biggest contributor, especially the floor assembly. As indicated the floor is also the main strength contributor, and there is not much scope for conventional weight reduction, e.g. removing current material without replacing them wisely. As per the previous section there can actually be a weight increase in the king pin and door frame support area to prevent possible failure.

The floor is generally stressed to rather low values, and potential problem areas are highly localised. Ideally speaking the floor can be made of a lighter construction except above the I-beams, king pin, at the side and at the front and rear edges. Theoretically such a complex glass lay-up and construction is possible, but practically not feasible.

In the floor itself the wood boards is the main weight contributor. Lighter and stiffer alternatives with the same strength are not readily available, not with cost as governing factor. The best alternative is a wood of a better quality, with a thinner cross section. The currently used floorboards are 32 mm Cape laminated pine. If 24 mm wood boards are used the weight is decreased by about 100 kg. Another advantage of the laminated boards is that their strength is almost similar in both directions, whereas for pine planks the ultimate stress decrease with a factor of at least 5 in the transverse direction. If aluminium is inserted inside the flooring, 18 mm board can be used.

The use of high quality laminated floorboards with a Formica™ topping was proposed by A. Da Cunha from Busaf Bauer. This type of flooring is used quite extensively in Europe. Given that the bonds between the boards can be watertight, this is an effective manner to eliminate weight and additionally improve product

quality. Another European trend is to use a continuous high-density rubber layer. These floors are capable of handling forklift imposed loading and the like. However, worn pallets might scratch through the relatively soft rubber layer, again breaking the vapour barrier.

The floor beams can be made lighter, and again the main advantage of floor beam modification will be the labour savings. Subsequently it will be discussed in the process paragraphs below.

For the side panels the main weight contributor is the outside skin. This skin is made of 2×450 chopped strand mat (CSM) with a 0.6 mm gel coat layer. The skin as manufactured by Busaf Cape is fairly on par with the stated theoretical values. According to the NCS data packs and literature the thickness for a 2×450 CSM layer is 1.87 mm. Plus the 0.6 mm gel coat it must be 2.47 mm. Measured thicknesses varied from 2.3 to 2.7 mm. From actual production samples the 2×300 CSM layer is somewhat too thick, indicating a mixing ration of 3:1 instead of the required and standard 2:1.

For pure comparative reasons, theoretical layer weights will be used for the following calculations, in view of the fact that not all of these skins are currently manufactured by Busaf. From the finite element analyses the outer skin is not stressed that much, and from a strength viewpoint the current 900 $g.m^{-2}$ lay-up can be reduced to 600 $g.m^{-2}$. Also instead of two 450 $g.m^{-2}$ CSM layers a single 600 $g.m^{-2}$ CSM layer will save labour. With the single 600 $g.m^{-2}$ CSM layer a surface tissue can also be applied to improve appearance. The weight increase of the extra tissue layer is almost negligible since it will use the same resin as the glass layer. This change will save about 72 kg for the semi-trailer. To further save weight, woven roving (WR) can be used together with a surface veil. The woven roving uses less resin per square metre as it has a mixing ratio of 1.5:1 instead of 2:1 for CSM. For glass fibre manufacturing a saving in weight is almost directly proportional to a cost saving, given the same basic type of materials are utilised. The WR lay-ups are considerably stronger than the CSM lay-ups. (Theoretically 265%, and in-house considering gel coat layer influence, 53%).

Following the same logic the side inside panels can also be manufactured from woven roving. The analyses showed that this skin together with the wood layer is the predominant load-carrying member in the side assembly. Although a high surface gloss in the semi-trailer inside is esthetical superior to a woven roving print-through, the weight benefits might be more advantageous than a glossy appearance, which is in any case seldom seen. For the roof the 2×300 CSM layers can be replaced with 1×450 CSM or even lighter woven roving layers.

Theoretical potential weight savings by altering skin lay-ups are listed in table 10.1. This table excludes gel coat weight. For all the CSM skins a mixing ratio of 2:1 and for the WR1.5:1 are assumed.

Skin	Current : [kg.m^{-2}]	Proposed : [kg.m^{-2}]	Saving [kg]
Side outside skin	2×450 CSM : 2.7	1×450 WR+Veil : 1.4	104.7
Side inside skin	2×300 CSM : 1.8	1×450 WR: 1.2	48.4
Roof out / inside skin	2×300 CSM : 1.8	1×450 WR: 1.2	47.4
Bulkhead inside	2×300 CSM : 1.8	1×450 WR: 1.2	4
Bulkhead outside	2×450 CSM : 2.7	1×450 WR+Veil : 1.4	8.7
			213.2

Table 10.1: Skin weight savings

As mentioned, the use of WR will lead to print through, but structurally and hygienically speaking the semi-trailer is similar.

The 6 mm wood next to the inside skin is inserted for impact protection. This damage will come from either the payload, or the loading mechanisms, be it forklifts or pallet jacks. Weight-wise the wood layer is equivalent to a 900 kg.m^{-2} CSM layer. The wood is stiffer than the CSM gel coat combination, and almost equivalent to WR and gel coat. It is because it is stiffer than the inside CSM layer, or floor layer, that it will fail before the skin, since its ultimate strength is lower. The question must be asked if it is really necessary to have this wood layer, and if a stronger inside skin layer would not be sufficient? As mentioned in chapter 4 there is quality problems in the wood bonding process. Also, the influence of moisture on the wood is more detrimental than on glass fibre. It is also realistic to assume that most impact would be in the bottom third of the skin height, and that reinforcement in this area would be sufficient.

In most semi-trailers aluminium side kick plates are inserted, making the wood layer even more redundant. If only a third of the current height is covered, it would translate in a weight saving of 137 kg. Also one resin bond (assumed 1 mm thick) is eliminated, saving another 100 kg and additional material cost.

Considering all of the above ideas it is possible to save about 450 kg in the box construction without radically changing the design.

The next possible area to save weight is the chassis construction. In the neck section, material needs to be added to stiffen the current construction. As indicated in the detailed analyses this additional material would weigh approximately 160 kg for the semi-trailer as shown in the finite element model. Realistically this 160 kg will actually fall to about 100 – 110 kg since the steering kit and other stiffening structures were not included in the model. In the remainder of the chassis construction there is some weight to save. The I-beams are only stressed to high values near the king pin area. For the remainder of the chassis the stresses are low, to very low. The flange material can be made of a lighter section. If 8 mm flat bar is used for the rear sections about 100 kg can be saved. The web plates can be constructed form 4 mm plate, even for the rearmost beam section. In the sub-structure analyses these changes were investigated and the stress influence seemed acceptable.

The I-beam height in the mid-section can be decreased, but the weight to save is minimal. The suspension brackets can be welded onto pedestals to keep mounting height correct, but the extra welding will probably lead to a cost increase, and all the extra welding might create more locations where fatigue failure might originate.

Material cost considerations

For manufacturing in general, inexpensive material is usually of an inferior quality. For semi-trailer manufacturing the same rule holds, but it is important to remember that the material quality must match the application. To use high strength steels where the stresses are seldom above 70 MPa is a careless waste of money. Even more so when the high stressed area is at a welded joint, since the apparent high strength material is basically reduced to standard 300W when welded. For fatigue especially allowed stresses in the welded condition are almost similar for mild steel and high strength steels.

In the chassis construction the use of Supraform need to be reconsidered, especially for the web sections. The ultimate strength of Supraform is similar to that of 300 WA, its yield strength is however 26.7% more. It was most probably originally used for its good forming capabilities for the folded cross members instead of its increased strength. The material can be folded to tighter radii, 1.5 to 2 times the plate thickness, whereas normal 300 WA will tore at such tight radii. If the bending press can be set-up with round bending radii there is no reason why 300 WA would not suffice.

The cost increase from 300 WA to Supraform is considerable at 26%. Some of the data from the steel material table is repeated in table 10.2 below. 300 WA is used as the base cost index. The last column is the ratio of strength over the cost index. With this combined index, a selection considering strength and cost can be made. The column is somewhat misleading since yield strength properties are used. As mentioned above, if fatigue limit stresses and welding are used as the design criteria the yield or ultimate stresses are not that significant and the standard cost index will be the driving selection criteria.

Description	**Ultimate Tensile [MPa]**	**Yield Tensile [MPa]**	**Cost Index**	**Strength / Cost Index**
30 Oak	618	463	1.11	417
ROQ-Tuff	852	791	2.5	316
Supraform TM 380	450	380	1.26	302
300 WA	450	300	1.00	300
BS4360-50 C	490	355	1.2	296
Corten	480	345	1.18	292
BS4360-50 A	490	345	1.2	288
BS4360-50 B	490	335	1.2	279
300 WC	450	300	1.10	273
BS4360-43A/B/C	430	275	1.01	272
3CR12	530	380	2.25	169
Stainless 304	600	310	4.1	76
Com Quality	~	(230)	0.8	288
Supraform TM 420	490	420	~	~
ROQ-Last	1095	739	~	~
Alum 545	220	125	~	~
Domex – 690 XP	750	690	~	~

Table 10.2: Steel cost comparison

30 Oak is exceptionally suited for its application as the I-beam flange material. For designs where stress is more important than stiffness the ROQ-Tuff would also be a more economical option. For semi-trailers however, adequate stiffness is almost more important than safe stress values and the use of ROQ-Tuff is an overkill since its Young's modulus is the same as 300 WA. Also the welding next to ROQ-Tuff is subjected to higher stresses, and the web material will fail long before the flanges. The use of 8 mm 50B at the king pin location should be investigated. The material is only 8.9% stronger (ultimate) than 300 WA, and cost 20% more. The use of commercial quality material (commonly known as Com-Quality) is a risk. The stated yield of this material is 280 MPa, but this is not guaranteed. It does cost considerably less, but the danger always exists that it might find its way into chassis construction if standard materials are not available. The use of 300 WA is therefore strongly advised throughout the manufacturing process for cross members and web plates. 30 Oak can be the default flange material.

On the GRP side, inadequate material quality can greatly influence total product appearance. The two outside skin panels greatly influence the overall aesthetic appearance and care must be taken to ensure that they have a high gloss and smooth appearance. Inferior bonding resin or technique will greatly reduce skin strength, and long-term vehicle quality. A proper resin needs to be consistent and predictable. This will help prevent expensive large scale manufacturing blunders when the resin sets too soon or to late. Another part of resin quality is the after sales service. With resin manufacturing there is a considerable number of production variables, and these variables must be checked or rather controlled by trained professionals to ensure a smooth lay-up and assembly process. The supplier must be able to inform and advise with regard to specific applications. Also if there is a clear problem definition the solution must be found quick with minimal disturbance to production. Without design changes the current material usage is already near optimum, it is just the wastage that must be controlled. This will be discussed fully in the next section.

Manufacturing process changes

The original manufacturing process does allow for a large number of potential manufacturing inaccuracies. These in turn could lead to inferior appearance, or worse

mechanical failure. The complete manufacturing process is rather labour intensive, and as indicated by the costing breakdown and labour cost saving could lead to a considerable decrease in overall production cost. An increase in product quality is just as, if not more important than lowering the cost. The labour practises greatly influences quality, and the discussions below will focus on the quality and cost alike.

The first labour group to be addressed is the GRP processes. An area where definite change is necessary is the design and manufacture of the floor, side and roof beams. These members are manufactured by laminating wood, polyurethane foam, glass cloth and steel sections together. These beams are then placed inside steel moulds and left to cure. The process takes long, and dimensional tolerances are not tight. The strength of these beams is also not adequate for the imposed loading. Especially after they are ground to be within dimensional specifications, the corner sections are weakened considerably. Pultruded glass fibre beams will be a far better solution. These beams are of exact dimensions, and their strength is also far better than the current assembled beams. The beams can even be pultruded with the core material in-place. Fibretek[30], in the Strand, quoted for a die for these extrusions. The cost is in the vicinity of R25 000. This cost roughly relates to 500 man-hours, which will easily be recovered given the hours it take to manufacture these modified beams. The material cost for these new extruded beams will be close to the original assembled beams. Even if the beams are not extruded with the cores intact it will still be better to use the extruded outer profile for beam manufacturing and insert the core material as required. The resin can be injected under pressure from the centre, and complete bonding can be obtained inside the pultruded beam. These beams can now be ordered as a stock item, decreasing internal lead times, and also occupying less factory floor space.

No finite element analysis of this beam comparison was done. The main advantage of the pultruded sections is the increased inner bonding strength, and this can not be built into the model. Also the current beams failed where the grinding process above damaged them. This manufacturing damage is difficult to simulate, and it would not be a fair comparison otherwise. It was decided to evaluate the new design with an

---

30 The contact person at Fibretek is Philip Nieman, +27 021 850 3085

experimental test set-up. An extruded type beam was compared with the current design in a three-point bending test configuration. A die with the exact dimensions of the current beam was not readily available. A slightly smaller beam was manufactured, and the maximum load was scaled with respect to section modulus for correct comparison with the larger and current beam design. The extruded beam is 180% stronger than the current design.

Another area of concern is the lamination of the side panel edges. This is a dispute that has been on-going for the last few years. This corner laminations wrap around the complete panel to floor corner assembly. Not only does this give mechanical strength to the connection, but it also serves as an extra vapour barrier. The panel core will absorb moisture, and due to the large temperature difference between the inside and outside of the refrigerated box, moisture condensation will form on the outside panels, especially near the corner sections where the steel inserts will decrease the thermal resistance. If moisture condenses here, it will move into the panels through capillary action, and core degradation might follow. The glass mat is not waterproof, and will not entirely prevent the flow of moisture, but it would lead to a considerable decrease. The application of these corner laminations is advisable, and the extra cost will be negligible. Also a water-resistant resin could be used when these laminations are applied, making them even more effective in preventing core failure. These outer skin laminations are also important at the bulkhead cutout and other open panel sections to increase transverse panel strength.

It is important to note that there are some pre-requisites when the corner laminations are assembled. The steel surface below must be clean of rust, dust and oil. Preferably the surface must be shot blasted. The Ciba Polymer structural adhesive guide[31] gives detailed instructions, and list cleaning agents for various bonding surfaces. From a process viewpoint it is recommended that all steel surfaces be shot blasted, prior to cleaning with an acetone solution. The glass fibre must also be free from loose dust and oil. A gross mistake that were made in the earlier production process is the use of standard factory compressed air to remove dust and particles from the bonded surfaces. This compressed air came from the central factory compressor, where oil is

---

31 Instruction manual No.A.15L – GB, February 1995

injected into the supply line to lubricate the air machinery. This oil necessarily ends on the glass fibre and other bonded surfaces. The epoxy glue and polyester resin do not bond to these oiled surfaces. Since the discovery of this shortcoming, air filters that trap moisture and oil were placed in the GRP factory section.

The current floor and side panel connection design is inadequate. Photo 10.1 below is a typical view of the current side to floor connection. Clearly visible is the voids and associated improper bonding. The specific trailer will get an aluminium floor and is fitted with 18 mm laminated pine floorboards. Also visible is the floor beam and the manner in which the glass side wall was ground away. The use of the pultruded corner section as analysed in the sub-component analyses will greatly reduce labour costs, and also increase quality to a great extent. This self-aligning corner cappings will act as a jig, forcing the panels to be square.

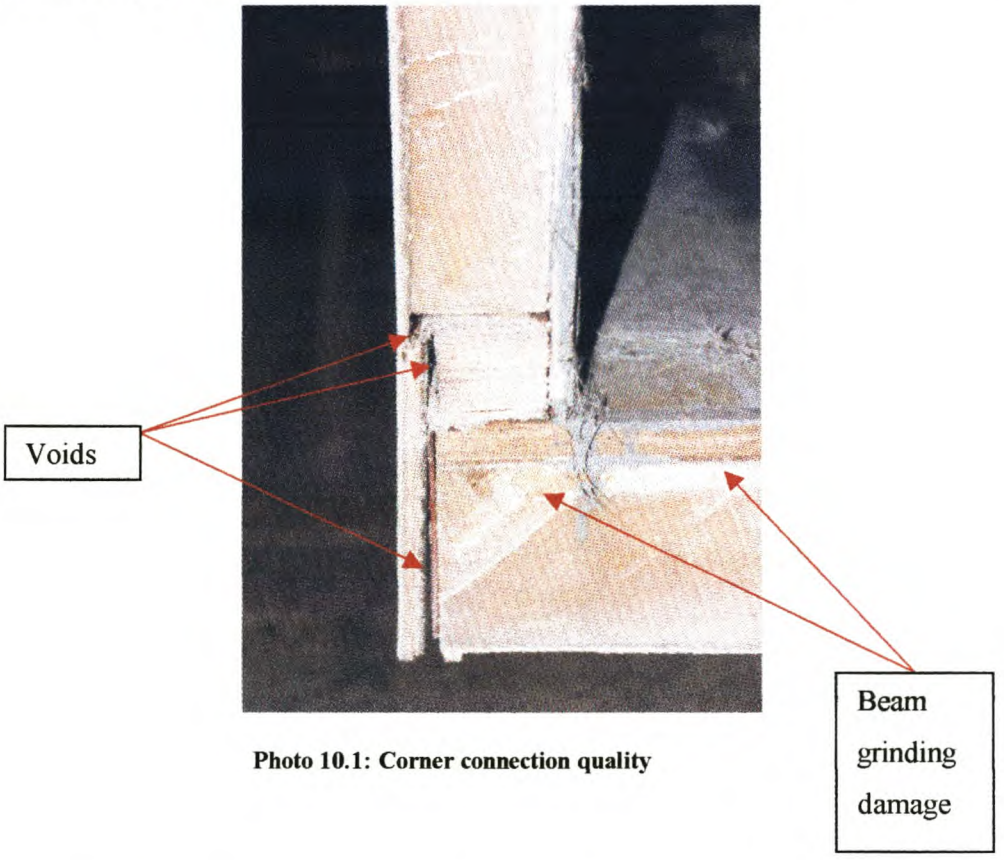

Photo 10.1: Corner connection quality

Over and above the self-aligning corner cappings the manufacturing process will greatly benefit if panel sizes can be standardised. Also with these standard sizes

complete jigs, e.g. holding two sides square at a set distance, can be made. The manufacturing process can also benefit if less layers are used during panel lay-up. Instead of say two 300 $kg.m^{-2}$ CSM layers one 600 $kg.m^{-2}$ CSM layer could work just as well.

Another area where improvement is called for, is the overall workshop lay-out, and especially the lack of quality orientated work methods. The biggest concern is all the loose dust inside the vacuum lay-up area. The skin layout area is isolated from the assembly area, and its air and surfaces are reasonably dust free. In the manufacturing and lay-up area there are however a vast amount of loose dust and oily grime. This dust and dirt inevitably ends between the bonded surfaces and this necessarily reduces bond strength. The biggest contributors to the dust are the open air sawing and grinding practises. The big panel saw produces tremendous amounts of fine dust, which is spread throughout the whole factory. Ways to eliminate this problem were investigated, and vacuum dust removal systems for the panel saw and the bench saw are proposed. For the panel saw an extraction unit will cost about R20 000[32]. This is a small price to pay if the decrease in workshop cleaning labour and increased quality is considered. Both the panel saw and the bench saw are however also worn, and dimensional accuracies are low. Proposed refurbishment of the panel saw would be in the vicinity of R15 000 to R20 000. A new bench saw (with built-in vacuum system) is in the vicinity of R60 000. The hand held grinders must also be equipped with extraction units. These modifications and replacements will greatly improve quality and reduce labour costs since the first time would be the right time and rework would be minimised.

---

32 Price obtained from Robert Steenkamp, Kooltron Pty. (Ltd.).

The overall appearance of the GRP shop is below industry expected standards, as evaluated in appendix B. In photo 10.2 below the resin decantering area is indicated. Clearly there is wastage. If a pump instead of decanting process is used there would be more precise volume control, and less wastage. A cleaner environment would also improve workshop pride and end product quality improvement will follow.

Photo 10.2: Resin decantering

Photos 10.3 and 10.4 fall in the same league. These are the wood panels that are to be placed in the side panel construction. They are obviously dirty, and the resin will not bond tightly to these surfaces. Skin delamination is possible. The main contributor to these dirty panels is the lack of workforce education. The workers should be made aware of the importance of a clean environment.

Photo 10.3: Dirty side floor boards

Photo 10.4: Close-up of photo 10-3

Acacio Da Cunha[33] of Busaf Bauer proposed a completely different manufacturing concept. Instead of the current GRP side construction the side and roof panels are to be constructed form zinc plated Chromaprep metal skins filled with expanded polyurethane core material. This construction would immediately reduce side

[33] Design engineer at Busaf Bauer.

delaminating problems, and the manufacturing process will simplify to a great extent. The panels will be standardised and outsourced. Assembly is now more modular, and the structure will align itself. The current floor design is to be kept, and a new aluminium side capping is to be designed. Door and bulkhead assemblies are also modular and outsourced. An estimate strength analysis of this concept was done, together with a modified chassis construction, which incorporated most of the proposals set forth in this chapter. This analysis is discussed in the next chapter.

For the chassis there is also scope for improvement. Here the process changes are more focused on cost than quality, except for the steering system that will be discussed on its own. To save cost it is advised that the cutting of the web plates and cross members be outsourced. Furthermore the neck section and beam sections must be standardised. There are only two standard vehicle coupling heights, e.g. 1280 and 1320 mm, and if two standard "kits" for these heights can be pre-cut, and possibly outsourced the cutting labour would be reduced. Also if the suspension ride height can be standardised the necessity of different designs can be eliminated. If this is not possible an adapter configuration at the rear section might achieve this in an indirect fashion.

Laser cutting of mild steel is highly competitive and material wastage is minimal, dimensional accuracy is also superb. At a small cost, positional markings and web cut-outs can indicate the positions and allow for accurate fitment of the cross members, outriggers and landing leg assemblies. The assembly process can almost proceed without the use of a measuring tape. The workers won't make dimensional mistakes since the assembly fits together in only one certain way.

The chassis centres must be standardised, with only two options. One design for a dual and on for a super single tyre configuration. This would also decrease design, drawing and manufacturing time alike. A suspension cross member with its gusset plates can be stock items, instead of raw material. The same logic is applicable to the king pin, land leg, rear light box and underrun protection assemblies. The manufacturing process can almost begin with the assembly process, instead of the

current time consuming cutting and bending process. This will greatly reduce delivery time, a great concern with most buyers.

Another idea that justifies further investigation is the more frequent use of bolt-on assemblies. Structures like the rear light-box and the landing leg assemblies are currently bolted on. This concept can be extended to the underrun protection assemblies, suspension cross members, and even apron plate assemblies. Bolted connections are far more fatigue friendly, and the wide use in truck frames confirms its successful application in the transport field. Care must just be given at the design phase to ensure the bolts are loaded in the correct fashion, and that effective methods be used to lock the bolts in a vibrating environment.

The steering mechanism is currently the main cause of vehicle downtime. The 6.3% contribution to manufacturing cost is also considerable, and this is excluding the extra labour associated with its installation. The design is now in its third major modified stage, and it needs to be seen if this design will give less breakdowns. The first system used dual cables, and it is believed that the dynamic cable behaviour lead to rapid fatigue failure of various components. This design also had a high part count. The next design used a single steering beam, and a much simpler mechanism. It still failed repeatedly when the front slewing-ring mounting bolts failed. The high neck and apron plate stresses from the finite element analyses confirm the high bolt loading. The main design mistake was to put the bolts in tension. Due to plastic deformation of the apron plate the load were not distributed evenly among the bolts. When subjected to a high overload the bolts will either break or loose their pre-tension. When the bolts loosen, the whole assembly is separated from the apron plate, leading to excessive apron plate wear and complete structural failure. Rather expensive design modifications were done on these systems that were already sold. A structure was welded in place above the front slewing-ring, to ensure that the bolts do not carry the complete vertical load. The next design update incorporated this design principle, and also the unit can now be removed from the bottom, without moving the complete GRP box section.

It is hoped that the third generation design would have addressed the shortcomings of the first two designs. The repeated failure, and obligatory expensive repair of systems in service should have been a good learning ground for the manufacturers to validate new designs before marketing them.

As indicated in appendix A the steering system is used to ensure the semi-trailer follows the turning path of a standard 9 m wheelbase semi-trailer. This can also be achieved if the last axle is a self-steering axle. In this arrangement the axle is not forced in a direction, but rather it follows the path of least resistance, in effect it steers itself. The tyre wear would be reduced, and more importantly from a manufacturers viewpoint the tare weight would reduce. The main setback however comes when the semi-trailer reverses. The axle will jack-knife and the vehicle will be uncontrollable. This problem can be overcome if the axle locks, or its' turning offset can swing around so that it follows the reverse direction. Lockable self-steering axles are available, and a reversible designs as well. Unfortunately they come with a high cost, and the current, albeit elaborated forced steering system, is still the more economic option. This is however only considering initial capital investment. It is believed that the reduced maintenance of the self-steerable axle will be the superior long-term investment. Also, if trade agreements can be arranged with the reversible axle manufacturers this will certainly attract market interest. Ridewell, an American axle manufacturer, patents the concept. To import a new axle type just for the steering axle is not viable. If however a local axle can be retrofitted on the Ridewell systems, the option is maintainable and therefore viable.

Chapter 11: Analysis of a Proposed New Design Refrigerated Box Section

The proposed modular design, which utilizes coated steel out- and inside skins for the refrigerated compartment is analysed in an estimated model. The model is estimated in the sense that the bottom corner capping and individual inter-locking panel connection are not modelled in complete detail. The purpose of the model is to the compare overall structural effectiveness, and to assure that the proposed new design will be capable of resisting the applied loading.

The new side panel inner skin is manufactured form a 0.6 mm Textradeck PVC coated steel layer. This outer skin is 0.6 mm thick and manufactured from enamelled zinc-plated chromaprep steel plate. The isolation material is expanded polyurethane foam. The big difference and advantage is that the polyurethane foam is expanded between the 2 steel layers, ensuring a high quality chemical bond, without the possibility of foreign material deteriorating bond strength. These panels are available in certain set lengths, approximately 2.5 m long, and the full height of the refrigerated box section. The panels are further totally outsourced, and are available at short lead times. They will fit together, aligning themselves to form the square refrigerated box section.

Before the finite element mesh is created a stiffness comparison is made to indicate possible overall structural influences of this design modification. A section of panel, 1 m high, perpendicular to the semi-trailer's axial direction is taken as a sample area. The polyurethane core material is left out of this comparison due to its very low stiffness contribution. Steel is used as the base material, and the CSM and wood scaled with respect to their corresponding Young's modulus.

Layer	Material	Thickness [m]	Young's Modulus [GN.m^{-2}]	Steel Equivalent Thickness [m]	Second moment of area [m^4]
Inside 1	CSM	0.002	2.2	0.000022	1.83333E-06
Inside 2	Wood	0.006	11	0.00033	0.0000275
Outside	CSM	0.0025	2.2	0.0000275	2.29167E-06
Total					0.000031625

Table 11.1: Original design equivalent stiffness

Layer	Material	Thickness [m]	Young's Modulus [GN.m^{-2}]	Steel Equivalent Thickness [m]	Second moment of area [m^4]
Inside	Steel	0.0006	200	0.0006	0.00005
Outside	CSM	0.0006	200	0.0006	0.00005
Total					0.0001

Table 11.2: New proposed design stiffness

From these calculations the new panels are about three times as stiff as the current design. It is therefore safe to assume that the change in panel construction will have a marked influence in the overall structural stress distribution.

For the finite element model the chassis construction underneath the new box design is similar to the original design, with only the neck area strengthened by means of diffuser plates. Only the bending and torsional load cases are considered for the estimate analyses.

For the gravity load case the overall chassis deformation is 6% less. The stresses in the neck area increase on average with 44% from the original design. In figure 11.1 below the highest stress values are indicated.

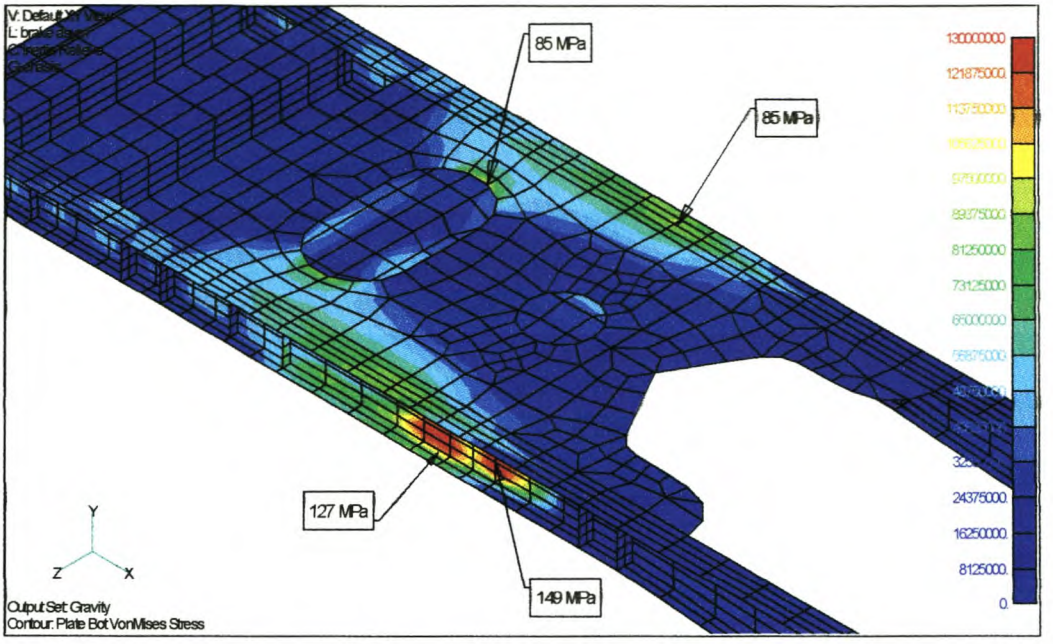

Figure 11.1: Stresses in neck area with new stiffer panel construction

layers are scaled to an equivalent steel layer with the respective Young's Modulus ratio. For the torsion load case the stresses are also higher. If figure 11.2 and 11.3 are compared, the increase in floor stresses are marked. The upper legend value is however low at 80 kPa. This conservative value was used for the improper bonding

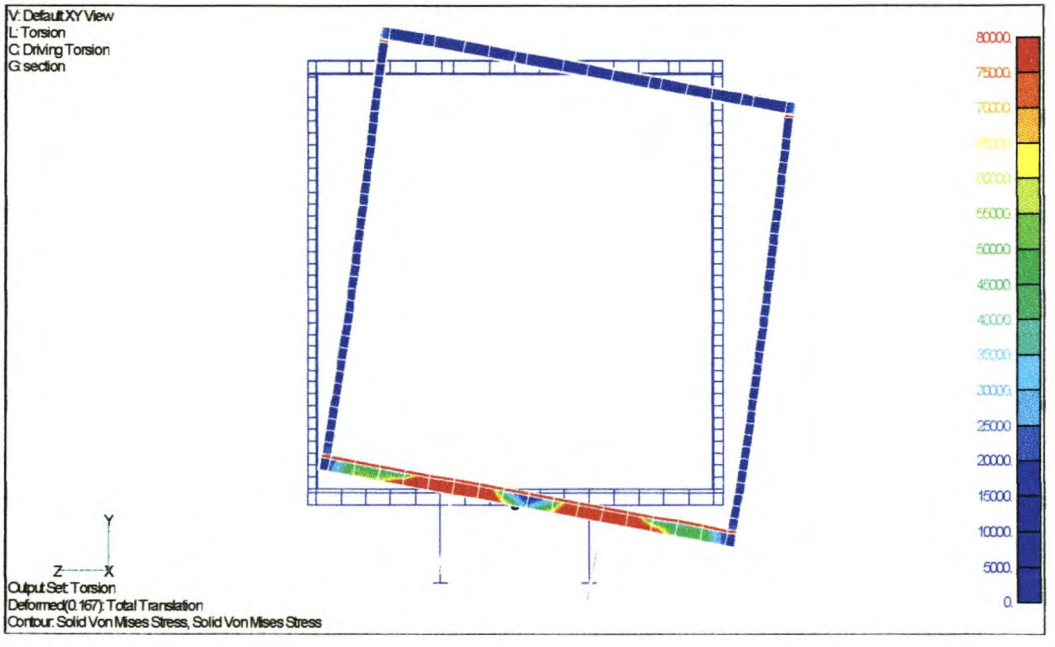

Figure 11.2: Mid-section, torsional stresses for current design

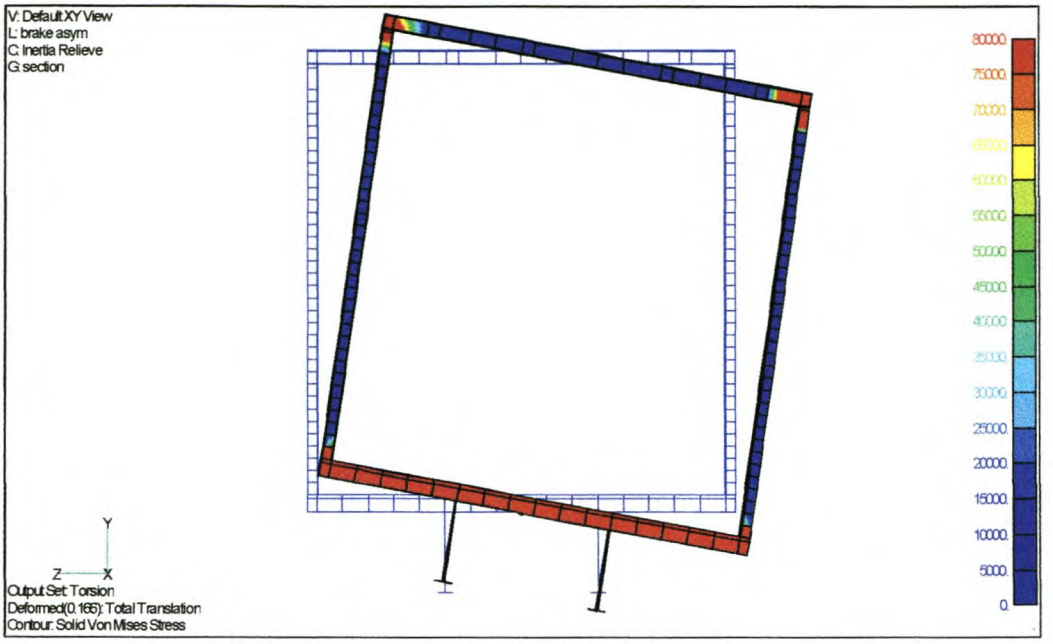

Figure 11.3: Mid-section torsional stresses for new side panels

that is common for the current manufacturing process. The new design with the higher quality panels will be capable of transferring significantly higher shear stresses. If overall chassis deformation is considered the effect is not considerable, but it is unclear why the chassis deformation is more, when it is expected to be less since the box section is stiffer. A possible cause might be the better transfer from the suspension loading to the rest of the structure since a forced displacement load and not a given force was applied. For the original, less stiff structure, there will be more local buckling and for the overall stiffer structure the displacement will be more uniform. This might also explain the higher neck stresses.

Position	Full [mm]	New [mm]	Difference [%]
Front curb-side	16.82	17.48	3.92
Front off-side	-17.60	-18.8	6.82
Rear curb-side	16.82	18.14	7.85
Rear off-side	-26.03	-29.9	14.87

Table 11.3: Chassis displacements for new side panel construction

The stresses in the side panels themselves are different from the original design. They are not only higher, but the distribution is also transformed. In figure 11.4 the gravity distribution is indicated, and in figure 11.5 the torsion load scenario is shown.

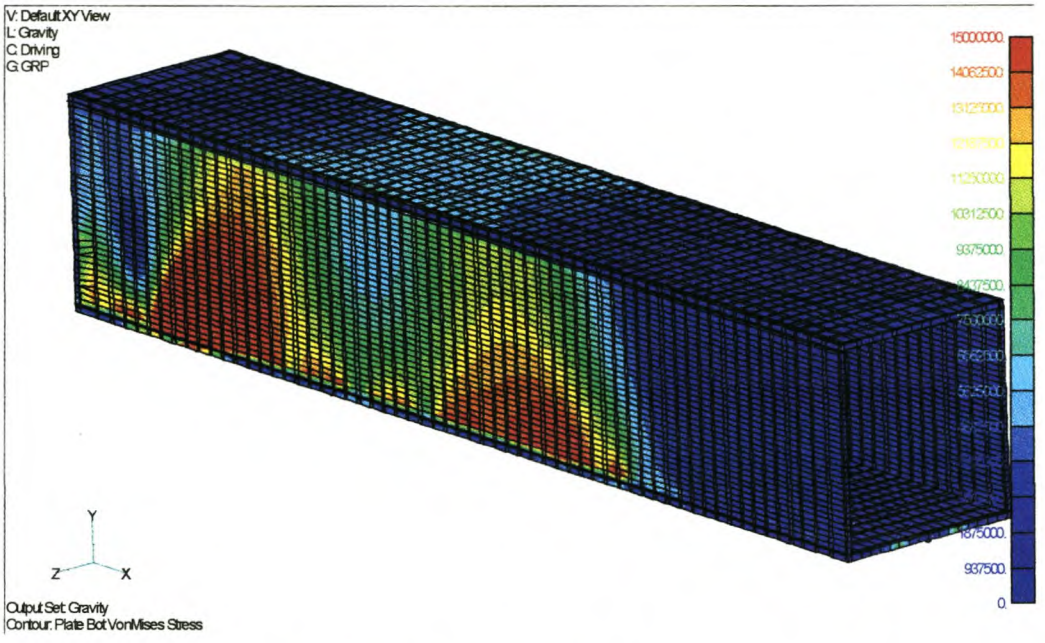

Figure 11.4: Side panel stresses for new panel design, gravity

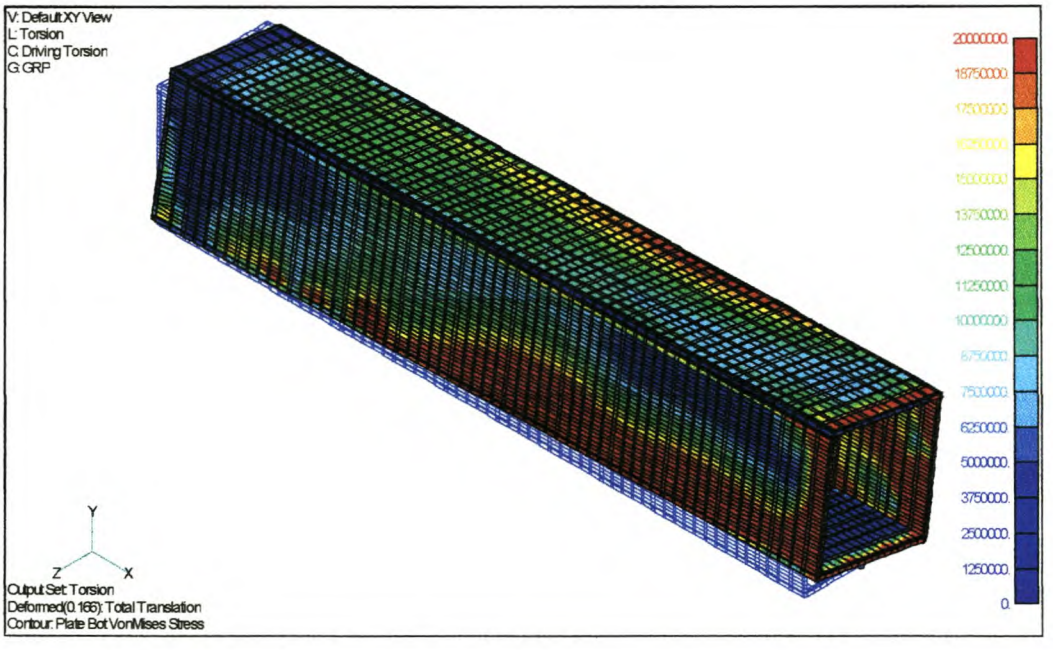

Figure 11.5: Side skin stresses for new design, torsion

Although the stresses in the sides and roof are high they are still within material capabilities. The stress inside the polyurethane core material is also low and from this analysis no failures are expected. In the floor section there is a slight decrease in the peak stress, however the mean floor stress increased to a small degree. The stresses in the bottom skin, polyurethane, as well as the main floor beams showed increased values.

Over and above the stress analyses a further estimate thermal isolation comparison is also done. The comparison is made for 1 square metre of panel construction. For the current design the gel coat and CSM layer with bonding resin were assumed to be one

Layer	**Material**	**Thickness [m]**	**Heat Transfer Coeff. [$W.m^{-1}.K^{-1}$]**	**Thermal Resistance [$m^2K.W^{-1}$]**
Inside 1	CSM	0.002	0.25	0.008
Inside 2	Wood	0.006	0.115	0.052
Isolation	PU-Foam	0.05	0.023	2.174
Outside	CSM	0.0025	0.25	0.010
Total		0.0605		2.244

Table 11.4: Current design thermal resistance

Layer	**Material**	**Thickness [m]**	**Heat Transfer Coeff. [$W.m^{-1}.K^{-1}$]**	**Thermal Resistance [$m^2K.W^{-1}$]**
Inside 1	Textradeck	0.0006	43	0.00001
Isolation	PU-Foam	0.06	0.023	2.60870
Outside	Chromaprep	0.0006	43	0.00001
Total		0.0612		2.60872

Table 11.5: Proposed design thermal resistance

material. From table 11.4 and 11.5 it is clear that the new panels have a greater thermal resistance than the current design. For a 50 degree Celsius difference, 1 m^2 of the current design will loose 22.3 Watt, and the steel plate design will loose 19.2 Watt. From this estimate comparison the new design is therefore the more superior isolation material with a considerable 14%. Considering that both the sides, roof, bulkhead and rear door panels are to be manufactured from this new material the decrease in cooling capacity is 414 Watt. This reduction will lead to reduction in cooling costs. It must however be pointed out that in the above comparison only

conduction is considered, and no radiation or convection losses are compared. According to Holman[34][14] the solar radiation absorptivity constant for white paint and white pigments are approximately the same. Form this it might be safe to assume that the white-pigmented gel coat and white enamel coated outside layer will have the same radiation absorption. Also, convection will be the same, since the surfaces have almost the same appearance and the same shape factor. Conduction therefore seems to be the only area where design changes will have a marked influence.

A weight comparison for the two alternatives is also done. The values listed in table 11.6 and 11.7 are for one square metre of panel. The new side construction is 3.92% lighter than the current design, assuming that the core material density will stay the same. Another assumption is that the density of the inside and outside coated steel plate is similar to plain steel. For the total area considered this increase will lead to a weight saving of 62.51 kg.

Layer	**Material**	**Density [kg.m^{-3}]**	**Thickness [m]**	**Weight [kg.m^{-2}]**
Inside skin	CSM	1200	0.002	2.4
Inside skin 2	Wood	425	0.006	2.55
Isolation	PU-foam	35	0.05	1.75
Outside skin	CSM	1200	0.0025	3
Bonding resin				2.29
Total				11.99

Table 11.6: Weight properties of current side panel

Layer	Material	Density [kg.m^{-3}]	Thickness [m]	Weight [kg.m^{-2}]
Inside skin	Steel	7850	0.0006	4.71
Isolation	PU-foam	35	0.06	2.1
Outside skin	Steel	7850	0.0006	4.71
Total				11.52

Table 11.7: Weight properties of proposed side panel

From these analyses and comparison there are considerable change in structural stresses and method of internal load distribution. The king pin construction is still the most highly stressed area in the chassis and refrigerated box section. Further from a

---

34 Heat Transfer, J.P. Holman, 7th edition, McGraw-Hill ©, 1992 Table 8.3.

stress viewpoint careful consideration must be given to the side to floor and side to roof connection areas. Since the side and roof panels are considerably stiffer, these joints will necessarily transfer higher loads. The current method of joining will not be sufficient. The joint method proposed by A. Da Cunha might be sufficient, but further calculations are advised. This joint method was not built into the finite element model. Elastic bonding will be a good method to join the side to floor and side to roof; given the corner cappings can transfer the implied loading. Continuous elastic bonding will also produce a more watertight connection. In the book: Elastic bonding, published by Verlag Moderne Industrie, © 1998 [34], these bonding techniques and the design principles to adhere to are described in detail.

The insulation properties of the new panels are better, and this on its own is a big advantage. Although the weight comparison above showed the new panels to be the lighter alternative, the stress calculations showed the need for improved corner capping design. The weight saved in the panel will most probably be added in the corner capping design. It is believed that the end weight would be fairly similar or even slightly more than the current design.

The major advantage of the new side panel construction is the modular assembly and proposed labour savings. The second important aspect is increased product quality. Given that the design is sound this will be the better method of manufacturing refrigerated semi-trailers. However, the change from the current design is considerable and careful design and prototype verification is advised. Also if the market will accept a totally new concept is a valid question, but given the advantages the market could be convinced.

Chapter 12: After Sales and Warranty Considerations

A big concern with semi-trailer customers is the extent to which the warranty contract conditions will cover semi-trailer failures. Especially in the GRP market sector, floor failures and its associated expensive repairs have had tremendous influences on perceived semi-trailer quality. For the manufacturer on the other hand the big concern are what failures can be related to design inaccuracies or inferior workmanship, and what failures can be related to operator misuse.

The standard vehicle warranty period against faulty design or workmanship is one year. However, this one-year period is often extended to keep good customer relations at a premium. Even if it might be suspected that failures were caused by misuse, repairs are done under warranty conditions to secure future orders. This is an unhealthy situation since the customers expect that they can get their semi-trailers repaired in this fashion regardless of the cause of failure.

Structural semi-trailer maintenance is mostly of an inferior quality, or all-together lacking. Whereas as the running gear are frequently serviced and usually kept in a good condition the chassis and GRP box are not inspected to prevent structural failure. The main reason for this is that tyre wear is closely linked to bearing deterioration, and to minimise expensive tyre operating costs the running gear are also kept in good condition.

If the chassis and GRP box section were to be checked for failures at more regular intervals, vehicle downtime and expensive repair work could be minimised. If say a cracked I-beam fillet weld are repaired when it only separated from the flanges the repair is easy and might even be done on-site. If however this crack is unattended, it can propagate through the flanges and web, and even lead to failure in the GRP section. Naturally to repair the structure now, would be far more expensive and take longer, in which time the operator will loose revenue.

To address this problem there are some solutions. First of all the semi-trailer operators must be educated with regard to structural maintenance, so that they can

realise that they can reduce downtime and losses when their trailers are kept in a premium condition. A service manual was compiled with this purpose in mind, which must be issued with each new trailer. Refer to appendix H. If the operator doesn't adhere to conditions set out in this manual he will forfeit his warranty conditions. Admittedly it will not be easy to enforce such maintenance procedures and in most cases it will be hard to prove that preventive maintenance was not done as per required documentation. However the operator will be made aware of the importance of proper maintenance, and there is some form of indemnity form the manufacturers side.

A second warranty possibility might be to have two different warranty contracts, a one-year standard and say a three year extended coverage contract. For the extended warranty, the semi-trailer operator will have to pay a certain amount, but with this he gets the peace of mind that his trailer will be covered for a longer period of time. For larger and regular customers this extended warranty may be the standard without extra payment. Under this contract the client agrees to obligatory yearly semi-trailer inspections. This inspection might even be done on his premises, eliminating his downtime. If it is required that repair work must be done under contract conditions, he will be obliged to have the semi-trailer fixed. If the damage is due to design or workmanship it is for the manufacturers account, and if it is fair wear or damage it is for the operators account.

Also the possibility of a maintenance contract exists. From discussions F. Pitts[35] had with the Fast and Fresh group it seems that they will be willing to pay up to 25 cent per kilometre, excluding tyre wear, if Busaf will take over their complete trailer maintenance. Maintenance will now cover faulty design and workmanship as well as wear. For both parties this arrangement might work very well. On average a GRP semi-trailer does 750 km per day. Given this average is for 25 days a month, e.g. 18 750 km, it means that Busaf will receive R4 687 per trailer per month. If this maintenance is not just for new trailers, but the complete fleets for various clients, the turnover can easily grow into a million or even more per month. This fund can then

35 General Manager of Busaf Cape and Busaf Bauer

be used as an insurance type fund, from which maintenance and warranty claims are funded. This maintenance contract can only work well if it is controlled in an effective manner. Dedicated personnel will have to be appointed and keep excellent record of each semi-trailer to ensure that semi-trailer maintenance is done at optimum levels and intervals. Under such contracts it might be possible for Busaf to have loan trailers for the customer, further minimising downtime making the proposal even more attractive. The feasibility of such contracts must be investigated in more detail. If one considers that the operator receives on average R5 per km, this trailer maintenance entails to only five percent of its turnover. The big advantage is the minimising of downtime, since this is each operator's worst enemy.

Another side of warranty repairs is the engineering feedback that must be gained. In the current warranty situation the original designer, or even manufacturer does not always conduct repair jobs. The semi-trailer is fixed, but the true cause of failure is not always documented. To enable effective design evaluation and engineering change a warranty analysis form was compiled, included in appendix J. With this form it will be possible to analyse the warranty repair jobs, and improve the current design. Also repeated faulty workmanship will be highlighted which might indicate equipment deterioration or process shortcomings.

Chapter 13: Modern Design Techniques Available to the Transport Industry

As mentioned in chapter 11, various software tools apart from finite element analysis packages have been created to aid in the design of vehicle structures. In this chapter a more ideal design and production method is described. The methods and processes are by no means idealistic, of futuristic, they are unfortunately just not implemented. The economic feasibility of these analyses methods is also investigated.

As chapter 11 emphasised the current design methods are laboriously adapted around marketing, and not optimised towards manufacturing or design. They are also not optimised from a profit viewpoint, as the next few paragraphs will indicate.

It would be a better scenario if you could first engineer a new design and make sure it is 100% fit for operational use before selling it. In doing this you will prevent negative market sentiment, which might arise if there are structural failures. The client / semi-trailer operator will minimize his downtime, and the manufacturer will also minimize his investment risk. Figures 13.1 and 13.2 are adopted from MSC-Africa literature where this concept is depicted.

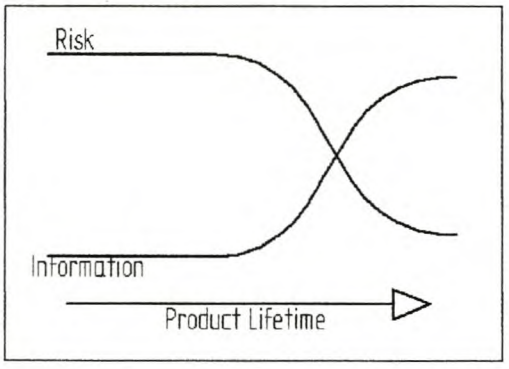

Figure 13-1: Risk vs. information

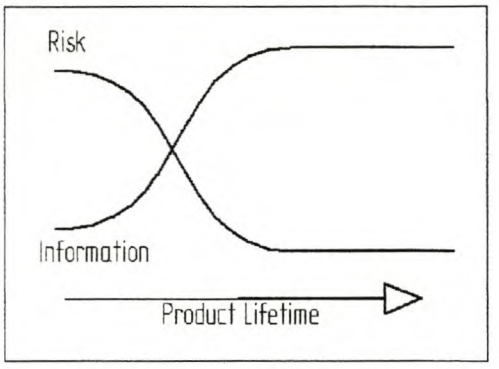

Figure 13-2: Modified risk vs. information

From these two figures it is clear that with the increase of information about your product and its operational conditions the associated manufactures risk decreases. If

the risk decreases reward will increase. The product life time is usually fixed by market trends, and as figure 13.2 indicates the sooner you can reduce your risk component the sooner your product can be marketed with success and achieve higher profit margins.

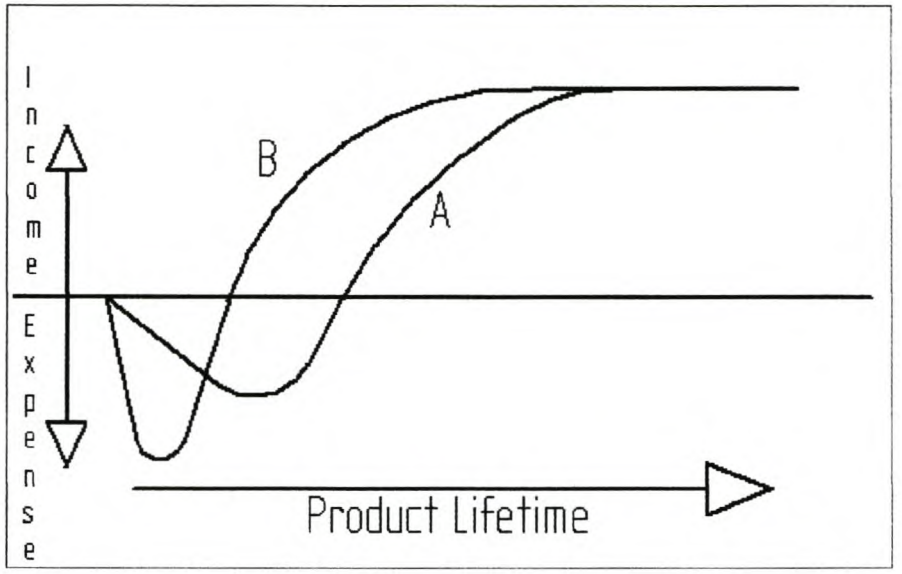

Figure 13-3: Income vs. expense thru product life

To increase the rate at which information is gathered will necessarily mean increased initial capital investment. If the concept design can come closer to the optimum, the profit gained right through the product life will be higher. This scenario is illustrated in graphical form in figure 13.3. The area under the line is the profit to be made from the product, negative indicating expenses and positive indicating profit. Line B represents a product where more detailed designs were undertaken at the development phase, hence the higher expenses. This product turns profitable faster than the original design method since it will have a positive market sentiment. Over the expected product life, scenario B will have a greater profit (positive area under the graph) than scenario A.

The graphs above are however typical for a product where considerable effort are invested into the development phase. As mentioned earlier this is not the current status quo for semi-trailer design. The designs are based on previous designs, so for a typical trailer design the investment versus return on investment graph will rather look

like graph A in figure 13.4. The design starts of as a new design and slowly obtains a bigger market share. It suffers a few design flaws during its life and possible negative market sentiment, indicated by the downward spikes. At the end of its lifetime the market interest in this model will decrease and the design will most probably be replaced by a new more profitable design. If this scenario is compared with line B where more money was invested into the design phase, the product will suffer less costly design changes and it will definitely obtain a bigger market share if it proves to be a reliable and well-designed semi-trailer. Considering this complete product lifetime, option B will render greater return on investment.

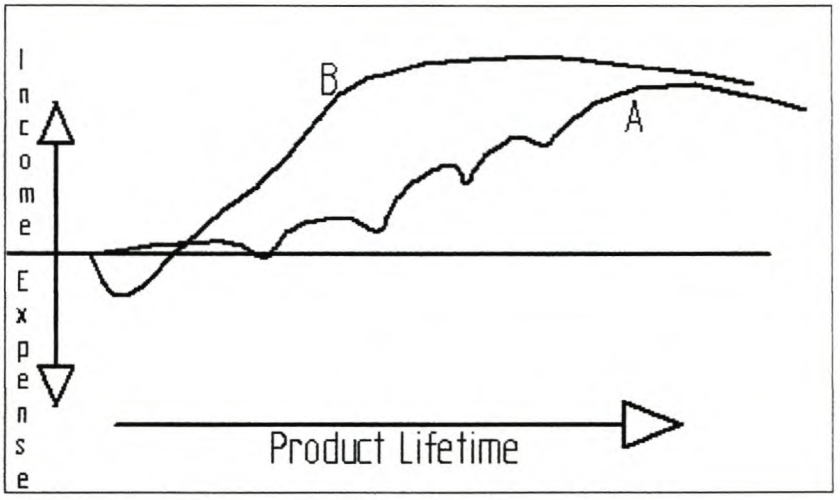

Figure 13-4: Typical semi-trailer income vs. expense thru lifetime

How do you increase the rate at which information is gathered about your product, without going the usual build it and repair it route? A first step is to simulate your design using numerical simulations. These simulations are not only applicable to stresses in the structure as this FEA analysis focuses on, but also complete vehicle layout and handling can be assessed.

In 3D modelling packages such as Pro-Engineer™ or Solid Edge™, vehicle clearances and part interaction is easy to investigate. Assembly methods can be compared and functionality evaluated. Also from these detailed solid models, design changes are easy to investigate, and passed through to the production area far more easily. Detailed part and substructure drawings can be created from the parametric solid

model and dimensions and part listings updated effectively. Of course this won't come easy, and considerable effort will need to be invested into the first model to make sure it can be used as a basis for future manufacturing.

At a higher level, the vehicle dynamics and handling characteristics can be verified using modern structural design packages such as ADAMS™. Now different concepts can be evaluated with respect to turning radius, road stability, structural forces and stresses and the like. From these models the worst loading cases can also be calculated, which in turn can be used to do realistic FEA analyses with software such as NASTRAN.

This is however not the end of it all. Numerical simulation is far better than estimating or intuitive engineering feeling, but it can never completely replace physical testing. After the first prototype is manufactured it can be tested and structurally verified for its complete expected lifetime before it is sold to potential customers.

One option is to use a development partner and that the semi-trailer is used for a designed lifetime in which time the design deficiencies will emerge, and the design can be updated. This is however a long term undertaking. A more effective solution is to test it at dedicated testing facilities such as Gerotek were equivalent lifetime testing can be done. However, on the Gerotek test track a truck will need to go through the same testing procedure as the semi-trailer, and at the end of the day both the trailer and a truck is written off. Another and more economical option is to only test the semi-trailer on a stationary hydraulic test bed. When using hydraulic cylinders and prescribed testing amplitudes, only the semi-trailer will be tested not the truck as well. Also, the load can be transferred via the axle hanger brackets, saving the axles, hubs and tyres form wear and damage. To determine the load amplitude and cycles, acceleration measurements can be conducted on a typical representative vehicle. During the testing procedure the same accelerations can be measured to serve as test control feedback. If this experiment is set up once, testing of further designs will be far less expensive, which will not be the case with testing on a track such as Gerotek.

Discussions and proposals for such an automated hydraulic test arrangement have been started and the University of Stellenbosch is well equipped with a thorough knowledge base and expertise to handle such experiments. They have been successfully conducting such testing on 30-tonne container tanks for various tanker manufacturing companies.

If a new design is verified in the manner depicted above, the possibility that unexpected failure will arise through the product commercial life is greatly reduced. The engineering, financial and marketing departments as well as the end user will benefit if this design approach is adopted.

If only one or even two detailed design projects are undertaken per year it would not make sense to buy these software suites. It would be far more economical to make use of outsourced contractors who knows the software, and more importantly, knows the transport industry.

It is estimated that it would take two to three weeks to create a complete parametric model of a GRP semi-trailer. Including software and man-hours this totals to about R20 000. From this model it would take about two to three days to create a full set of 2D manufacturing drawings in electronic format with its BOM, which would relate to about R3 000 to R4 500. If this first model is operational minor changes such as king pin offset, wheelbase or chassis centre distance will be easy to accommodate and can be incorporated possibly within a day. Obviously time to market will increase considerably and technical design staff can spend their hours in improving design concepts and manufacturing processes, instead of doing tedious drafting work.

A dynamic vehicle handling model creating will also cost approximately R15 000 for the first model. If the solid model already exists in a compatible format this cost could be halved. Variations in this model will also be quick and inexpensive, making it easy to compare different vehicle configurations.

A typical FEA analysis on a three axle GRP semi-trailer would cost in the vicinity of R30 000 to R40 000. For semi-trailer structures the link between the manufacturing solid model and the FEA analyses model would not be so smooth and seamless as claimed by the software suppliers.

Chapter 14: Conclusion

The finite element method was successfully applied to the semi-trailer structure and realistic and yet revealing information about the stress distribution within the main load bearing and surrounding structures was obtained. From the stress results the method by which the structure resist the applied loading became clear. Certain current design deficiencies were highlighted, and methods to overcome these design deficiencies were successfully investigated. The importance of certain structural members and the necessity of high quality manufacturing procedures were further pointed out. Noticed structural failures can now be verified and the cause and prevention thereof determined with a higher degree of accuracy.

The finite element method was furthermore successfully applied to certain substructure analyses, which were used to investigate general design concepts.

Methods to reduce weight and increase reliability were also investigated and discussed. It was shown that it is possible to remove about 400 kg in vehicle weight, without considering alternative running gear configurations and possible steering mechanism changes. Considering all of the above even as much as 1 tonne can be cut from the current tare weight.

The similarity between predicted overstressed areas and observed failures further indicated the effectiveness and importance of detailed stress analyses. For the current design the repeated neck failures, or rather slewing ring separation, could for instance have been prevented. Also the weight disputes could have been investigated in more detail and solutions obtained before large-scale manufacturing commenced.

Modern design techniques available to the transport industry were also introduced, and their effectiveness in increasing total product design life profits and decreasing development risk, indicated.

Considering the finite element analyses results and other discussions in this dissertation it is clear that there is scope for design improvement. A paradigm shift is

not necessarily necessary. With subtle design improvements, Busaf can remain a competent force in the South and Southern Africa region since there is enough scope for improvement from a weight and fatigue life viewpoint.

Together with the proposed labour cuts, these design modifications will increase Busaf's market share and profits. The complete new design proposal, which incorporates thin metal skins instead of chop strand mat, will greatly reduce labour hours and improve manufacturing quality, alike. From the estimate analyses it was shown that the structure would be capable to resist the applied loading. However, the analysis also pointed out that the replacement would lead to considerable changes in chassis stresses. The adequacy of the current chassis to resist the applied loading need to be investigated before the concept can be sold as a new proven design. The advantage that controlled experimental verification will have on prototype development was also discussed.

To conclude: The major importance of careful design practises and considering all alternatives early in the design phase is clearly indicated. Furthermore, the key importance of high quality manufacturing procedures and labour directly influences the effective structural strength.

Appendix A: Semi-Trailer General Arrangement and Design Motivation

To give more insight into the specific vehicle layout and its functionality, the dimensional and weight layout will be explained in more detail. The most important legal limitations will also be highlighted and their influence on this particular combination explained. The economic feasibility of the steering axle concept is also investigated.

The overall vehicle layout is indicated in figure A.1. The truck used with the semi-trailer is the International Eagle 9700. Figure 1 is what is generally referred to as the General Arrangement (GA) drawing. Indicated on this drawing are the relevant vehicle tare weights, overall dimensions, achievable payload and axle load values.

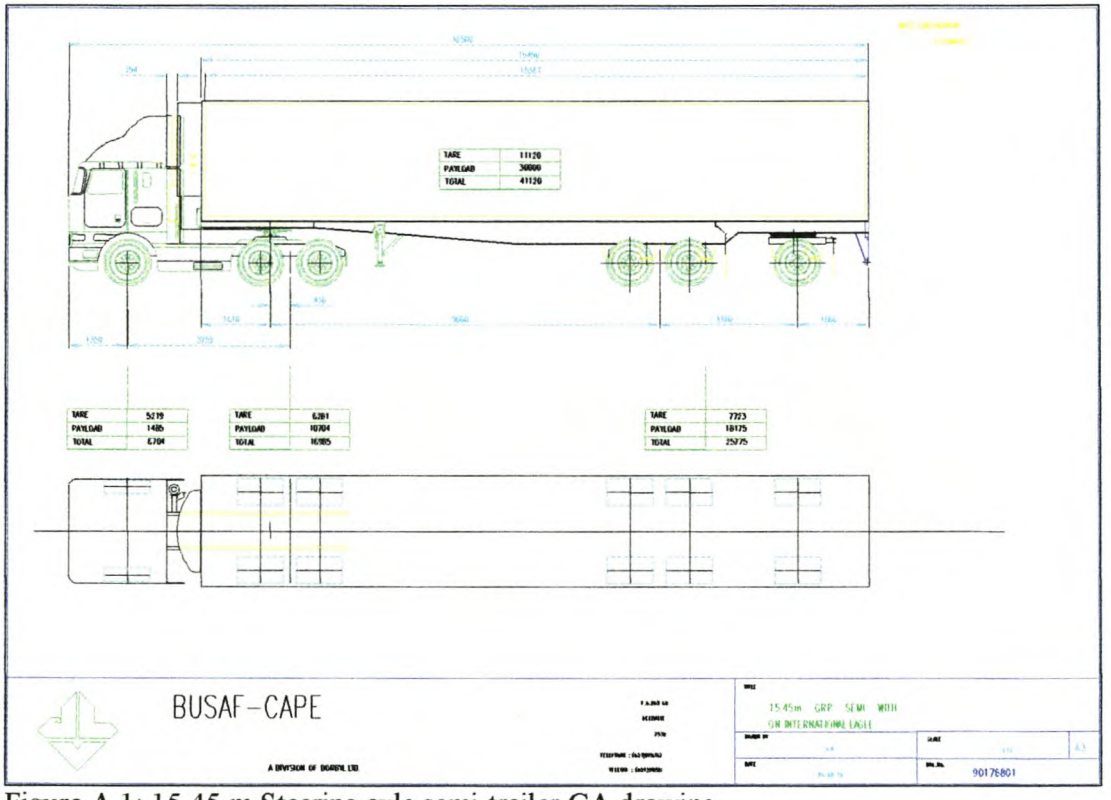

Figure A.1: 15.45 m Steering axle semi-trailer GA drawing

With the GA drawing the total vehicle layout and its legal compliance is visually summarized. The actual weight and dimensional detail is calculated with a spreadsheet[36], as indicated below.

VDV INTERNATIONAL 9700 SBA (THERMOKING SMX HIGH CAPACITY)90180701
Dim 'a' = 5th wheel pos. (+)ahead and (-)behind bogie ctr

SEMI TRAILER (* REQUIRES INPUT)						
Body length	*	15640	Unit	*	780	
Wheelbase	*	9000	Body mass	*	6640	
Front overhang	*	1610	Bogie		3700	
Load centre from bulkhead	*	7820	Tare		11120	
			Payload	*	30000	
KINGPIN LOAD			BOGIE LOAD			
Unit		903	Unit		-123	
Body		2617	Bogie		7723	
Payload		11825	Payload		18175	
Total		15345	Total		25775	7.40% OVER (5% ALLOWED)
Max	*	15000	Max	*	24000	
TRUCK TRACTOR (* REQUIRES INPUT)						
Front overhang	*	1359	5th wheel	*	0	
Wheelbase	*	3759	Total tare		8344	
Opt.dim 'a'		489	Max payload		16656	
Dim 'a'	*	458	Bogie spread	*	1350	MERC 1350;MAN 1400
FRONT AXLE			BOGIE			
Front tare	*	4834	Rear tare	*	3510	
Front load		1870	Rear load		13475	
Front total		6704	Rear total		16985	-5.64% OVER (5% ALLOWED)
Front max	*	7000	Rear max	*	18000	
Front axle load as % of combination mass					13.55	11% min.
Traction ratio					34.34	20% min.
Overall combination length					18690	
Combination tare					19464	
GCM to max axle					49000	
Permissible combination mass (D/T)				*	0	
Payload to max axle					29536	
Payload to bridge					28986	5% OVER ALLOWED

BRIDGE FORMULA :	DIM.	ROUNDED	BRIDGE	CALCULATED	VARIANCE (+over; -under)
AXLES 1 - 6	14436	14500	48450	49464	2.09%
AXLES 2 - 6	11352	11400	41940	42760	1.96%
AXLES 4 - 6	3180	3200	24720	25775	4.27%

With this spreadsheet the effect of various dimensional and weight changes can be investigated and the optimum vehicle layout established. The semi-trailer as indicated above, differs from the one on which the finite element model is based, in the sense that the front overhang is not the same. For this example the front overhang is

36 Spreadsheet designed by J. Barry – Busaf Cape

1610 mm, whereas for the model it is the maximum allowed 1800 mm. This 1800 mm is only possible with special refrigeration units, which have tight swing clearances. The 1610 mm is however the more common front overhang, and to stay conservative this overhang is chosen as the standard for this particular weight calculation.

From the spreadsheet and drawing the following important data can be gathered as an overall summary.

Weight criteria	Weight [kg]	Legal limit [kg]
Total tare	19 464	
Truck tare	8 344	
Semi-trailer tare	11 120	
Total payload	30 000	
King pin load	15 345	
Truck front axle	6 704	7 000
Truck bogie	16 985	18 000
Semi-trailer bogie	25 775	24 000
Gross combination mass	49 464	56 000
Payload efficiency	60.65%	

Table A.1: Vehicle weight data

The trailer rear bogie is obviously overloaded, with 7.4%. The law does allow for a 5% overshoot, but if you break the 5% tolerance the fine is worked back to 0%. The reason the weight is calculated for this obvious illegal layout, is that this is what the operators would like to achieve. The standard pallet weight is 1 tonne; therefore the 30-pallet semi-trailer must be able to carry 30 tonnes. Also the king ping load is slightly over the manufacturer's limit of 15 000 kg, although this is still acceptable. The gross combination mass (GCM) is within limits. The vehicle length is also within the 18.5 m maximum length. All the bridge formulae[37] restrictions are met. The last row in table A.1 is the ratio of the payload to the GCM. This is an easy way to compare different vehicle concepts with each other, the higher the payload efficiency the more economical the vehicle layout. Vehicle tax is paid per tare weight, thus the lighter your semi-trailer, the less tax you pay and the more legal payload you can carry.

37 The bridge formulae stipulates that the maximum load (in kg) on a given length of road shall not be more than the length (in mm) x 2.1 + 18 000 kg. A 5% tolerance is allowed.

To render the layout legal for the 30 000 kg payload and 1610 mm front overhang the maximum semi-trailer tare weight must be below 9 400 kg. This is a weight reduction of 950 kg from the current design.

As mentioned, the front overhang can be changed to 1.8 m if the new generation refrigeration units are used. If this is done the layout is legal without any weight reduction necessary, albeit within close margins (4.5% overload on tridem bogie).

The driving force behind the steering axle design is the shift of trailer tare- and payload weight from the semi-trailer to the truck bogie. As can be seen in the spreadsheet the truck bogie is not loaded to the maximum allowed values while the semi-trailer is already overloaded. This tendency would be even more pronounced if the semi-trailer where not of the steering-axle type.

If the last axle can be steered it can be legally placed at an extended offset. This is allowed since the turning behaviour is still similar to a standard 9 m wheelbase semi-trailer, according to which roads and buildings are designed. (The three axles are unfortunately still considered to be one tridem unit for weight calculations. If it were considered as a tandem plus a separated single unit, the allowed load would have been 3000 kg more). In real terms this means that the semi-trailer wheelbase is mathematically extended while the centre of gravity of the trailer (excluding running gear) and payload stays the same. The end effect is that more weight is transferred to the truck bogie.

To steer the last axle does have increased cost implications, not only from an initial capital investment viewpoint but also its lifetime maintenance cost. From a 14.6 m standard configuration to a 15.5 m steering axle semi-trailer a further investment of roughly R60 000, or almost 27%, is required. The payload capacity only increases with 7%. Although tyre and diesel costs should not increase considerably, downtime and maintenance cost will increase. (For the current steering mechanism in particular.)

However, if one estimates that the operator can get 4% more income on a R80 000 monthly turnover, this extra income of R3 200 per month will repay the original investment in 18.75 months, ignoring the time value of money. The designed vehicle lifetime is 5 years, and it can further be assumed that the trailer works for 11 months a year. The increased profit over the complete vehicle lifetime is in the vicinity of R116 000. Compared to the total turnover over 5 years this is a 2.64% increase in profit, which is worth the investment, given that the system works satisfactory.

Appendix B: GRP Process Evaluation Grid

The following grid is adapted from an article by B. Lacovara: "The Optimum Composites Shop"[3]. It gives certain criteria according to which a glass fibre workshop can rate itself to evaluate its current position, and how far it is from being an optimum composites workshop. The situation describing the current workshop position is typed in bolt face. Where there is overlapping classifications more than one selection is made.

	Worst	Better	Best
Plant location	City or suburban area within 400 m of residential housing, offices, public facilities or retail stores. Property line less than 60 m from plant.	**Commercial industrial area. Industrial neighbours engaged in manufacturing. Nearest residential properties 800 m. Property line greater than 60 m from plant.**	Isolated industrial area. Nearest occupied industrial facilities further than 400 m. Nearest residential properties 800 m or more. Property line greater that 150 m from plant.
Building type	Wood frame. Brick wood interior and wood roof joints.	**Metal or concrete block metal roof.**	Metal or concrete block metal roof, fully insulated.
Temperature control	**No temperature control. Minimum heating capabilities in winter. Temperature drops lower on coldest days. Hot and cold spots in production area.**	Capability of maintaining constant temperature at all times. Few hot and cold spots in production areas.	Able to maintain a uniform temperature at all times, in all production areas.
Ventilation system	**Random placed wall or ceiling fans. No spray booths. Open doors no airflow control.**	**Strategically located exhaust units serving specific area. Spray booths. Some control over plant airflow.**	Specifically designed directed flow. Ventilation system integrated with make-up air system. Spray booths modified to directed flow type.
Make-up air system	**No make-up air, relay on natural flow.**	Make-up air brought into central location in production area.	Make-up air designed into directed flow system to create air blanket over parts.
Ventilation system capabilities	Average styrene exposure TWA 100 ppm.	**Average styrene exposure TWA 50 ppm.**	Average styrene exposure TWA < 25 ppm.
Fire suppression system.	**Fire extinguishers. No alarms.**	Fire extinguishers, fire hoses, internal alarms.	Fire extinguishers, fire hoses, automatic alarms wired to local fire service, sprinkler system.
Loading area	**No loading dock. Truck to ground.**	External loading dock.	Internal loading dock.
Materials storage	In work areas.	**Random storage sites in plant.**	Designated & segregated storage areas.
Resin storage	**Drums throughout shop.**	Tote tanks in central locations.	Bulk tank serving entire shop.

Resin handling	**Individual pumps in drums.**	Wall mounted pumps feeding from resin storage.	Central pumping system feeding from bulk tank.
Laminating process	**Spray-up (chopping) or hand lay-up with resin spray application.**	Hand lay-up wet out with pump fed rollers, flow coaters or impregnators.	Vacuum infusion, vacuum bagging, RTM, other closed processes.
Resin application equipment	**Air atomised spray gun. High-pressure airless spray gun.**	Airless air assist spray equipment. HVLP spray equipment.	Pressure fed rollers, flow coaters, impregnators.
Gelcoat application equipment.	**Air atomised spray gun. High-pressure airless spray gun. Disposable cup gun.**	Low-pressure airless air assist.	HVLP spray equipment.
MEKP delivery system	**"Old style" 2 gallon tanks.**	Newer 1 gallon pressure tanks.	Slave pump delivery system.
Clean-up solvents	**100% Acetone usage. Worse methylene chloride.**	Partial acetone usage with some high boiling point solvents or water based emulsions.	100% Water based emulsion detergents or high boiling point solvents.
Resin types	High styrene content, >40%, long gel time.	**Low styrene, <35%, or styrene suppressed**.	Suppressed low styrene, <35% with fast gel time. Flash above 90°F, no red label.
Dust Control	**Uncontrolled girding in general area.**	Dust extractors on grinding and cutting tools. Grinding in discrete areas.	Down draft grinding booth. Dust extractors on grinding and cutting tools.
Production floor lightning	**Gel and laminating areas – 50 foot-candle illumination. Widely spaced lights cast shadows.**	Gel coating and laminating areas 70 foot-candle illumination.	Gel coating and laminating areas – 100-foot candle illumination. Closely spaced lights eliminate shadows.

Waste generation	No regards to the volume of solid waste or liquid hazardous waste generated.	**Program to use materials efficiently. Effort made to reduce quantity of waste generated.**	Product design, materials specified and employee training focus on waste minimisation.
Employee training	**No formal training program. Employees trained on-the-job by other workers.**	1-2 hours per month of formal training. New employees instructed.	Up to 4 hours per month of formal training conducted by qualified personnel. New employees trained in off-line situations, then placed in training crews. Detailed assessment of individual progress.
Quality assurance system	None. Management reacts to customer complaints. No in-coming material QA.	**Management committed to improving the situation. End of line inspection by QA inspectors. Some incoming material QA.**	Top priority commitment from upper management to hourly workers. QA system using procedural quality control along with statistical quality assurance. Extensive incoming QA.
Spill incidence	**Frequent spills of resin or solvent. Catalyst spills or drips common.**	Occasional small spill of resin or solvent. Catalyst spills are rare and cleaned immediately.	Spills are rare. All liquids are handled carefully with the proper equipment.
Container discipline	**Lids are often left open. Solvents in non-approved containers.**	Lids are usually closed. Solvent in approved containers.	Lids are always closed. No volatile solvent is used in plant.
Shop floor condition	**Covered with resin and dust. Generally dirty, rough and cluttered.**	Resin and dust confined to immediate work areas. Floors cleaned on a daily basis. Uncluttered.	Work areas clean. Only small amount of resin on removable floor coverings directly under moulds. Floors cleaned at end of each shift.
General housekeeping	**Dirty it, leave it. Poor work habits.**	**Dirty it, clean it. Good follow-up.**	Work clean, avoid making mess. Excellent follow-up.
Equipment maintenance	**Fix it when it breaks.**	Enough preventive maintenance to avoid most breakdowns.	Real preventive maintenance. Replace everything that wears or can break before problems can

			occur. Scheduled rebuilding.
Personal safety equipment.	Used only on special occasions or by few individuals. No specific training.	**Required by company. Required training. General use is proper.**	Strict company policy, even for management. Thorough training and complete compliance. Part of production culture.
Employee facilities	Restrooms dirty. Workers eat lunch where they can sit down.	**Restrooms reasonably clean. Segregated lunch area.**	Restrooms clean and maintained everyday. Showers and locker room. Clean comfortable well maintained lunchroom.
Job training	High degree of job specialisation, poor teamwork.	**Some overlapping of job skills, some teamwork.**	Extensive cross training, high level of teamwork.
Production procedures	Verbal only. Changes by word of mouth.	**Important procedures in writing. Some documentation available on product and process specifications. Important changes in writing.**	Detailed written procedures used throughout plant. Extensive documentation on specifications, quality procedures and process steps. All workers trained to same procedures, all changes in writing.
Production record keeping	Occasionally write something down that might be important.	**Keeps record of materials and part serial numbers.**	Document material batch and lot numbers to each specific part. Record equipment settings, environmental conditions and personal assignments on a daily basis.
Regulatory compliance	Find out your are not in compliance when inspection occurs. Not sure of all the permits and filings you are responsible for submitting.	**Have a good general idea of the requirements and have completed all major permits and periodic filings.**	Know exactly what is required and have resource for information and regulatory assistance. All regulatory requirements are met.

Appendix C: Polyurethane Material Properties

In the same manner as the glass fibre lay-ups and wooden beams, the polyurethane core material was tested to obtain or validate available material properties. Cylindrical test samples were cut from a polyurethane sheet. In total seven panels were tested for material consistency and material properties. The cylindrical test specimen was 65 mm in diameter and in height.

The test specimen were first measured and weighed to calculate the density. Thereafter it was subjected to an axial compressive test. During this test the compression load and associated displacement were sampled. From this load / displacement data the Young's modulus and crushing stress could be calculated.

From the density values it seemed that the material density is rather consistent throughout the panel. For example the average density for the supplied 35 $kg.m^{-3}$ material was 36.7 $kg.m^{-3}$. From the load / displacement data it was also evident that the maximum load did not vary to a great extent between the different test specimens. The material rapidly reached a point, which was in a way similar to a steel specimen yield point, and thereafter the material failed in an uniform manner.

An interesting observation is the 25 N (equivalent to approximately 19 kPa) range on the load / displacement curves. If the load is released before the 19 kPa value is exceeded, the specimen will return to its original state, e.g. elastic behaviour. If it is loaded above this value, the specimen will compress permanently. The permanent deformation is not plastic in nature, but rather like horizontal plane of cells that crush in unison. This "crushing plane" moves through the sample until the whole specimen is compacted. At this point the material behaviour is again stable and the applied load will increase again, until a pressure of 150 kPa. However the specimen is completely destroyed, and this upper stable region does not have significant meaning.

The most interesting observation from this experiment is the manner in which the material failed. As mentioned, at a compression stress of 11 kPa the cells

disintegrate. These stresses are easily produced during the manufacturing process, due to handling and lay-up vacuum pressures. Also this damage is always on the outside of the panels, where the polyurethane is bonded to the glass fibre or wood skins. If it failed, no permanent bond is possible, and the overall structural integrity is lost.

A summary of the experimental data is given in table C.1 and C.2. Experimental data plot, graph C.1, is for a typical test specimen.

Sample Description	Surface Crushing Stress kPa	Maximum Stress kPa
35 $kg.m^{-3}$ # 1	19.4	310
35 $kg.m^{-3}$ # 2	17.3	320
40 $kg.m^{-3}$ # 1	19.43	330
40 $kg.m^{-3}$ # 2	N.A.	330
80 $kg.m^{-3}$ # 1	N.A.	2 800
80 $kg.m^{-3}$ # 2	18.7	1 660
40 $kg.m^{-3}$ wet # 1	19.43	270
40 $kg.m^{-3}$ wet # 2	18.71	260

Table C.1 Polyurethane compressive test, data summary

If figure C.1 is studied, the first phase described the original elastic behaviour. The second phase is the horizontal area where the strain increased without a stress increase. The third phase is the area where the material failed continuously but with increasing load-carrying capability. For design purposes the first phase stiffness was used. A Poisson's ratio of 0.44 was assumed for both densities, following guidelines proposed in literature sources[38].

Sample Description	First Phase $GN.m^{-2}$	Third Phase $GN.m^{-2}$
40 $kg.m^{-3}$	0.00131	0.00447
80 $kg.m^{-3}$	0.00106	0.051

Table C.2: Compression stiffness / Young's modulus for polyurethane foam

38 Specifically: **Introduction to composite materials technology**, P.A. Coetzer, © MMS Technology.

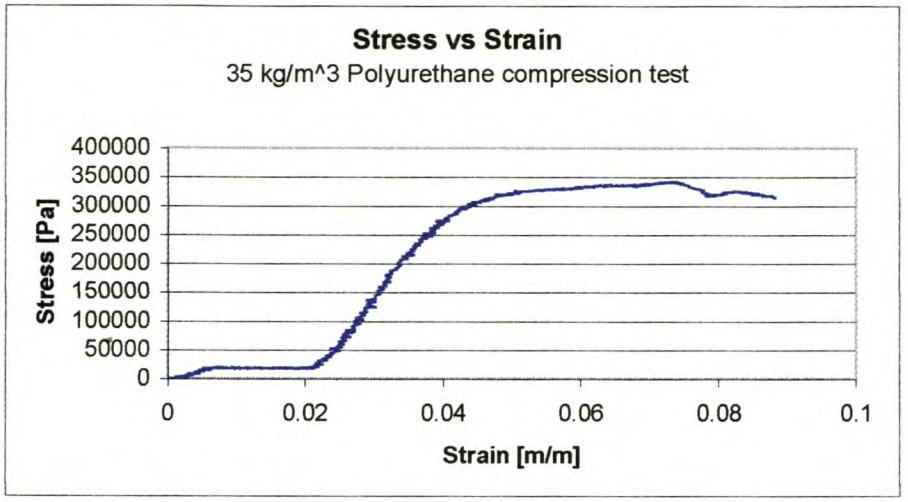

Figure C.1: Stress versus strain plot for a polyurethane foam specimen

From the above data it is evident that the core material is indeed structurally weak. The material is however used for its exceptional insulation characteristics[39], and not as a direct load-transferring member. The foam does however form an integral part of a sandwich panel construction, for which moderate shear strength are necessary. The material properties as given in table C.2 were used throughout in the finite element analysis.

The density for the 40 $kg.m^{-3}$ and 80 $kg.m^{-3}$ were modified from the actual values in the FEA models. This was done to include the weight of the resin bonding the polyurethane foam to the glass layers. In the table below the resin masses and modified foam density is indicated.

	40 $kg.m^{-3}$	**80 $kg.m^{-3}$**
Mass in FEA model [kg]	356	222.5
Resin surrounding Foam [kg]	305	195
Required total mass [kg]	661	417.5
Increasement factor	1.86	1.87
Modified density [40 $kg.m^{-3}$]	74.23	150.11

Table C.3: Modified foam density

39 For 40 $kg.m^{-3}$ the k value is 0.023 $W.m^{-1}.K^{-1}$, obtained from http://www.Matweb.com.

Appendix D :Wood Properties

The wood as used in the construction of the GRP refrigerated box was tested to obtain more accurate material properties than those readily available.

The test was in the form of a 3-point bending test. The load applied at, and the vertical displacement of the centre point, were measured. Three different wood types were tested. The wood was tested in both beam-bending directions. The first two was of the same type, with different suppliers. Wood properties perpendicular to the grain were ignored, since the wood is seldom loaded in this fashion in the semi-trailer structure.

For each beam type, 10 bending tests in each direction was done from which the Young's modulus could be calculated. An indication of the ultimate bending stress was also obtained by loading one beam until in failed.

Graph D.1 is a typical example of such a test. The wood is of a laminate ply type, 18 mm thick. On graph D.2 and D.3 the data set for the ultimate failure test is illustrated.

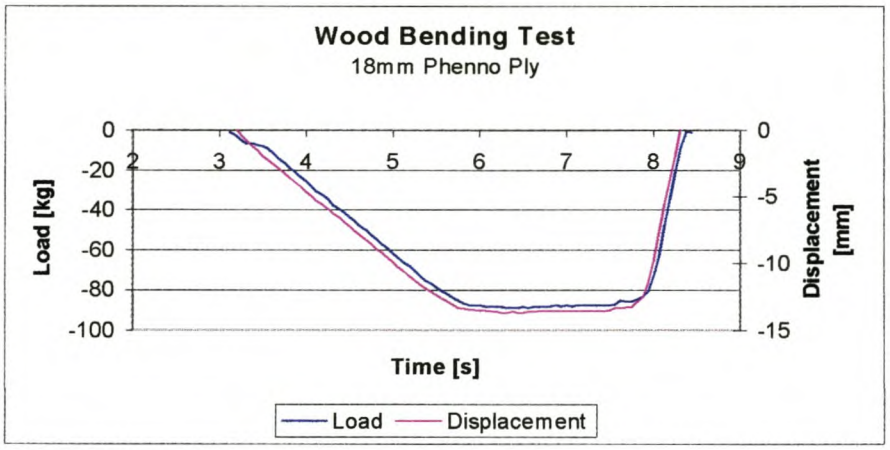

Figure D.1: Typical wood 3-point bending test data plot

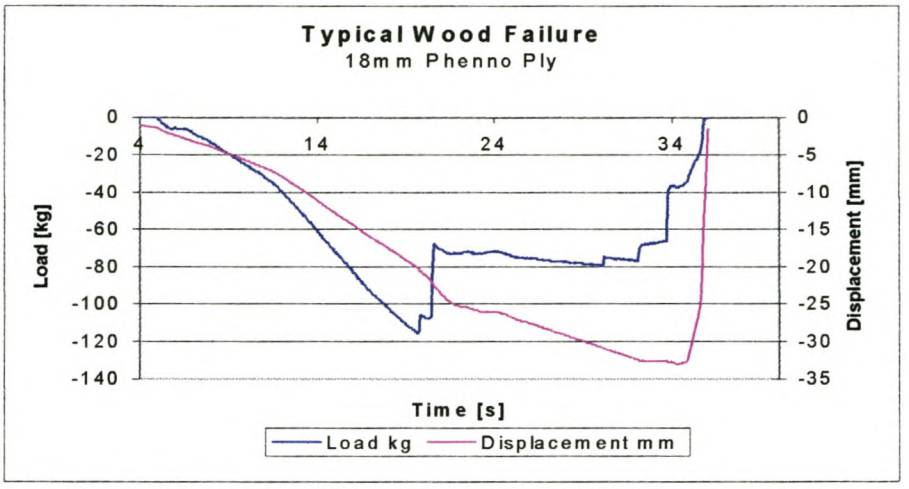

Figure D.2: Typical load and displacement curves for beam failure

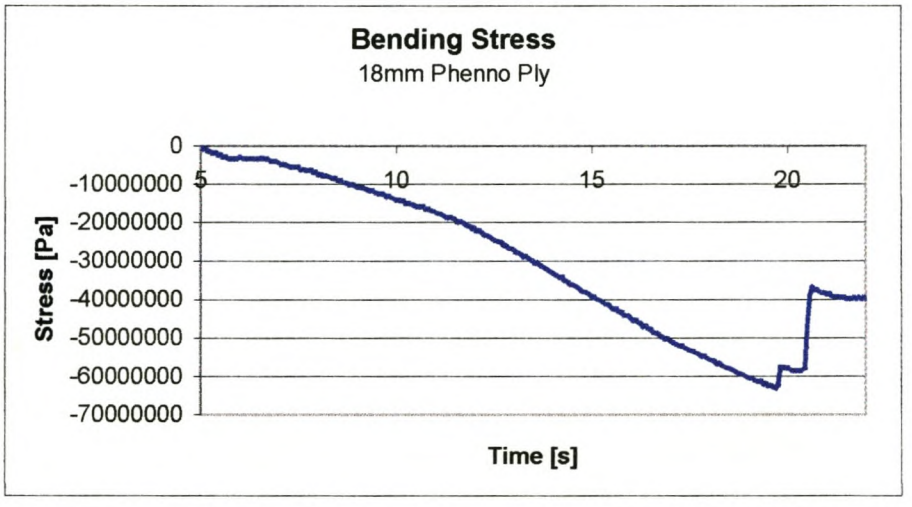

Figure D.3: Stress plots for failure

Using standard deflection formulas for a centre loaded, simply supported beam the relation between the load, deflection and stiffness could be found. [25]. The maximum bending stress could also be calculated with the familiar bending stress formulae.

$$d_{max} = -\frac{Fl^3}{48EI}$$

For displacement:

Where,

d_{max} = displacement at beam centre [m]
F = Load at centre, [N]
L = Span length [m]
E = Young's modulus [$N.m^{-2}$]
I = Second moment of inertia [m^4]

For bending stress [Pa]:

$$\sigma_{Bend} = \frac{My}{I}$$

Where,

M = Applied bending moment [N.m]
Y = Distance from neutral axis to outer fibre. [m]
I = Second moment of inertia [m^4]

Solving for the Young's Modulus and bending stress in the above formulas for each data point in each experiment gave the following average material properties.

Wood Specimen	Young's Modulus [$GN.m^{-2}$]	Ultimate Bending Stress [MPa]
18 mm Phenol Ply, A Direction 1	11.2	63
18 mm Phenol Ply, A Direction 2	2.2	-
18 mm Phenol Ply, B Direction 1	11.1	59
18 mm Phenol Ply, B Direction 2	2.2	-
Lamtico Bearer Direction 1	3.3	-
Lamtico Bearer Direction 2	3.5	53

Table D.1: Average wood properties

The test data showed good repeatability, and the values are deemed accurate for the finite element analyses done. The values are considerably less than those available in available literature. From "Materials Science for Engineers" [35] the stiffness for Douglas fir is 13.4 $GN.m^{-2}$ and the ultimate tensile strength is 85.5 MPa. (Parallel to the grain)

Appendix E: Glass Lay-Up Properties and Finite Element Correlation

To ensure that the finite element model resembled actual material behaviour a detailed analysis, combined with experimental measurements, was done for the glass fibre lay-ups as used in the refrigerated cooling box. Uniaxial tensile test specimens were cut form various production samples, following the SABS 141-1992: "Glass reinforced polyester laminates" testing directive. During this experiment the various strains, loads and displacements were measured and logged. From these data sets and subsequent calculations a more accurate estimate of in-house material properties were obtained. Even though the lay-up comprised out of a gelcoat and glass layer, a comparative plate element with one isotropic material property was created which resembled the actual laminate lay-up. The use of this single plate element made model creation and result interpretation easier.

A model with laminate material properties was first created to evaluate the test data. A second model, with the plate property, was subsequently created on which the material properties were altered to agree with measured strains and stresses.

The test specimens were constructed so that pure tension was generated at the measuring point, as depicted in the stress contour plots below. The effective neck area was 30 mm in width, and the thickness varied from specimen to specimen, with an average of about 2 mm.

Photo E.1: Tensile specimen

The experimental set-up comprised of the tensile specimen, on which a rosette strain gauge was placed (Photo E.1).The tensile load was measured with a load cell and the axial displacement was measured with an inductive type transducer (Photos E.2 and E.3). A hydraulic cylinder generated the axial load while swivel mounted clamps ensured that no bending moments were introduced.

Photo E - 3: Tensile set-up - overall

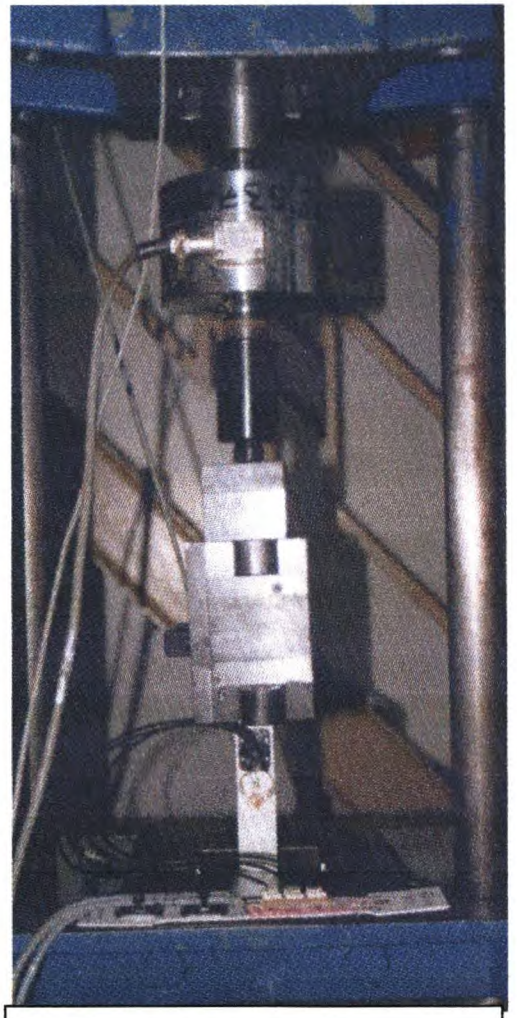

Photo E - 2: Tensile set-up – close-up

The strain gauge was bonded to the gelcoat side of the lay-up. The gelcoat was assumed to behave as normal cast polyester resin, with a Young's Modulus of 0.7 $MN.m^{-2}$. For the chop strand mat (CSM) lay-ups, failure was in the form of complete specimen failure, e.g. through the gelcoat and glass mat on one clearly

defined section. The woven roving (WR) lay-up failed in a de-lamination fashion, e.g. the glass separated from the gelcoat layer. It is therefore acceptable to assume that the measured strain did resemble actual strain, since gelcoat separation was only present near ultimate failure. Slip was also encountered with some specimens, but only to a limited degree and it did not influence the results adversely. The slip characteristics were clearly visible from the data plots as sharp local contour variations.

In total 15 specimens were tested. From each particular lay-up of three samples, two were loaded until failure, and one sample was only loaded to about half the ultimate failure load. The complete experimental data pack is on the data CD included with this thesis. A summary of the test data is given in table E.1. A sample calculation for one data set is included herewith to demonstrate the analysis procedure.

The data set and calculations is for a 1×450 CSM lay-up. This specimen did not fail, and the strain stayed within linear limits. A maximum load of 168 kg force was applied. The glass thickness was 0.6 mm and the gelcoat 0.9 mm.

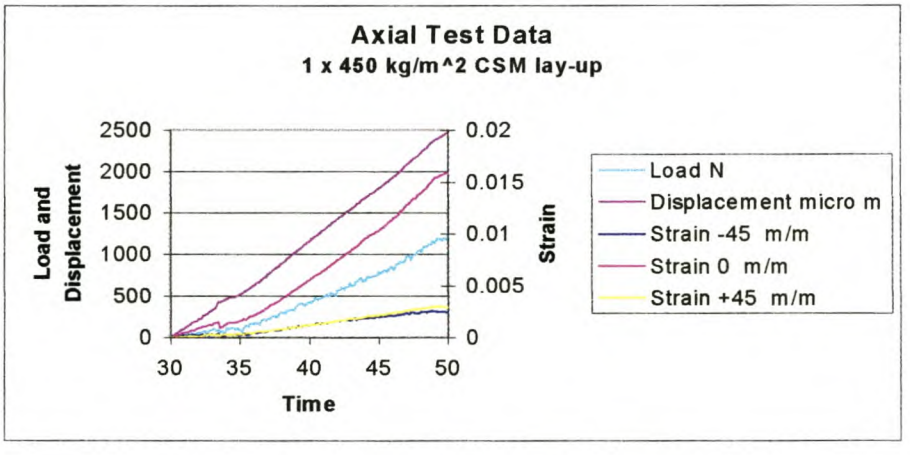

Figure E.1: Test data for tensile test: 1x450 CSM specimen

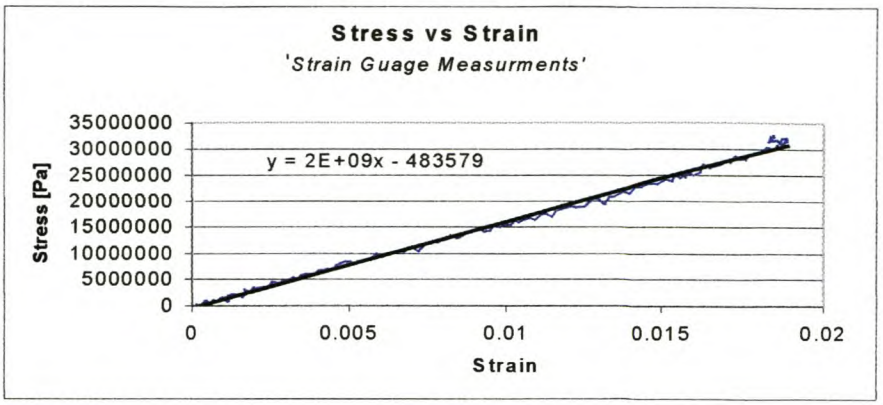

Figure E - 2: Stress versus strain plot, strain as measured with strain gauge

The strain in graph E.2 was measured with the stain gauge in the 0° direction. The stress is for the effective area of the glass and gelcoat combined. The average gradient of the above data was near 2 $GN.m^{-2}$. A second method of obtaining the strain was to divide the displacement with the original length, graph E.3. Again the gradient was about 2 $N.m^{-2}$.

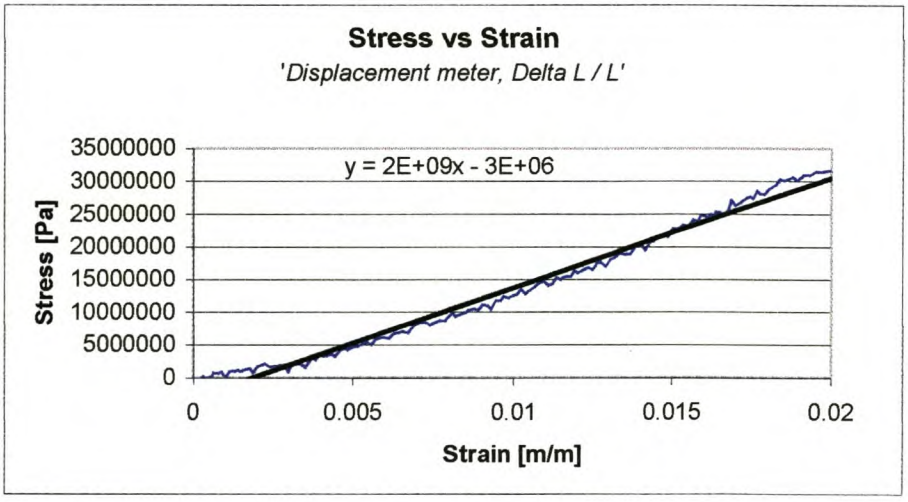

Figure E.3: Stress versus strain plot, strain calculated with displacement

If these two stains are plotted together, good correlation is visible. From the plots it is also possible to conclude that the strain gauge started to slip, or detach from the specimen after about 54 seconds. If this was not the case, the specimen might have been cracking at a different location, e.g. local strain did not increase while the specimen length increased. However this should not be a problem, since the Young's

Modulus was calculated throughout the whole data set, and the possible slip is only near the end of the data set.

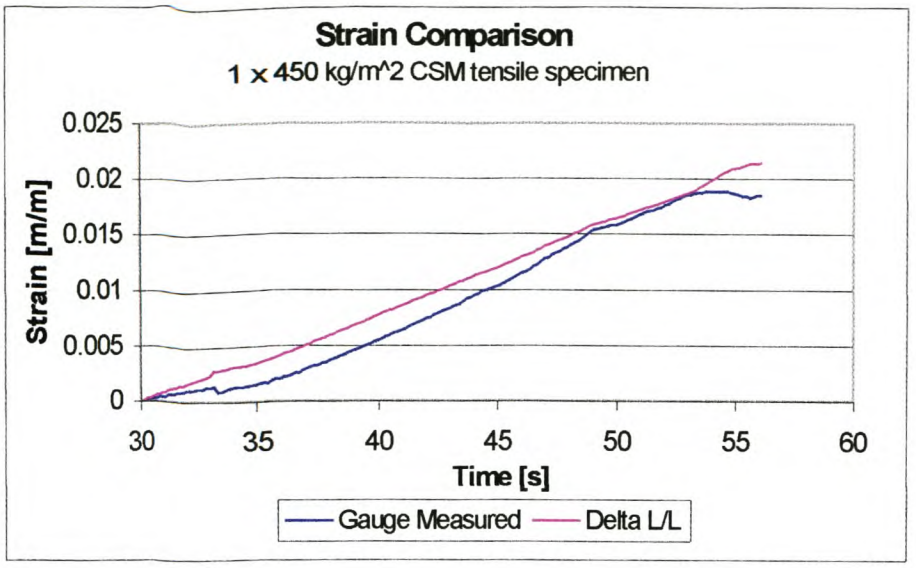

Figure E.4: Strain comparison

To calculate and compare the stress within the material, a data point was taken at a time of 53 seconds.

Time [s]	Strain 45° [m.m^{-1}]	Strain 0° [m.m^{-1}]	Strain 45° [m.m^{-1}]	Displacement [mm]	Axial Load [kg]
53.12	0.00212435	0.01858031	0.00303627	2.823	150

Table E.1: Strains at 53 seconds, 150 kg force

From this strain data the two principal stresses and von Mises stress could be calculated with the following formulae[40].

$$\sigma_{1,2} = \frac{E}{2}\left(\frac{\varepsilon_{-45} + \varepsilon_{45}}{1-\nu}\right) \pm \sqrt{(\varepsilon_{-45} - \varepsilon_0)^2 + (\varepsilon_0 - \varepsilon_3)^2}$$

40 Formulas obtained from: **Measurements Group Data Sheet**, Raleigh North Carolina, 1979

$$\sigma_{VM} = \sqrt{\sigma_1^2 - \sigma_1\sigma_2 + \sigma_2^2}$$

Where E is the Young's Modulus of the specific material, and ν is the Poisson's ratio. For this analysis the following material properties were used [18,19].

	Glass	Gelcoat
Young's Modulus	7 $MN.m^{-2}$	0.7 $MN.m^{-2}$
Poisson's Ratio	0.26	0.26

Table E.2: Material properties for Laminate Analysis

The strains are defined according to the drawing below.

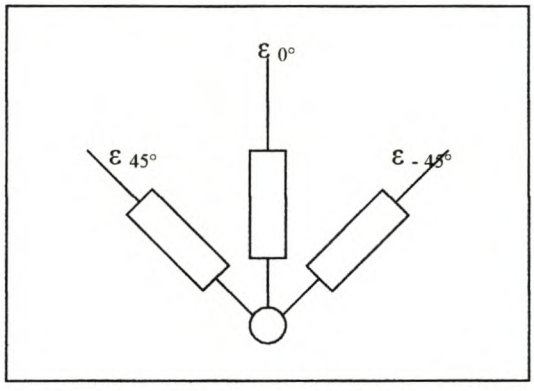

Drawing E.1: Gauge orientation

The principal stresses (σ_1 and σ_2) as well as the von Mises stress (σ_{VM}) were as follow:

Gelcoat Layer			Glass Layer		
σ_1 [MPa]	σ_2 [MPa]	σ_{VM} [MPa]	σ_1 [MPa]	σ_2 [MPa]	σ_{VM} [MPa]
11.33	-6.45	15.59	113.3	-64.52	155.94

Table E - 2: Stresses at selected data point

For the representing laminate finite element model the maximum stress in the Glass layer was 145 MPa and 14.5 MPa in the gelcoat (figures E.5 and E.6). This compares favourable with the measured results. The displacement values were also near the correct, or measured values. The predicted value is 3.08 mm, which differs 9.1% from the measured 2.823 mm. In the following two contour plots the laminate stress distribution is displayed. The legend is in MPa.

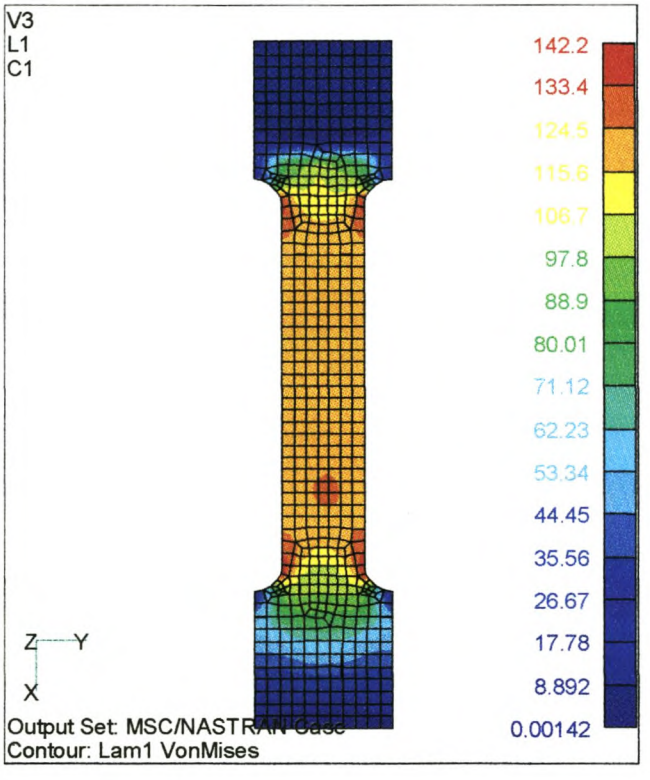

Figure E.5: Gelcoat stresses for laminate model

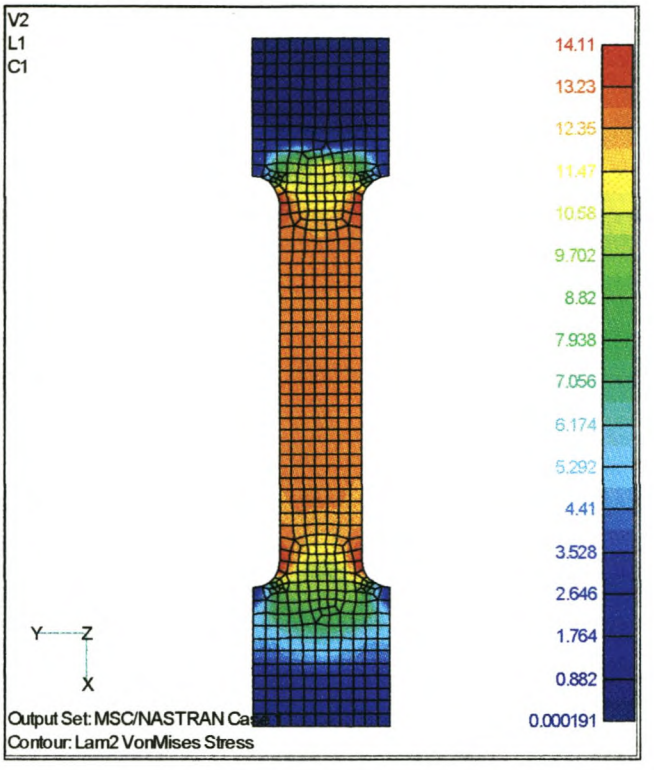

Figure E.6: CSM stresses for laminate model

As mentioned earlier, a second model with isotropic material and plate properties was also created. For this model the Young's modulus used was obtained from the experimental data, e.g. 2 $GN.m^{-2}$. The model showed excellent correlation with the measured data with respect to stresses, and displacement. If the effective specimen area is used in axial stress calculations, the stress amounts to 30.6 MPa.

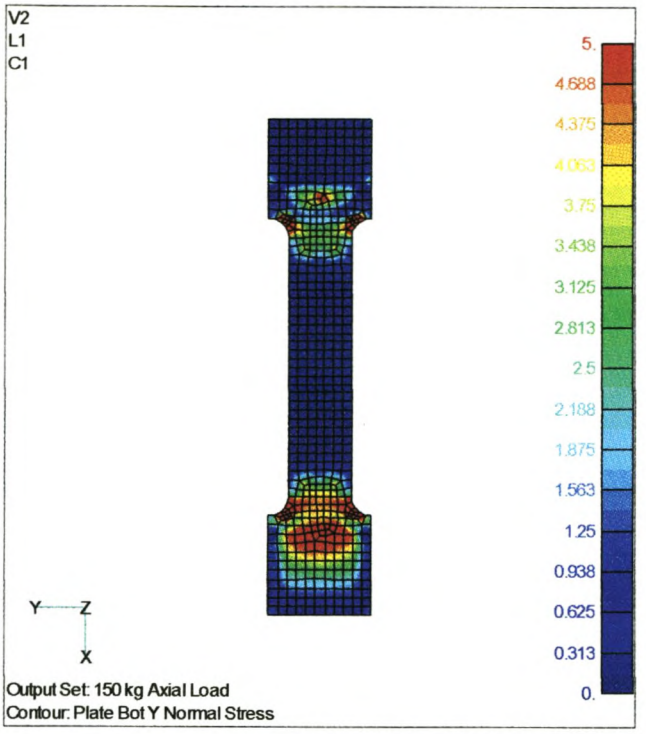

Figure E.7: Gelcoat stresses for plate model in Y-Direction

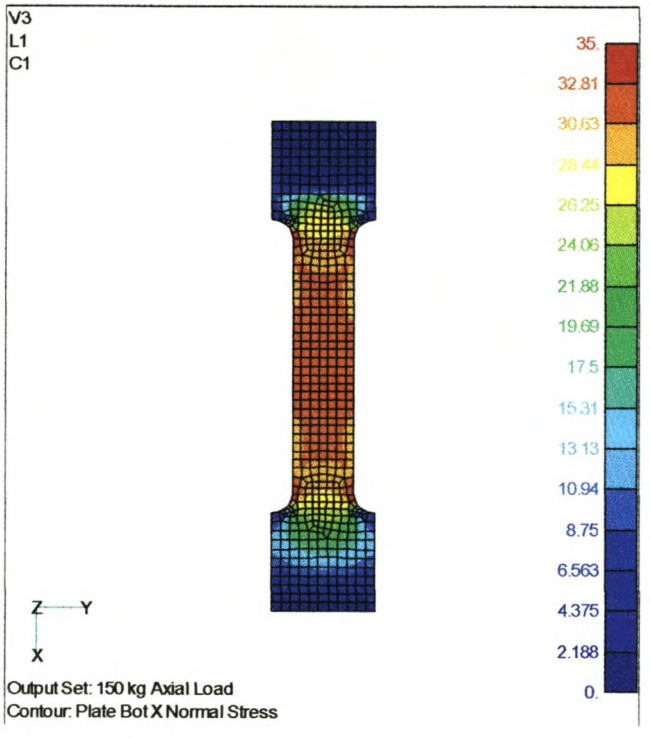

Figure E.8: CSM stresses for plate model in X-Direction

From the contour plots the similarity is apparent. From these analyses it is evident that either the laminate or plate elements can be used to analyse the semi-trailer structure. As mentioned earlier the plate element is more convenient when it comes to result interpretation. For the majority of analyses this element type was subsequently used.

The only estimated value was the maximum allowed stress. This value did show some scatter during the experiments. It appears that the in-house material strength is lower than the normally stated values. The reason for this is the comparative thick gelcoat layer on each lay-up. The gelcoat would increase the ultimate breaking strength to some extent, but not as much as a chopped strand mat layer of the same thickness. A thicker chopped strand mat layer will also increase the overall stiffness. For weight considerations it must also be included into the model. The most realistic assumption was to take the average experimental breaking stress, based on the total specimen section area. Only two classifications were made, chop strand mat and woven roving. It is further believed that a factor of safety of at least two must be utilised during design evaluations to cover manufacturing and process variations. The same experimental analysis as above was done for the remainder of the test specimens. The table below is a summary of the test results.

Material	**Ultimate Tensile Strength [MPa]**	**Safe Strength [MPa]**	**Effective Young's Modulus [$GN.m^{-2}$]**
Chop Strand Matt	55	28	2.2
Woven Roving	84	42	2.5

Table E.3: Summary of test results

Appendix F :Investigating Inertia Relieve

To test the validity of the inertia relieve constraint method (MSC/Nastran proprietary name) a test model was created. A 50 mm thick 200×200 mm steel plate was loaded at one corner point with a 10 kN static load. The analysis evaluates the behaviour (quasi static) if a shock point load is applied. The plate is free to move, and its own inertia is the only mechanism resisting steady state movement as per figure F.1.

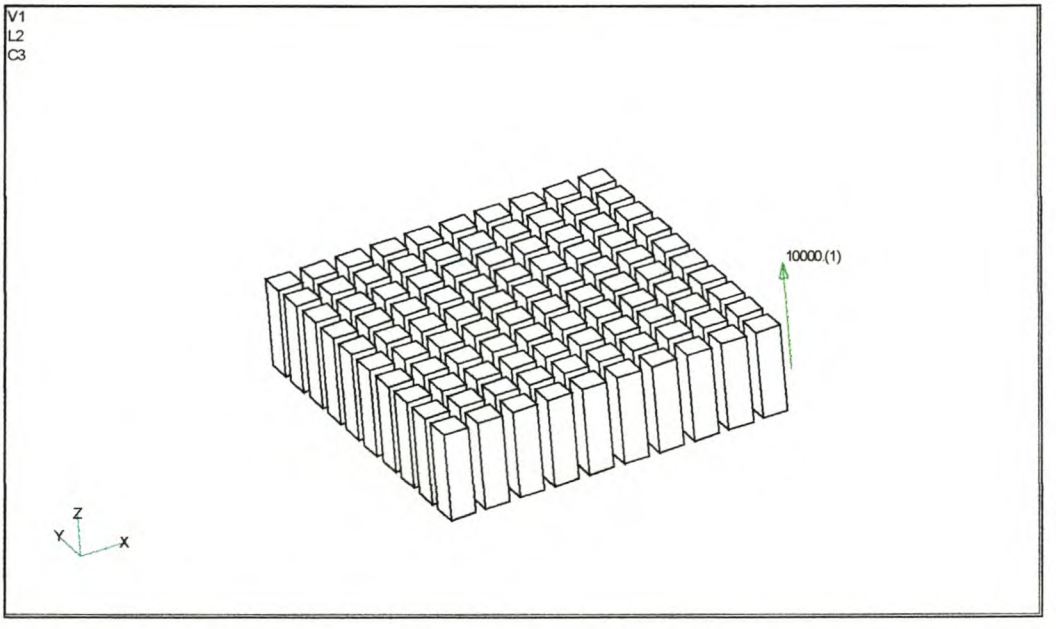

Figure F.1: Inertia relieve test model

Following the procedure as set out in the MSC/Nastran for Windows documentation Update, Volume II, the plate was constrained in all six degrees of freedom. For a first analysis this was done at one node near the plate's centre of gravity. The stress contour plot can be viewed in figure F.2. If this contour plot is compared to the same analysis without the inertia relieve constraint method, the difference is remarkable, figure F.3. Obviously the stress results of the second analysis cannot be correct if the plate is free to move. The effect of constraint placement was also investigated. The six degrees of freedom is now separated to six different nodes. The result was exactly the same, as per figure F.4.

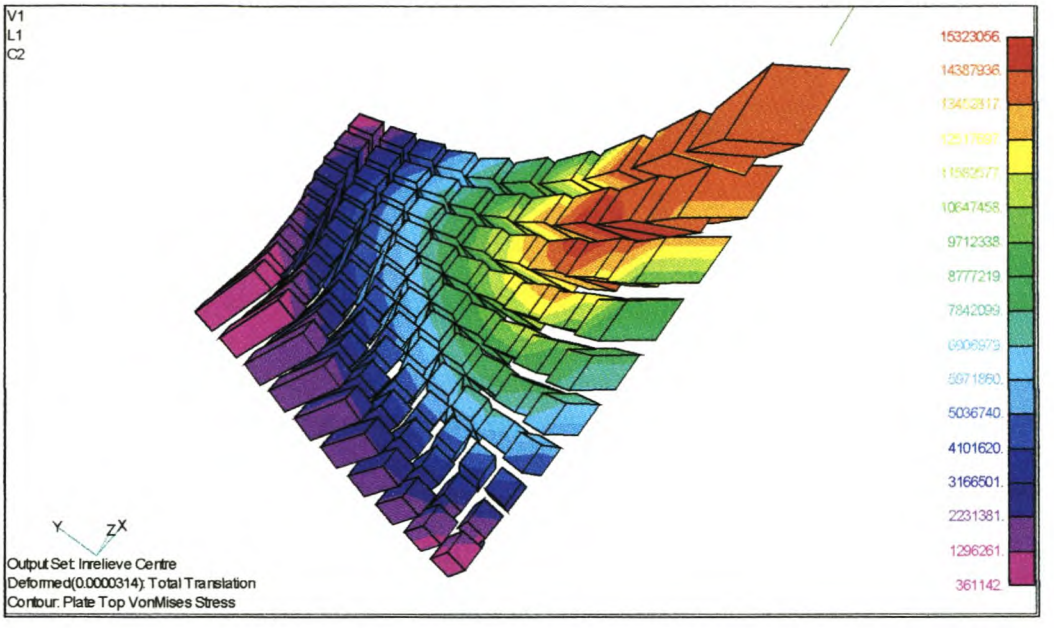

Figure F.2: Inertia relieve contour plot, centre fixed

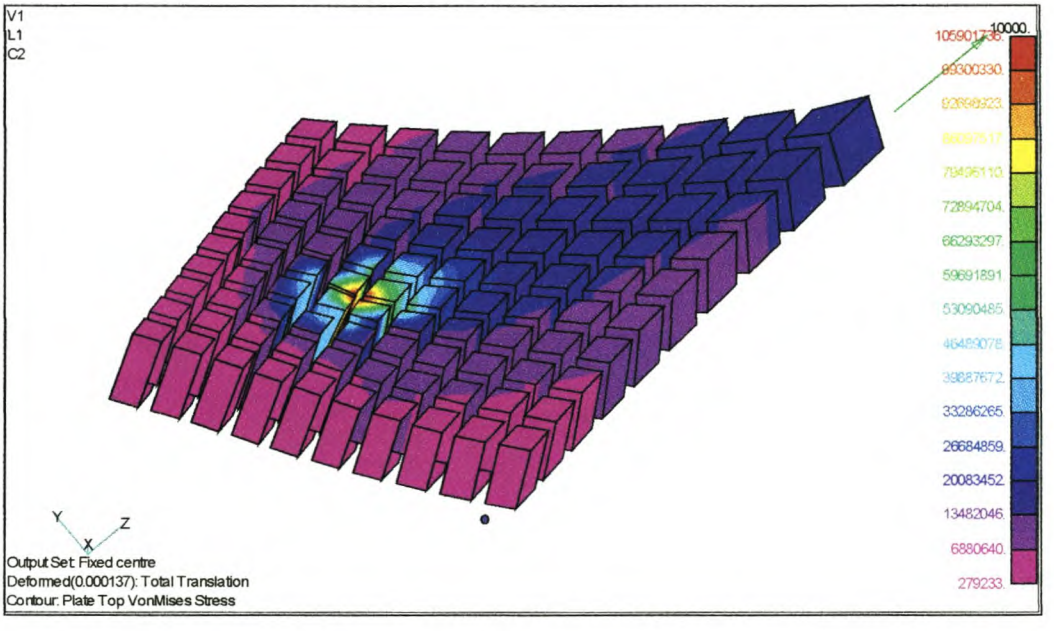

Figure F.3: Standard static analysis, centre fixed

To further verify the results of the inertia relieve method, a dynamic model of the plate structure was made, also in which no constraint was applied. For the dynamic analysis the plate was free to move in all directions, and the impulse load was applied at the same location as for the first three analyses. From the time history data it was evident

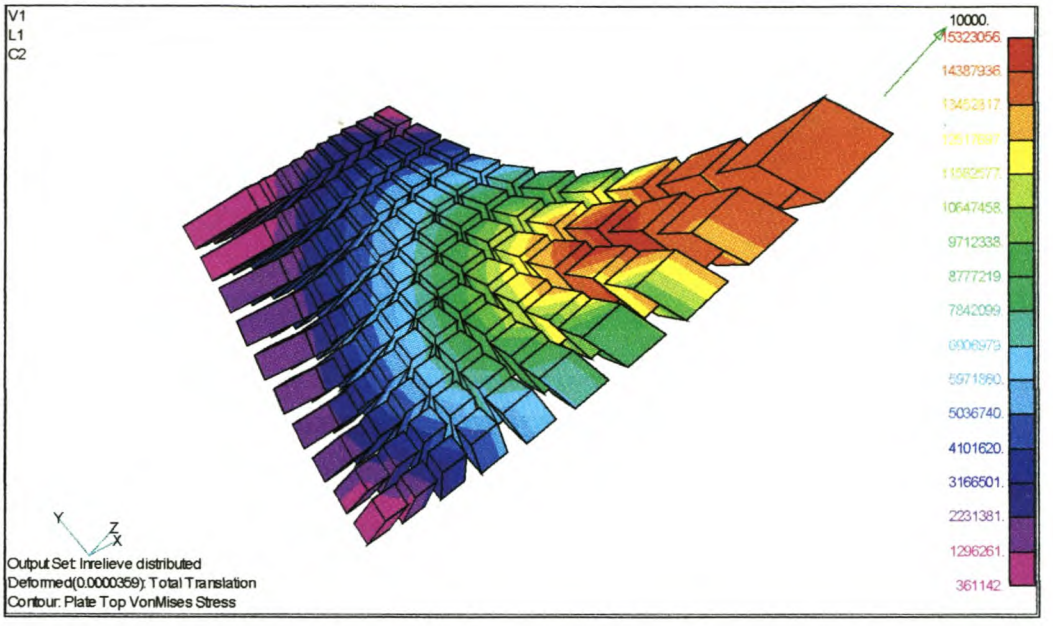

Figure F.4: Inertia relieve contour plot, distributed constraint set

that the plate moved a considerable distance in a spinning and vertical translation fashion. This behaviour is to be expected since there is nothing resisting this movement. The stress contour is almost exactly the same to the inertia relieve analysis, the difference being 70 Pa (0.0004%) on the maximum value of 17.46 MPa.

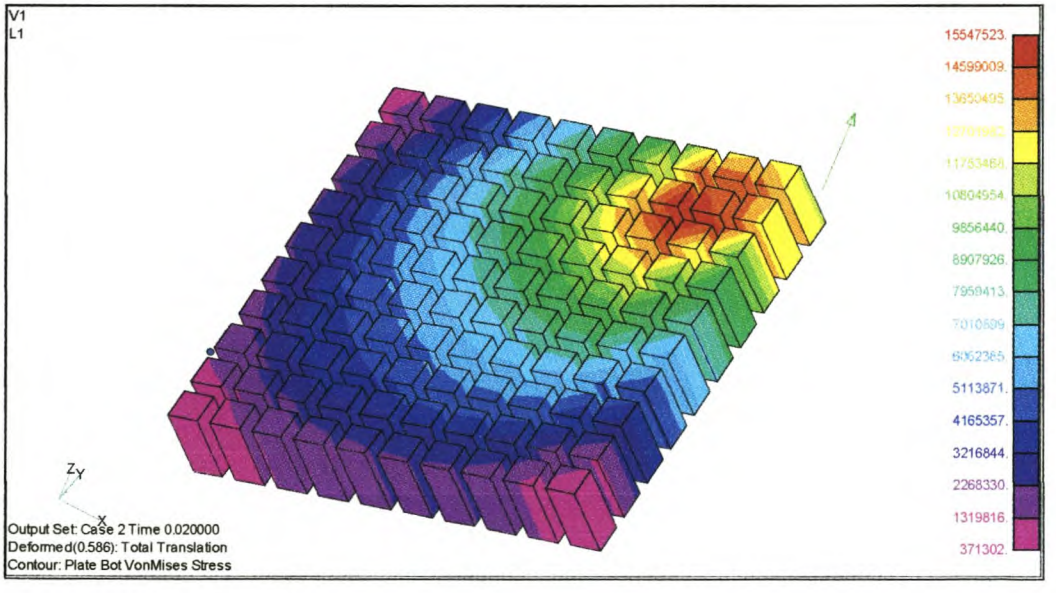

Figure F.5: Dynamic analysis contour plot

It was however not possible to compare the deformed shape, since as mentioned the plate just moved through space for the dynamic analysis. From this comparison the inertia relieve analysis seemed to be a good method to efficiently analyse free body movement and the stress results seems realistic. However for the above comparison the investigated model was structurally stiff. To apply it with confidence, the method has to be investigated for a structure having a much lower overall stiffness. A new model was created, namely a 200×200 mm of 50 mm thick 80 kg.m^{-3} polyurethane block, sandwiched between two 5 mm steel plates as per figure F.6. A 1000 N load was applied to a corner of the bottom plate. The six-point constraint was applied to the centre of the upper plate.

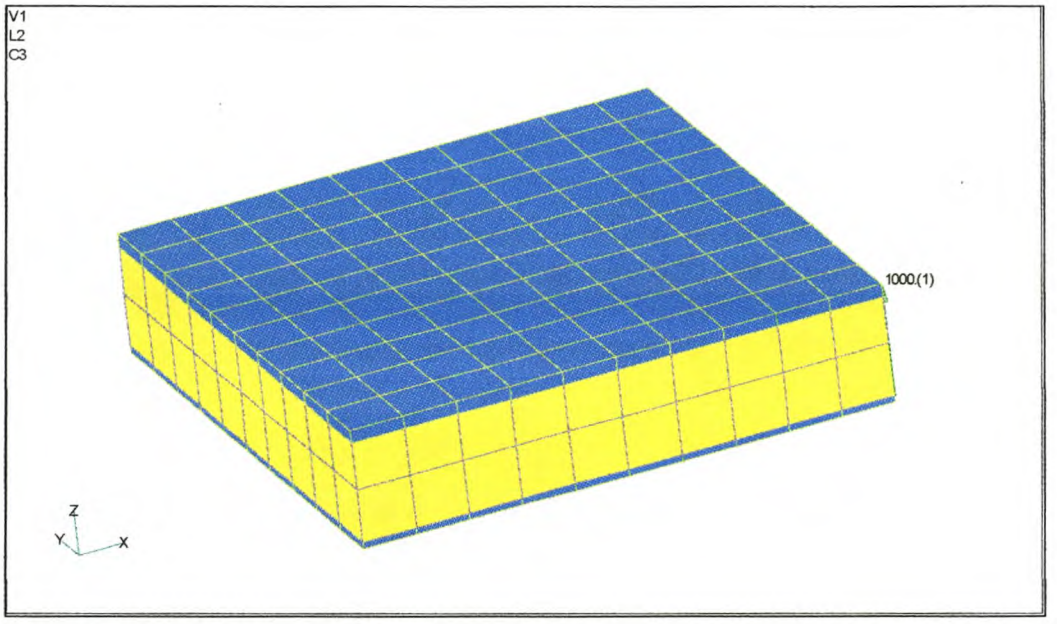

Figure F.6: Sandwich panel investigation

From the contour plots in figure F.7 it is clear that even though the point constraint was applied to the top plate, the high stressed area remained in the lower plate. This situation is to be expected since the polyurethane cannot transfer the strain. The stress distribution as per figure F.7 seems logic. The result of the standard static analysis is as would be expected, totally wrong, e.g. the fixed constraint dominates the stress distribution, figure F.8. To validate the stress values a dynamic model of this structure was also analysed, with the contour plot displayed in figure F.9.

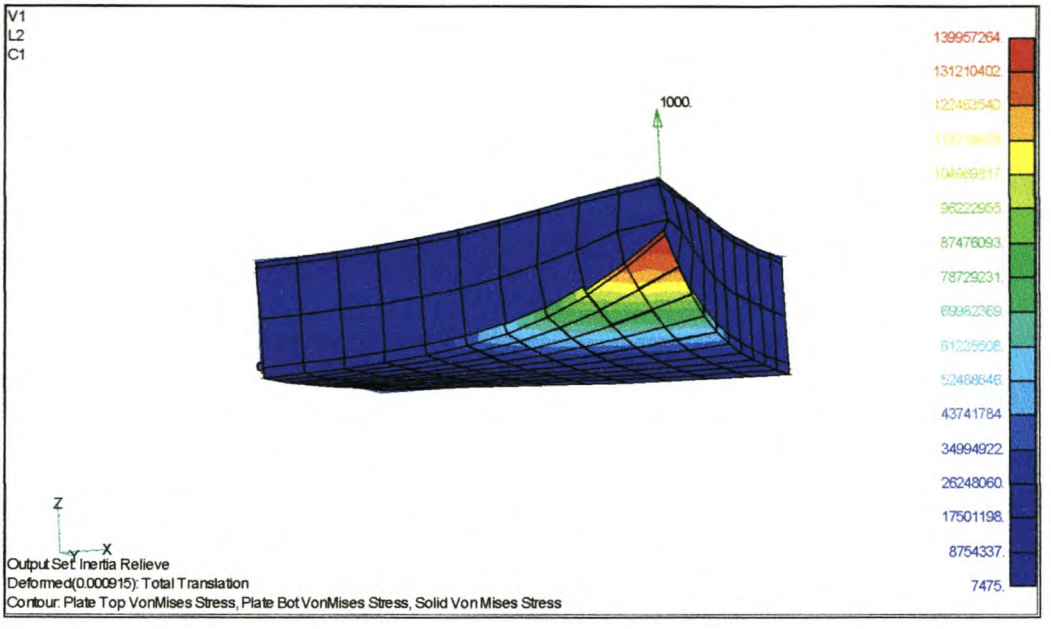

Figure F.7: Contour plot of sandwich model, inertia relieve analysis

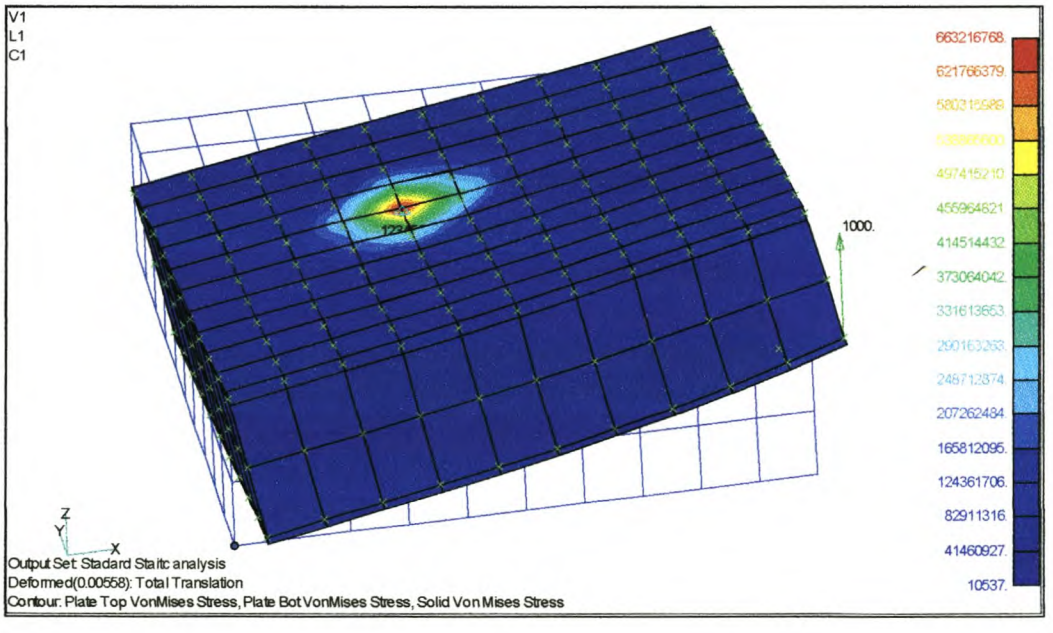

Figure F.8: Contour plot of sandwich model, standard static analysis

The stress contour plots display the same tendency as for the above analysis. The maximum stress differs only with 0.007% from the above analysis. From this comparison it can be seen that even for this relatively flexible structure the inertia relieve method still gives realistic and highly accurate answers. The only setback is

that whole body translation dominates displacement plots for the dynamic analyses and displacement contours have to be viewed as such.

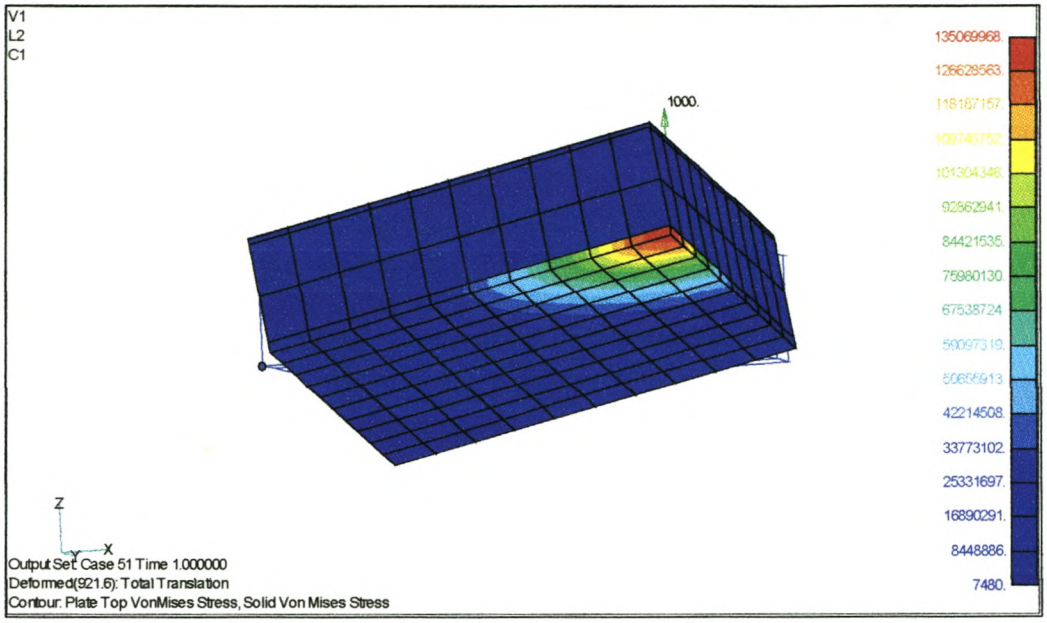

Figure F.9: Dynamic analysis of sandwich panel

Appendix G: Wheel Alignment Tool and Process

Tyre wear is a large contributor to vehicle maintenance cost. Incorrect wheel alignment can quickly cause permanent and irrevocable tyre damage. In one instance a new set of tyres was damaged to the extent of needing replacement in one Cape to Johannesburg round trip since the steered axle was misaligned. This is a loss of about R24 000. To permit easy and accurate wheel alignment, an alignment plate tool was developed which was used to lock the steering mechanism in an axial direction. The tool was positioned closely around the king pin, and had an accurate V-groove to align with the steering block. This alignment plate was laser cut and machined afterwards to ensure tight tolerances. The whole plate could be adjusted by a screwing mechanism to turn and lock the front steering system. To ensure that the system was aligned with the axle assembly, a laser measurement system was used. Figure 1 below is a drawing of the guide tool. With the aid of the figure the two alignment processes are described.

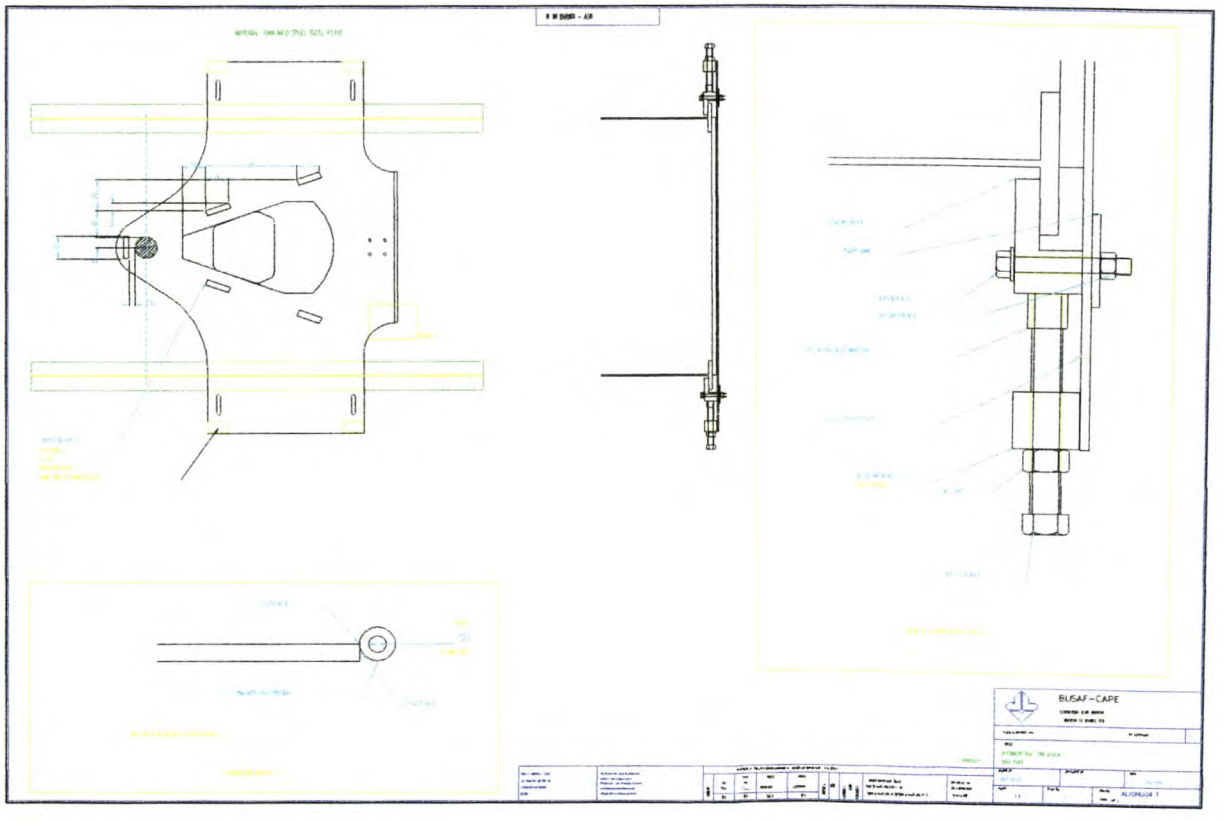

Figure G.1: Wheel alignment tool

Alignment method

Step 1 Align axle A2 with respect to KP

Step 2 Align axle A1 with respect to A2 and KP.

Step 3 Align axle A0 with respect to A1 en A2.

Step 4 Align axle A3 with respect A0.

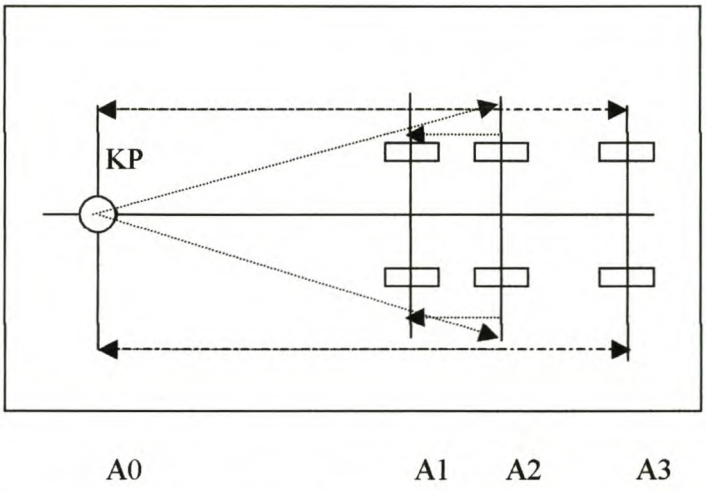

Figure 6.2: Wheel alignment diagram

The vehicle is first parked after being driven in a straight line. The truck is un-coupled, and the tool plate is positioned around the king pin. The V-block must be loosened and re-tightened to facilitate a close and secure fit. The first (A1) and second (A2) axles are aligned in the normal fashion with the king pin as origin. The tow-in and camber are also done in the usual fashion. The laser pointers are then positioned on the centre (A2) axle. With the aid of the alignment tool, the front turntable assembly (A0) is turned to ensure that the V-block and king pin are in a straight line. This is achieved by pointing the lasers at a board in line with the king pin position and one at an offset from the king pin. If the readings on either side of the centre are the same for all four measurements, the two boards must be parallel and perpendicular to the vehicle centre axis. The steering arrangement is now locked and the rear axle (A3) can be aligned again to the king pin centre point. All three the axles will now follow the same running point and the bogie will follow the vehicle direction of travel without internal scuffing.

Appendix H: Maintenance Manual for Steering Axle Semi-trailer

[1,4,5,9]

BUSAF CAPE

Maintenance Manual

30 Pallet Steering Axle GRP Semi-Trailer

Introduction

Congratulations on the purchase of your new BUSAF CAPE 30 pallet steering axle GRP Semi-trailer. By adhering to the enclosed instructions you will not only extend your vehicles lifetime to the maximum but also minimize downtime losses.

Your semi-trailer was manufactured according to the latest road regulation act with SABS approved manufacturing procedures. We are confident that you have bought the best value for money GRP semi-trailer on the South African market, backed by a team of highly skilled and professional staff. Be assured of our continual support and assistance, and do not hesitate to contact us if there any questions regarding your semi-trailer and its operation.

General Information and First Service

To ensure trouble free operation and minimum repair work the key word is continuous inspection. If any abnormalities, e.g. abnormal tyre wear or chassis cracks are detected immediate action should be taken. Contact our repair and technical staff if there is any doubt as to the severity of the abnormalities.

Strict maintenance scheduling is important during the first few hundred kilometres. We strongly recommend that you study the "BPW trailer axle and suspension" maintenance instruction booklet over and above this maintenance manual.

After 200 km.

Check the following		
Wheel nuts	M22x2	430 Nm

After 1 – 3 weeks.

Grease stabilizer bearings		
Check U-Bolts for firm seating	M24	600-650 Nm
Check spring pivot bolts	M30	700-750 Nm
Shock Absorber fastening	M24	400-450 Nm

Maintenance Instructions

Suspension & Axles

Initially after two weeks

Grease stabilizer-bearing bushes with BPW special long life grease ECO-Li 91 and check for wear.

Check U-Bolts for firm seating.	M24	600-650 Nm
Check spring pivot bolts.	M30	700-750 Nm
Shock Absorber fastening.	M24	400-450 Nm

Every 12 weeks

Grease stabilizer-bearing bushes with BPW special long life grease ECO-Li 91 and check for wear.

Twice annually

Visual inspection.

Check all component parts for damage and wear.

Check condition of air bags.

Check air suspension level valves for condition, seal tightness and firm seating.

Annually

Check U-Bolts for firm seating.	M24	600-650 Nm
Check spring pivot bolts.	M30	700-750 Nm
Shock absorber fastening	M24	400-450 Nm
Check air bag fastening	M8	19 Nm
	M12	66 Nm
	M16	230 Nm
Check stabilizer fastenings	M10	53 Nm
	M30	700-750 N

Brakes

Daily

Drain reservoir tanks.

Monthly

Check line filters. Clean or replace.

Annually

Check diaphragm and all other parts, replace if worn.

Check valves and fitting for leaks, tighten or replace.

Steering Mechanism

General

It is of the utmost importance that the steering mechanism is kept in premium mechanical condition. The system is intolerable of excessive play or misalignment and any deviation from the designed status will lead to degraded vehicle handling characteristics as well as excessive tyre wear.

Front slewing ring

Grease every 5 000 km.

Ensure that the mounting bolts are tight (160 Nm).

Check for excessive play at each greasing interval.

Steering beam

Check for structural integrity, every 20 000 - 30 000 km.

Check support pads every 20 000 - 30 000 km.

Check bolt flanges, tighten to 65 Nm every 100 000 km.

Check for play at end bearings every 100 000 km.

Rear turntable

Grease every 5 000 km.

Check bolt torques (120 Nm) every 20 000 - 30 000 km.

Check dolly for cracking and deformation, 20 000 - 30 000 km.

Landing Legs

General

Never drop semi-trailer onto the landing legs. Before unhitching the semi-trailer, ensure the landing legs are fully extended.

Grease at three-month intervals.

King Pin

General check, every 100 000 km.

Check torque on mounting bolts, 180 Nm

Check king pin and apron plate for excessive wear and deformation.

Ensure fifth wheel is greased frequently and adequately!

GRP Body Work

General maintenance

The Glass Reinforced Plastic (GRP) bodywork should be checked for cracking and damage on a continuous basis. If there is any damage, immediate repair should be done to prevent moisture form entering the GRP sandwich panels or propagation of the cracking. Small repair work can be done in-house, but if the damage could have affected structural integrity, repair work must be done by an official appointed Busaf Cape repair facility.

Conditions of sale

Not included with thesis

Conditions of repair and repair branches

Not included with thesis

Maintenance Diagram

Drawing H-1 will serve as a workshop aid. It conveniently gives the torque requirements and service intervals for the major chassis components. If you require additional, or larger or laminated copies contact our Busaf Cape technical office.

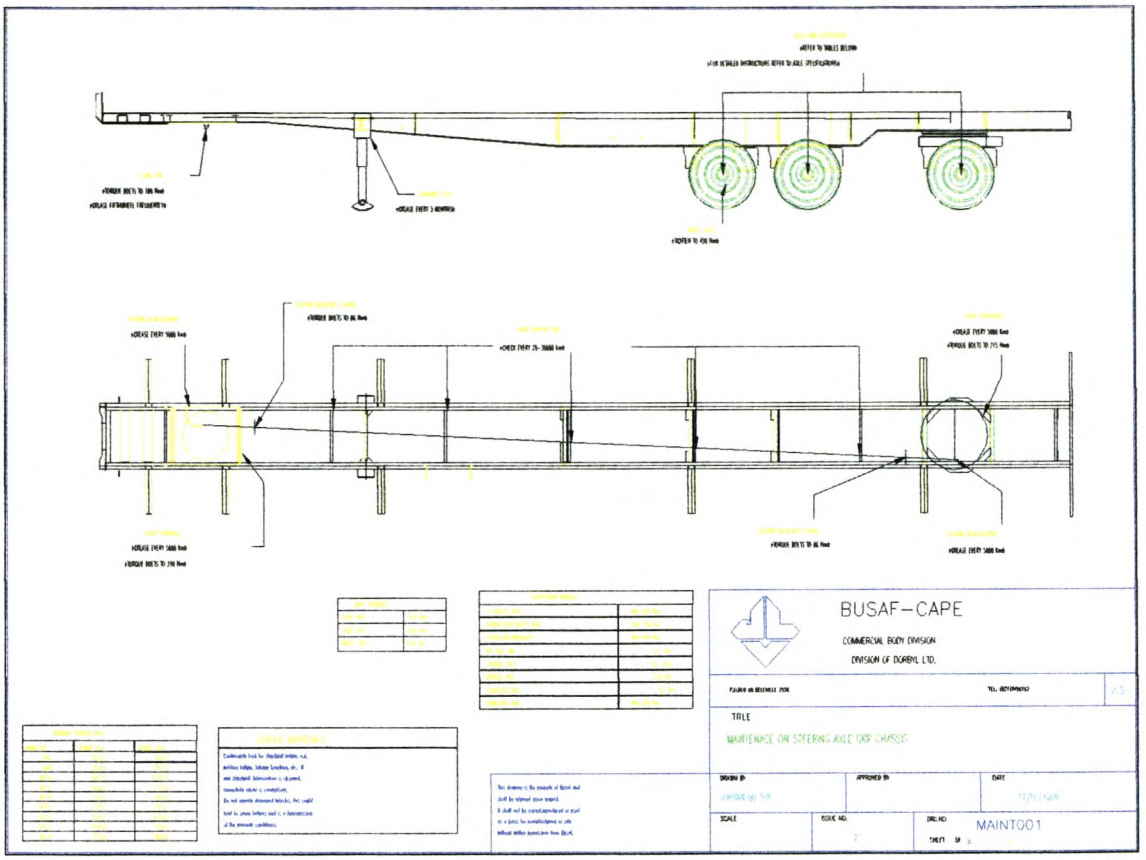

Figure H.1: Maintenance diagram for steering

References

1. Air-suspended running gear AIRLIGHT, **General information**, BPW ALV 96/1 e [5001]
2. B. Burchardt, et al, **Elastic Bonding**, Verlag Moderne Industrie, 1998
3. B. Lacovara, **The Optimum Composites Shop,** CFA 1994
4. BPW Axles with air suspension SL, **Trend-setting chassis technology**, BPW O/95/1 e [5001]
5. BPW Axles with air suspension, **Installation Instructions**, BPW EAO/94/1 e [3002]
6. Data Sheet, **Iscor,** Plate to BS 4360 Grade 43, September 1984
7. Data Sheet, **Iscor,** Plate to BS 4360 Grade 50, September 1984
8. Data Sheet, **Iscor,** Supraform TM340-500, September 1987
9. GRP Semi-trailer, Quality Procedure Manual, Busaf Cape
10. Product Data Sheet, **NCS**, PolyLite 31 000
11. Toyota Forklift Truck, **Vehicle specifications**, Toyota Motor Corporation 5FG/D10-30/e-8606/J/Printed in Japan/No.72006/22,600
12. HJ Beermann, **The analysis of commercial vehicle structures**, Mechanical Engineering Publications Limited, 1989
13. WA Lees, **The Ultimate Vehicle – a bonded composite?**, Reinforced Plastics, September 1987
14. JP Holman, **Heat Transfer**, 7th ed, McGraw Hill, 1992
15. Alcan Canada Products Limited, **Strength of Aluminium**, 5th ed, 1983
16. SSAB Tunnplåt AB, **Sheet Steel Handbook**, 2nd ed, 1996
17. Middelburg Steel and Alloys, **Pocket guide to stainless steel & 3CR12**
18. Scott Bader, **Crystic Polyester Handbook,** 1994
19. Composite Profiles cc., **CP Design Guide**
20. Society of Automotive Engineers, **Fatigue Design Handbook Notes**, Date Unknown
21. SJ Maddox, **Fatigue Strength of Welded Structures**, Abington publishing, 1969

22. OW Blodgett, **Design of welded Structures**, James F. Lincoln Welding Foundation, 1966
23. RS Sabo, **Procedure Handbook of Arc Welding**, 13th ed. Lincoln Electric, 1994
24. TB Jefferson and G. Woods, **Metals and how to weld them**, James F. Lincoln Welding Foundation, 1954
25. PP Benham, RJ Crawford & CG Armstrong, **Mechanics of Engineering Materials**, Longman, 1987
26. SABS SV 1051: Part 1-1980, **Braking Part 1: General**, The council of the South African bureau of standards
27. Data Sheet, **Iscor,** ROQ-tuff: Alloy Grades, September 1986
28. Data Sheet, **Iscor,** Corten, October 1987
29. Linpac Insulation, **Products report Ref. DSA-015**, 26 April 1995
30. Article, Telford Round-up**, Transport Engineer,** June 1996
31. D Garzanzich, **Tailored Trailers**, Transport Management – August 1996
32. Product Data sheet, **Structafoam,** Data Sheet 3.5, Polyurethane and Polyisocyanurate rigid foam – July 1991
33. Technical Letter, **David Graves**, Macprac (UK) Ltd., 19 September 1997
34. Bernd Burchardt, et al., **Elastic bonding**, Verlag Moderne Industrie, 1998
35. J.F. Shackelford, **Material Science for Engineers**, Macmillan Publishing Company, 1992
36. SABS 141-1992, **Glass reinforced polyester laminates**